University of Sheffield

Changing ice flow geometries of the British and Irish Ice Sheet: Applications of model-data comparisons

PhD Thesis

Submitted in accordance with the requirements
for the degree of Doctor of Philosophy

Remy Lawrence John Veness

2023

Abstract

Over time, changes in climate and subglacial processes result in shifts in ice sheet flow direction and extent, collectively referred to here as ice sheet geometry. For palaeo-ice sheets, changes in flow geometry are recorded in the form of glacial landforms and sediments, and can be simulated using numerical models. However, the modelled and observed flow geometries of palaeo-ice sheets have rarely been compared. In this thesis, I combine modelled ice flow geometry with observations of glacial landforms and sediments of the last British Irish Ice Sheet, to gain insight into model fidelity, the conditions of drumlin formation, and erratic transport. In Chapter 3, I use observations of ice flow direction and indicators of ice extent to evaluate an ensemble of ice sheet model simulations, curating a list of 'not ruled out yet' simulations. In Chapter 4, I use the 'best-fit' simulation as an 'observational environment' to investigate conditions associated with drumlin formation. I compare 85,834 drumlins against 15,000 years of modelled ice sheet conditions, observing an association between drumlins and a distinct velocity (>50-100 to <350 ma^{-1}) and thickness ranges. I interpret these as the conditions of drumlin formation. In Chapter 5, I develop and implement a simple flowline model of erratic transport which I test by reconstructing the dispersal of 2295 erratics from six sources (Shap, Ailsa Craig, Galway Granites, Glen Fyne, Cheviots and the Sperrins). I find the best-fit model matches 82% of erratics, and that the transport model can be used to assess model fidelity with regards to ice flow geometry. Overall, this thesis contributes to the growing field of palaeo-ice sheet model-data comparison, demonstrating both how data can help constrain models, and models can help us understand processes.

Acknowledgements

There are several people how I would like to thank and acknowledge. Firstly, I would like to thank my supervisors, Professor Chris Clark and Dr Jeremy Ely, both of whom have provided me with support, encouragement and enjoyable discussion across a breadth of academic and informal discussions. Their guidance and support has been unparalleled and I am truly grateful.

I would also like to extend my gratitude to the PalGlac team both for the scientific collaboration, but also for the who's regular Palglac Pizza Puzzle (despite lacking in pizza), which were a much needed lifeline during a long pandemic PhD.

Similarly, I would like to thank the ICERS Research Group, who have nurtured my glacial interests since first joining the department for my Masters in 2017. From the ICERS Group, I would like to give specific thanks to Darrel Swift and Andrew Sole; their input has been formative to my career and ideas.

Similarly, I would like to thank my glacial cohort fellows Christiaan and Pete who similarly were a bastion of support during the pandemic, along with 'the bubble'.

This work would not have been possible without funding from the University of Sheffield, Hossien Farmy Scholarship, and the Grantham Centre for Sustainability.

I would like to my family for their support and guidance, but specially to Judith, who could not be here to see this work completed, but I hope would have been proud to see it in its final state,

Finally, I would like to say a special thank you to Natalie for your unwavering support throughout through the years, and for helping me see the bigger picture when I needed it most.

Declaration

I, the author, confirm that the Thesis is my own work. I am aware of the University's Guidance on the use of Unfair Means. This work has not previously been presented for an award at this, or any other university.

Table of contents

List of tables

List of figures

List of abbreviations

AFDA - Automated Flow Direction Analysis
APCA – Automated Proximity Conformity Analysis
ATAT – Automated Timing accordance Tool
BIIS – British and Irish Ice Sheet
CV – cumulative velocity
DEM - Digital Elevation Model
EIS – Eurasian Ice Sheet
EIS- FenoscandinavianF Ice Sheet
GIA – glacial isostatic adjustment
HPC – High Performance Computer
MSGL - Mega Scale Glacial Lineation
NGRIP – North GReenland Ice core Project
NROY – not ruled out yet
PISM – Parallel Ice Sheet Model
RSL – Relative Sea Level
SIA – Shallow Ice Approximation
SSA – Shallow Shelf Approximation

Chapter 1 - Introduction

Our planet's climate is in a state of flux, alternating between glacial and interglacial states. The largest bodies of ice are called ice sheets - exceeding thousands of metres thick and many hundreds of kilometres in spatial extent. During the Quaternary Period (the last 2.6 million years), the total volume and number of ice sheets varied, as we transitioned through cyclical ice ages (Agassiz, 1842; Milanković, 1920; Weertman, 1976). During these cycles of waxing and waning, ice sheets sculpted the landscape, eroding away mountains and redistributing the resulting sediment into their proximal environment. Interpreting this glacially sculpted landscape is the aim of palaeoglaciology. As these palaeo ice sheets melted they released gigatonnes of water into the oceans, raising global sea level, and submerging low lying land (Lambeck & Chappell, 2001; Patton et al., 2017). Today, the Greenland and Antarctic Ice Sheets are the last of a once expansive network of ice sheets that covered almost all of the high latitude land masses (Batchelor et al., 2019). Together, the Greenland and Antarctic ice sheets today store enough water to cause 70 m of global sea level rise if completely melted (Church et al., 2001). With projections indicating future climate warming, society needs to predict the volume and timing of water that will be released as they melt further (Nicholls and Cazenave, 2010; IPCC, 2023). The systems which govern the demise of ice sheets are far from fully understood (e.g. Kirschner et al., 2011; Pollard et al., 2015). Thus, improving our understanding of the palaeo ice sheet record, to gain understanding into ice sheet processes, could have significant societal implications. This thesis looks to use these palaeo ice sheets as an observational laboratory to better understand the processes which governed the formation of their geomorphological and sedimentological record.

Modern humans have lived through a comparatively stable period of glacial activity known as an interglacial period (Sigman and Boyle, 2000). Extensive satellite observations of ice sheets during this comparatively stable period go back only sixty years, making up less than 0.05% of a single glacial cycle (120 kyrs). To understand how ice sheets behave over a longer period, we cannot rely on the contemporary observational record. To extend the glacial record beyond the era of satellites, palaeo-ice sheets can be reconstructed and used to understand the past (Stokes et al., 2015;

Pearce et al., 2017). In addition to extending the ‘observational’ record, investigating former ice sheets allows for the possibility of examining ice sheet processes. Some of these processes pertain to potential catastrophic ice sheet events associated with the terminal demise of an ice sheet, analogues for which have not yet occurred in the contemporary record (Batchelor et al., 2023). Whilst other phenomena are of intrinsic value to the understanding of ice sheets, acting as intricate clues which help uncover the larger intellectual puzzle of glacial processes.

In a similar manner to contemporary observations, records of the palaeo glacial environment alone provide only a partial picture of the past, suffering from either spatial or temporal discontinuity. Although some palaeo glacial records can provide a continuous record of the past such as lake varves (c.f. Boygle, 1993), these are limited in spatial extent, often acting as single points in space. In contrast, other records can be more continuous spatially but record only single points in time (Hughes et al., 2014). Collectively, these can be pieced together to provide a relatively spatially and temporally continuous record (e.g. Clark et al., 2022). However, this record from palaeo glacial reconstruction must be caveated with the need for extrapolation and interpolation between these inherently point based observations.

The final piece of the puzzle for reconstructing the past comes in the form of numerical ice sheet models (e.g. Tarasov and Peltier, 2004; Gregoire et al., 2016; Gandy et al., 2021). These benefit from being able to calculate a spatially and temporarily continuous reconstruction, using our understanding of the physical processes that govern ice sheets, and either records (for hindcasting) or projections (for forecasting) of ice sheet forcings such as climate. The resulting simulations from these models, however, are only as good as the understanding of the components that drive ice sheet processes. To improve numerical models, we need improved understanding of the ice sheet system. Despite this, models can also be used to help explain glacial processes (e.g. Gandy et al., 2019; Jamieson et al., 2012; 2014). With further knowledge of these processes, they can then be incorporated into models, and used to improve our understanding of contemporary and palaeo-ice sheets.

1.1 - The British-Irish Ice Sheet

With the aim of understanding the Greenland and Antarctic ice sheets, glaciologists often look for analogous palaeo-ice sheets, which can help them to understand key ice sheet processes. One of these palaeo-ice sheets was the British-Irish Ice Sheet (BIIS; Clark et al., 2022) which became connected with the ice sheets of

Scandinavia and the Barents Sea to create the Eurasian Ice Sheet (EIS) complex (Hughes et al., 2016). This most recently occurred during the Devensian, which spanned approximately from 31-15 ka. Throughout that period, the BIIS reached its maximum extent asynchronously (Clark et al., 2022). The BIIS is of particular interest to understanding some of the mechanisms which may also affect the Antarctic Ice Sheets. In particular, this ice sheet can be seen as analogous in some respects to the West Antarctic Ice Sheet, both being extensively marine based (see Figure 1.1). Furthermore, the BIIS is perhaps one of the most intensely studied ice sheets (with regards to studies per km^2 of ice sheet), meaning it has one of the most extensive palaeo glacial records available based on the number of reconstructions, and the percentage of landforms mapped. This is highly beneficial when asking questions of model fidelity (in other words 'how accurately does my model recreate reality?'), or process experimentation.

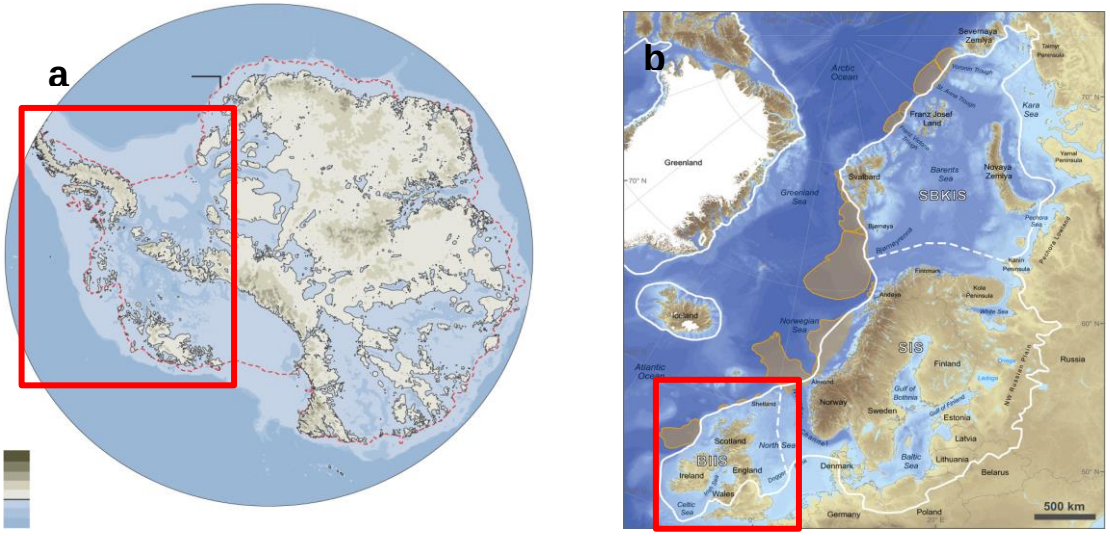

Figure 1.1: The Eurasian Ice Sheet complex, an analogue of West Antarctic Ice Sheet. 1.1a the Antarctic Ice Sheet, with current ice extent indicated by the dashed red line - from which it is evident that large parts of the ice sheet are grounded below sea level (land above sea level is shown in grey colours) (Modified from DeConto & Pollard 2016). The solid red box highlights the approximate area of West Antarctica. 1.1b shows the last EIS complex with contemporary landmasses and estimated maximum glacial extent in white corresponding to the Devensian maximum ice extent (Modified from Hughes et al., 2016. The solid red box highlights the BIIS.

1.2 - Ice sheet flow geometry

Ice sheet flow varies spatially and temporally, with regions of fast and slow flow, and with changing flow directions over time (see figure 1.2). This is because ice flow

direction is mainly dependent on the ice surface slope which shifts and adjusts to changes in precipitation regime and ice evacuation. The direction and speed at which an ice sheet moves varies dramatically over the course of a glaciation. The configuration of this flow pattern I refer to as the 'ice sheet flow geometry'. To understand future ice mass loss, we must be able to correctly simulate future changes in ice flow geometry. This is because flow geometry is crucial to understanding mass transfer from ice sheets to the ocean, and/or to lower elevations where it then melts. Changes in flow geometry are important as they can be observed (directly or indirectly) as markers of changes in inputs, outputs, or rates of change. In other words, ice sheet flow geometry arises from some combination of climate controls and ice sheet dynamics (e.g. ice velocity),

Many factors combine to dictate an ice sheet's flow geometry, as it is the result of a complex set of surface, internal and subglacial conditions, and mass balance. For example, dome geometry can be directly driven by prevailing precipitation regimes shifting the ice sheets' centre of mass, ice divides, and outlet glaciers (See figure 1.2b). Shorter scale processes also likely play an important role in ice sheet geometry, with diurnal variation in ice-bed coupling allowing for rapid variation in velocity (Bartholomew et al., 2010; Tuckett et al., 2019). Similarly, subglacial bed topography and basal material properties can play an important role in the mechanisms which dictate ice flow (Winsborrow et al., 2010; Jamieson et al., 2012). Terminus conditions are also important. Land-terminating outlet glaciers often form lobate margin positions, with flow geometry at the terminus becoming splaying. On the other hand, marine terminating portions of an ice sheet often form ice shelves when terminating on shallow marine shelves. Ice shelves can slow the flow of ice through buttressing (Thomas, 1979). This means that the geometry of an ice sheet is the culmination of several factors including, but not limited to regional climate and subglacial conditions. Therefore, a better understanding of ice flow geometry may reveal more than simply the shape and flow direction of an ice sheet.

The processes which lead to changes in ice sheet geometry are complex, interconnected and not fully understood. Fortunately, as an ice sheet's geometry and the processes controlling its velocity change, ice sheets often leave an imprint on the landscape, often preserved once the region is deglaciated (Stokes and Clark., 2001; Windsborrow et al., 2010; Livingstone et al., 2012a). This takes the form of landforms and deposits which can be interpreted as indicators of ice flow, including erratics (e.g.

Sutherland, 1984; Greenwood, 2008; Livingstone et al., 2012), striations (Klassen, 1994), and subglacial bedforms (Clark 1993, Hughes et al., 2010).

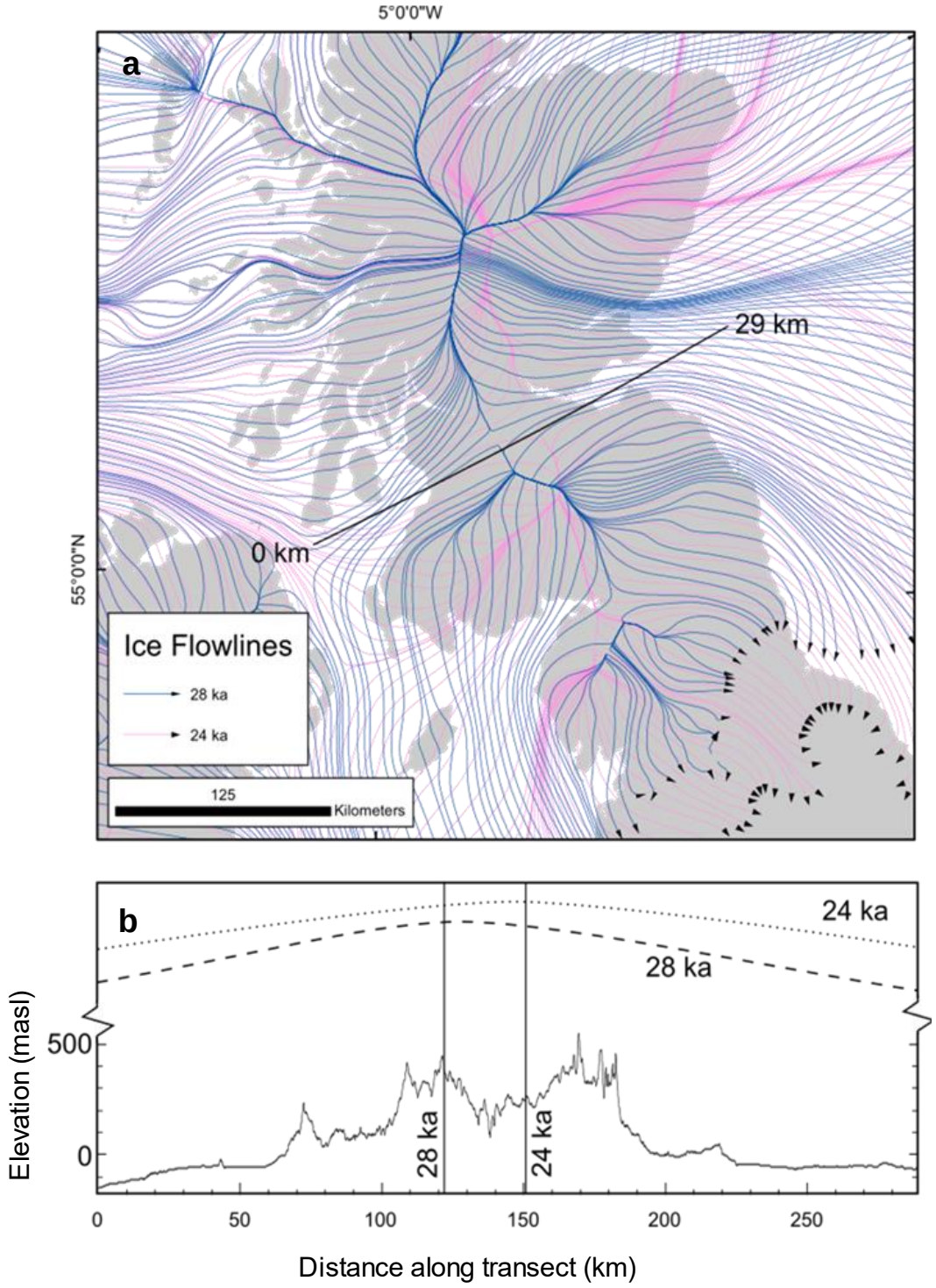

Figure 1.2: Ice flow geometry of the BIIS. Note how changing ice divides are unimpeded by basal topography between 29 ka and 24 ka. Flowlines in 1.2a indicate ice flow direction over time with regions of divergence (ice divides) from the BC model (Clark et al., 2022). 1.2b shows subglacial topography (Clark et al., 2022), with vertical lines indicating the location of ice divides and dashed and dotted lines indicating ice surface with distances in km and heights in m.

1.3 - Numerical ice sheet modelling and observations of palaeo-ice sheet activity

Numerical ice sheet models are computer programs designed to solve a series of equations which approximate the processes of ice sheet flow. The range of applications of numerical ice sheet models is broad, from accounting exercises used to calculate the amount of ice mass lost at an ice sheet scale, to investigations of processes such as ice streaming or ice shelf buttressing (e.g. Tarasov and Peltier, 2004; Gregoire et al., 2016; Jamieson et al., 2016; Gandy et al., 2021). A pragmatic challenge of all modelling efforts is the need to balance model fidelity with computational expense. In practice, the trade-off is played out at all levels, from the mathematical complexity of the ice physics (Kirschner et al., 2011), the temporal and spatial resolution of the model domain (e.g. Rutt et al., 2009), to the breadth of parameters calculated (e.g. Jouvet et al., 2017). Also, a number of challenges hinder the modelling of ice sheets. Some issues stem from poorly understood processes, such as the coupling between an ice sheet and its bed, whilst others stem from attempting to maximise a model's fidelity to a particular ice sheet with a limited computational expense. Answering these questions of model fidelity are challenging when looking to model future ice sheet changes and contributions to global sea level, given the limited temporal span of direct observations we can use for model validation.

Hindcasts are model simulations which recreate past conditions. Using this approach, it is possible to assess model skill against glacial events that have already happened. The advantage of this method is that (providing you have sufficient evidence of past glaciations) hindcasting predictions can be empirically tested, and model fidelity evaluated (Aschwanden et al., 2013). Using hindcasting modelling of ice sheets, it is possible to experiment on aspects of numerical modelling, performing parameter sensitivity analyses, and experiment with the importance of different glacial processes and their incorporation into ice sheet models (Ely et al., 2021).

To effectively use hindcasting for numerical model development and to learn about processes, we need empirical observations of the palaeo glacial environment. Fortunately, glacial processes leave an extensive sediment record which can be interpreted to reconstruct the ice sheet processes which deposited them. The palaeo glacial record is rich with landforms, which can be interpreted using satellite, field, and

lab based methods to provide a complex picture of how an ice sheet behaved (Mark, 1974; Clark et al., 2004a; Smith et al., 2006; Fuchs and Owen, 2008). Specifically, characteristics like ice extent, flow direction, and thermal regime can be inferred from observations of specifical landforms, sediment structures, or the absence of such structures (Kleman 1994; Kleman and Borgström, 1996; Greenwood and Clark 2009b; Hughes et al., 2014; Dulfer et al., 2022; Clark et al., 2022; Boyes et al., 2023). The history and methods of these reconstructions are discussed in more detail in Chapter 2.

As well as incorporating empirical observations into ice sheets simulations to assess how well the model performs, we can also incorporate numerical models into our observations to test our understanding of the observations (e.g. Clason et al., 2016; Livingstone et al., 2016; Jamieson et al., 2016; Gandy et al., 2019). In doing so, it is possible to enrich the palaeo observational record by extracting parameters which cannot readily be observed from the sediment record, such as timing required for formation and glacial conditions associated with a landform. This is to say, if we can accurately reconstruct the past, this can help explain previously confounding landforms or processes of past glaciations.

The landforms associated with palaeo-ice sheets most utilised by this thesis are drumlins. These small hills form in the direction of ice flow and cover up to 70% of the palaeo glacial landscape of Britain and Ireland (Clark et al., 2009). Drumlins provide a palimpsestic record of ice sheet flow geometry. That is to say, they record episodic events spread throughout time (Clark, 2010). I also use moraines, which delineate ice extent and are one of the earliest tools used in glacial reconstruction (Geikie, 1897). Broadly, moraines are accumulations of sediment which demarcate the edges of an ice mass (Barr and Lovell, 2014). The final piece of the palaeo glacial record I use in this thesis, is the glacial erratic. Erratics are surface boulders, cobbles (lodged in till), and indicator grains (constituting till) which have been found outside of their geological source area (Klassen and Gubins, 1994). As with moraines, glacial erratics have a long history of use for glacial reconstruction, supporting the first hypothesis of widespread glacial reconstruction in the 1840’s (Buckland, 1941; Lyell 1941; Agassiz, 1941). Glacial erratics stand out as a powerful intermediary of drumlins and moraines, proving the potential of allowing for the inference of both ice extent and flow direction (Charlesworth, 1953; Sutherland; 1984, Greenwood, 2008). Despite this, in recent years glacial erratics have fallen out of favour with those who conduct glacial reconstructions.

The palimpsestic nature of the geomorphic record of ice sheets conceptually compliments numerical ice sheet modelling (Ely et al., 2019a). The empirical record highlights discrete glacial events over time but requires interpolation between these events if a continuous record is required (e.g. Clark et al., 2004a). In contrast, numerical ice sheet models can provide a continuous record of the past, and benefit from being validated against the points in time from the past. Unfortunately, historically poor interoperability between numerical ice sheet models and empirical observation mean models and data are rarely combined (Kirschner et al., 2011; Ely et al., 2019a). In this thesis I look to develop methods for improving interoperability between models and data. Specifically, I focus on observational data which can help to validate a model's fidelity to reconstructing flow geometry. I also reverse the model-data comparison process to use an ice sheet simulation to explore drumlin formation and how this relates to ice sheet velocity, and potentially the subglacial environment. Similarly, I aim to contribute to the reintroduction of erratics as a mainstream tool deciphering ice sheet geometry and explore the potential of using erratics as a model data comparison tool.

1.4 - Thesis aims and objectives

The overall aim of the thesis is to make advances in the emerging field of model-data interoperability, to reduce the disconnect between numerical ice sheet models and empirical observations. I address this both from the perspective of using empirical observations to test model fidelity, but also that of using numerical models to explore glacial processes. More specifically, the last BIIS is used as a data-rich palaeo-ice sheet to address the objectives below.

Objective 1: Assess the fidelity of an ensemble of 200 numerical model simulations of the BIIS against empirical observations of ice flow direction and ice extent (drumlins, moraines & erratic's). To achieve this, I will score, rank and identify simulations which best recreate palaeo-ice sheet flow geometry (Chapter 3).

Objective 2: Given a model-simulation that best captures empirical observations of flow direction, as identified in Objective 1, examine the modelled glacial conditions (e.g. velocity and thickness) associated with the formation of drumlins. The intention here is to attempt to use a numerical ice sheet simulation as an 'observational' environment to gain insights (Chapter 4).

Objective 3: Develop a simple debris transport modelling approach for use with numerical model simulations, and assess the extent to which it can reasonably explain the observed dispersal of glacial erratics across the British Isles (Chapter 5).

Objective 4: Explore the potential for the glacial erratic record to test modelled flow geometries of the British and Irish Ice Sheet (Chapter 5).

Chapter 2 - Empirical reconstructions and numerical ice-sheet model simulations of the last British-Irish Ice Sheet.

2.1 - Introduction

With the realisation that modern glaciers are changing comes the urge to know what they were like before. Initially, these thoughts would likely have remained internal musing of shepherds, hunters and mountain guides. By the 1700's these musings were formally being paired with observations such as striations in front of a glacier or glacially transported boulders (e.g. Martel, 1744; Besson, 1780, in Charlesworth 1953). Such ideas became increasingly complex to the point that Scientists started to recreate past glacial environments based on observations - we call these glacial reconstructions. Initially, reconstructions were based entirely on observations drawn together in maps. However, more recently these reconstructions have used increasingly sophisticated tools including satellite observations, numerical dating methods, and numerical ice sheet models (e.g. Clark et al 2012; Ballantyne and Cofaigh 2017; Ely et al., 2019a). This shift in methods has come both naturally with time but accelerated by the realisation that melting ice sheets in Greenland and Antarctica will likely play an important role in years to come (Bamber and Aspinall, 2013).

In this chapter, I outline the history of glacial reconstructions of the British and Irish Ice Sheet (BIIS), specifically focussing on lineated bedforms and moraines as indicators of flow direction and extent. I do not include the discussion of the history and use of erratics as these are addressed in detail in chapter 5. I also highlight some of the key methodological developments which have helped improve ice sheet reconstructions. Furthermore, I introduce and outline the basis of the numerical ice sheet model on which much of this thesis is based.

2.2 - Reconstructions of the British-Irish Ice Sheet

2.2.1 - Empirical reconstructions of the British-Irish Ice Sheet

The notion of ice sheet scale glaciation of Britain and Ireland was slow to gain traction. It was not until Agassiz's 1842 visit that discourse truly began on the possibility that an entire nation could go from ice covered to ice free. Gradually evidence of moraines and striations began to accumulate and in 1894, Geike published the first empirical reconstruction of the entire BIIS (Geike, 1894), as shown in figure 2.1. The fact that an ice sheet scale reconstruction could be developed by a single individual in the 1800's is remarkable, especially when you consider that observations were largely collected on foot or horseback. Geike was a geologist, and his main observations were on the composition of sediments. Although he mainly used till composition, striations and some glacial landforms were also widely used to infer flow direction and extent. Given that the evidence base was sparse (especially offshore), Geikie must have used a large degree of well thought out conjecture to build his reconstruction (See Figure 2.1). At this point in time glaciers were still considered to be relatively static bodies of ice which homogeneously expanded to a maximum extent before retreating. Therefore, Geike only presented a maximum ice sheet extent and a single set of flow geometries represented by flowlines. At this time, there was still little consensus as to how drumlins related to ice sheet geometries, so it is likely these did not play a central role in Geikie's reconstruction. It was several decades before the reconstruction by Geikie was further refined by the work of Charlesworth (1953). Charlesworths work culminated in an improved glacial reconstruction which used a broader range of palaeo glacial records including drumlins.

Implicit in Charlesworth and Geikie's work is the notion of a relatively stable ice sheet, without the dynamic, asynchronous switching proposed by ice sheet reconstructions today. It was not until the 1980's when Boulton began to suggest the varying dynamics of ice sheets that the notion of fast flowing ice streams arose (Boulton, 1987). This notion of a dynamic asynchronous ice sheet posed substantial challenges to palaeoglaciologists looking to reconstruct the BIIS as it put to question the notion of a single maximum extent (Clark et al. 2004; 2012).

The advent of remote sensing and widely accessible optical and DEM data (around the turn of the century) revolutionised what was possible for palaeo glacial reconstructions. This allowed a much larger body of data to be collated and ice sheet scale mapping of glacial landforms could be conducted by a single researcher with a consistent method and approach. This was the premise of the BRITICE project (Clark

et al., 2004a), which was followed by the work of Greenwood and Clark (2009b) and Hughes et al., (2014). A landmass wide approach was used to generate observations of drumlin orientation, and flow event grouping. These works supplemented an extensive revisiting of till geochemistry, and ice sheet chronology (e.g. Evans et al., 2010). As a combination of increasingly high resolution spatial reconstructions, and changing shift in understanding of the timings of ice sheet geometry it became apparent that the BIIS was much more dynamic than previous works by Charlesworth and Geikie's reconstructions suggested (Clark et al., 2012). To combine this theoretical understanding of dynamic ice sheets, with the observations of margins, field observations needed to be tied to geochronometric dates.

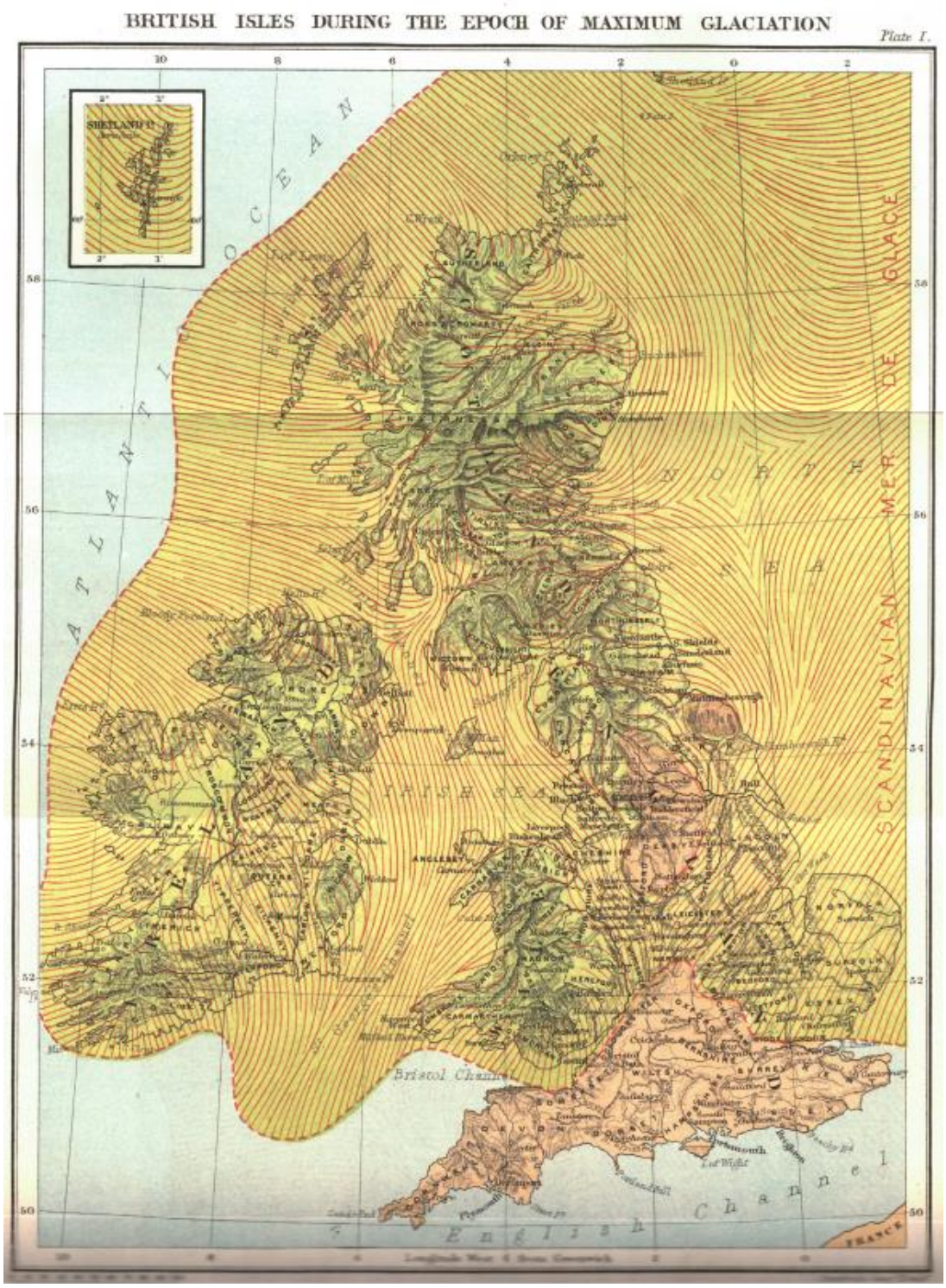

Figure 2.1: The first empirical reconstruction of the last British-Irish Ice Sheet by Geike (1894). Glacial extent in most regions aligns well with current thinking (e.g. Clark et al., 2022). Small discrepancies include glaciation of Norfolk, which is now believed to have occurred prior to the last glacial maximum.

The next bottleneck overcome in empirical reconstructions of the BIIS was that of constraining glacial chronology (Clark et al., 2021). Dating methods had been implemented for decades (Libby, 1961; Benedict, 1967; Dyke et al., 2002), and the early 2000's saw a rise in dating projects on the BIIS, many of which were increasingly alluding to the importance of the complex, largely undocumented offshore record (e.g. Scourse,1991; 2001; Carr, 2004; Carr et al., 2006; McCabe, 2007). However, it wasn't until dating could be paired with large scale mapping datasets and that a sufficiently large body of paired dates were accumulated (both on and offshore). At this stage as well as focussing simply on the maximum extent and single main flow direction, nuances of crosscutting flow geometries recorded in subglacial bedforms began to be proposed (Rose and Letzer, 1977; Evans et al., 2009; Greenwood et al. 2009; Clark et al., 2009; Livingstone et al., 2012; Hughes et al 2014). The benefit of combining large scale mapping with dating observations, is that a number of sites can be linked together to create isochrones which delineate the extent of the ice sheet through time. In Clark et al. (2012), the reconstruction determined ice extent to the edge of the continental shelf at the maximum extent. Clark et al. (2012) presented seven isochrones documenting retreat, pattern and timing. It was noted in Clark et al. (2012) that many more dates, especially offshore, were needed.

The BRITICE CHRONO project dramatically improved both the quality and quantity of data available by combining ice sheet scale observations with the collection of many hundreds of dates (Clark et al., 2018; Clark et al., 2022). Three main data outputs from the BRITICE-CHRONO project are highlighted for this work. Firstly, a comprehensive remote sensing mapping campaign identified 170,000 glacial landforms features which likely represents the majority of land-based features in Britain and Ireland (Greenwood et al. 2009; Clark et al., 2009; 2018; Hughes et al 2014). Secondly, 18,000 km of bathymetry and 377 cores were collected for the BRITICE-CHRONO Project, which allowed for offshore moraine complexes to be extensively mapped and at times sampled for dating (Clark et al., 2022). Finally, 690 strategically located geochronological dates were collected to supplement the mapping and existing work, meaning the chronology of the BIIS could be more robustly constrained (Clark et al., 2022). Significantly, this improvement in data has allowed for a new glacial reconstruction which combines empirical observations of ice flow directions, relative timing, with geochronological data. Observations of timing and extent have been used to create a series of isochrone extents. This BRITICE-CHRONO reconstruction is referred to throughout this work and can be seen in figure 2.2. Significantly this empirical reconstruction identified a number of key events and chronologies. These include a rapid offshore collapse of the marine sectors of the BIIS, followed by rapid

stabilisation of the onshore sector, and an asynchronous maximum extent across nine sectors of the ice sheet (Clark, et al., 2022).

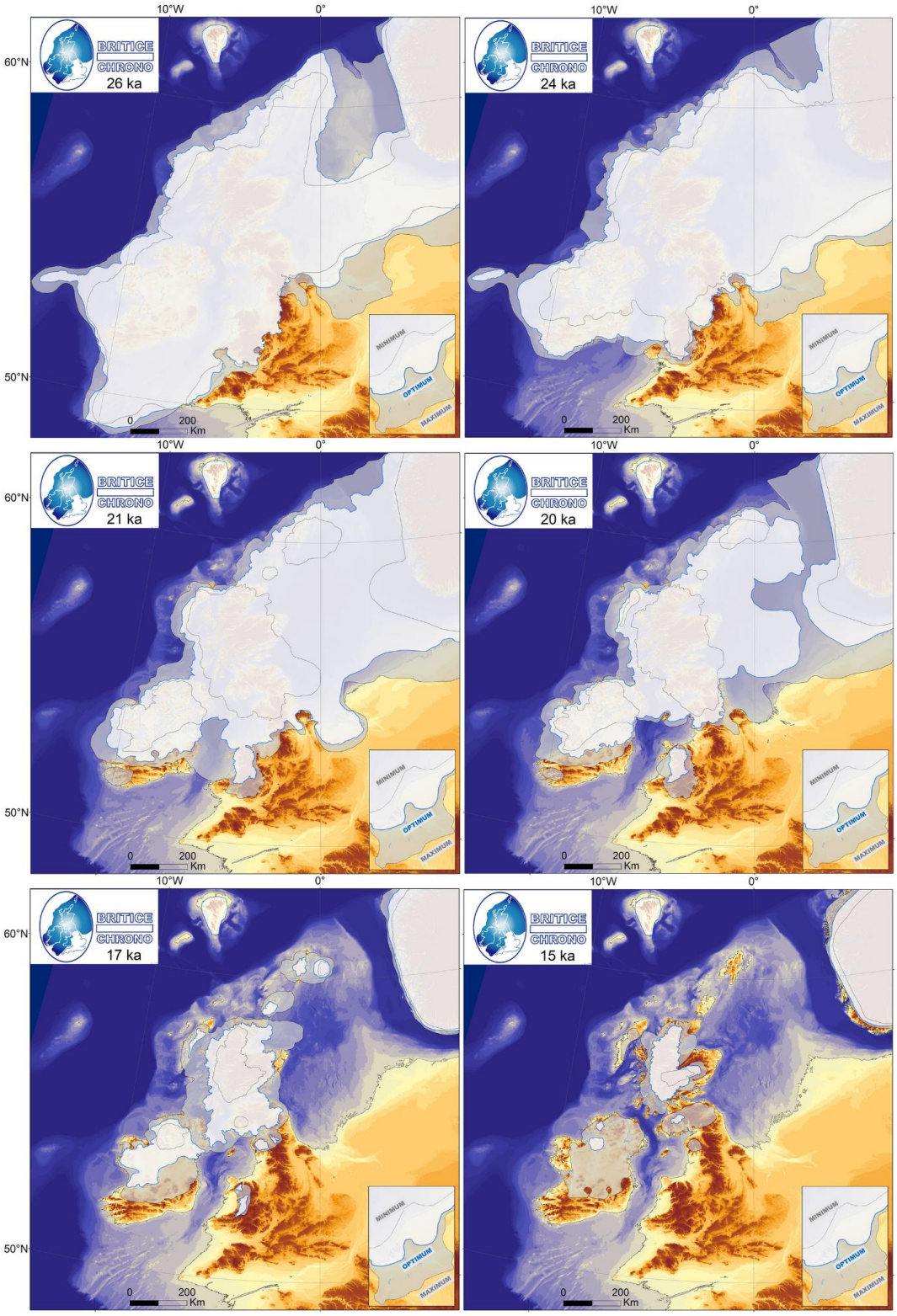

Figure 2.2: The BRITICE-CHRONO empirical reconstruction of the BIIS. Empirical reconstruction of the last BIIS at 26, 24, 21, 20, 17 and 15 ka from Clark et al. (2022). The degrees of confidence are accounted for with shades of white, with the white (blue boundary) representing the optimum and grey representing the maximum (illustrated in the insert key).

2.2.2 - Numerical modelling simulations of the BIIS

In addition to the long history of empirical reconstructions of the ice sheet, numerous numerical modelling approaches have also been trialled. The first numerical modelling reconstructions were carried out by Boulton, et al. (1977) (see figure 2.3a). These approaches were pioneering for the era using perfectly plastic ice based on Nye's (1952) equations to reconstruct the ice sheet to fit an empirically reconstructed boundary. These early models assumed a constant basal shear stress of 100 kPa. As a consequence of using simplified ice physics, these models did not recreate ice streams (Boulton et al., 1977; Sugden et al., 1977). This was largely in line with conceptualisations of ice sheets at this time being made up entirely of sheet-flow; the importance of ice streams had not yet been appreciated. Despite the lack of very fast ice flow both Boulton et al. (1977) and Sugden et al. (1977) recreated the lobate form of ice stream termini. Significantly, these simulations were conducted at a time when current glacial understanding of mid latitude palaeo-ice sheets was that they were much thicker, similar in surface elevation to their contemporary counterparts in Antarctica and Greenland (Boulton and Hagdorn, 2006). Under such assumptions a thick Scottish Ice Sheet (approximately 30% thicker than current estimates) was needed to create the observed ice extent. Thanks to subsequent glacial isostatic adjustment modelling, and an appreciation that ice streams can help achieve large extents with low surface ice slopes, we know this is not likely to be the case for the BIIS or other palaeo mid latitude ice sheets, which were much thinner and had lower angled surface slope than their high latitude counterparts (Shennan et al., 2006).

The next incremental improvement in numerical modelling of the BIIS came from Boulton in 1991 (see figure 2.3b). A particular innovation of this work was the use of varying basal shear stress in offshore regions. Boulton et al., (1991) used comparatively high basal shear stresses by modern standards of 70 kPa for onshore regions and 30 kPa for offshore regions. This simulation did not allow the margin to migrate and instead used a prescribed ice margin derived from empirical observations (Boulton and Hagdorn, 2006).

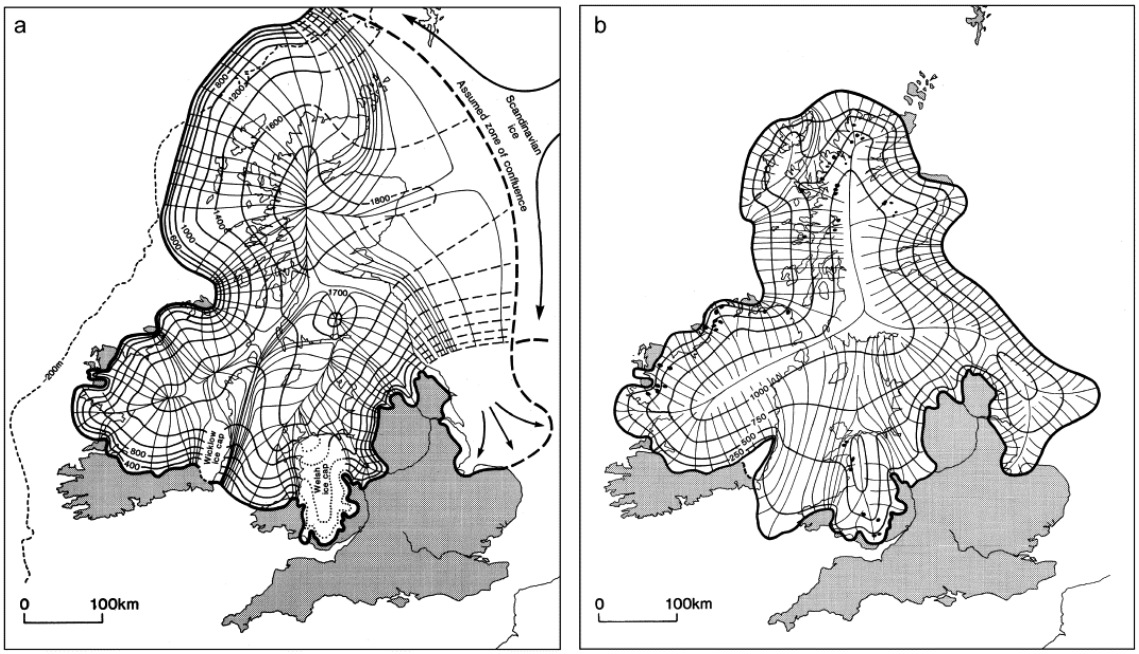

Figure 2.3: Early numerical models of the BIIS. 2.3a The first numerical ice sheet model reconstruction of the BIIS modified from Boulton et al. (1977). A constant shear stress of 100 kPa was used. 2.3b shows Boulton et al. 1991 numerical model with different shear stresses onshore (70 kPa) and offshore (30 kPa). Both modified from Boulton and Hagdorn (2006).

The next major advance in model reconstruction of the BIIS came in Boulton and Hagdorn (2006), where their used a variety of climate and physics led approaches to reconstruct the ice sheet. Here, they varied (tuned) input parameters to best match empirical observations of the ice sheet. A number of model runs were conducted exploring the significance of varying climatic and basal conditions. A particular innovation of this work was the use of varying basal shear stress in ice stream locations (marine troughs), by up to an order of magnitude. The modelling utilised a new method of thermomechanically solving ice flow mechanics. This work in many ways set a precedent for the future modelling of the BIIS further highlighting the dynamic nature of the ice sheet.

The next major step forward in reconstructing the BIIS came in 2009 when Hubbard et al. (2009) published the first higher-order enhanced SIA numerical ice sheet reconstruction. By using higher order ice physics to solve longitudinal (membrane) stresses to reproduce ice stream dynamics, Hubbard et al. (2009) were able to recreate more realistic ice streaming. Hubbard et al. (2009) paired the computationally expensive zones of high longitudinal stresses with a traditional SIA model so as to balance computational efficiency with physically realistic results. Thanks

to these compromises, Hubbard et al. (2009) were able to run an ensemble of 350 model runs. This work also introduced the use of systematic model data comparison for the BIIS. Hubbard et al. (2009) used a version of Automated Flow direction Analysis (AFDA) (which is discussed in more detail in chapter 3) to perform their model data comparison and filter out poorly performing models (Li et al., 2007).

Zooming in, Patton et al. published a series of papers first modelling the Welsh Ice Cap, (2013a; 2013b), and later modelling the entire Eurasian Ice Sheet complex (2016; and 2017). Significantly the modelling of the Eurasian Ice Sheet was one of the first numerical ice sheet model which successfully reconstructed the joining of the BIIS and the Fenno-Scandinavian Ice sheet (FIS) (Siegert et al.,2001; Patton et al., 2016). The model used to reconstruct the BIIS and the EIS by Patton et al (2013a; 2013b) did not allow for the build up of ice shelves, although did account for ice sheet calving. Despite modelling the complex confluence of the BIIS and the FIS, Patton et al. (2016) did not succeed in reconstructing the full extent of the Norwegian Channel Ice Stream.

The complexities of ice streams still posed issues with reconstructing the last BIIS. Ice streams were the focus of the work of Gandy et al., (2018; 2019; 2021) who used the higher order ice sheet model BISICLES with an improved subglacial hydrology model. They utilised the L1L2 physics from the Full Stokes equations to calculate membrane stresses (Kirchner, 2011). In this series of papers, Gandy et al. looked to test key ingredients required for ice streams to form in the correct places. Initially they explored the marine ice sheet instability hypothesis on the BIIS, at the Minch Ice Stream in Northwest Scotland, finding the importance of ice shelf buttressing which was previously omitted from modelling of the BIIS (Gandy et al., 2018). Gandy et al. (2019) looked at the ingredients needed for the positioning of ice streams in the BIIS finding bed topography and marine margins to be key. Unlike previous modelling efforts which have aimed to accurately reconstruct the BIIS, Gandy et al. (2019) used an idealised glacial cycle (climate) aiming to use the BIIS as an experimental laboratory, rather than recreating realistic simulation of the past. Most recently Gandy et al. (2021) modelled the build-up and collapse of the BIIS over the North Sea using a model ensemble suite of 70 runs and used AFDA (discussed in more detail in chapter 3) to assess how well modelled ice flow recreated empirical records from drumlins.

The most recent ice sheet modelling reconstruction of the BIIS comes from the culmination of the BRITICE CHRONO project. The Parallel Ice Sheet Model (PISM) (Winkelmann et al., 2011) was nudged to fit the empirical ice extent margins (see figure 2.2) to yield a combined empirical and model physics simulation of the ice sheet history (Clark et al., 2022). Figure 2.4 illustrates several time slices from the BRITICE

CHRONO model simulation. Further experiments using the same model, this time as part of a 600 ensemble runs not nudged to fit empirical ice extents, but instead varying in extent as a result of climate and model set up (Ely et al., in prep.) These model runs are the focus of the remainder of this chapter.

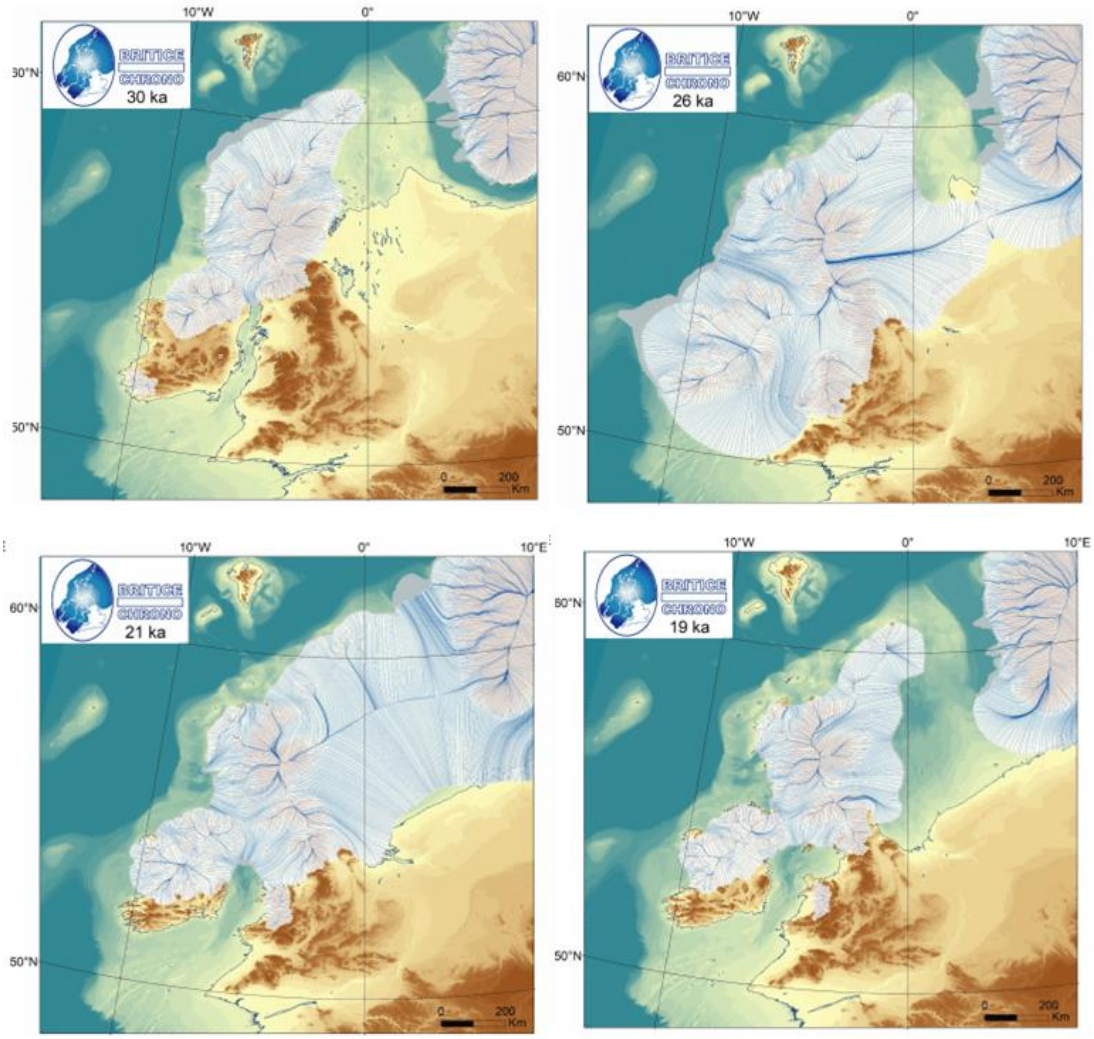

Figure 2.4: Nudged numerical reconstruction of the BIIS. Modelled ice extent and ice flow direction (indicated by blue flowlines) for 30, 26, 21 and 19 ka are nudged to empirical observations of ice extent.

2.3 - Numerical modelling of the British-Irish Ice Sheet in PISM

Numerical modellers of palaeo-ice sheets are faced with a complex balancing act: weighing the computational expense of the simulation vs accounting for the inherent uncertainty in how the past played out and the specific model set up parameters. The model user can choose to run a single simulation using a computationally expensive model of the best estimate model parameters and climate conditions (e.g. Boulton and Hagdorn, 2006). The advantage of such an approach is being able to use a computationally expensive model environment (e.g. at high spatial resolution), with the disadvantage that you may make a mistake in choosing your model parameters. The alternative, which is becoming increasingly popular is to run a large number of less computationally expensive simulations called an ensemble, with a range of plausible input parameters so as to see which best represents past glacial conditions (e.g. Hubbard et al., 2009; Gandy et al., 2021). This is possible because when reconstructing past glacial activity, we have records (and reconstructions) of what the ice sheet is believed to have done which we can compare against. This allows us to learn what elements (or parameters) an ice sheet model needs to correctly recreate. This ensemble approach is what has been taken by Ely et al. (in prep.) and from which model simulations are selected in this thesis.

PISM is an open source 3D numerical ice sheet model (Bueler and Brown, 2009; Winkelmann et al., 2011). Unless otherwise stated all model outputs shown in this work were generated using PISM version 1.2. PISM is a hybrid Shallow Ice Approximation and Shallow Shelf Approximation (SIA/SSA). SIA/SSA models use two simplifications of ice sheet flow, one for grounded ice and one for ice shelves, to provide improved ice sheet realism over purely SIA models (see figure 2.5). Use of these hybrid SIA/SSA approaches allow the modeller to have a shelfy-streamy area which has been shown to be important in creating marine terminating ice streams (Bueler and Brown 2009). In addition to using this hybrid model approach, PISM also allows for subglacial hydrology and till modelling. When combined with the highly parallelised approximation-based approach these factors allow PISM to perform well compared to significantly more computationally expensive models at a fraction of the computational cost of a higher order model. A combination of low computation cost, and high fidelity mean PISM is a widely adopted tool for modelling ice sheet scale

processes. Having been extensively used in experiments on both palaeo and contemporary ice sheets (e.g. the Laurentide (Gowan et al., 2023), Greenland (Zeitz et al., 2021) and Antarctic (Albrecht et al., 2020)).

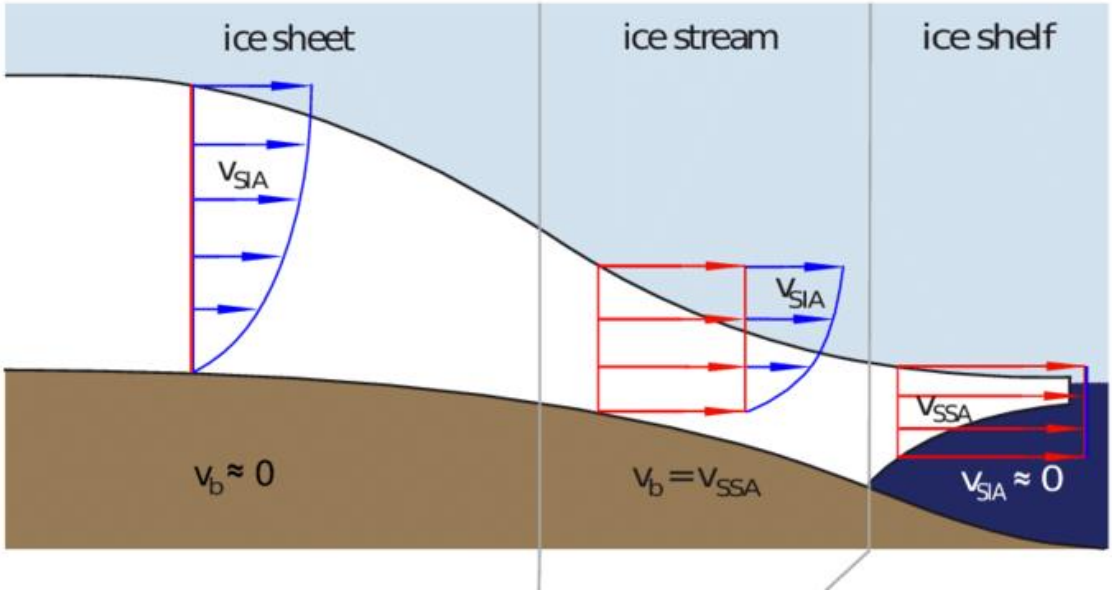

Figure 2.5: Idealised SIA-SSA interaction. Modified from Winklemann et al. (2011) showing how SIA (blue arrows) and SSA (red arrows) are applied in isolation and in combination to produce varying ice velocities using one of both ice flow laws.

2.3.2 - Modelling approach: Ensemble and best estimate

All numerical ice sheet models used in this work were produced by Jeremy Ely as part of Clark et al. (2022) or Ely et al. (in prep). These can be split into two classes: i) best estimate or nudged models (Clark et al., 2022); and ii) model ensemble reconstructions (Ely et al., in prep).

2.3.3 - Best Estimate (BC) Model

This thesis uses and references the BC model simulation. This is a best estimate model produced to match the empirical isochrones from BRITICE-CHRONO (Clark et al., 2022). The BC model run is a PISM model simulation based on a set of ensemble parameters which performed well in model data comparison tests (Ely et al., 2019a; Clark et al., 2022). This method has the benefit of being able to be run at a higher resolution than the ensemble runs as the model user already has a good estimate of what the best model parameters are for recreating ice extent. The model

run used a numerical ‘nudge’ to fit specific extents at specific times. Using this approach, key margins can be met, obtained by decreasing ice extent by inducing additional melt at the margin.

The process of generating the BC model simulation is outlined, and more details are available in Clark et al. (2022). The approach is iterative in an attempt to get both the ice extent and ice thickness correct, while also accounting for glacial isostatic adjustment (GIA), sea level changes and ice streams and shelves. First, ICESHEET 1.0 a computationally cheap, plastic-ice flow, numerical model, developed by Gowan et al. (2016) was used. This model computed a static ice sheet that exactly fits the optimum extent defined by the empirical reconstruction. There is no climate forcing it is merely a steady state, plastic ice sheet model. Variations in basal shear stress were explored such that the ice mass reasonably recreates the sea level and GIA constraints (Bradley et al., 2023). At each 1 ka timestep these ice elevations were input to the more physically realistic PISM model driven by a more realistic climate field. The PISM simulation could then extend beyond the empirical limits (dictated in ICESHEET 1.0). When the ice sheet exceeded an empirically derived margin, additional melting was applied locally to encourage the margin back within the empirical extent for that time period. Similarly, the ice shelf melt rate and calving rate were varied through time to encourage the ice to extend to known dated marine margins at key times.

This nudging capability must be used sparingly so as not to significantly alter the ice flow in the interior for perhaps the wrong reasons. To achieve rapid variation in ice flow, the PISM simulation is restarted every thousand years, causing a stop-start modification to the internal ice flow. Although this is not apparent for certain applications, this would likely reduce the model users ability to use some of the model data comparison tools discussed in Chapter 3 and to observe subglacial processes (e.g. chapter 4); the model is designed to produce 1000-year snapshots, rather than a fully transient simulation. At this stage it seems important to reiterate the opening rhetoric of this chapter, there are inherent issues in all models, but this doesn’t remove their usefulness in the right applications.

The nudged approach used in the BC model is useful for approximating certain attributes of the BIIS, such as mass loss, the location and velocity of ice streams, timings of glaciation and for general visualisation of the ice sheet. As with all models this method is ‘wrong’ but highly useful for certain uses as it represents in many ways, the best estimate of what the ice sheet was like. Despite aligning well with empirical

observations of ice extent, this work does not use the BC model as its primary model run, because the nudged approach introduced a number of undesired artefacts. Ideally for comparison of modelled flow geometry with drumlins and erratics we need model simulations optimised for flow geometry rather than just ice extent.

2.3.4 - PISM ensemble approach for optimising flow geometry

Two hundred ensemble runs of PISM driven by climate and sea level fields and unconstrained by empirical data were conducted by Ely (in prep.) and provided for use in this thesis. The model runs were conducted at a 5 km spatial resolution with results recorded at 100-year intervals. Input parameters for the models were sampled from a range of variables outlined in table 2.1 using a Latin hypercube sampling technique. The models were run on a 5 km palaeo bed topography from a quasi-coupled GIA model, where the bed is altered every 1000 years (Bradley et al., 2023).

Ice motion in PISM is derived from internal deformation and sliding. Internal ice deformation (ϵ) is calculated using the Glen-Paterson-Budd-Lliboutry-Duval flow law:

$$\epsilon_{lj} = E\, A(T,\omega)\tau^{n-1}\tau_{i,j} \qquad (2.1)$$

Where E is the ice flow enhancement factor, A is the ice softness (which is related to the ice temperature (T), and liquid water fraction (ω)), τ is basal shear stress imposed on the ice and n is Glen's flow law exponent. The ice flow enhancement factor E is varied between each model ensemble run to account for uncertainty of other parameters. Changing the value of E allows the ice to be more or less deformable. The same value for E is used for both the SIA and the SSA calculations.

Basal sliding is calculated using a pseudo-plastic sliding law which relates basal shear stress τ_b to the sliding velocity of grounded ice (u_b) in the SSA. In PISM sliding only occurs when basal shear stress (τ_b) exceeds the basal yield stress (τ_c).

$$\tau_b = -\tau_c \frac{u_b}{u_0^q |u_b|^{1-q}}, \qquad (2.2)$$

The grounded ice velocity is modelled in a non-linear manner due to the exponent constantly remaining below 1 in the 200 model ensemble members used in this work. All parameters used for, PISM set up are outlined in table 2.1.

Table 2.1: Parameters used for model ensembles modified from Ely et al (in prep). Each parameter was selected using a Latin hypercube from the parameters space. MR 400-500 use a sliding regime defined by the basal till friction, whilst MR 500-600 use a prescribed sliding regime. The parameter ranges were reduced from an initial 400 simulations conducted at a lower horizontal resolution. All model ensembles considered in this work are forced by the GRIP ice core record.

	Parameter name	Main effect	Value range
Ice Physics	Ice flow enhancement factor (E)	Deformation rate of the ice	0.53 to 1.46
	Sliding law exponent (q)	Rate of basal sliding	0.001 to 0.663
	Maximum water thickness in till (m)	Rate of basal sliding	1.1 to 4.9
Climate	Temperature offset (°K)	Ice sheet size and ice temperature	-1.53 to 2.92
	Precipitation offset (%)	Ice sheet size	74 to 146
	Positive degree day factor for snow (m/a)	Ice sheet size	0.0026 to 0.0030
	Positive degree day factor for ice (m/a)	Ice sheet size	0.0056 to 0.0082
	Forcing factor	Constraint to empirical reconstruction	0.0005 to 0.0030
Ocean	Calving thickness threshold (m)	Ice shelf extent	68.6 to 171.6
	Subshelf melt factor	Ice shelf extent	0.002 to 0.048

Four methods of assigning basal yield stress were tested in the initial 600 run model ensemble, but only two methods of assigning the basal yield stress are used in the numerical ice sheet models used for this work (Ely et al., in prep.). These are prescribed yield stress and the prescribed till friction. The first method uses a map to prescribe a yield stress value for each pixel based on characteristics of the palaeo glacial bed. Five categories of yield stress were used, which are, from lowest to highest value: i) palaeo-ice streams reported in the literature (Gandy et al., 2019); ii) marine sediments; iii) thick sediments, as indicated by the occurrence of drumlins and on sediment thickness maps; iv) discontinuous sediment, as indicated by subglacial ribs and on sediment thickness maps; and v) bedrock, as indicated by sediment thickness maps and the characteristic rough surface evident on DEM's (see table 2.2, Pollard et

al., 2023). The second method uses a map of prescribed till friction angles (see table 2.2). Other methods were explored in the initial 400 ensemble members but were deemed unsuitable for further investigation in the ensemble (Ely et al., in prep). To calculate yield stress, the till friction angle (ϕ), till cohesion value C_0, and effective basal pressure (N_{till}) are used in a Mohr-Coulomb criterion:

$$\tau_c = c_0 + (tan\phi)\, N_{till} \qquad (2.3)$$

To calculate N_{till} the following basal hydrology model is used to calculate water thickness (W).

$$\frac{dW}{dt} = \frac{m}{\rho w} - C \qquad (2.4)$$

Where m is the basal melt rate, ρw is the density of water and C the rate of water drainage from the till. This model does not allow for lateral transfer of water, or conservation of water once a water thickness exceeds the set value in table 2.1. This second method of calculating the yield stress uses equation 2.3, with values of ϕ prescribed according to the same categories as the prescribed shear stress map (see table 2.2).

Surface type	Prescribed τ_c, experiment 1 (kPa)	ϕ for experiments 2 (°)
Palaeo-ice stream	20	12
Marine sediment	25	15
Drumlins	60	20
Subglacial ribs	90	25
Bedrock	130	30

Table 2.2: Prescribed values for τ_c and ϕ based on geomorphological classification of landforms (Pollard et al., 2023; Ely et al., in prep).

Climate is the largest unknown when hindcasting palaeo-ice-sheets (Clark et al., 2012; Stokes et al, 2015). In PISM, climate is represented by a variety of spatially continuous input fields and offset parameters. These can be conceptualised as maps of

a parameter (e.g. precipitation), which can be varied over time, from a climate record (e.g. an ice core), with a predefined relationship. The model ensemble used throughout this work employs a novel climate field produced in Ely et al. (in prep). This climate field is produced using an iterative process of GIA corrected model runs. To create this climate field, PIMP 3 scenarios (Barconnot et al., 2012) were used in conjunction with a simple 1D ice sheet simulation fitted to the empirical reconstruction of Clark et al. (2022) using ICESHEET 1.0 (Gowan et al. 2016). By comparing PIMP3 with a palaeo surface topography temperature and precipitation fields were produced at 1000-year resolution. A bespoke index was produced for each 1000-year climate field to calculate sub millennial variation in parameters based on the NGRIP record. Furthermore, each simulation had a temperature and precipitation offset randomly selected between the ranges described in table 2.1.

2.4 - Summary

This section has outlined the history of modelling and reconstructions of the BIIS specifically drawing on how empirical evidence has become increasingly powerful in informing model input and outputs. The key take home from this chapter is numerical models are more advanced than ever, however, they are still not perfect and decisions must be made by the model user so as to best use the (model) tools at our disposal. It has been outlined as to how a physically sophisticated ice sheet model (PISM) was nudged to fit empirically defined margins (the BRITICE CHRONO model simulation), and how more freely varying (not nudged) ensemble runs were used to build an ensemble of 200 simulations. Some of these runs are likely to better capture the flow geometry of the ice sheet and will be used later in this thesis.

Chapter 3 - Evaluating ice sheet model ensemble simulations against observed indicators of flow direction and ice extent

3.1 - Introduction

No ice sheet simulation will ever be a perfect replica of the past. This is the reality of attempting to reconstruct complex landmass scale phenomena (such as an ice sheet) given the vast range of uncertainties in ice sheet and climatic processes paired with real world computational constraints (Kageyama et al., 2012; Osman et al., 2021). Numerical ice sheet modelling is therefore a constant balance of attempting to optimise uncertainty in parameters with the computational expense of the modelling process (Stokes et al., 2015; Ely et al., 2021). In an effort to address this, modellers sometimes look to use a range of plausible input parameters so as to recreate many possible variations of the past glacial environments (Tarasov and Peltier, 2004; Boulton and Hagdorn 2006; Jamieson et al., 2012; Patton et al., 2016; Ely et al., in prep). Perturbed parameter ensembles allow for the range of uncertainty in input parameters to be simulated and accounted for, before running numerical reconstructions of ice sheets (see chapter 2). The consequence of running model ensembles (in contrast to single best estimate simulations) is that the model has multiple outputs. In the case of the BRITICE-CHRONO project, 200, 5 km resolution, model outputs were produced (section 2.3.4). The challenge then becomes selecting model runs which represent the best compromise for the specific questions posed of a past ice sheet. This is where mode-data comparison is needed.

Given empirical ice sheet reconstructions existed long before numerical models, it is unlikely any numerical ice sheet reconstruction has been conducted without some degree of model data comparison taking place. In many cases, this may be as simple visually comparing a model output against an empirical reconstruction. Increasingly however, this comparison against empirical data is becoming a key element of the modelling process, particularly since the move towards ensemble modelling simulations (discussed in chapter 2). This is because ensemble modelling usually relies on being able to distinguish between resulting end members, so as to select the most appropriate simulation. The process of eliminating poorly performing model runs is called sieving. The aim of sieving is to ‘rule out’ models for being implausible, gradually

decreasing the list of models ‘not ruled out yet’ (NROY) until a sufficiently small selection of realistic model outputs are curated for the model users' intended observations or analysis. When curating a list of NROY reconstructions, modellers use evidence of how a modelled ice sheet is believed to have behaved to rule out unrealistic model simulations. A variety of glaciological metrics have been used to assess glacial model quality (Ely et al., 2021), including but not limited to ice extent (e.g. Napieralski et al., 2006; Jamieson et al., 2012), ice flow direction (e.g. Li et al., 2007), ice thickness (e.g. Jouvet et al., 2017), glacial isostatic adjustment (GIA) (e.g. Tarasov and Peltier, 2004) and ice volume (e.g. Gregoire et al., 2016).

The sieving process begins simply by asking what is the intended use of the model simulation? This is crucial to framing the question: ‘what makes a good model simulation?’ and therefore the process (or tests) used to identify such a model simulation. In this thesis, I look to understand the relationship between ice sheet flow geometry and glacial processes (such as erratic transport and drumlin formation). Therefore, ice sheet geometry (e.g. flow direction and extent) is the most important modelled characteristic for this work. For this I ask the questions: does the modelled flow geometry align with observed flow geometry (see figure 3.1a)? This chapter outlines how this can be scaled and used for sieving 200 model ensemble components. I use indicators of flow direction (drumlins) (see figure 3.1a) and ice extent (moraines) to identify which models best represent the empirical data, so as to answer the following question: Which ensemble simulation best recreates ice flow geometry? I do this both to select a model ensemble member for use in subsequent chapters, but also so as to extract the modelled ice conditions associated with that period of model data match for subsequent use in chapter 4 (see figure 3.1b).

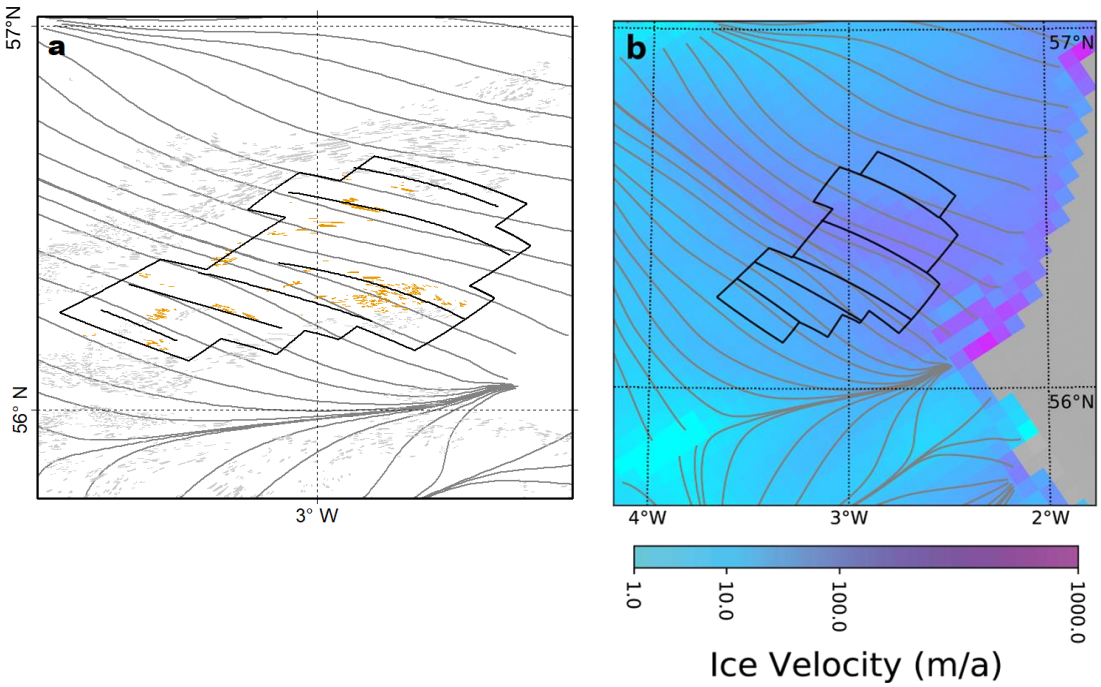

Figure 3.1: Example of data and modelled ice flow geometry comparison workflow. 3.1a shows a drumlin flowset. Lineated observations are coloured based on flow regime (Orange) with observations not considered in this flowset in grey. 3.1b shows lineated observations compared against model output. Both a and b show modelled flowlines produced from the simulation in b (grey lines).

3.1.1 - Model-data comparison for ice sheet flow geometry

Ice sheet geometry is a function of regional variations in inputs, outputs, and rates of ice movement (e.g. velocity). Some of these metrics can be testing for sieving, whilst others require proxies to infer their rate of change. In an ideal world one model simulation would clearly perform best in all model-data comparisons. In reality, achieving this is improbable given the computational limitations and climatic uncertainties which affect ice sheet modelling (Ely et al., 2021). Therefore, as more levels (tests) are added to the sieving process increasing compromises are met with regards to performance in some metrics so as to match other metrics. Hence, a conscious and deliberate choice must be made as to which metrics are most important for the desired simulation use. This will therefore inform which and how many tests are used for sieving. With this in mind, here I briefly review three ways of constraining ice sheet geometry which are ice flow direction, ice extent, and approximation of ice mass.

Perhaps the most common metric used in model data comparison is ice extent. The first uses of ice extent in numerical ice sheet modelling were using margins from empirical reconstructions as a static ice extent to reconstruct ice surface geometry (e.g. Boulton, 1977). However, as numerical ice sheet models began to derive their own ice

extents, model users began to compare these modelled extents against those from empirical extents. Initially this process consisted of visually comparing the margin location of a numerically modelled ice sheet with known moraine systems (Sugden et al., 2002; Boulton and Hagdorn, 2006). As numerical ice sheet modellers began to produce larger model ensembles, the need for quantifiable methods of comparing against ice sheet extent, which could readily be automated emerged (Napieralski et al., 2006; Jamieson et al., 2012; Patton et al., 2016; Jouvet et al., 2021). Broadly speaking these methods either consider the margin as a line or a point. Point based margin matching benefits from being computationally simple to implement, by measuring the distance between the ice margin, and the known palaeo margin. Jouvet et al. (2022) for example, measures the distance along a central flow line from the modelled margin to the observed palaeo margin. Jamieson et al. (2012) adopt a similar approach using marine grounding line wedges to estimate retreat of the Marguerite Trough Ice Stream. Both these studies in essence use a 1D approximation of the margin position measured along a central flowline to give a measure of model data fit to ice extent. This flowline method works well in a topographically confined valley setting, but is difficult to successfully implement at the margin of a topographically unconstrained ice sheet. Another method is therefore to use the entire moraine as a line demarking the known palaeo margin. This approach could be seen as preferable when looking to constrain ice extent in areas of low topographic relief and high observational confidence. The difficulty with considering an entire margin is it requires more than a single measure of distance along a flow line - the margin has a 2D shape. Napieralski et al. (2006) developed a tool to account for this issue called Automated Proximity Conformity Analysis (APCA).

Ice extent can also be considered in terms of timing of occupation. This is increasingly becoming a powerful concept in assessing how well a numerical ice sheet simulation hindcasts a palaeo-ice sheet as it allows a test of the rate of change. Numerical dating can either be paired directly with a moraine complex, or at times simply provide a time for when a point on the map needs to be ice free (e.g. Jouvet et al., 2017). As with ice extent, initially this ‘test’ would simply be done by eye, by asking, is the maximum extent consistent with dates for the extent? As margin matching becomes automated, age constraints can also be included to ensure appropriate timing of margins matching is also met (i.e. match the maximum extent, then the retreat extent, rather than vice versa) (Ely et al., 2019b). In such a process a Bayesian age model can be fitted to the retreating moraine complexes so as to incorporate

knowledge of chronology of model/data fit into the retreat pattern (e.g. Chiverrell et al., 2013).

Ice sheet flow direction is not frequently considered when sieving numerical ice sheet simulations. This is perhaps unusual when consider that glacial landforms are one the key components of traditional glacial inversion reconstructions (Kleman and Borgström 1996; Margold et al., 2013; 2015; Greenwood et al., 2008; Duffer et al., 2022). Subglacial bedforms for example have been proposed to indicate direction of ice flow and perhaps glacial conditions (such as thickness and velocity). This is particularly significant as the location of glacial catchments is in part defined by the surface topography which is highly challenging to approximate from other records and an important maker for a climate (see Chapter 1, cf. dome geometry response to climate). Despite being frequently acknowledged in the literature to be a useful tool for understanding ice sheet flow geometry, there are only small number of published works which compare palaeo indicators of flow direction with model outputs to rule out implausible model outputs (Hubbard et al., 2009; Patton et al., 2016; 2017; Gandy et al., 2019; 2021; Ely et al., 2021). Comparison of flow direction to modelled ice have historically been conducted using the Automated Flow Direction Analysis tool (AFDA) (Li et al., 2007).

Several methods of estimating a palaeo-ice sheet mass exist and have been used in numerical ice sheet simulations. These approaches primarily revolve around three metrics: the GIA signal of the earth's crust (e.g. Bradley et al 2023); the relative sea level (e.g. Tarasov and Peltier 2004; Gregoire, et al., 2016); and the ice thickness using empirical observations (Mas e Braga et al., 2021). In reality, most methods involve a combination of two or more of these tools in conjunction. The challenge with using ice mass as a sieving criterion for ice sheet geometry is establishing the spatial relationship between ice sheet geometry and total ice mass. I see ice sheet mass therefore as an important sanity check of a plausible ice thickness for eliminating model runs, rather than identifying model runs that have a suitable ice flow geometry.

3.2 Empirical indicators of ice sheet geometry

In this thesis, I use observations of flow direction to test the fidelity of palaeo ice models to reconstructed geometry. I use the term observed indicators of flow direction as a catch-all term to describe glacially lineated bedforms which can be observed using

remote sensing and that form parallel to ice flow. Significantly, this definition excludes subglacial ribs which form perpendicular to ice flow (e.g. Dunlop and Clark, 2006). Observed indicators of flow direction can broadly be split into three classes: sediment, bedrock, and hybrid. Sediment bedforms are primarily drumlins and MSGL. Hybrid bedforms are predominantly crag and tails. Bedforms in the final category are composed solely of bedrock (e.g. roche moutonnée, whalebacks and grooves). Most observations in this dataset were mapped as drumlins or undefined sediment lineations. I did not propose new regions observed indicators of flow direction, instead I used published shapefiles which provided complete cover of terrestrial areas (see figure 3.2) (Hughes, 2014; Greenwood and Clark, 2009a) supplemented by data of submarine areas where available. For these latter cases, it was necessary to georeference mapping and regroup flowsets (see table 3.1).

I used published mapping of lineated bedforms of Britain and Ireland included in the BRITICE project and conducted by Anna Hughes in mainland Britain (Hughes et al., 2014) and Sarah Greenwood in Ireland (Greenwood and Clark, 2009a). As part of the BRITICE project, mapping of Britain was classified into specific landforms (drumlins, ribs, MSGL) and grouped into flowsets (Hughes et al., 2014). Mapping and flowsets of the island of Ireland were taken from Greenwood (2008). Unlike flowsets from mainland Britain, lineated landforms in Ireland were not assigned specific landform types when mapped (with the exception of ribbed moraine). Lineations were therefore only classifiable as sediment or bedrock landforms. Both Sarah Greenwood and Anna Hughes used bedform context to ascertain the likely process associated with their formation. Specifically, they classified their interpretation of the stage of glaciation (e.g. advance or retreat), the certainty, and the style of event which likely produced the drumlin (e.g. a single isochronous event or a multi-phase transgressive event). For both Britain and Ireland I used the published flowsets, and only included flowsets which had been mapped as ‘isochronous’ (therefore thought to represent a single point in time) and ‘certain’ for model data comparison.

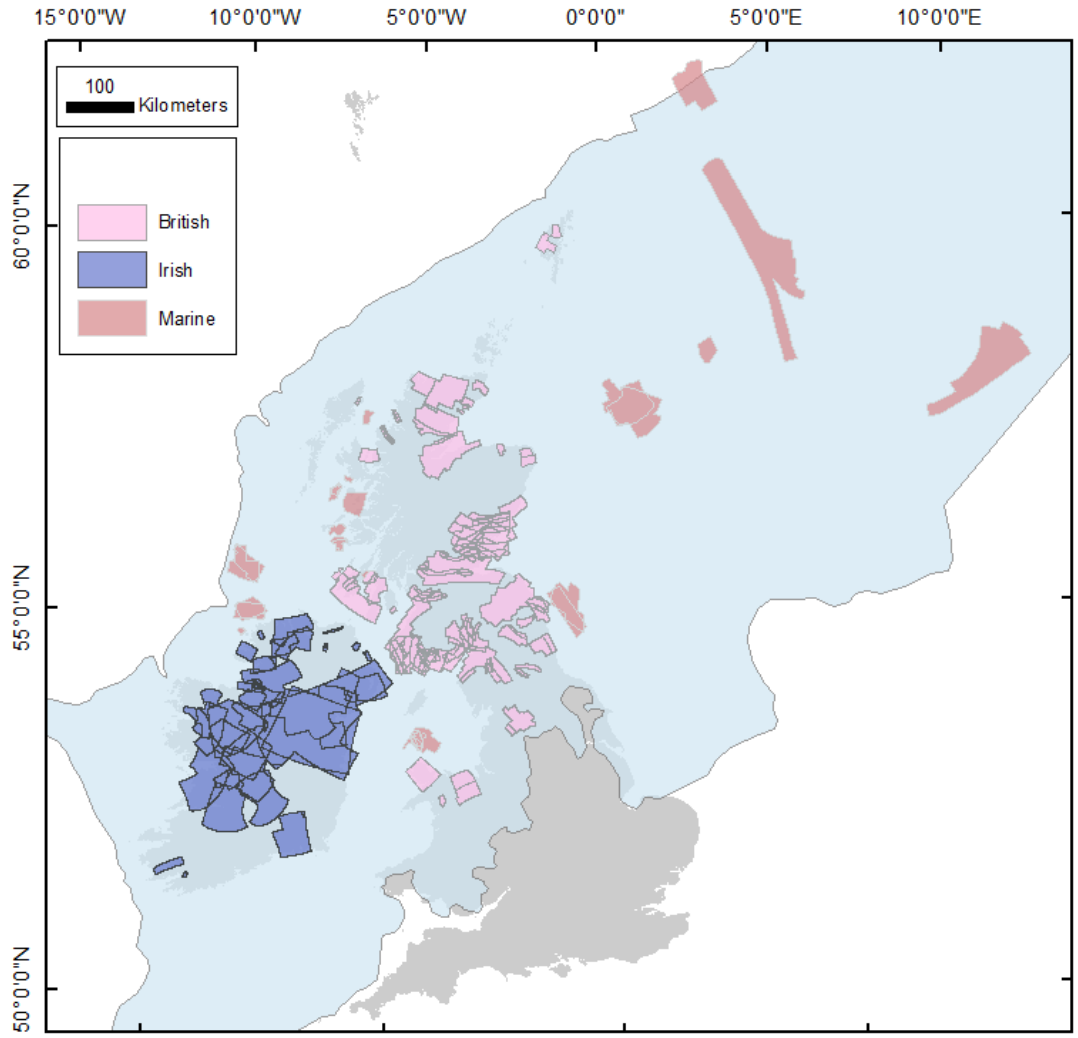

Figure 3.2: Map of flowsets used as indicators of ice flow direction. Irish flowsets mapped by Sarah Greenwood in blue, British flowsets in pink and marine flowsets compiled from the literature for this thesis in red (see table 3.1). Devensian maximum ice sheet extent in light blue.

No comprehensive mapping of the offshore lineated landforms of Britain and Ireland exists due to the lack of a sufficiently high resolution freely available bathymetric map. To improve the spatial distribution of indicators of ice flow direction I chose to incorporate published mapping of offshore lineated bedforms where available. Offshore bedforms primarily come from spatial discrete mapping based on privately purchased or collected bathymetric data (see table 3.1). Every endeavour was made to include all published work prior to the November 2021 census date. Only mapping explicitly published as lineated bedforms was included. All offshore data was georeferenced from published maps and flowsets were produced specifically for this project. Using this hybrid approach, it is hoped that flowset grouping will remain constant across the bathymetric flowsets. Given the low coverage of bathymetric data, it is likely that many more offshore flowsets exist.

Table 3.1: Supplementary offshore data sources. Bathymetry data used for mapping offshore indicators of flow direction off shore of Britain and Ireland. Observed landforms are included as well as the method of data extraction.

Area	Feature type(s)	Data type	Reference	Source
Norwegian Channel Ice Stream	MSGL	Georeferenced map from - bathymetry and 2D/3D seismic data	Ottesen, et al., 2016	https://doi.org/10.1016/j.sedgeo.2016.01.024
Moray Firth/North Sea lobe	Lineations	Georeference map from Bathymetry	Roberts, et al., 2019	https://doi.org/10.1002/esp.4569
Northwest Ireland	Drumlins	Georeferenced map - Bathymetry	Benetti, et al., 2012	https://doi.org/10.4113/jom.2010.1092
Irish Ice Stream	Ribs Drumlins and MSGL	Georeferenced map - Bathymetry	Van Landeghem, et al., 2020	https://doi.org/10.1016/j.quascirev.2020.106526
Malin Shelf	Drumlins	National Seabed Survey	Dunlop et al. ,2010	https://doi.org/10.1016/j.margeo.2010.07.010
Minch	Streamlined bedforms	Georeference map	Bradwell, et al., 2007	https://doi.org/10.1002/jqs.1080
Sea of Hebrides	Drumlins and streamlined bedforms	Georeferenced map - Bathymetry	Howe, et al., 2012	https://doi.org/10.1016/j.margeo.2012.06.005
Inner Hebrides	Bedrock and sediment lineations	Georeferenced maps - Bathymetry	Dove, et al., 2015	https://doi.org/10.1016/j.quascirev.2015.06.012
Minch	Streamlined bedrock, drumlins	Georeferenced map	Bradwell, et al., 2015	https://doi.org/10.1111/bor.12111
Norwegian Channel Ice Stream	MSGL, Lineations	Georeferenced map	Graham, et al., 2007	https://doi.org/10.1016/j.quascirev.2006.11.004

To check modelled ice extent I used moraine complexes mapped as part of regional reconstructions of the BRITICE-CHRONO project (Bradwell et al, 2021a; 2021b; Evans et al., 2021; Chiverrell et al., 2021; Scourse et al., 2021; Ó Cofaigh et al., 2021; Benetti et al., 2021). Only margins which could clearly be identified as ice marginal were included with minimal connecting of moraine features. Each moraine was assigned an age range using Bayesian age modelling from (Chiverrell et al., 2013, Scourse et al., 2021). This process resulted in 97 margin positions and geometries, which could be used to test ice extent (see figure 3.3).

The final resulting dataset used for sieving and model data comparison consisted of 121 isochronous flowsets and 97 margin positions with associated Bayesian age modelling chronologies.

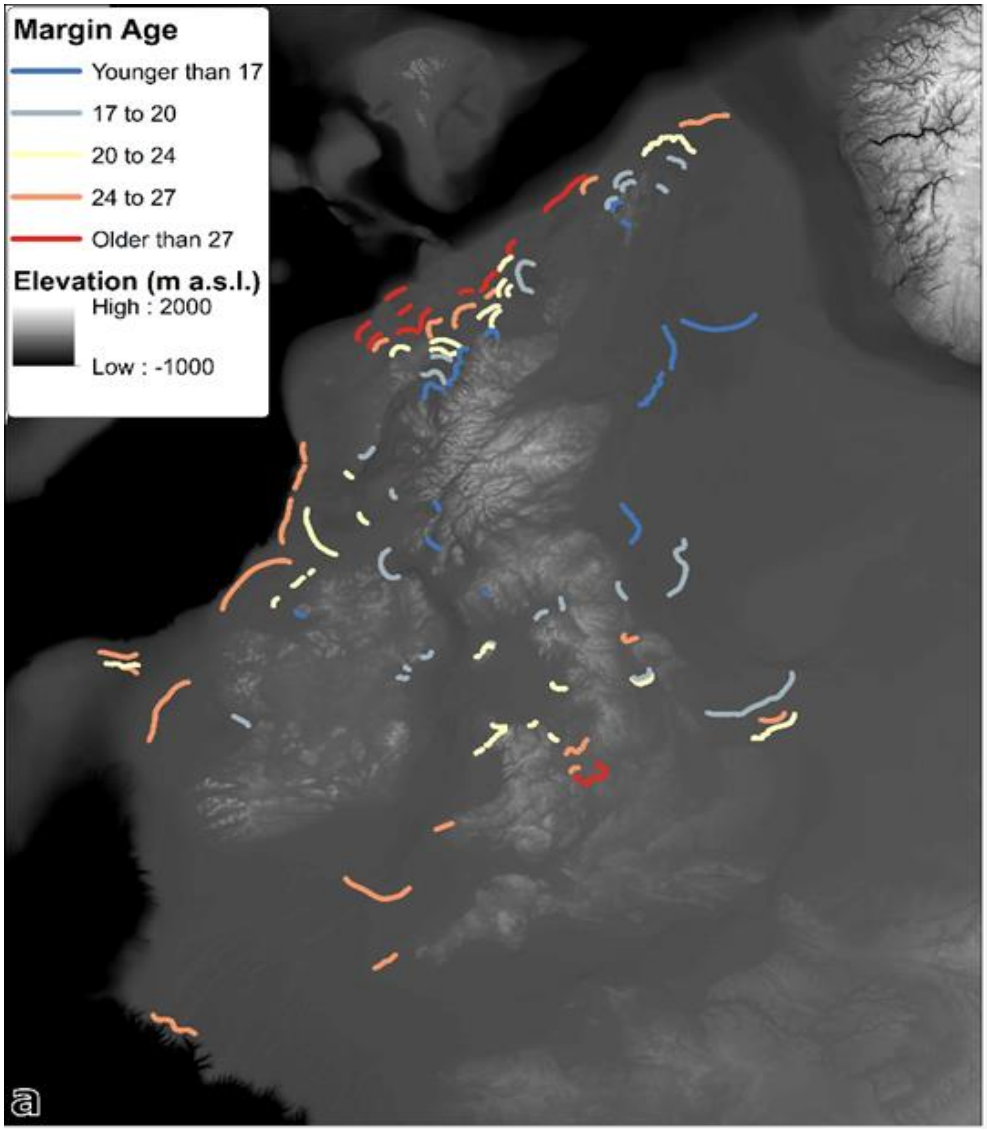

Figure 3.3: Bayesian moraines and ages. 97 moraines used for model-data comparison of the BIIS, figure modified from Ely et al. (in prep).

In addition to the data used for sieving ensembles an additional check was conducted against a model simulation nudged to meet ice extent and volume produced in Clark et al. (2022) (known as the BC model) and discussed in detail in Chapter 2. The BC model was nudged to meet ice thickness (mass) derived from Bradley et al. (2023). I use this as a final sieving pass to ensure my NROY simulations sit within reasonable thicknesses.

3.3 - Methods

The aim of this chapter is to use flow directional data and ice margin extent to sieve 200 model ensembles of the BIIS. Sieving was conducted with regards to the aim of this thesis which is to explore the relationship ice flow sheet geometry has with the palaeo glacial record. Two data driven metrics were chosen to select simulations deemed to be suitability for use in reconstructing erratic transport: 1) direction match to lineated landforms such as drumlins/crag and tails; and 2) margin match (to moraines). These tests are connected in parallel and combined for initial sieving. These criteria should produce a model simulation which can be used for inferring timing of ice parallel bedforms with a view of examining the modelled glacial conditions associated with these times (discussed in chapter 4). As a final check, I compare the ice thickness and volume of my NROY simulations against a GIA corrected best estimate model simulation which uses the same margin (discussed in chapter 2).

3.3.1 - Automated Flow Direction Analysis (AFDA) workflow

Flow direction analysis is the process of comparing observations of palaeo ice flow geometry against modelled flow geometry and scoring how well both align. I use AFDA to systematically perform and scores these comparisons. To perform analysis using AFDA observations of flow directions are grouped into synchronous clusters of landforms. These clusters are best estimates of representative flow events and are called flowsets (Clark, 1997). Each flowset is compared against each time step of each model simulation. This produces a score for each flowset, at each point in time (see Figure 3.4 and 3.5). AFDA is performed at the model resolution (5 km), meaning mapping of flow indicators is coarsened to match modelled resolution in some cases necessitating some generalisation of flow orientation (see Figure 3.4c&d). This generalisation provides advantages when considering ice sheet scale flow because minor directional changes around small topographic features are below the scope of SIA and this project. For each grid cell the angular offset between data and model is computed and forms the basis of quantitative matching score.

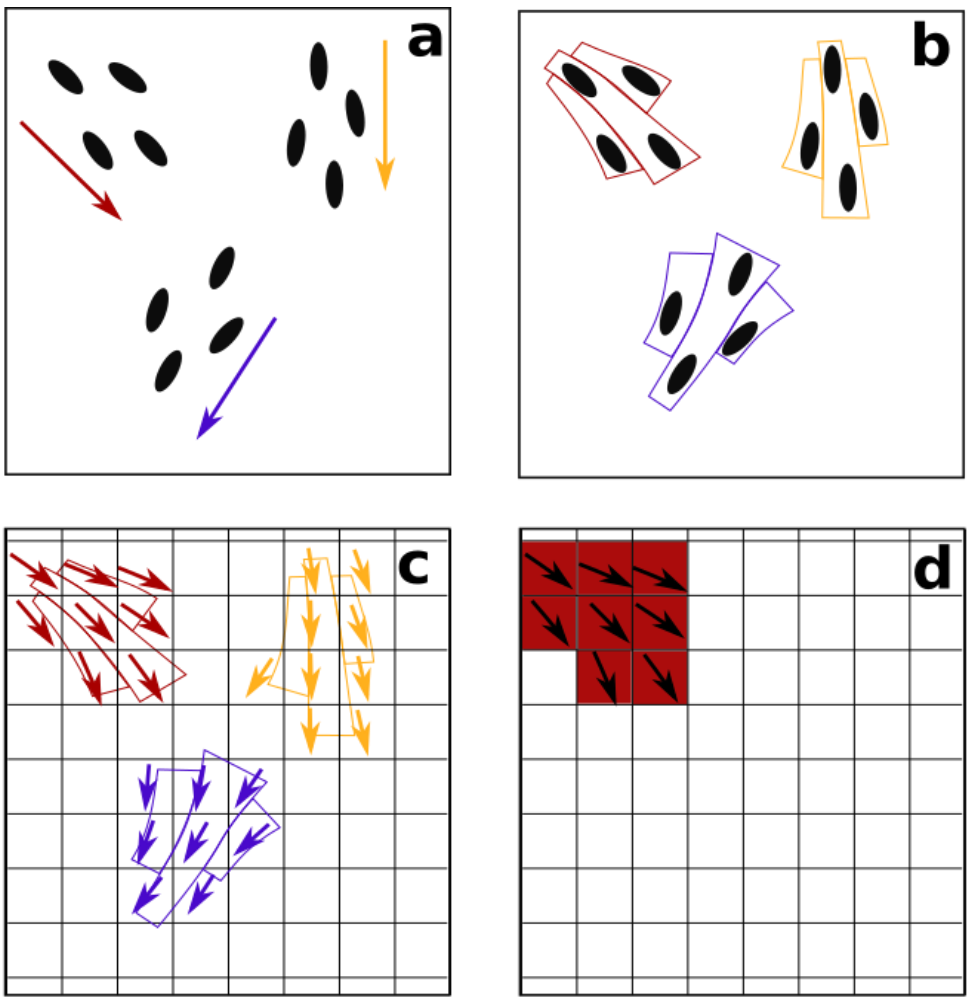

Figure 3.4: Preparing a palimpsestic drumlin record for model-data comparison. Converting observations of drumlins (a) into flowsets (b), then transforming to the model grid (c), and separating them out into individual arrays of cells that represent flowsets (d).

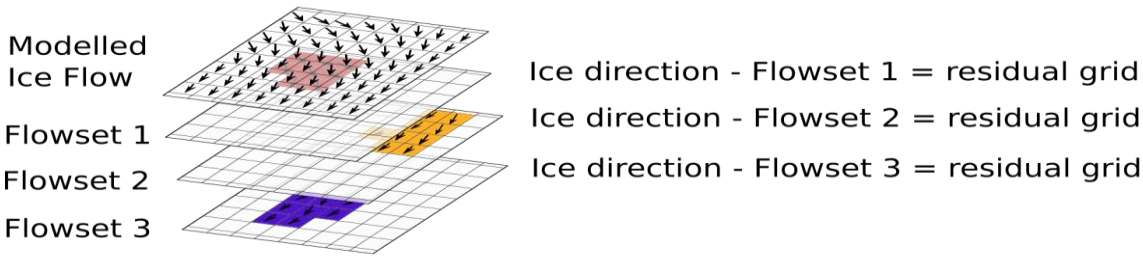

Figure 3.5: Idealised model data comparison in AFDA. Modelled ice flow at a particular time step is compared to a multitude of flow sets to ask which has the best match. AFDA calculates residual angles (between model and data) on a pixel-by-pixel basis to produce a residual layer documenting the angular difference between modelled directions and that in the flowset for each point in model time and space, for each flowset.

The scoring of a flowsets' match to the model is composed of two metrics: the flowset average angular offset, called the 'mean residual vector' and a measure of the match in shape of the flowset called the 'mean residual variance' (i.e. does the model form a converging ice stream when the data shows a diverging one? (see Figure 3.6)). A combination of these two measures allows for the differentiation between the model fidelity with an inferred direction (mean residual vector) and with the inferred flow field geometry (mean residual variance), as illustrated in Figure 3.6. This is important when used for examining the processes involved with bedforming. The mean residual vector can vary from 0 degrees which is the best possible match, to 180 degrees indicating the ice flow direction is reversed (see Figure 3.6). A mean residual vector of 90 degrees, for example, would mean ice flow was perfectly perpendicular to observations. The quality of the shape of the match is calculated as the mean residual variance (see Figure 3.6). High mean residual variance values mean a poor match in shape. In vector-space in Figure 3.6 (d, e & f) higher mean residual variance is visualised with a large area between the solid and dashed line meaning that there is a poor match in shape. A combination of both metrics helps understand a breadth of model data match types without having to plot maps. For example, figures 3.6a&d illustrate good model/data fit with low mean residual variance and low mean residual vector: the model simulated as converging ice flow, and the empirical observations also indicate flow converged. In contrast, the Figure 3.6 b & e have a similar residual vector (to 3.6a), but a higher variance due to the simulated diverging ice flow. The difference between 3.6a and 3. 6b would be minimal if considering mean residual vector alone.

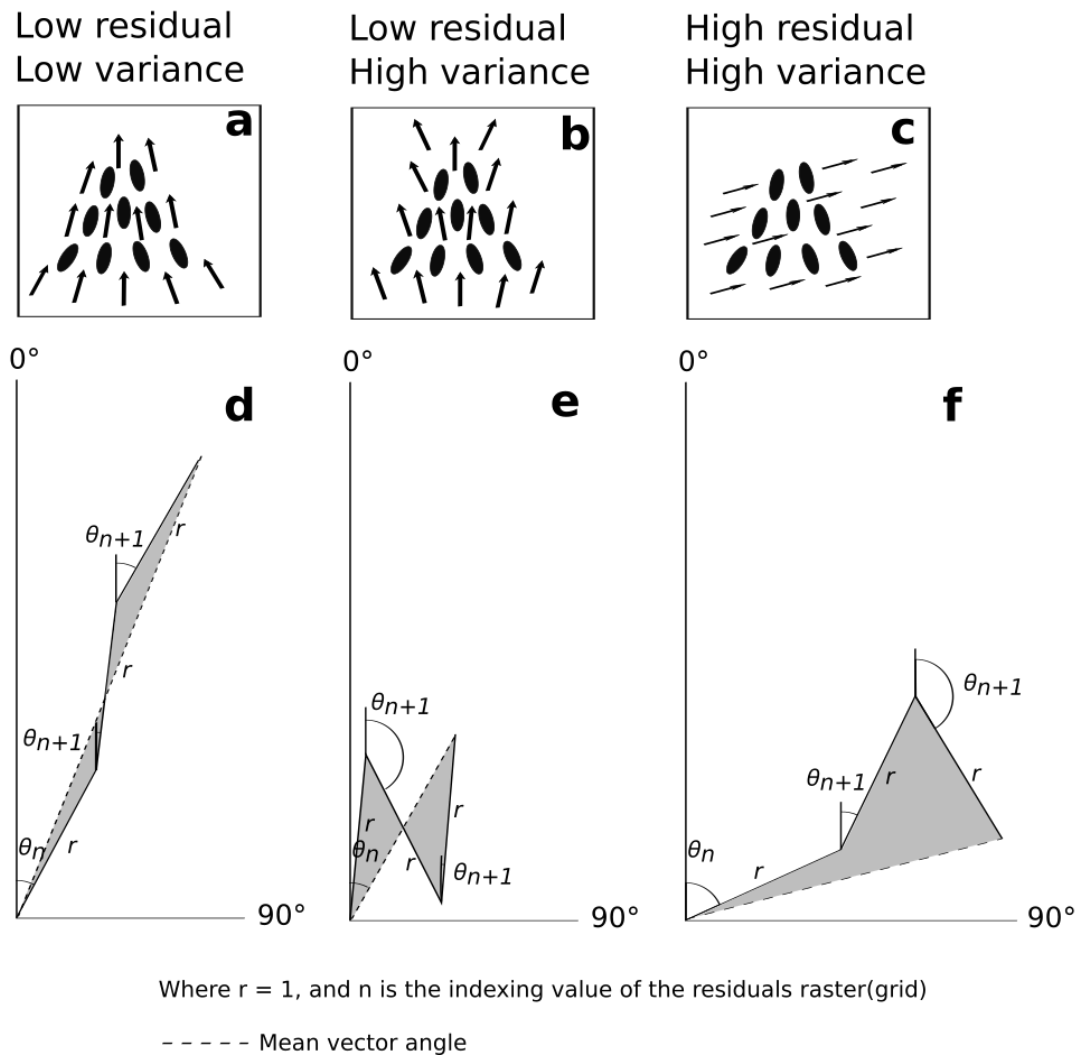

Figure 3.6: Idealised model data matches in AFDA. drumlins and modelled ice flow as arrows (a, b & c) for three cases to illustrate different degrees of matching in terms of both average angular offset and match of shape of flow set. In 'a' we have the best match and in c the worst (80 degrees off). In b however the general direction is good giving a reasonable angular offset score, but the shape match is poor. These two measures are computed using directional vectors, where each cell is visited in turn and the angular offset computed. Conceptually these are then plotted as in d, e & f starting at the origin with r being a standard length and the angle theta being the residual. The next cell visited starts from the end of the last one. In d, e & f, a , b & c are represented with three cells represented by line segments. This method allows the mean angular offset (dashed line) of the whole flow set to be computed, and the degree to which the overall flow set shape matches can be qualified by the variance, here visualised as the grey area between the solid vectors and the dashed line.

Model-data matches are considered good when the metrics are below user defined threshold values in both the mean residual vector and the mean residual variance (see Figure 3.7). Using these two measures of model data fit (mean residual

vector and mean residual variance) it is possible to ascertain which flowsets are potential matches to which model timesteps.

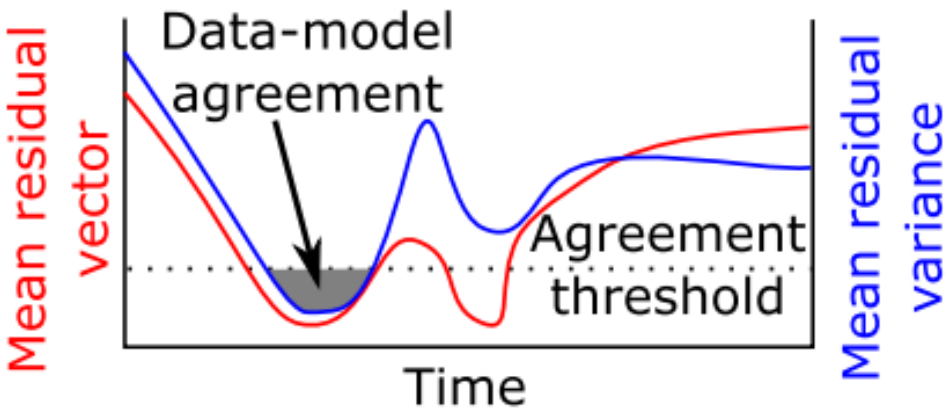

Figure 3.7: Idealised model-data comparison AFDA results. Mean residual vector (and variance scores vary over time. When both scores are lower than the predetermined threshold they are deemed as a good fit (i.e. during the shaded "data-model agreement" region). Figure modified from Ely et al., 2021.

3.3.2 - Flowset regridding for model data comparison

When comparing modelled flow directions with observed indicators of flow direction the spatial resolution of both datasets must be consistent. Traditionally, observed indicators of flow direction are stored as vector files consisting of polygons and polylines. In contrast numerical ice sheet models run on a grid, with outputs for each pixel of the grid. In this work all data is resampled to the model grid resolution of 5 x 5 km, to match the model grid.

Due to the large number of flowsets being compared two novel 'ArcMap Tools' were produced. The first 'ArcMap Tool' takes a single shapefile with all the polylines inferring ice direction for a flowset and divides them into 5 km line segments with a single point in the centre of each polyline. Direction is then calculated for each line segment before each flowset is split into its own file. The second 'ArcMap Tool' is then run on batches of flowset polylines to assign the directions of the line segments to a blank grid extracted from the ice sheet model. This tool uses the nearest line segments to the model grid centroid to define the direction with the exception of lines pointing geographically north where a single value is used (to avoid anomalous averages of 359 and 1 degrees). The second script results in one raster per flowset, with each raster having identical gridding to the numerical model outputs. The extent of the flowset can be identified by the boundary between values greater than 0 and no data values (-9999). The final step in preparing the flowset data for analysis is to combine all the flowset rasters into a single NetCDF with one layer per flowset.

3.3.3 - Automation of the flow direction workflow

AFDA analysis in this study consists of three python scripts. The first script performs the AFDA calculations, the second and third scripts relate to plotting and initial analysis of the results so as to allow a first pass/filtering of results.

AFDA is written and designed for large scale model data comparisons, however a number of minor modifications were made to the script initially written by Ely et al. (2021) to further automate the process. Despite these changes the first script remained largely unchanged mathematically. The additions allow the script to be more effectively run across multiple model simulations with added input tolerances to run across normal variation in input (size & shape). This initial AFDA script outputs two tables per model run with dimension FS^n+1 by M^t+1. Where FS^n is the number of flowsets (121) M^t+1 is the number of time steps run in the model (170). One table is filled with the mean residual vector values, and one with mean residual variance.

The second script written specifically for this thesis, summarises AFDA results on a simulation-by-simulation basis. This script combines the mean residual variance and mean residual vector values into one table per flowset per model run. This data is also combined into a series of plots of mean residual vector and mean residual variance over model time (see Figure 3.7). Furthermore this script assigns each mask to a discrete classification based on a combination of mean residual vector and mean residual variance values (see table 3.2).

Table 3.2: Thresholds used for discrete AFDA classifications.

Match name	Mean residual vector	Mean residual variance
Match	45	0.1
Ok	30	0.1
Good	20	0.1
Excellent	10	0.1
Exceptional	5	0.1

The second script produces a figure for each model-data match that meets a user defined threshold or criteria. Each plot can be paired with pre-produced flowlines generated using a MATLAB script written by Igneczi (Igneczi pers. comm.). Each plot is centred on a predefined xy centroid and uses a polygon (not the NetCDF raster) to illustrate the approximate area of the flowset, the ice surface topography and ice velocity (see Figure 3.8). This plotting feature was primarily used for selecting thresholds for subsequent model data competition tests. Using this plotting feature adds significant computational expense to the script, and can increase running time by an order of magnitude. Despite the increase in running time this step can be useful in visualising the quality of the match and is recommended for pilot work or visualising the 'best model runs'.

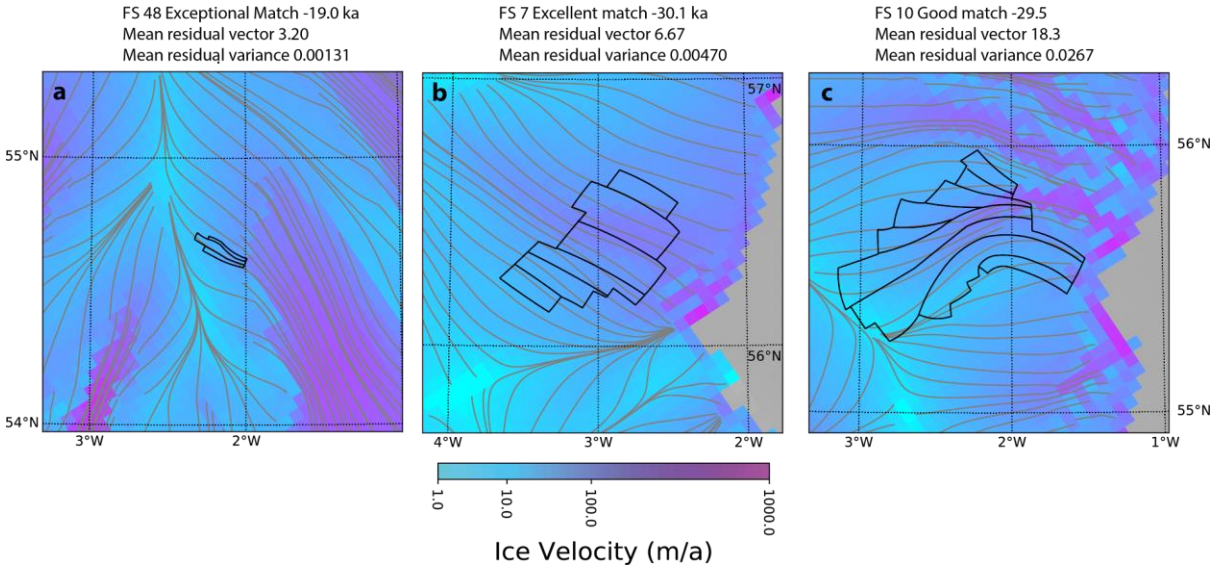

Figure 3.8: Example model data matches. Examples of top three match classifications with flowset box in black, flowlines in Grey and a raster basemap of velocity. All plot areas are equal size, therefore illustrating the relationship between flowset size and quality of match.

The third script summarises the results of the AFDA comparisons for all of the model simulations in the ensemble, producing a table of summary statistics. These include counts of each match type per simulation, as well as summarising each flowset across all model runs (e.g. flowsets which never matched). This script is useful for identifying which model run has performed best as these metrics are used later in the analysis for the combined model ranking. It also helps identify systemic model data mismatches.

As AFDA analysis on this scale is reasonably computationally expensive, a number of techniques were implemented to reduce the time required for analysis. A centralised high-performance computer (HPC) at Sheffield was used to run AFDA, yet

each comparison still took several hours of computing time to process. AFDA has been written to run on a single HPC core, however, multiple reconstructions were run independently in a quasi-parallel workflow where eight reconstructions were analysed using eight cores at once. This quasi-parallel computing method was achieved by submitting single job script seeds to sequentially run all three components of the AFDA analysis before queuing the jobscript for the following model run. Eight jobscript seeds were initialised, sequentially looping through the model runs until intersecting the next seed point. Using this method, all 200 model runs could be analysed in <12 hours (with plotting disabled).

At this stage I have a mean residual vector and variance score for each flowset at every model time step. To summarise how well a simulation has performed, I want a single metric which can be compared between ensemble members. As the 'quality' of the match varies, simply counting the number of matches below a threshold would lose information about match quality. I therefore opted for a normalised measure which favoured high quality matches and matches a large fraction of flowsets. To do this, I have developed what I call an 'excellence ratio' which gives a score for each simulation. To create this metric I take the best score for each flowset against a model simulation. Ideally all matches would have a low mean residual vector score, but failing this, if they suggest the ice is flowing in the right direction, this is better than not including the score. If the mean residual vector is >45° ('match') the flow vector is primarily not in the direction of observed flow. Therefore, I only consider flowsets where the match is less than 45. However, the best model is likely not necessarily the model which matches the most flowsets with this basic level of match. Instead, the best model ideally matches the flow direction in many places more closely (<10°). The best model run in terms of matching observed indicators flow direction therefore has a high ratio of matches <10°:<45° but also provides a high number of total matches. This rationale led to the following method of deriving the excellence ratio.

$$\frac{number\ of\ matches <10°}{number\ of\ matches\ \epsilon\ (10°,45°)} \times total\ number\ of\ matches\ < 45° \quad \text{(Equation 3.1)}$$

This metric gives a hypothetical max score of $(FS^n)^2$, if all flowsets match with a score of <10°, where FS^n is the number of flowsets being used in the comparison. The higher the excellence ratio the better the model is deemed to have performed in terms of matching modelled flow direction against observed indicators of flow direction. Using this metric models are ranked from best (1) to worst (200).

3.3.4 - Automated Proximity and Conformity Analysis (APCA)

To ensure members of the model ensemble simulate an ice sheet of appropriate size I use the Automated Proximity and Conformity Analysis tool (APCA) (Napieralski et al., 2006). Moraines represent perhaps the most obvious marker of ice sheet extent. ACPA systematically compares moraines to each timestep of a numerical ice sheet simulation. The comparison of ensemble end members to ice sheet extent was conducted by Ely et al. (pers. comm.). I used these results, to inform my selection of the most appropriate ensemble end member. Here I outline the process of creating an APCA model ranking.

APCA's assessment of the model data match consists of two metrics. The proximity score and the conformity score. The proximity score is a numeric quantification of how close the modelled ice sheet margin is from an observed moraine (e.g. black arrows 3.9a). Whilst the conformity measure is a quantification of the match in moraine shape, based on the variation in proximity measurements (see Figure 3.9). Each metric is measured at each model time step, allowing the model user to observe the degree of match in both metrics over time. If the ice sheet reconstruction and observation were perfect, the model would exactly match the margin at a point in time. Unfortunately, this is rarely the case, and a threshold for levels of match must be used to ascertain which models can be preserved as NROY's.

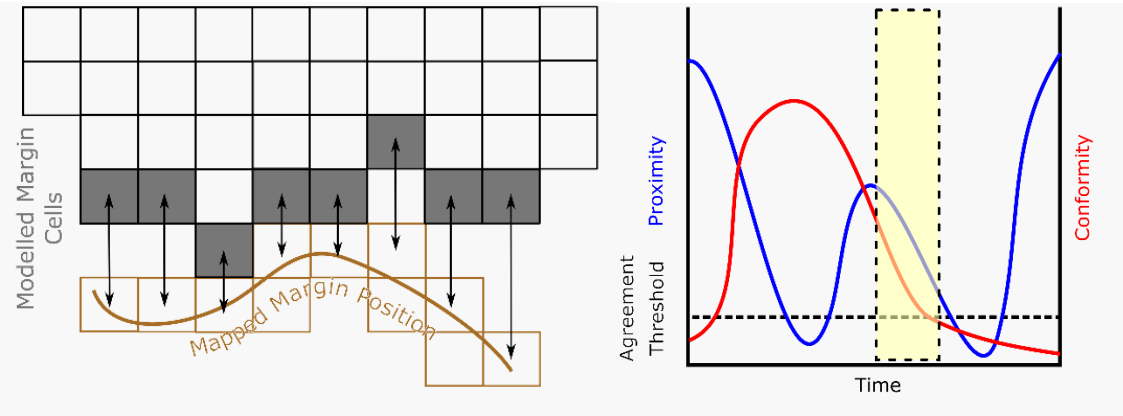

Figure 3.9: Idealised APCA process and results. Modified from Ely et al., (in prep) showing method for quantifying margin match using the APCA method. Left shows idealised modelled ice extent compared against moraine margin and right shows APCA proximity and conformity scores over time.

To perform APCA, major moraine complexes are re-gridded to binary rasters at the numerical model resolution (and grid shape). The ice margin extent is then systematically compared against each binary moraine raster, for each model time step.

This results in a conformity and proximity measurement for each moraine complex at each point in time (See Figure 3.9). In this study, a proximity threshold of 15 km and a conformity threshold of 3 km were used. These thresholds are similar to those published by Ely et al. (2019) and Napieralski et al. (2006). These moraines must match within the time window specified by the Bayesian moraine limits outlined in Clark et al., (2022). Using this method, I identify how many moraines each model run has matched. Each model run is then ranked from best match to moraines (1) to worst (200).

3.3.5 - Combining AFDA and APCA into one measure of relative model data fit

Once I have a rank for each model simulation, for each test, I need to combine both metrics to give a single score which accounts for my preferences as what metric to compromise on. In this study ice sheet reconstructions are to be used for two primary roles: i) empirical exploration of the parameter space under which lineated glacial landforms such a drumlins form; and ii) modelling of transport pathways of glacially transported sediments. As discussed previously this study has therefore prioritised numerical ice sheet reconstructions which flow in the most appropriate direction, followed by ice sheets which have realistic glacial extents. This should mean the NROY models are the most likely to move sediment in the correct direction but not exceed plausible ice boundaries.

To produce a list of NROY models which primarily have the best approximation of ice but also fit within a plausible ice extent, I use what I call a weighted suitability score (equation 3.2). This score combined both ranks, resulting in a weighted suitability score with lower scores relating to better or more suitable models for the model users intended purpose. The main feature of the weighted suitability score is the ability to weight one test more favourably that the other. In this work, models which perform poorly with regards to their rank on flow direction are more heavily penalised with regards to their final weighted suitability score than models which perform badly in regard to their APCA Rank (margin matching). I used a weighting of 1.5 but experimented with no weighting (1) and double weighting (2). Varying this weighting demonstrated some sensitivity in the ranking order of the top three NROYs, but which simulations ranked in the NROY list (discussed further in section 3.4.1). This weighting factor allows for the tests to be applied in parallel, whilst still accounting for the model users testing priority (or rationale).

$$Weighted\ suitability\ score\ =\ APCA\ Rank\ +\ Excellence\ Rank * 1.5 \quad \text{(Equation 3.2)}$$

Using the weighted suitability score, the 200 model simulations from the ensemble were ordered from best to worst. The best performing NROY is the simulation which received the lowest weighted suitability score. Using this ranking I can choose a model which is the best representation (ranked 1st/200) of flow direction and ice extent, or a bad representation such as the 75th percentile (e.g. ranking 151st/200).

3.4 Results

3.4.1 Automated sieving results

Using the combined weighting suitability score all 200 model runs were ranked from most to least suitable. The rankings of the top ten simulations are summarised in table 3.3. The best two ranking simulations are considered the most suitable for further investigation with a weighted suitability score of 18.5 and 19.5 respectively. For contrast, I also considered the third best ranking model run which scored 42 in the weighted suitability score. 4th-10th scored between 61 and 78 on the weighted suitability score. The top three ranking NROY's selected are 441, 453 and 586. The relative AFDA performance of a model (AFDA rank) did not appear to relate directly to the relative APCA rank although the best three NROYs all sat within the top 12% of AFDA model runs as the weighted suitability score favours flow direction as a metric for simulation 'quality'. In other words, the best simulations with regards to flow direction, did not generally perform well with regards to ice extent. Only one model simulation ranked within the top 5% of both APCA and AFDA rankings. This was simulation 453 which ranked second overall in the combined ranking (see table 3.3). Model run 453 ranked 7th with regards to flow direction and 9th with regards to ice extent. In chapters 4 and 5, I focus on the top ranking model simulation which ranked 1st with regards to ice flow directions and 17th with regards to ice extent (see table 3.3). It should be noted that although model run 441 ranked 17th with regards to ice extent it only matched 3 moraines fewer than 453 (matching 55 rather than 58 moraines).

The top three ranking model simulations were not consistent in regard to ensemble parameters used. The percentage of parameter space used varies from 1% to 80%. The smallest range in potential parameter space used was 1.18% in the sliding exponent q (see table 3.4). The two parameters which were observed to vary most were subshelf melt and precipitation offset which were seen to vary by 80.2 and 76.0% of the total possible range respectively. This aligns well with previous studies showing modelling uncertainty which suggest climate and ice shelf dynamics to be both significant and uncertain (Teng et al., 2015; Bauer and Ganopolski, 2017; Bulthuis et al., 2019). However, model ensembles 441 and 453 (ranking first and second respectively) used much narrower parameter ranges for precipitation and sub shelf melt (when we exclude the third ranking ensemble 586). With the sub shelf melt factor varying by only 8.05% of the total range and precipitation offset varying by 56.2%

MR	Match $\epsilon(45,30)$	Good $\epsilon(30,20)$	Ok $\epsilon(20,10)$	Excellent $\epsilon(10,5)$	Exceptional $\epsilon(5,0)$	Total Matches $\epsilon(45,0)$	Excellence Ratio	Excellence Rank	APCA (moraines)	APAC RANK	Weighted sum	Final Rank
441	7	22	30	34	17	110	95.1	1	55	17	18.5	1
453	6	17	39	35	13	110	85.2	7	58	9	19.5	2
586	11	21	27	35	12	106	84.4	12	53	24	42	3
496	10	19	34	36	10	109	79.6	33	56	12	61.5	4
451	12	17	33	38	10	110	85.2	8	46	57	69	5
479	14	17	32	36	12	111	84.6	9	46	58	71.5	6
583	6	26	31	38	8	109	79.6	34	54	23	74	7
467	11	16	36	36	11	110	82.1	21	50	43	74.5	8
463	11	18	33	33	14	109	82.6	17	47	51	76.5	9
443	6	22	35	32	14	109	79.6	35	53	25	77.5	10

Table 3.3: NROY simulations. The 10 best performing NROY's using the weighted sum of AFDA and APCA scores. MR (model run) indicates simulation name from the ensemble; the number of models in each mean residual vector range (written name and numerical mean residual vector score range) all matches must meet a threshold of 0.1 mean residual variance. The excellence ratio (with high values indicating better scores), and the excellence rank (1 best to 200 worst). APCA bayes moraines indicates the number of moraine complexes matched (higher values are better performance), with APCA rank indicating the moraine match performance relative to the ensemble (lower value resulting in better relative performance). The weighted sum indicates how the performance of the model runs based on a combination of APCA and AFDA, with the final rank indicating how well the model performed in both APCA and AFDA relative to the other model ensembles.

	Temperature offset (°K)	Precipitation offset (%)	Forcing factor	Positive degree day factor for snow (m/a)	Positive degree day factor ice (m/a)	Calving thickness (m)	Sliding exponent: q	Ice flow enhancement factor: E	Subshelf melt factor	Maximum water thickness in till (m)
441	1.867	1.083	0.002769	0.004852	0.007981	120.9	0.002843	1.449	0.002968	3.661
453	2.187	1.392	0.002937	0.004203	0.008155	147.4	0.003350	1.179	0.01781	2.427
586	-0.3729	0.8415	0.001746	0.004604	0.008020	137.3	0.01064	1.321	0.03984	2.101
Observed Range	2.5600	0.5507	0.001191	0.0006490	0.0001740	26.49	0.007797	0.270	0.03687	1.560
Possible Range	4.45	0.72	0.0025	0.00280	0.0026	103	0.662	0.93	0.046	3.8
% of range used	57.5	76.0	47.6	23.2	6.69	25.7	1.18	29.1	80.2	41.1

Table 3.4: Parameters used for best three NROY Simulations. Percentage of range used shows how clustered within the parameter space the three NROY's are for that specific parameter. Low percentage of range used could be indicative of parameters which could be fixed in future modelling attempts. MR 441 and 453 use similar climate parameters and flow parameters but differ more significantly with regards to ice removal (subshelf melt, carving, till thickness). 586 in contrast uses markedly different parameters to 453 and 441, using a colder climate and a smaller precipitation offset

One sliding law was used in the PISM experiments (see chapter 2, equation 2.2) with two schemes for deriving the basal yield stress τ_c. The first method is known as the prescribed yield stress, where values of τ_c are defined using a till map; the second method prescribes ϕ to calculate τ_c using equation 2.2. Simulations using a sliding law where τ_c is calculated from ϕ performed better than those using a prescribed τ_c map (as defined by their weighted suitability score) (see Figure 3.10). On average models using a variable sliding regime based on basal friction performed 17% better than the median average. The difference in performance of the two sliding regimes is more apparent when we consider the top and bottom ranking regimes and note that 14 of the top 20 ranking simulations use the elevation dependent sliding regime. In contrast the reverse is apparent in the bottom 20, where 16 of the simulation use a prescribed sliding regime.

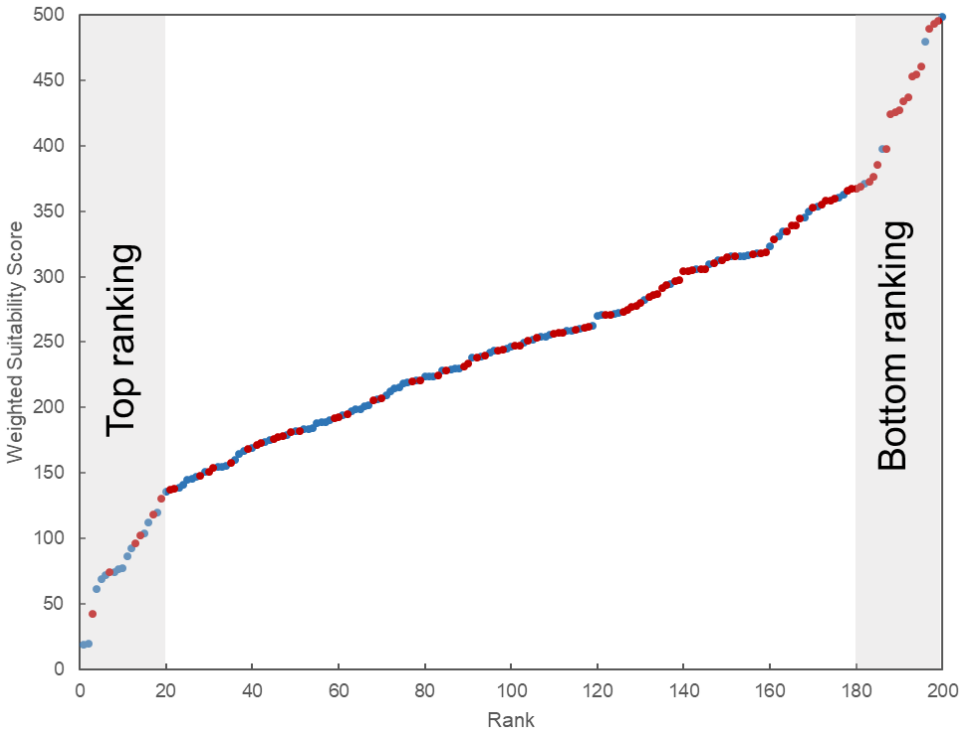

Figure 3.10: Model ensemble rank over weighted suitability. Note rank is derived from weighted suitability score but does not relate to the score in a linear manner. Model runs in blue use a sliding regime whereby till friction angle was prescribed (MR400-500), whilst points in red use a prescribed sliding regime (MR 500-600) (see chapter 2 for description of sliding regimes). Models using a prescribed sliding law are on average awarded a higher weighted suitability and rank more highly with a mean rank of 83.5 (where a mean rank of 100 would mean both models perform equally). Figure highlights the spread of weighted suitability scores within the top bottom ranking models.

3.4.2- Comparing simulations to ice volume

The best performing simulations achieve relatively consistent extents when compared against the worst ranking model runs (see figure 3.11). This indicative of the margin matching component of the weighted suitability score which favours model runs which align with observation of ice extent. In contrast, due to the weighted suitability score not considering glacial volume, limited systematic variation can be observed between the best ranking NROY runs and the worst.

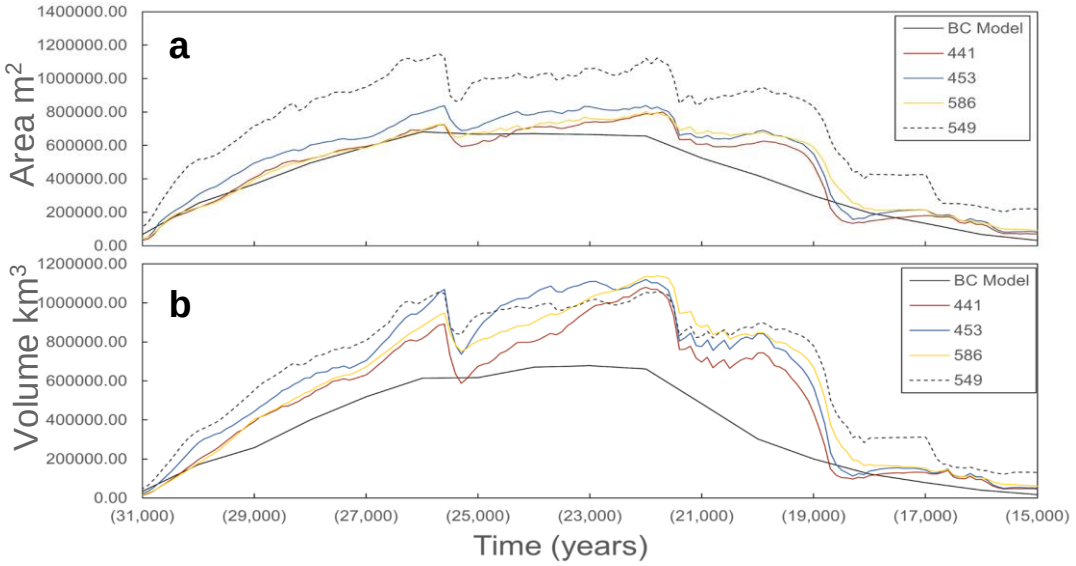

Figure 3.11: Comparison of NROY ensemble area and volume against reference nudged simulation and a rejected NROY. Top three ranking NROY simulations (441, 453, 586 ranking 1st 2nd 3rd respectively), the nudged BC a rejected ensemble member (549). 3.11a shows area over time, note the three NROY's align when will the nudged BC area, whilst the rejected NROY is considerably larger. 3.11b shows volume over time, note that ensembles generally exceed the volume. This is least pronounced during build up and late retreat (when most model data matches occur). This likely therefore suggests ensembles are thicker than implied from the GIA signal, although the largest volume mismatch also align with the largest area mismatches, the increase volume is likely not simply a thickness signal

In an effort to estimate thickness uncertainty I calculated the mean thickness required to produce the modelled volume (from ice extent). I do this for both the nudged BC model and ensemble 441 and calculate the difference between both over time (See Figure 3.12). This analysis suggests on average ensemble 441 produced ice thicknesses in the region of 206 m thicker than suggested by GIA observations.

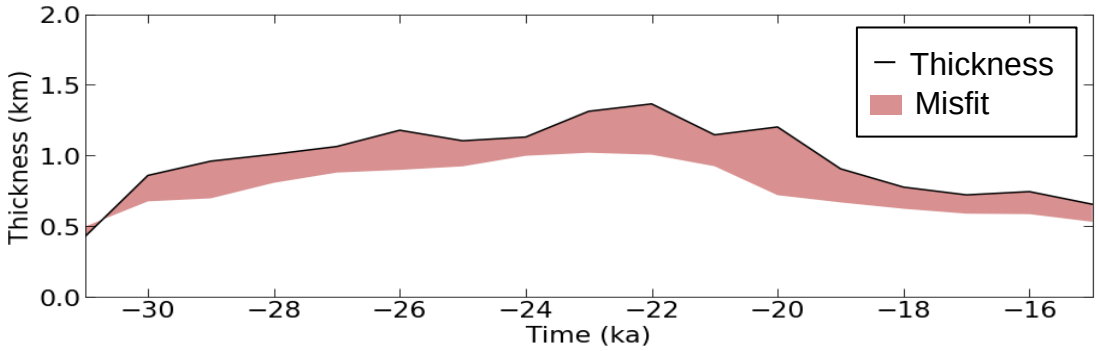

Figure 3.12: Thickness misfit of NROY. Mean thickness of ensemble member 441 with residual thickness (under or overestimate) residuals relatively to the GIA nudged BC simulation. The ensemble 441 generally overestimates ice thickness. Note BC ice thickness is only nudged to the GIA signal at 1000-year intervals hence lower temporal resolution ensemble thickness than in Figure 3.11.

3.4.3 - Comparing model runs to traditional empirical measures

Once initial automated sieving had been conducted, I performed visual validation checks on the three top ranking NROY's. I select a number of key extents and features from the 2022 BRITICE CHRONO reconstructions accounting for the chronology and timing (Clark et al., 2022). These include:

Maximum extents:

- 30-29 ka Northern sector (Minch & Otter Bank) (e.g. Bradwell 2021b). Transect 8 in Clark et al. (2022).
- 27-26 ka West and Southwestern sectors (Malin, Hebrides, Galway, Donegal, Irish Sea Ice Stream) (e.g. Callard et al., 2018) Transect 7 in Clark et al. (2022).
- 23-22 ka North sea sector (North sea, Norwegian Channel Ice Stream) (e.g. Sejrup et al., 2016) transect 2 in Clark et al (2022).
- 28 ka Irish Ice Stream established (e.g. Bradwell 2021a) transect 3 in Clark et al (2022)
- 20 ka separation of the BIIS and EIS (e.g. Evans et al. 2021) transect 2 in Clark et al (2022).
- 16 ka separation into the Irish and Scottish Ice Sheet (e.g. Bradwell 2021a) transect 3 in Clark et al (2022).

Each model's performance in relation to the key characteristics are highlighted in table 3.5, and these can seen in Figures 3.11, 3.12 & 3.13.

	441	453	586
Maximum extent in the Northern sector at 30-29 ka	✓	✓	X
Maximum extent in the West and South Western sectors between 27 and 26 ka	✓	✓	✓
Maximum extent of the North Sea sector between 23 and 22 ka	✓	✓	✓
28 ka Irish Ice Stream established	X (already established)	X (already established	✓
20 ka separation of the BIIS and EIS	X (later 18.7 ka)	X	X
16 ka separation into the Irish and Scottish Ice Sheet	X	✓	X

Table 3.5: Visual model data comparison. Visual assessment of events (and their timing) with 1000 years leniency proposed by the BRITICE Chrono project in Clark et al 2022 based on visual inspection of ice sheet deglaciation maps.

Simulation 441 ranked first in the sieving, matching 110 flowsets and 55 moraines, giving it a weighted suitability score of 18.5 (see table 3.3). Simulation 441 also performs well with regards to key timings and observations laid out by the BRITICE-CHRONO project (Clark et al., 2022). The simulation reaches its maximum extent on the northern sector of the BIIS at approximately 27 ka. At this time, ice streams (Minch and Rona) extended to the edge of the continental shelf. However, the model deglaciated more rapidly in the northern sector than suggested by offshore observations (e.g. Bradwell et al., 2021) having significantly deglaciated by around 25 ka. Some growth of the southern sector can be observed between 27 ka and 25 ka,

however by 23 ka the southern sector is beginning to advance. This southern advance is synchronous with large scale ice streaming in the northern sector around the Minch, Rona and Foula Ice Streams (Stoker and Bradwell, 2005, Bradwell, 2008, Gandy et al., 2019). The confluence of the BIIS and the EIS occurs at approximately 24 ka, although extensive marine ice shelves have intermittently connected both ice sheets since 24.5 ka (see Figure 3.13). Extensive ice shelving is not observed between ice sheets until at 18.8 ka when both the Irish Channel and the North Sea begin to rapidly form ice shelves and collapse. The Irish Ice Shelf collapses at 18.7 ka with the North Sea Ice Shelf almost entirely collapsing by 18.5 ka. The separation of the Irish and Scottish Ice Sheets is therefore premature in simulation 441 occurring almost 3 ka years before estimated in Clark et al. (2022).

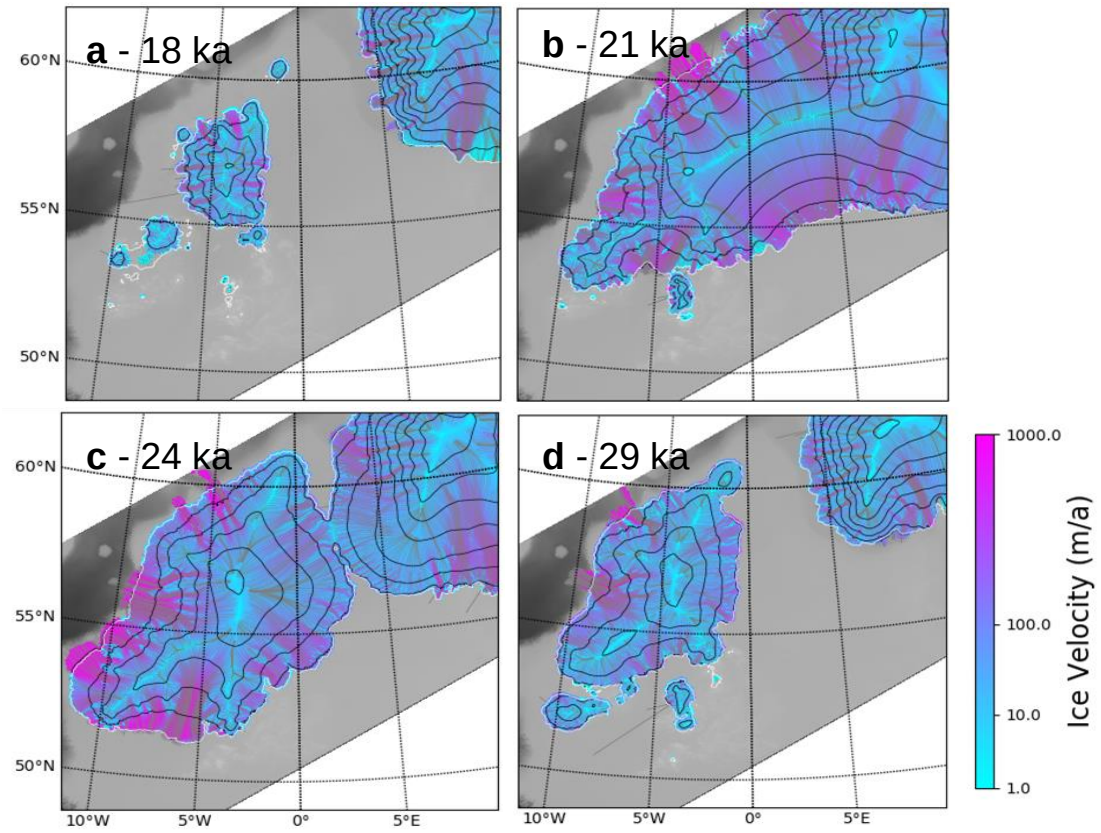

Figure 3.13: NROY simulation 441 which performed best in the weighted combined ranking of AFDA and ATAT. Figure shows a greyscale palaeo topography with an overlaying ice velocity map, 500 m ice elevation contours in black and grounding line contours in white. Grey lines indicate computed flow lines which were produced using code modified from Igneczi, (pers. comm. 2020). MR 441 performed well with regards to meeting benchmarking events, however, the timing of events is not consistent with the empirical reconstruction (Clark et al., 2022).

Simulation 453 ranked second in the sieving with matching despite matching the same number of 110 flowsets and more moraines (58). This was because on

average the flowsets were matched less precisely giving a lower score for the same number of matches resulting in a weighted suitability score of 19.5 (see table 3.3). Simulation 453 performs best out of the three top ranking NROYs runs with regards to the empirical markers selected for manual assessment. Beginning with the northern sector, the simulation extends to the continental shelf at 27 ka. In this sector the ice flow is characterised by a large number of ice streams. These ice streams are in addition to the Bara, Minch, Rona and Foula, but are generally small and do not persist (see Figure 3.14). During this time, the southern sector is still gently expanding until 25.6 ka when it begins to retreat. During the retreat of the southern sector, a pronounced Irish Ice Stream emerges from what is initially a wide zone of fast flow spanning the entire southwest margin (but not extending deep into the interior) to a deep reaching ice stream confined mainly to the Irish Sea by 25.3 ka. The Irish Sea Ice Stream dominates the southwestern sector of the ice sheet for almost 7 ka until the eventual collapse of the sector at around 19 ka. By 19 ka the original Irish Sea ice Stream has retreated back almost to the Isle of Mann. Approximately 300 years after the breakdown of the Irish Sea Ice Stream the Scottish and Irish ice sheets separate. Simulation 453 simulated this unzipping of the two ice sheets to occur through a network of ice shelves over 200 years, before a rapid collapse back to grounded ice in both Ireland and Scotland. Simulation 453 produces an earlier collapse of the marine sector of the North Sea than suggested in the literature, with much of the Norwegian Channel deglaciating between 19 and 18.3 ka (Evans et al., 2021). This unzipping for the EIS is preceded by fast flowing ice which rapidly transitions into extensive areas of shelf which do not persist for more than 100 years before collapsing.

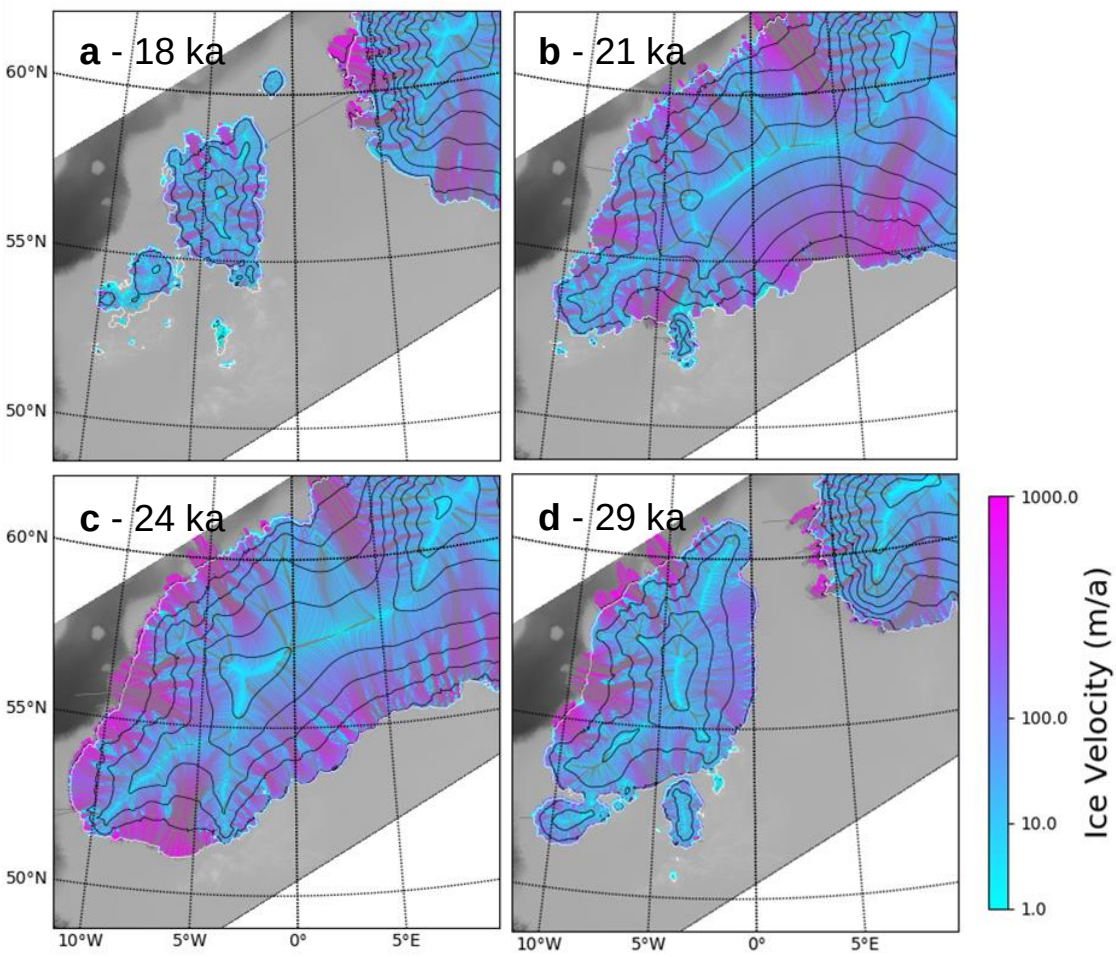

Figure 3.14: NROY simulation 453 which performed second best in the weighted combined ranking of AFDA and ATAT. simulation 453 was the only model to perform in the top 12% of both AFDA and ATAT, and in many regards could be considered an equal NROY to 441. Figures shows a greyscale palaeo topography with an overlaying ice velocity map, 500 m contours in black and grounding line contours in white. Grey lines indicate computed flow lines which were produced using code modified from Igneczi pers. (comm., 2020). Simulation 453 performed best of the three highly rated NROYs with regards to meeting benchmarking events. The most notable shortcomings of simulation 453 are its synchronous retreat in the north and south when an asynchronous north south (advance retreat) pattern is observed in the palaeo record.

MR 586 ranked third in sieving, matching 106 flowsets and 53 moraines, giving it a weighted suitability score of 42 (see table 3.3). Simulation 586 expands more gradually than 441 and 453, not reaching its maximum extent in the southern sector until 25.6 ka. Shortly after reaching its maximum extent, the southwest sector goes through a large-scale speed up for approximately 200 years. This speed up is followed by a substantial decrease in area before settling into a new configuration with the Irish Channel Ice Stream establishing itself to evacuate much of the southwest sector. This

configuration with the Irish Ice Stream is maintained until 20 ka when the sector experiences a final phase of rapid and extensive ice loss (see Figure 3.15). Unlike Simulation 441 and Simulation 453, Simulation 586 does reproduce the unzipping which is proposed to occur through the development and collapse of extensive Irish Channel Ice Shelves. Instead, I observe a primarily grounded unzipping at approximately 16.8 ka. Similarly to the Irish Channel, the unzipping of the EIS and the BIIS between 18.3 and 18 ka shows less evidence of ice shelves, and is primarily a terrestrial retreat of grounded ice.

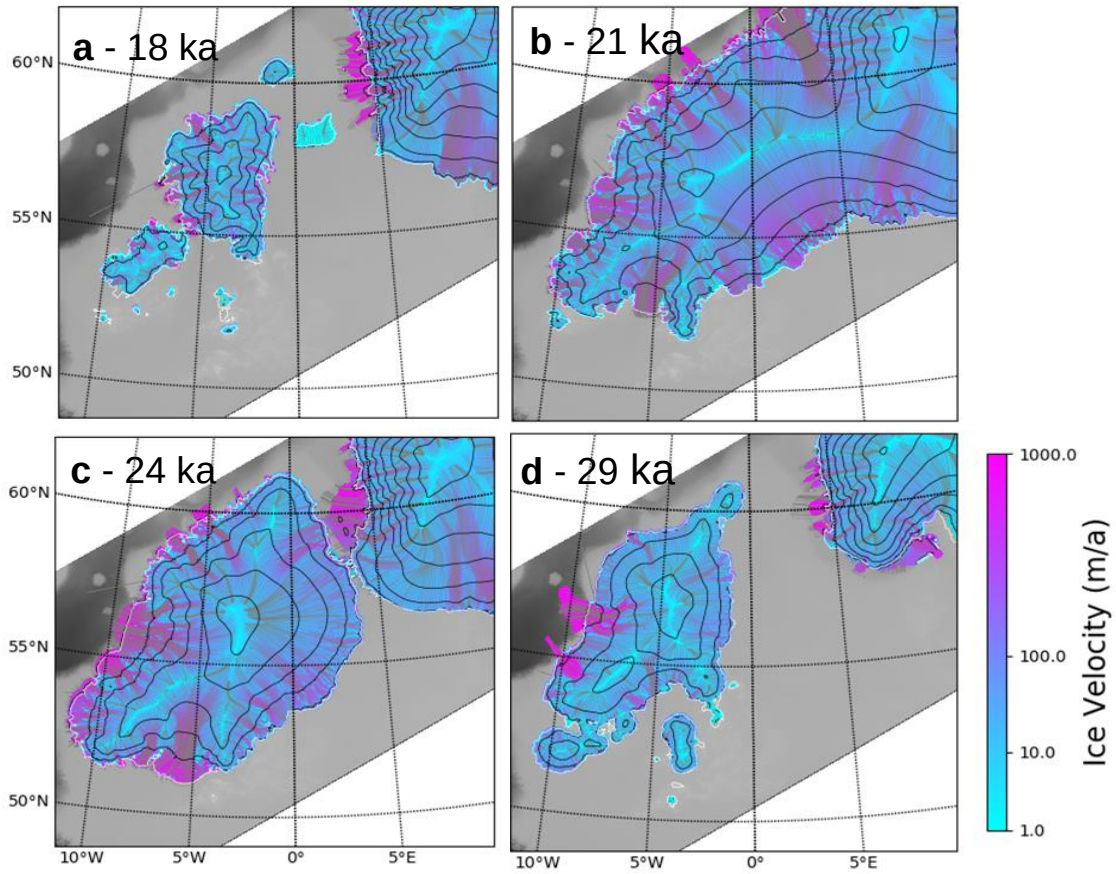

Figure 3.15: NROY simulation 586 which performed third best in the weighted combined ranking of AFDA and ATAT. Figures shows a greyscale palaeo topography with an overlaying ice velocity map, 500 m contours in black and grounding line contours in white. Grey lines indicate computed flow lines which were produced using code modified from (Igneczi, pers. comm.2020).

3.5 - Discussion

In this chapter I have used sieving to curate a list of NROY simulation from a model ensemble by assessing fidelity with regards to recreating ice sheet geometry. The broader motivation for this work is twofold: firstly, to learn about the glacial

processes related to ice sheet geometry (e.g. drumlin formation and erratic transport); secondly to learn more broadly about numerical ice sheet models and their ability to reconstruct palaeo-ice sheets. The remainder of this chapter focuses on the latter.

3.5.1 - The skill of top ranking ensemble members at recreating observed flow direction

Using automated tools to assess flow geometry, I was successful in identifying a number of high fidelity simulations (NROY). Of the top 10 ranking NROY simulations, all were successful in broadly recreating flow geometry matching over 100/122 flowsets (see table 3.3). The majority of matches had mean residual vectors of less than 20 degrees. The highest ranking NROY MR 441 also produced the highest number of matches <5 degrees. This, however, comes with the caveat that the best matches (e.g. <2%) across all model runs were on the smallest flowsets (being statistically most likely to align perfectly across all pixels). Similarly, the top ten NROY predominantly matched over 50 moraines with the overall top three matching between 53 and 58 moraines (see table 3.3).

More broadly, almost all flowsets were matched at some point by at least a simulation in the ensemble. Only four flowsets were never matched by any ensemble member with a match <45 degrees (Two marine, one Irish and one British). 45 degrees is a loose measure of model data fit. That being said only, 14 flowsets were never matched at <20 degrees. Indicators of ice extent performed similarly to indicators of ice flow, in so far as the majority of moraines were matched at least once. Seven moraines were never met, with all bar one of them being offshore (See Figure 3.16).

Recreating a large number of indicators of flow direction and ice extent optimistically highlights PISM's skill at broadly recreating ice flow geometry. Furthermore, given the general fidelity shown across the ensemble the initial investigation of parameter sensitivity was successful in removing unrealistic parameter combinations. More critically however, it also highlights the need for a large number of observed indicators of flow direction to be used to rigorously ascertain if a model is indeed matching well with flow geometry (rather than coincidentally matching five to ten flowsets). As the number of observations matched and rigor of tests increases, uncertainty about equifinality (or coincidentally getting a good set of model data test results) of the icesheet gradually decreases adding confidence to the sieving processes.

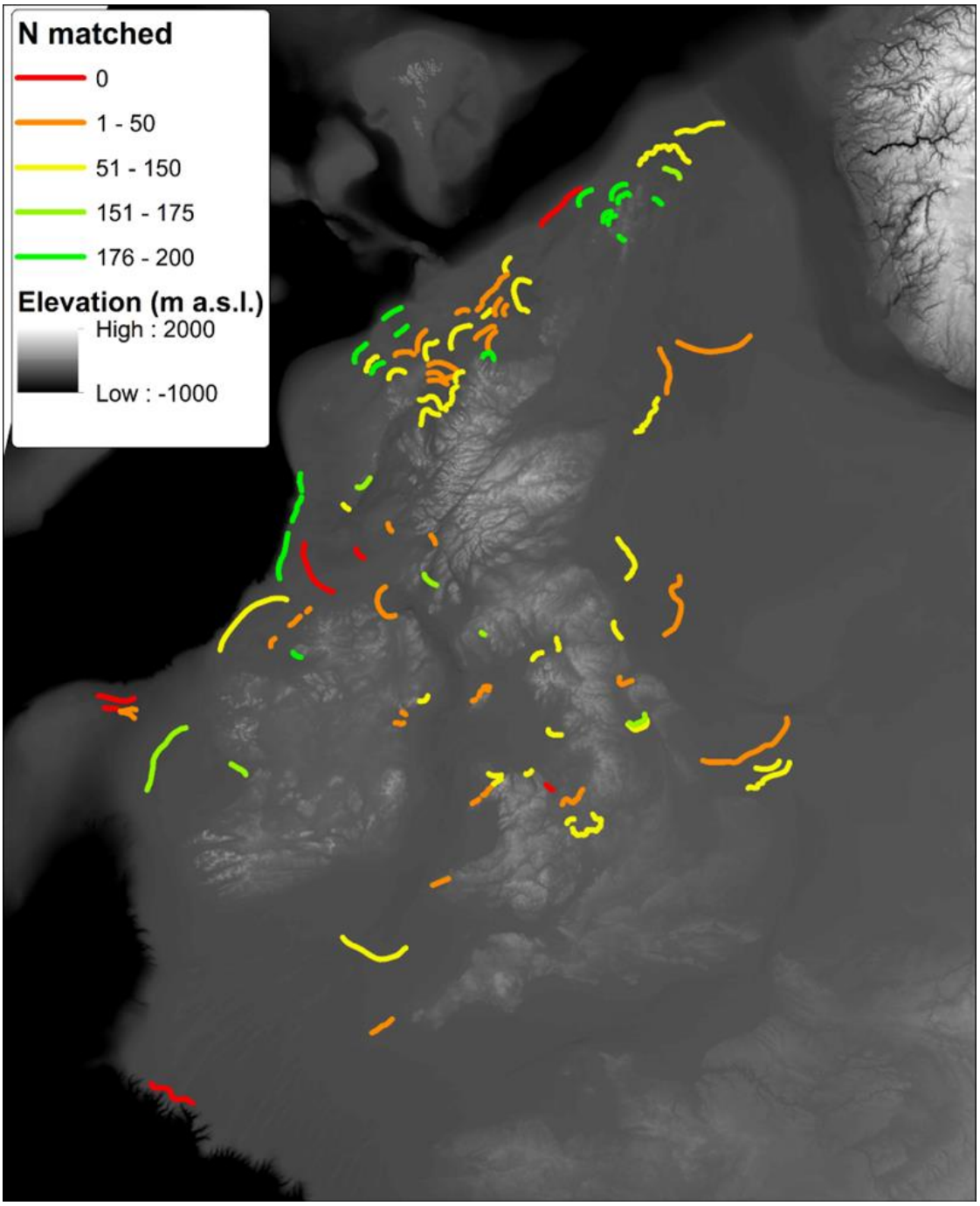

Figure 3.16: Number of matches per moraine. Moraines used for model-data comparison of the BIIS colour coded based on the number of matches, figure modified from Ely et al. (in prep).

The top ranking NROY simulation shows a similar pattern in model data fit of flowsets to ice extent. Mid latitude terrestrial flowsets generally match, whilst ice marginal flowsets at higher and lower latitudes and marine sectors do not (see figure 3.17). Several factors may be at play, such as the distribution of similar flowsets being higher in regions with higher matches (therefore preferentially selection models which perform better in these regions); or that increased data availability in this region

improved the input data for these regions (e.g. shear stress input maps); or that primarily terrestrial regions are easier to numerically model than the land terminating sectors. Quite possible some combinations of these factors may be at play, therefore highlighting these as considerations for future modelling and model data comparison endeavours.

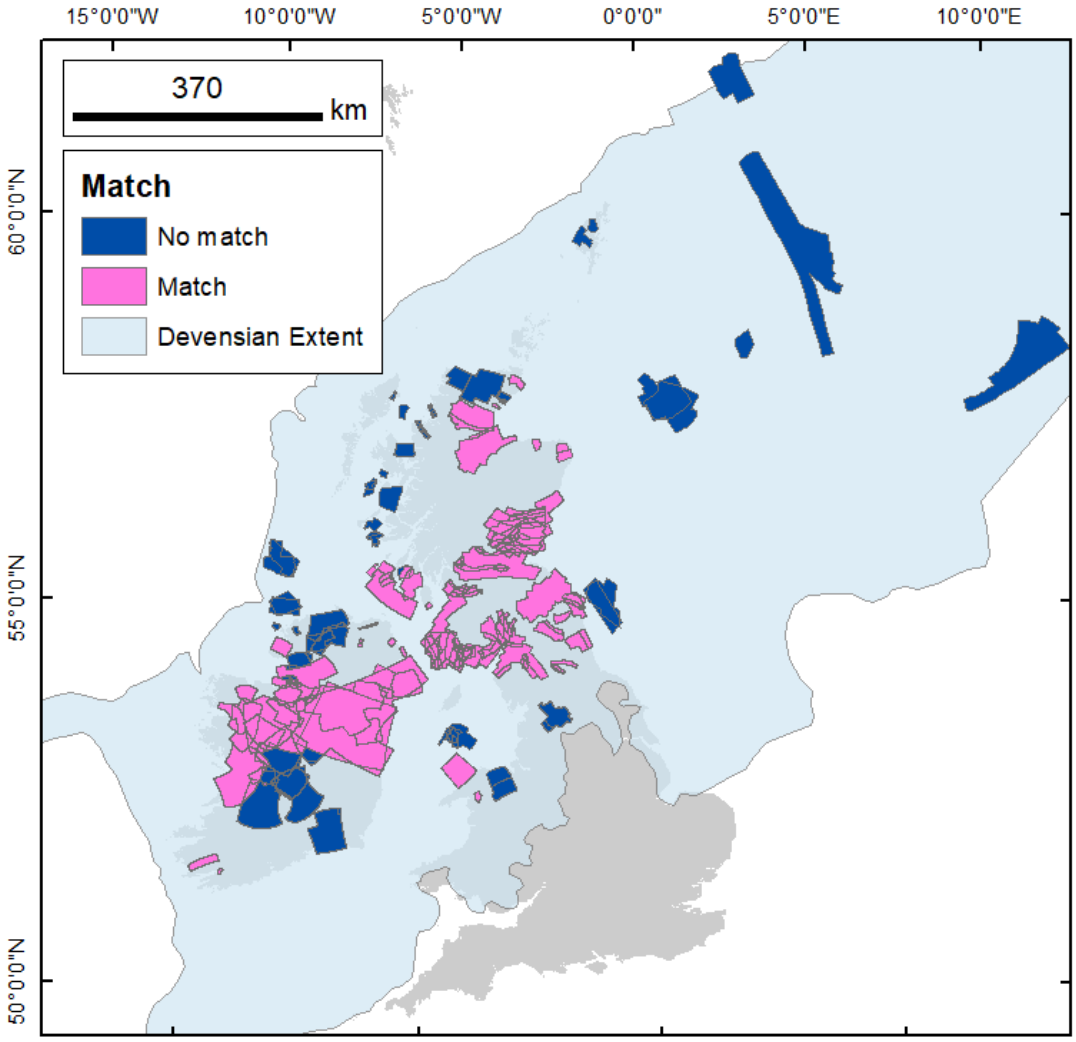

Figure 3.17: Distribution of matching flowsets from MR 441. Flowsets with a match score of <20 degrees. Matching flowsets are focused around the central latitudes of the BIIS.

3.5.2 - Implications for reconstructions of the BIIS

Qualitative investigation of ensemble members is still useful, and provides a different insight into the processes. For example, the retreat of ice extent along the northwest coast of the BIIS (around the Minch and Rona Ice Streams) was recreated much more consistently in high ranking NROYS. Such observations are not apparent when considering match scores alone. I propose that this is a by-product of the relatively extensive (by marine standards) offshore evidence in the form of moraines

(e.g. Bradwell et al., 2007; 2008; Clark et al., 2022) (see figure 3.16). The quality of the ice flow geometry feeding the Minch is also important, as it represents one of only a few empirical and numerical testing grounds for work on the marine ice sheet instability (e.g. Gandy et al., 2018). This instability is proposed to have the potential to rapidly remove ice mass from an ice sheet, and correctly estimating the rate at which ice is supplied to such an area could be significant for future work on the mechanism.

Despite lacking explicit indicators of ice shelf extent, growing evidence constrains the offshore grounded ice extent (see figure 3.16). The NROY simulations in this chapter's ability to model retreat of offshore ice shelves (without using observations of grounding line wedges) suggests that ice sheet geometry is an important factor in controlling mass movement to ice shelves. Although systematic comparison to previous modelling efforts has not been included, the ability to 'naturally' bridge the Norwegian Channel (unlike many previous modelling efforts, e.g. Patton et al. (2016), is likely a result of more realistic distribution of ice mass, in addition to improved ice physics to recreate ice shelving. Despite important improvements in the style of offshore glaciations (e.g. extensive ice shelves), the poor offshore performance with regards to ice flow direction suggests there is still considerable room for improvement in ice flow geometry.

3.5.2.1 - Interesting behaviour in data poor regions such as the North Sea

Variation in the timing of ice shelf collapse in this chapter helps to highlight the importance of the marine sector in controlling the timing and geometry of an ice sheet. Unfortunately the marine sector of the BIIS (specifically the North Sea), remains relatively data-sparse with regard to empirical observation of flow direction. Although an increasing number offshore markers of palaeo ice flow geometry have recently been identified such as drumlins, MSGL, and moraines (e.g. Dunlop et al., 2010; Van Landeghem, et al., 2020; see table 3.1), the marine sector of the BIIS remains by far the most data poor portion of the ice sheet in terms of landform density. Landforms pertaining to ice shelves in particular are largely absent from the record. This is in part due to limited availability of high-resolution bathymetry, but also due the large volume of Holocene sediments which have built up (Evans et al., 2021). Despite this general lack of offshore indicators of flow direction for use in sieving, it seems the offshore ice performs largely as anticipated from empirical reconstructions (which also benefit from the use of the extensive sediment cores). An intriguing question therefore arises: if we successfully recreate the current terrestrial geometry, will we recreate the offshore geometry? We know the onshore record of ice flow direction for the BIIS is well constrained and offshore indicators of ice extent are comparatively good (compared to

several years ago (e.g. Patton et al., 2016; 2017) or for other ice sheets) in part due to new data from BRITICE CHRONO (Clark et al., 2022; Ely et al., in prep). Tentatively it appears that offshore indicators of grounded ice extent paired with comprehensive onshore indicators of ice flow direction may perform adequately with regards to ice extent, but not flow direction.

The challenge of glaciating the North Sea in numerical ice sheet simulation is well documented (Boulton and Hagdorn, 2006; Patton et al., 2016, Gandy et al., 2018). This is likely because of the deep depth of the Norwegian Channel (~700 m). This deep trough largely inhibits grounded ice from extending out from Norway. As a result, ice must predominantly be sourced from the BIIS for a confluence with the EIS to occur under plausible climatic conditions (Evans et al., 2021). Despite these challenges, the build-up of the marine sector of the BIIS and its coalescence with the EIS appears to be an essential aspect of the growth and decay of the sector (Sejrup et al., 2016; Gandy et al., 2019; Evans et al., 2021; Clark et al., 2022). As a result, confluence through ice shelving is still rarely accounted for in numerical ice sheet simulations prior to those included in this thesis (Gandy et al., 2021). Nor did all model simulations from the ensemble recreate the progressive confluence of both the BIIS and the EIS. Correctly distributing ice mass flow from the BIIS into the North Sea sufficiently early to produce ice shelves is likely a feature of model ensembles which perform well with regards to ice geometry.

3.5.2.1 - Persistent model-data mismatches

Although the northern portion of the BIIS performed well in some simulations, two persistent model-data mismatches in the ensemble suit were evident. Firstly, that of the marine sector of the Irish Sea Ice Stream. The timing and extent of the Irish Sea Ice Stream are contested, however recent work has suggested it extended to the Celtic Shelf rather than the Isles of Scilly (Lockhart et al., 2018; Scourse et al., 2019; Scourse et al., 2021). None of the ensemble models included in this thesis were successful in extending to the Celtic Shelf. This may be a result of incomplete reconstruction of the processes in PISM. Scourse and Furze (2001) for example suggest surge-type glaciation is required to reach the southern extent. Variation in the ice flow dynamics could perhaps be resolved with more geomorphic evidence of ice flow direction in the Irish Channel. Alternatively, the PISM simulations may appropriately reconstruct the ice extent and instead further empirical observation of timing of the glacial extent of Irish Sea Ice Stream may be required.

Further along the south-west margin of the BIIS, recent geomorphological evidence suggests the last BIIS extended out to the Porcupine Bank off the west coast of Ireland (Peters et al., 2015; Ballantyne and Ó Cofaigh, 2017; Callard et al., 2020; Ó Cofaigh et al., 2021). This is not reconstructed in any of the model simulations included in this thesis. This western most extent may prove to be significant in deglaciation of the BIIS and it would provide an important pinning point for a more extensive ice shelf to the west of the BIIS. Such an ice shelf would have significant buttressing effects and potentially substantially alter the location of ice divides over Ireland. Given the relative geographic proximity of these two persistent model-data mismatches I propose that a systemic under representation of ice sheet geometry may in fact cause both of these persistent model mismatches. I address the potential of a systemic issue with ice sheet geometry in Ireland further in Chapter 5.

3.5.3 - Lessons for ice sheet modelling

This work found evidence that the Mohr-Coulomb criterion, paired with a prescribed till friction angle (ϕ) map to calculate basal yield stress performed better with regards to recreating ice sheet geometry (see Section 2.3 on method & Figure 3.10). Of the top 10% of model simulations (ranked using the weighted suitability score), 70% calculated yield stress using the prescribed till friction angle (ϕ)' map, whilst 80% of the lower 10% scoring simulations used a prescribed yield stress to calculate sliding. This is perhaps a useful guide for future modelling endeavours, affirming that the rather laborious task of compiling maps of bed geology and ascribing shear stress values to different substrates is indeed preferable.

Due to the lack of a direct test of model fidelity with regards to metrics such as subshelf melt, ice shelf extent, or indeed climate, it is difficult to definitively answer all questions of model fidelity. I reaffirm that ice sheet flow geometry is an important proxy for these factors but nevertheless not a direct test. By incorporating a multi proxy, multi-level test of model fidelity I look to resolve some questions of equifinality. However, multiple ice sheet configurations may result in the same or similar results. Therefore, it is important for the trend in increasingly multi-proxy, model-data comparison approaches to continue.

3.6 - Summary and Conclusion

Numerical modellers have access to increasingly large computing resources, leading to the potential to run larger model ensembles with more computationally

expensive models. With this, however, comes the challenge of knowing which (of many) simulations is the most appropriate reconstruction of the past. A large range of metrics can be used for selecting a model ensemble member, however, each layer of sieving potentially compromises a more important metric. A central theme of this chapter is a deliberate model-data comparison rationale. Or in other words, acknowledging that no simulation is currently perfect for every task and attempting to select simulations appropriately suited to the task. In this chapter, I have made a deliberate effort to focus on ice sheet geometry above other metrics. I have presented a framework of tiered tests of decreasing priority, combing parallel (e.g. AFDA and APCA) and in-series testing. Using this framework, I have undertaken sieving to curate an ordered list of NROY from a model ensemble of 200 model simulations.

In this chapter, I have highlighted the importance of ice sheet geometry as an overarching tool for considering the complexities of marine terminating ice sheets. I interpret successful confluence in the North Sea as evidence that recreating terrestrial geometry in inferred accumulation zones increased fidelity offshore with regards to building ice shelves and confluences of ice sheets. I identify a number of persistent model-data mismatches that may have significant implications for retention of ice mass on the West and Southwest of the BIIS. I highlight that these model-data mismatches may be the result of a poor modelled ice sheet geometry, which I will investigate further in Chapter 5. The marine nature of both persistent model-data mismatches sites highlights the significance of ice-ocean interactions and the physics governing these processes.

Chapter 4 - Novel approach for using an ice sheet model simulation to ‘observe’ the physical conditions of drumlin formation.

4.1 - Introduction

If you look across the undulating topography of Ireland or North Yorkshire, the landscape is covered in regular undulations. These humps and troughs are often described as a ‘basket of eggs’ topography (see Figure 4.1). The human eye is fascinated by regular and recurring shapes, and it is little wonder that these undulating topographic features have drawn the attention of academics and hobbyists alike for centuries (Davis, 1884; Fairchild, 1929; Ely, et al., 2023). The collective term for these hills is subglacial bedforms (also referred to as bedforms in this thesis): formations of sediment and bedrock which developed beneath glacial ice (Ely et al., 2016). This chapter focuses on the most commonly studied class of subglacial bedform, drumlins (Clark et al., 2009). Subglacial bedforms have been the focus of extensive study, with drumlins being touted as the most studied landform on Earth, with >1300 works investigating them (Clark et al., 2009). Despite continued research in this field, to this day no consensus exists as to how a field of drumlins develops (Clark et al., 2017) or whether drumlin formation relates to a specific set of glacial conditions (Eyles et al., 2016; Iverson et al., 2017; Ely et al., 2023). For this reason, I have so far assumed the only information preserved by bedforms is the orientation of the ice flow under which they form (Clark, 1993; Spagnolo et al., 2010; Ely et al., 2016) (see Figure 4.1c). However, it is a long held hypothesis that drumlins morphology likely holds more information about a past ice sheet's behaviour (Clark 1993; Stokes and Clark 2002). The issue of finding a universal drumlin formation hypothesis has historically been known as the ‘drumlin problem’ (Dowling, 2016).

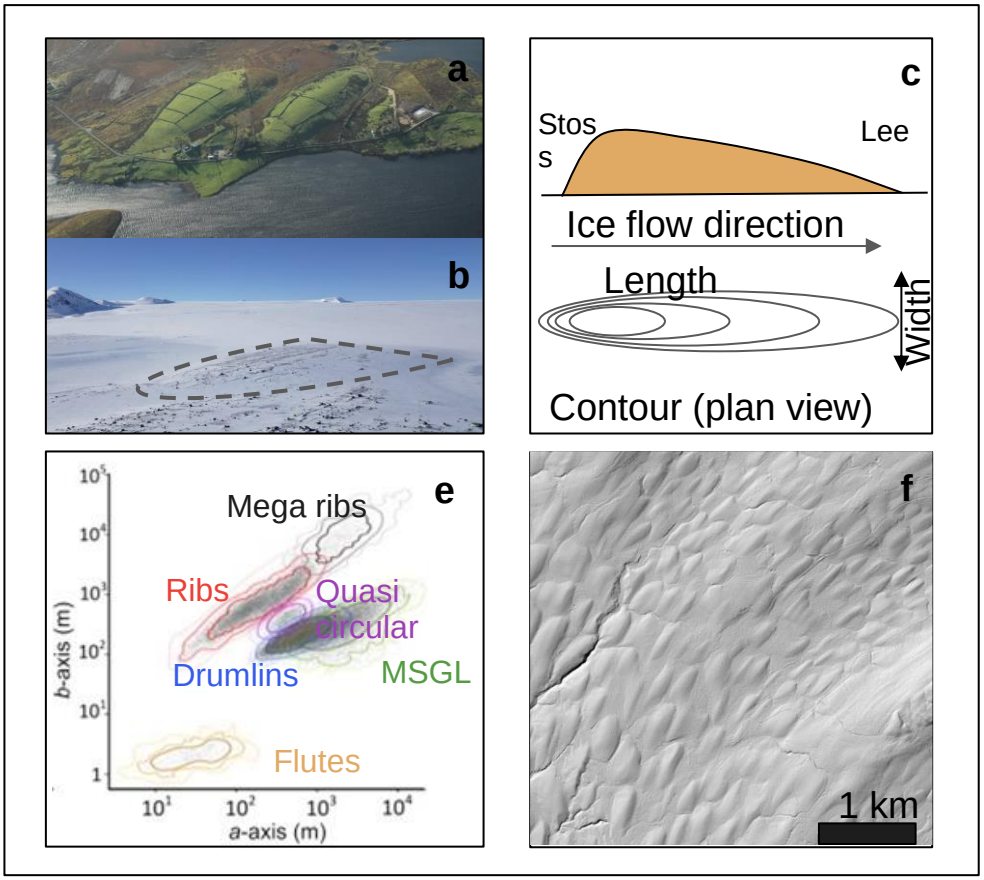

Figure 4.1: Drumlins and their descriptive attributes. 4.1a Aerial image of drumlins in Ireland (Michael Gibbons, 2015). 4.2b drumlin emerging from beneath the Hofsjokull ice cap. 4.1c Section view of drumlin with stoss and lee side annotated above, and plan with contour lines below. 4.1e Size/shape continuum of glacial bedforms from where the a axis is the distance down ice and b is the distance across ice (Ely et al., 2016). 4.1f is a relief-shaded DEM of part of a drumlin field in Ribblesdale, North Yorkshire. Produced from 2m Environment Agency LIDAR composite DTM and centred on [-2,305, 54,203].

Part of the motivation for such sustained study of drumlins stems from their anticipated relevance to both contemporary ice sheet dynamics and their utility in palaeo glacial inversion modelling and reconstruction (Stokes et al., 2013; 2015; Margold et al., 2013; Ely et al., 2019a; Gandy et al., 2019; Clark et al., 2022). Drumlins form at the ice sheet bed, and are thought to relate to a specific set of glacial conditions. The nature of these conditions is widely debated, but includes broad controls such as ice velocity (Clark, 1993, 1999; Hart, 1999; Stokes and Clark 2002; Stokes et al., 2013), ice thickness (Jauhiainen, 1975; Patterson and Hooke, 1995), effective pressure (Fowler, 2000), basal shear stress (Mitchell, 1994), consistent flow conformity (Wright, 1912), and smaller scale subglacial variations in till or bed characteristics (Eyles et al., 2016). For example, it has been proposed that drumlin formation would only occur if a saturated wet till is present and the effective pressure

(overburden minus hydrostatic pressure) is less than the shear stress over the coefficient of friction: or put differently a slightly wet, deformable till bed (Stokes et al., 2013). These conditions are traditionally very difficult for ice sheet glaciologists to observe as they all relate to subglacial conditions hundreds or thousands of metres below ice. Herein lies the issue and value in developing understanding of drumlins using contemporary glaciological methods: drumlins form underneath ice sheets, in parts of the ice sheet we do not fully understand and cannot easily observe. However, it is possible that such subglacial conditions are also associated with readily observable surface characteristics of the ice (e.g. velocity). Therefore, it may be possible to elucidate the glaciodynamic setting of drumlins from observations of the ice conditions during drumlin formation.

This chapter represents a first attempt at using PISM numerical ice sheet modelling outputs (discussed in detail in Chapters 2 and 3) to better understand the glacial conditions and environment that drumlins form in, so as to provide insight for testing drumlins formation hypotheses.

4.2 - Challenges with understanding drumlin formation

As with most phenomena, our first instinct when trying to understand the processes which lead to its occurrence is to try and observe the phenomena forming in nature. Such an approach is highly challenging with drumlins in the contemporary glacial setting, as formation occurs beneath ice sheets (e.g. King et al., 2007; Schlegel et al., 2022). These challenges are exacerbated by the fact that drumlin formation may occur over geological timescales, whilst also having the potential to remain ‘dormant’ beneath ice without affecting or being affected by the overlying ice (Clark 1993, Greenwood and Clark 2009b, Hughes et al., 2014). Historically, our understanding of drumlins has therefore primarily been derived from studying them in palaeo glacial settings (Clark et al., 2009; Ely et al., 2016). This offers two distinct benefits. i) the ease with which drumlins can be observed; and ii) the variety of endmember morphometries such a broad data set provides. Hundreds of thousands of drumlins have been mapped and analysed in a palaeo setting (Ely et al., 2016). In contrast, the number of drumlins observed in a contemporary setting (i.e. beneath ice) is likely less than 100. With this volume of palaeo drumlin observations comes countless hypotheses to explain their formation (Menzies, 1979; Shaw, 1983; Daris, 1985; Mitchell, 1994; Clark, 2010; Stokes et al., 2011; Dowlings, 2016, Eyles et al., 2016; Iverson et al., 2017). It is well beyond the scope of this chapter to address all of these hypotheses, and indeed many have been refuted (e.g. Shaw et al., 1989). However, I will touch upon some of the key

hypotheses I have considered in this work and some reasons for the breadth of hypotheses.

Likely one of the earliest sources of diversity in drumlin formation hypotheses stemmed from the breadth of bedforms attributed to the name ‘drumlin’ (Clark, 2010). This is not to say such definitions are ill founded, simply to highlight that the same formation mechanisms may not account for all bedforms known as ‘drumlins’. Stokes et al. (2013) highlights five main types bedform commonly attributed as drumlins in the literature: 1) mainly bedrock (or whalebacks); 2) part bedrock part till; 3) mainly till 4) part till/part sorted sediment; and 5) mainly sorted sediments. Though this is an oversimplification, it is a useful framework for understanding the type of processes which cause drumlin formation. Although such classifications exist, these are not universally used or recorded, largely due to the difficulty in identifying the internal structures without a sediment section or seismic/radar survey. Given the uncertainty about drumlin formation and difficulties distinguishing one class from another, in this thesis I consider all four classes which involve the reworking of sediment (2-5) to be drumlins. I therefore assume drumlin formation requires deformable sediment.

One of the few elements of drumlins which is not contentious is that drumlins form in the direction of ice flow (see figure 4.1c). Given this information and the prevalence of the bedform across deglaciated regions it is therefore not surprising that drumlins have a long history of being used to recreate past flow directions, and at times glacial conditions (e.g. relative velocity, thermal regime) (Charlesworth, 1953; Prest, 1969; Clark 1993, Greenwood and Clark 2009b; Hughes et al., 2014; Clark et al., 2022).

If drumlins do indeed require a specific set of glacial conditions, the presence or absence of drumlins could be used to specifically infer past glacial conditions (Clark, 1999; Clark et al. 2010; Strokes et al. 2013). Glaciologists therefore hope that drumlins may relate to very specific glacial conditions (e.g. velocity, thickness, shear stress, effective pressure), and if so, could in future be used to elevate palaeo glacial reconstructions.

4.2.1 - Bedform morphometry and ice flow conditions

One way in which glaciologists hypothesise bedforms may store information about palaeo glacial ice flow conditions, is through their morphometry: i.e. their size and shape. One of the most commonly described features of drumlins and glacial bedforms is their length (parallel to ice flow direction) or the ratio of such length to the (flow perpendicular) width which is known as the elongation ratio (Doornkamp and

King, 1971; Jauhiainen, 1975; Mills, 1987; Clark, 1993; Stokes and Clark, 2002; Stokes et al., 2013; Ely et al., 2016). The length or elongation ratio (length/width) is now widely used as a metric for distinguishing between the various bedforms such as drumlins and MSGL (see Figure 4.1c, e) (Clark et al., 2009; Zoet et al., 2021). Recent work has suggested bedforms (ribs, drumlins and MSGL) may form part of the same process, as a transition of length/width observations can be seen, suggesting they are members of a single continuous process which increasingly elongates the bedform (see Figure 4.1e) (Ely et al., 2016). A number of hypotheses have been put forward to explain variations in bedform length, with the most widely adopted hypothesis being that higher ice velocity causes longer more elongate bedforms (Clark, 1993; 1999; Hart, 1999 Stokes and Clark 2002; Stokes et al., 2013; Barchyn et al., 2016) (see figure 4.2).

Despite the prominence of the velocity/length relationship in the literature, a number of alternative hypotheses have been proposed including length as a function of sediment availability (Heidenreich, 1964; Rose & Letzer 1977; Barchyn et al., 2016), subglacial pressure (Jauhiainen, 1975), or a feature of the consistency of flow direction resulting in gradual elongation (Wright, 1912). It is important to point out that many of these hypotheses may not be mutually exclusive, and elongation may require a combination of factors. For example, flow consistency in part relates to the observation that more elongate bedforms are more parallel. However, increasingly parallel bedforms are also observed in the centre of ice streams which are regions with faster ice flow (Stokes and Clark 2002). A key element these hypotheses share is that of relating landform morphometry to specific glacial conditions such as velocity, or flow constancy. Frequently, this has been done by applying a conceptual ice sheet model to the palaeo glacial environment and inferring glacial conditions. Observing and identifying these metrics and contextualising them with drumlin formation observations has however proven challenging.

4.2.2 - Under which conditions do drumlins form?

One approach which has been used for understanding the ice flow conditions associated with drumlin formation has been to contextualise palaeo drumlin observations with respect to the wider palaeo glacial record. For example, Patterson and Hooke (1995) compiled a list of drumlin observations in the Northern Hemisphere and used palaeo records such as trimlines and margin position to estimate ice thickness. Similarly, Stokes et al. (2013) estimated the ice velocity under which bedforms are generated, by fitting a conceptual model of bedforms to a contemporary ice sheet setting (see Figure 4.2). Specifically, Stokes et al. (2013) observe that the

geometry of a field of lineation (consisting of ribs, drumlins and MSGL) aligns with that frequently observed in an ice stream and conceptually superimpose approximate velocities accordingly. This approach is not unique to Stokes et al. (2013) but provides an interesting approach to conceptually deriving and contextualising drumlin formation parameters.

Another approach to understanding the conditions associated with drumlin formation is to attempt to observe the process in the contemporary setting. This has been undertaken in Antarctica, with MSGL being identified beneath Rutford Ice Stream (e.g. Schlegel et al., 2022), Pine Island Ice Stream (e.g. Bingham et al., 2017), and Thwaites Glacier (Holschuh et al., 2020). This is the most direct approach for seeking drumlin forming conditions but is very expensive and logistically challenging, and as a result this has led to a small number of observations. Furthermore, simply because drumlins are observed beneath ice, does not mean that they are actively forming under those conditions; they could be a relic from previous ice flow.

Most recently, a third approach has been taken to understanding the formation of lineated bedforms which is that of model-data comparison. This method can be seen as the logical extension of the palaeo glacial inversion approach and used a numerical ice sheet model to calculate the glacial conditions associated with formation. Jamieson et al. (2016) used this model data comparison approach to infer the glacial conditions associated with palaeo MSGL in Marguerite trough, off the coast of Antarctica. The benefit of this approach is that a broader range of glacial conditions can be extracted such as ice velocity, shear stress and ice thickness which are hard to interpret in a palaeo setting.

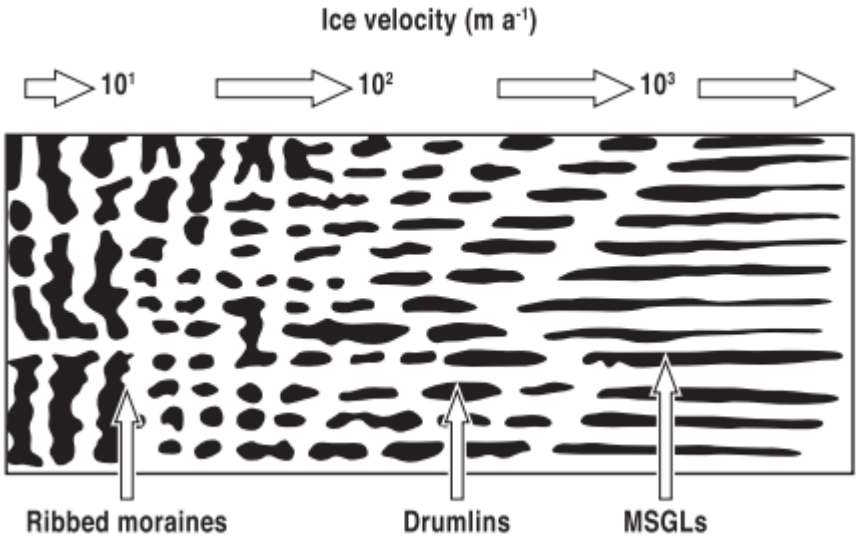

Figure 4.2: Proposed landform continuum and velocities from Stokes et al., 2013 (originally modified from Aario, (1977)) showing transition from ribbed moraine, through drumlins, to MSGL with increased velocity.

A third hybrid approach has also recently been implemented where emerging drumlins have been examined at the margin of the Hofsjokull Ice Cap in Iceland (Johnson et al., 2010; Benediktsson et al., 2016; Woodward et al., 2020). These works have combined satellite and field based observations with locations of known drumlin formation in an effort to combine the benefits of physically observing an emerging drumlin, with the benefits of observing ice flow associated with a drumlin. A pertinent question with all 'active' drumlin observations is, do they actually relate to the current ice conditions, or are the drumlins preserved from previous flow conditions?

4.2.3 - Does a drumlin forming switch exist?

A question which persists with all these methods of contextualising drumlin formation is: is the process continuous, or do drumlins relate to specific conditions (i.e. is there a 'drumlin forming switch' that turns on and off)? If there is no switch, then drumlins continuously form under all conditions. Continuous drumlin formation would suggest that drumlins were being reshaped until they became ice-free. Significantly, this would mean any drumlins observed beneath ice would be actively forming. At one extreme of such a hypothesis, the lack of any 'switch' would mean drumlins could provide no insight into glacial conditions as they would always form regardless of any changes in glacial condition. In contrast, the presence of an identifiable set of drumlin forming conditions, or 'switch,' could allow drumlin formation to halt, without drumlins being removed from the bed. If this switch related to a very narrow range of conditions, it could have significant implications for the understanding of both palaeo and subglacial drumlins, as episodes of drumlin formation to specific conditions. Similarly, in the contemporary environment, the existence of a drumlin forming switch would need to be carefully considered before drumlins presence could be used to infer subglacial conditions as they may be dormant. The growing consensus in palaeoglaciology is that some degree of a drumlin forming 'switch' exists. However, the specificity of the conditions required for such a switch is unknown. Several pieces of evidence suggest such a mechanism must exist. For example, if no switch existed, drumlins would continually reorientate, and we would expect all drumlins to align with ice marginal geometries which is not the case. Similarly, the presence of superimposed cross-cutting drumlins indicates the potential for multiple phases of formation (e.g. Rose and Letzer, 1977) again suggesting formation halted and recommenced (I discuss cross cutting drumlins further in Section 4.4.3). Despite this evidence, the presence of such a switch is rarely discussed in the context of drumlin observations beneath or in front of

ice, and subglacial crosscutting drumlins are yet to be observed subglacially (e.g. in Iceland or Antarctica).

4.2.4 - Contradicting drumlin formation hypothesis

Despite the complexities associated with observing drumlins and their associated formation mechanisms, numerous hypotheses have developed as to how drumlins form. Some of these have been operationalised as numerical models which can 'produce' bedforms; some of these explain the process mathematically, while some remain conceptual models of the process.

A core issue of the 'drumlin problem' has been adequately explaining how and why drumlins form from an initially flat bed. This aspect of drumlin formation has largely been absent from early formation hypotheses which are sometimes more adequately described as explanations of how a bump becomes streamlined (c.f. Clark, 2010). The lack of ability to account for this central process has stalled many hypotheses for decades as they frequently require preconditioning on the bed (e.g. Hart, 1997) which cannot explain the regularity of many drumlin fields (Clark, 2010; Ely et al., 2018, Clark et al., 2018). As an important aside, in defence of many early drumlin formation hypotheses, it should be noted that many hypotheses were put forward before the widespread acceptance of subglacial till deformation and the impact this had on glacial beds (e.g. Smalley and Unwin, 1968; Boulton, 1979; Boulton and Jones, 1979; Boulton and Hindmarsh, 1987). Similarly, many of these hypotheses also attempted to explain drumlins in isolation, whereas academic consensus now focuses on drumlin formation as part of a field (Ely et al., 2016). It was therefore not until the notion was put forwards of drumlins existing as peaks and troughs within a field, composed of a viscous till, that the new phase of drumlin formation hypotheses I focus in this chapter begin to arise.

In an effort to account for the challenges associated with understanding how drumlins form from an initially flat bed, Barchyn et al. (2016) created a 'reduced complexity model' which drew from sand dune modelling. Barchyn et al. (2016) looked to identify key elements of bedform formation and used these to build drumlins as part of a landform continuum. This work resulted in one of the most visually convincing sets of modelled drumlins (see Figure 4.3) and highlighted the importance of ice sheet velocity and subglacial sediment in the process of bedforming. The mass conserving model uses erosion and deposition to sculpt bedforms. However, it has been widely criticised for using incomplete physics of the process (Fannon et al., 2017; Fowler, 2018; Ely et al., 2023) This is largely due to the reductionist approach to modelling the system means that it does not "reflect the physically appropriate processes involving

water and sediment transport" (Fannon 2017, p.2). This is a key limitation with this model and is likely the core reason it has not yet been expanded upon since publication.

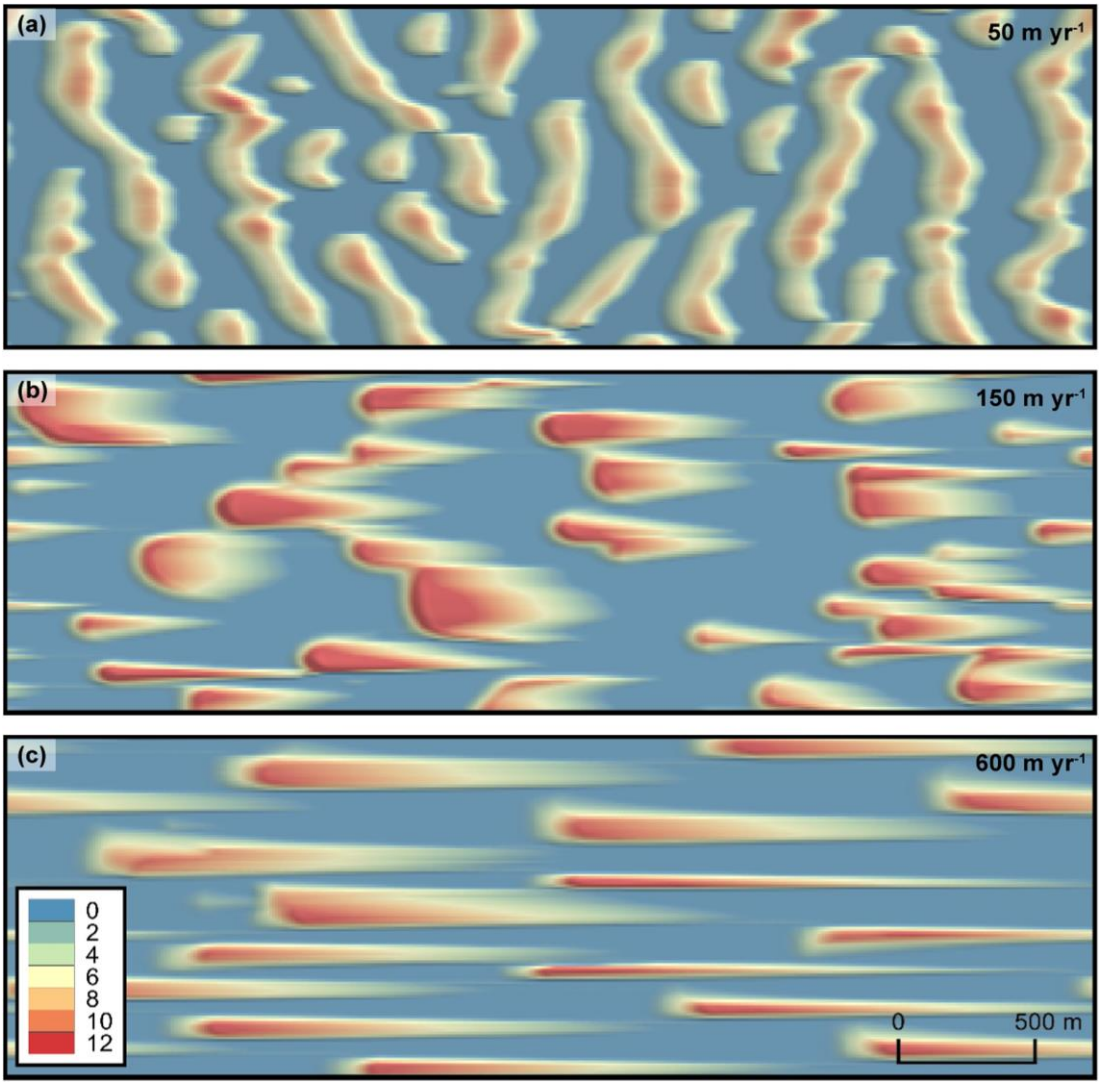

Figure 4.3: Modelled transition from ribbed moraine (a) to drumlins (b) into MSGL (c) reproduced from Barchyn et al. (2016) model of drumlin formation. Colour scale is not specified but assumed to be vertical height of bedforms (in metres). Barchyn et al. (2016) highlight modelled velocities that each bedform type develop under ranging from 50 to 600 ma^{-1}.

In contrast, the erodent layer hypothesis of Eyles et al (2016) suggests that drumlins form as the result of a purely erosional processing. The presence of contradictory landform evidence in the form of hybrid erosional and depositional landforms makes it difficult to expand upon this conceptual model (Johnson et al. 2010; Spagnolo et al., 2014).

In 2017, Iverson and colleagues published a drumlin formation hypothesis and mathematical model which addresses this dichotomy of erosional and depositional drumlin formation. Specifically they focused on the emerging drumlin field of Múlajökull on the Hofsjökull ice cap. Although this model accounts for both erosion and deposition, it employs a dual phase method, with erosion occurring during ice flow quiescence and deposition occurring during surges. This mechanism was based on the observation that proglacial drumlins terminating at the surging ice margin of Múlajökull were draped in an apron of till (Johnson et al. 2010; Benediktsson et al. 2016; Woodward et al., 2020). For this mechanism to be more widely applicable to all drumlins, surging glaciers would need to be more common than observed in contemporary ice sheets. Furthermore, an additional mechanism would be required to explain the regular spacing observed within drumlin fields (Ely et al., 2023). Questions therefore remain as to the wider application of such a mechanism. Alternatively, the till aproning event which is central to this hypothesis may be merely a confounding factor associated with surging over pro-glacial drumlins, and the internal bedding of sediments observed in Iceland (and elsewhere c.f. Spagnolo et al., 2014) may be the result of another process.

The final formation method I will discuss is the so-called ‘instability hypothesis’, a branch of mathematics first applied to the context of drumlin formation by Richard Hindmarsh (Hindmarsh, 1998a; 1998b;1999). This hypothesis stems from the notion that the interface between two viscous fluids is fundamentally unstable. A consequence of this instability is a positive feedback loop in which small perturbations will grow, leading to regularly spaced bedforms. In instabilities, transverse and longitudinal bumps preferentially grow at certain wavelengths, in our case producing a drumlin. This formation hypothesis has gained increasing traction over the last two decades as it is able to account for both the formation and subsequent shaping of a wide range of observations of bedforming by both deposition and erosion (Fowler, 2000; 2010; Schoof 2007; Stokes et al., 2013; Chapwanya, et al., 2014; Dowling et al., 2016; Fannon et al., 2017; Fowler 2018; Ely et al., 2023). A range of numerical models have been able to use the hypothesis to recreate 2D and 3D bedforms including, ribs, drumlins, herringbones, and potentially MSGL (Hindmarsh, 1998b; Chapwanya, et al., 2014; Fannon et al., 2017; Fowler 2018; Ely et al., 2023). Most recently, the work of Ely et al. (2023) was successful in using this hypothesis in a physics grounded model to build (grow) idealised ribs (See Figure 4.4a), drumlins (see Figure 4.4b) and MSGL (see Figure 4.4c) in three dimensions, from a flatbed.

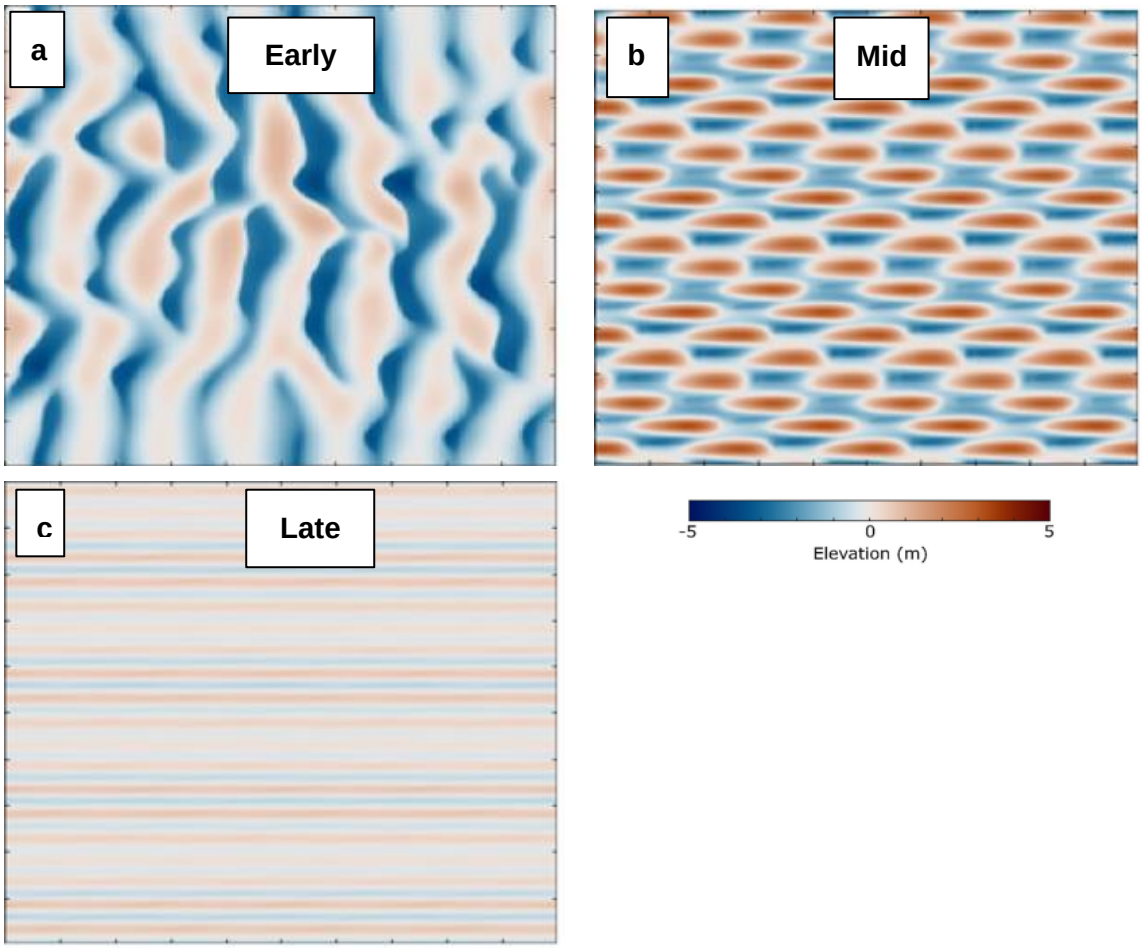

Figure 4.4: Numerical modelling of the bedform continuum developing as a continuous field. Bedforms can be observed to develop from ribbed moraine (panel a) into drumlins (panel b) then into MSGL (panel c) over modelled time. Note modelled ice flow from left to right across a 10 by 10 km domain. Figures are modified from Ely et al. (2023).

4.2.5 - Rationale

Despite the challenges in deciphering the relationship bedforms have with glacial conditions such as ice velocity and thickness, improved understanding might help produce the next generation of sliding laws. The prevalence of drumlins in the palaeo environment suggests they are likely a major component of the wider glacial context.

Although I have touched on only a fraction of the competing hypotheses for drumlin formation, as Shaw put it “There are almost as many theories of drumlin formation as there are drumlins” (Shaw, 1983, p.476). With promise from recent work that the issue may be partially resolved (Ely et al., 2023), I propose that a key element required to advance the ‘drumlin problem’ is to know more about the physical conditions under which drumlin form. Such knowledge might help establish which drumlin forming hypothesis or models are correct, or help inspire new developments.

Here I develop and apply a new method of exploring drumlin formation which uses a numerically modelled ice sheet simulation as an 'observational' environment. In doing so, I will be able to combine the benefits of the palaeo record (large extensive dataset of bedforms with a breadth of bedform types), with the benefits of numerical modelling, as a quantitative approximation of ice sheet conditions such as thickness and velocity. Using the British and Irish drumlin database (Greenwood and Clark 2009, Hughes et al., 2012) and a numerical ice sheet simulation (Ely et al., in prep) (see Chapters 2 and 3), this chapter answers the following questions:

1. What ice flow conditions (thickness, velocity) did drumlins form under?
2. From the model-data relationships, can we infer episodic events or continuous drumlin formation; i.e. is there a drumlin switch?
3. Does drumlin length relate to ice flow conditions?

4.3 Methods

In this chapter, I use a numerical ice sheet simulation of the BIIS (produced in Ely et al., in prep. and discussed in Chapter 2 & 3) to explore the physical environment of drumlin formation. I identify a number of points in time when modelled ice flow direction is found to be parallel with drumlin fields (see Chapter 3) which I propose to be potential periods of drumlin formation. I explore these phases of potential formation to extract the modelled ice sheet parameters at times and locations where drumlins may have formed. Using this approach, I am able to explore potential drumlin formation scenarios over long time scales. The crux of this approach is distinguishing between drumlin forming events, coincidental model/data matches and model or data errors. To achieve this, I have developed a novel combination of statistical and automated methods to establish when potential drumlin forming events may have occurred and to extract these modelled ice sheet parameters.

4.3.1 - Model data comparison

The core method used for this work is the flow conformity tool Automated Flow Direction Analysis (AFDA) discussed in Chapter 3, which was developed by Li et al. (2007) and expanded upon by Ely et al. (2019). In short, AFDA identified times when specific flowsets align with modelled ice flow directions. The fundamental assumption of this work is that if drumlin orientation aligns with ice flow, drumlin formation could have occurred at this time and under the modelled physical conditions. Based on this

assumption I explore a number of scenarios which may be associated with drumlin formation.

When selecting the ‘best model run’ in Chapter 3 I looked to identify if the ice sheet was broadly flowing in the right direction, and therefore used a mean residual vector threshold of 45 degrees as a fairly loose constraint. For drumlin formation investigation, a higher constraint is required and a lower threshold of 20 degrees was chosen. It should be noted that although a 20-degree offset may still seem high, this is a maximum mean value and in practice this results in a high level of conformity across most of the flow field when compared by eye.

4.3.2 - Model and data selection

The drumlin dataset consists of 122 drumlin fields across Britain, Ireland, and offshore (described in full detail in Chapter 3). The flowsets used in model selection had been subtly amended to remove a small number of pixels where no drumlins existed within a flowset (e.g. evidence of streamlined bedrock were used to connect voids within a drumlin field). These pixels accounted for less than 1% of those considered in Chapter 3.

A gridded dataset of drumlin lengths per flowset was produced to compare against model metrics. If a drumlin fell over multiple pixels, the total length of the drumlin was assigned to all pixels it overlapped. When multiple drumlins sat in a pixel the mean drumlin length was calculated. A raster layer was then created for each flowset, and combined into a single NetCDF file. This results in one array per flowset, with each pixel representing the mean drumlin length of the intersecting drumlins. Drumlin length was only calculated for terrestrial drumlins of Britain.

This chapter uses PISM simulation 441 as the numerical model run. This model run was identified in Chapter 3 as proving the best compromise between flow geometry and ice extent. The rationale being that optimising for flow geometry is crucial for identifying timings of potential drumlin formation, while optimising for ice extent is important for understanding the spatial relationship drumlins have to the glacial extent. Cross examination against a GIA corrected simulation suggested ice mass was well constrained through the selection process. Furthermore, if I correctly identify ice extent and flow direction, with a realistic ice volume it is hoped that this also results in realistic ice flow conditions (velocity, shear stress).

4.3.3 - Bedforming parameter extraction

To understand drumlin forming events I use two primary measures of the conditions a drumlin field has been exposed to. The first of which is the pixel value of a specific parameter (e.g. velocity, thickness, shear stress) and the second is the cumulative parameter (e.g. cumulative velocity). Pixel based parameters are the primary metric used for exploring the conditions of drumlin formation. Simply put, these are the model output parameters, in a gridded format (e.g. one value per 5 km cell). These parameters are extracted at the flowset level for the entire flowset, if the flowset has a sufficient AFDA score. This approach offers the benefit of statistical robustness in selecting timings of matches which are realistic with regards to the whole flow field, rather than extracting the parameters of an isolated drumlin during a match. A consequence of this approach however is that flow orientation may not align with every cell in a drumlin field (particularly with larger flowsets averaging may hide outliers). Pixel based measures are then either aggregated to produce summary statistics of that point in time, stored as discrete values without their geographic relationship (e.g. for the total number of cells which a specific magnitude), or preserved in their spatial configuration for comparison against other bedform metrics (e.g. length). Pixel based metrics are also the foundation used for calculating mean velocity and thickness over time.

To understand the potential impact of prolonged periods of potential drumlinisation or flow continuity, I developed a measure of bedform parallel ice activity called cumulative velocity (CV). CV represents the time transgressive sum of the pixel based parameter at an array scale. CV provides a metric for how much ice moved over an area (ice flux) of drumlinised terrain for the duration of the flow match period. The method of calculating cumulative parameters is initially identical to that of calculating pixel based parameters. However, each time step where the match criteria is met the array is combined with separate cumulative array. This results in a final array which preserves the geographic locations of CV in which each cell representing the cumulative metres of ice which has moved over the specific cell (generally represented in km).

4.3.4 - Data processing and filtering

A central source of uncertainty when exploring the potential drumlin forming match is which ice parallel events resulted in drumlin formation and which are merely coincidental model data matches. Consider a flowset that only matches modelled flow geometry once and for a brief period in time (e.g. 100 years). In such a scenario,

assuming the model and data are correct, I can infer the observed event formed the drumlins. These matches are preferential, but limited in number (two 100 year matches, less than ten 500 year matches). I therefore look to use longer model data matches and identify when the drumlin forming event took place. However, as matches become increasingly long or more frequent, the risk of observing coincidental matches increases. Therefore, when creating a frequency distribution of ice parallel velocities for a long match, I might observe two signals to be combined into one; a signal of drumlin forming velocities and a signal for coincidental non drumlin forming velocity. For example, observing the velocity of a long model data match, a bimodal distribution (see Figure 4.5a) is often produced. In contrast, a sample of the natural variation in ice velocity across the ice sheet produced a predictable unimodal distribution (Figure 4.5b), which aligns with the lower velocity peak observed in the drumlin forming events with wide possible timing constraints (Figure 4.5c). In practice, as match length increases, the signal progresses from a distinct unimodal signal, to a bimodal signal, with the magnitude of the lower velocity peak increasing with match length. To overcome these issues, I present a method of isolating the coincidental signal from the drumlin forming signal for longer model data matches (see Figure 4.5d). This filtering approach allows me to isolate the drumlin forming velocities from an observation of drumlin formation, where not all points in time or space obviously relate to a discrete drumlin forming event but where a distinct signal which is apparent above the background signal.

To perform distribution filtering, I take a random sample of a 2×10^7 values of an ice sheet parameter (e.g. velocity) over time and space so as to account for the natural variability anticipated across the ice sheet. Each pixel must meet the sampling criteria of a match (e.g. >10 m ice thickness, >10 ma^{-1} velocity, grounded ice, and sediment based) and are randomly sampled over time and space until the sample is of the specified size. This base distribution is then subsequently resampled to create a bespoke distribution of anticipated natural variation of the same sample size as the potential drumlin match. This new sample represents the distribution velocities anticipated from a coincidental match of the same spatial size and magnitude of a potential drumlin forming event. By resampling a larger natural variability sample, I avoid some of the issues with creating small ‘random’ samples of the ice sheet and consistently recreate a representative sample with the same natural distribution as the ice sheet. As total match length increases the magnitude of the background distribution must be scaled accordingly. I restrict the use of distribution sampling to flowsets and observations where a clear baseline and anomaly event is visible. When no such

anomaly is visible, distribution filtering is not used. All plots where filtering is used are clearly described in the figure caption as is distribution scaling magnitude.

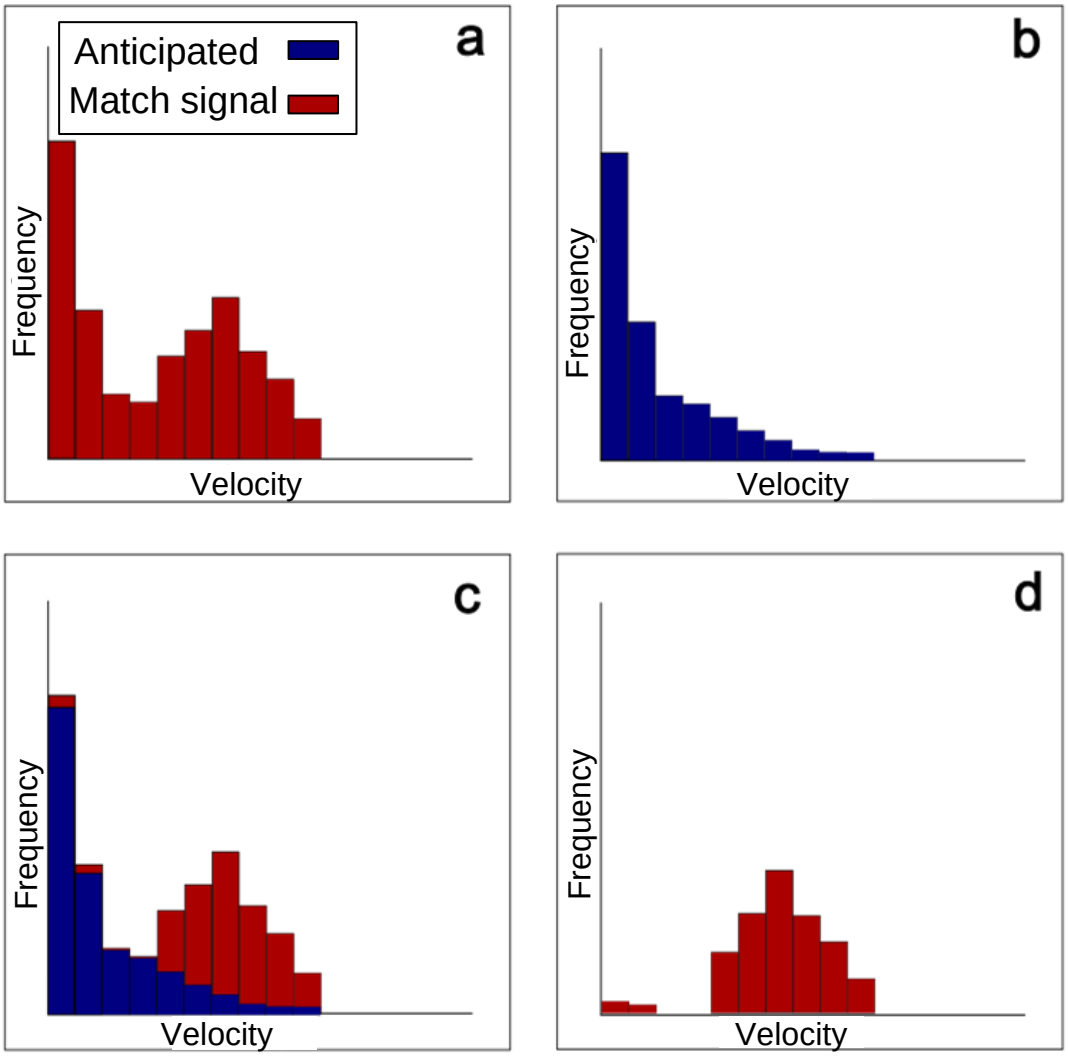

Figure 4.5: Filtering coincidental model data matches using distribution filtering. 4.5*a shows the initial mixed distribution combining likely drumlin forming events with coincidental matches.* 4.5*b shows the distribution of natural variability of the ice sheet velocity (i.e. anticipated coincidental drumlin match).* 4.5*c shows an anticipated coincidental match signal, derived from a random sample of natural variability of the ice sheet overlaid on a combined signal.* 4.5*d shows drumlin forming velocities (without anticipated coincidental match velocities).*

4.4 - Results

4.4.1 - The ice flow velocity and thickness during model-data matches

The initial premise of this chapter is that any point in time when a drumlin field aligns with ice flow could represent a drumlin forming or reorientation event. This provides a useful starting point as it frees us from excessive preconceptions of potential drumlin formation hypotheses. When we take this approach and apply it to all ice sheet velocities we observe a bi-modal distribution (idealised in Figure 4.5a), with a primary modal peak of 25 m and a secondary modal velocity of 200 m. We observe ice flow/bedform 'matches' lasting between 100 years and 15,000 years with most flowsets matching more than once. It is possible therefore that not all points in time where ice flow aligns with bedforms are representative for identifying bedforming conditions. Or in other words, some of these matches occur by coincidence or without forming drumlins. In an effort to account for the potential of coincidental matches, as match length increases, I remove the anticipated signal expedited from a coincidental match (Figure 4.5).

I use a statistical approach to try and filter out coincidental matches which I apply to the full dataset and a subset of matches (see Section 4.3.4). When we remove any anticipated coincidental samples from our observations we are left with a defined unimodal signal, and the data shows an association with modelled velocity of 100-350 ma^{-1} (see Figure 4.6). These velocities are also consistent with the short unfiltered individual matches (discussed in section 4.4.1.1) where there is less uncertainty about the timing of the event and therefore no anticipated coincidental signal. Furthermore, these filtered velocities are consistent with those observed for drumlins and MSGL beneath Rutford Ice Stream (King et al., 2006; 2007; Smith et al., 2007; Schlegel et al., 2022), Pine Island Ice stream (Bingham et al., 2017) and Thwaites Ice Stream (Holschuh et al., 2020), which are the three locations where subglacial lineations have been observed beneath an ice sheet. The relationship of these parameters to these contemporary ice sheets is further outlined in section 4.5.3.

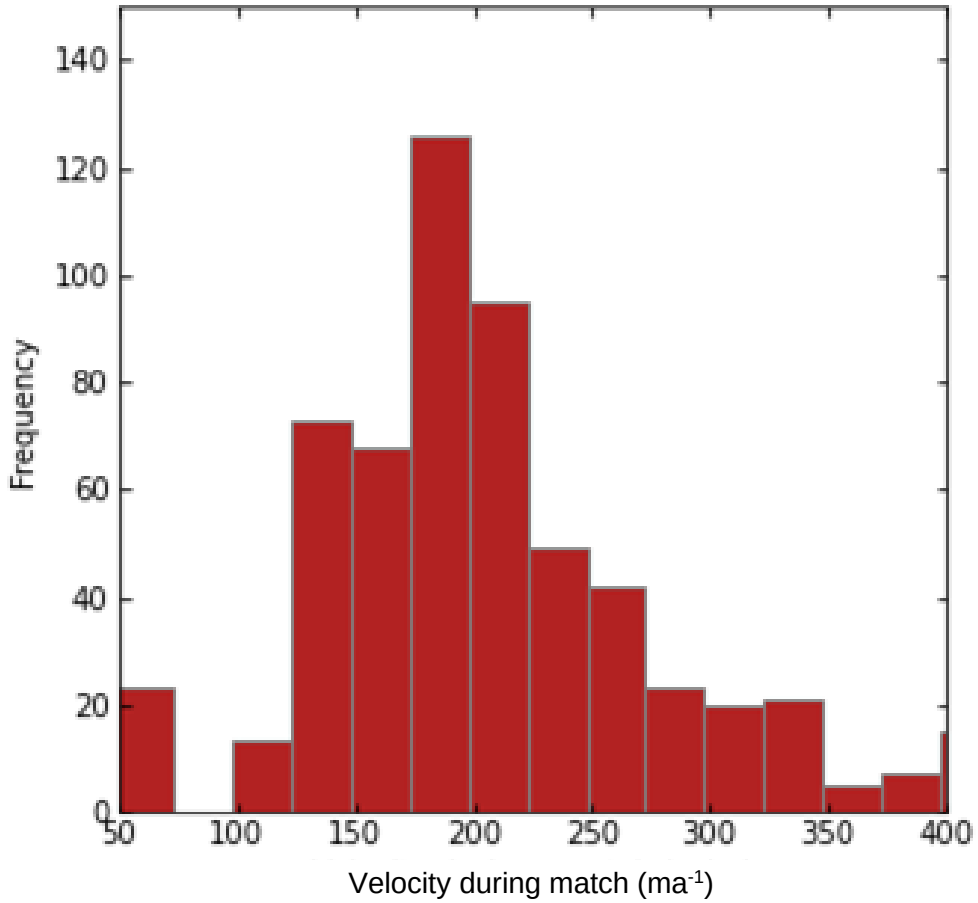

Figure 4.6: Distribution of velocities during a directional model-data match. All model data matches filtered using distribution filtering. Only velocities above the distribution of anticipated coincidental velocities are included. Drumlins are associated with a modal velocity of 175-200 ma^{-1} and sit within a range of 100-350 m/yr.

Ice thickness data shows a pronounced modal thickness of 1025 m during matches (see Figure 4.7). It should be noted, however, that unlike ice sheet velocities which appear to have a distinct modal velocity an order of magnitude above that of the modal background velocity. The modal match and baseline ice thicknesses sit within 1σ of the full dataset mode. The distribution of modal thicknesses within a match have a significantly lower range in comparison to the full distribution. In addition to the lower range drumlin matches have a higher amplitude than the upper and lower quartiles, meaning distribution filtering still results in a prominent peak at 1025 m ice thickness. A potential by product of the distribution frequency filtering is the removal of a secondary peak which can clearly be observed prior to filtering at 2500 m. This ice thickness could be considered in future work as a potential thickness of importance for drumlin formation.

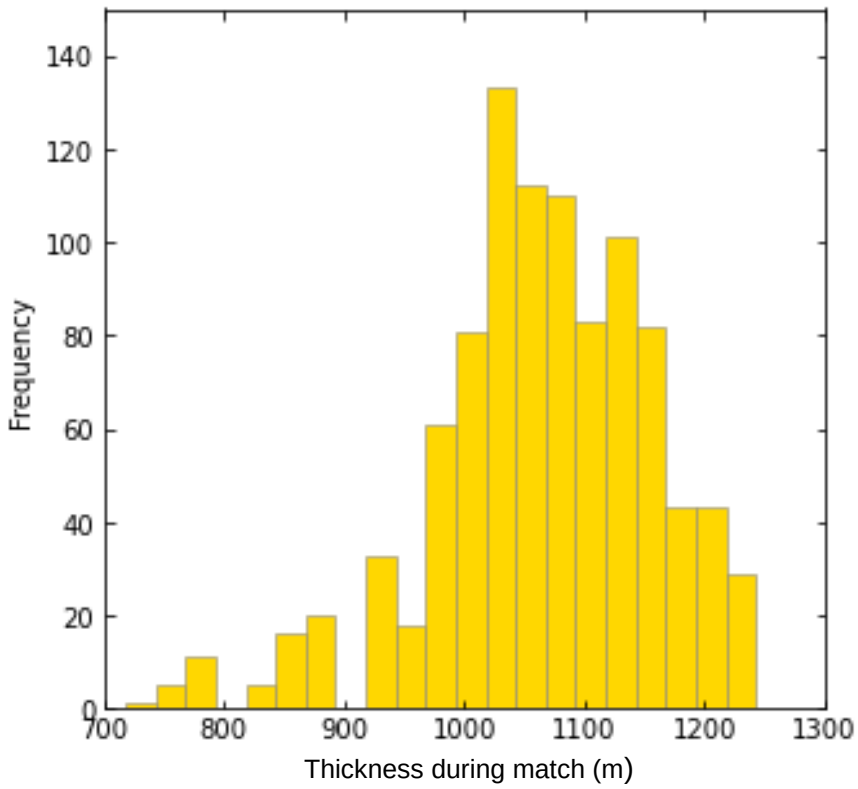

Figure 4.7: Ice thickness of drumlins with ice parallel flow. Frequency distribution of drumlins during matches with distribution filtering applied. A modal distribution of ice thicknesses can be observed at 1025 - 1050 m.

4.4.1.1 - Short and single matches

The association in velocity and thickness is observed across three types of model-data match: short unfiltered matches (likely the most robust), medium length filtered matches, and the full filtered dataset (including all lengths of matches). Short matches last from one to several hundred years and can be characterised by a well pronounced mode (see Figure 4.8a) as a result of minimal variation in ice flow velocity. In examining short matches, I anticipate only observing the ice flow conditions of the drumlin forming or reorienting event. Unfortunately, these short matches are limited in number (less than 10% of all matches) so result in a small sample size. However, some medium length matches (up to 1000 years) show a clear bimodal signal (4.10b). To retain some of the medium length matches where I am uncertain about the specific timing of drumlin formation, I implement distribution filtering to remove the coincidental (outlined in section 4.3.4 & Figure 4.5). Longer matches show a characteristic velocity distribution (see 4.10c), which sits between that of the pronounced bi modal (4.10b), and the coincidental signal (see 4.10d). As match length increases, the distribution trends towards that anticipated from a coincidental match.

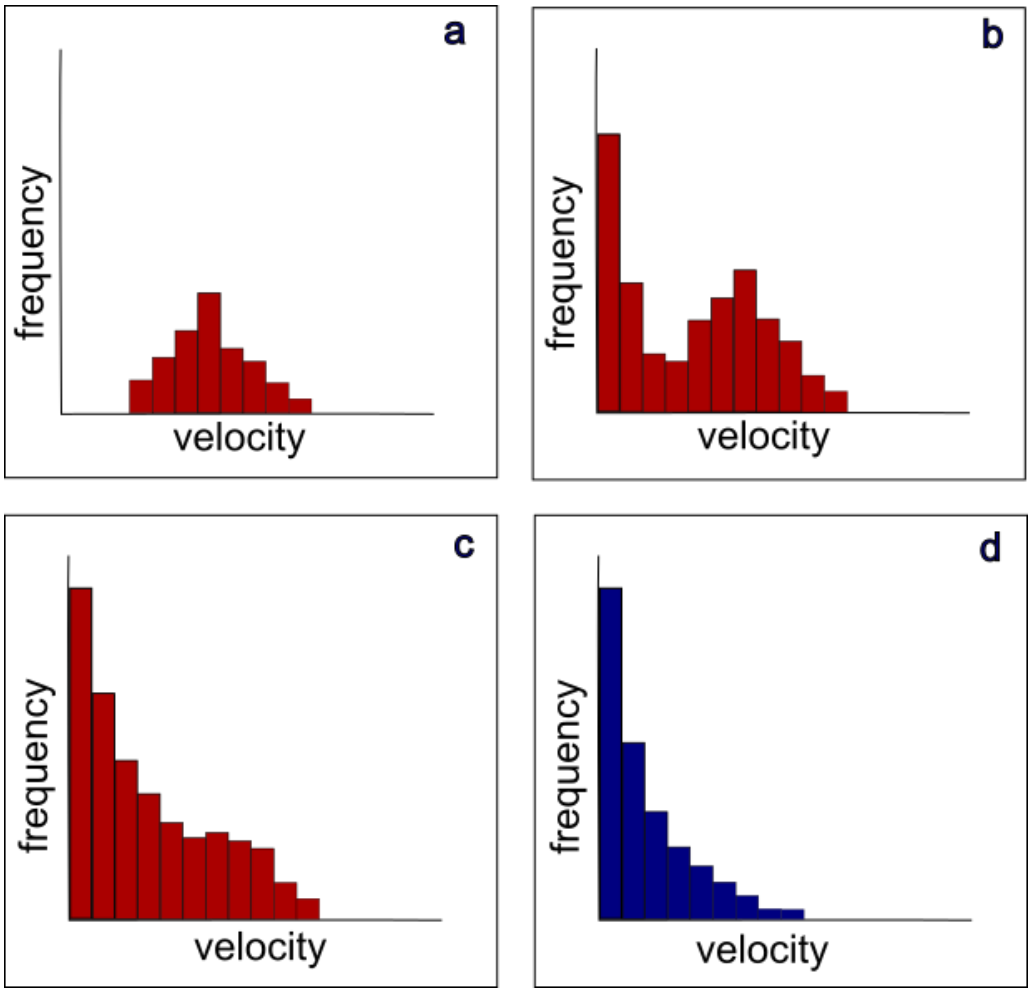

Figure 4.8: Unfiltered distributions associated with different match lengths. 4.8a shows the distribution of a short model data match. 4.8b shows a medium length match with a clear secondary peak, likely associated with drumlin formation. 4.8c shows a long match where the drumlin forming match is not obvious. 4.8d shows the distribution of the natural ice sheet (i.e. if we don't deliberately sample regions of potential drumlin formation). As match length increases the signal transitions from 4.8a, through 4.8b, to 4.8c, until the point in which it cannot be distinguished from 4.8d. Filtering method used to remove the coincidental signal is outlined in Section 4.3.4.

To validate the observations on the full dataset and further explore mechanisms of drumlin formation, I identify short matching events with high confidence in the timing and glacial conditions. To select these events I looked to limit uncertainty about timing. As a result, I selected flowsets which only matched for a single 100-year period (one model time step). In such scenarios, assuming the model is correct, and the drumlin field is of Devensian age and appropriately grouped, the observed model conditions must have formed the drumlin field. Only two drumlin fields met this criteria FSx4c (in Ireland) and FS35 (in Scotland). FSx4c is a topographically confined drumlin field at the southern extent of the last BIIS (see Figure 4.9b). FSx4c was mapped as part of a

larger diverging flowset, FSx4, but was identified as being a separate flow event as it was spatially separated from the rest of the drumlin field (Greenwood and Clark, 2009a). Model-data comparison puts FSx4c matching as part of a gradual retreat of the southwestern sector of the BIIS following a period of minor advances and retreats (see Figure 4.9c). This timing is in line with what was proposed in the detailed reconstruction of Greenwood and Clark (2009a). The data show a modal velocity of 240 ma^{-1}, which sits within the range of velocity identified for the full dataset (see Figure 4.6).

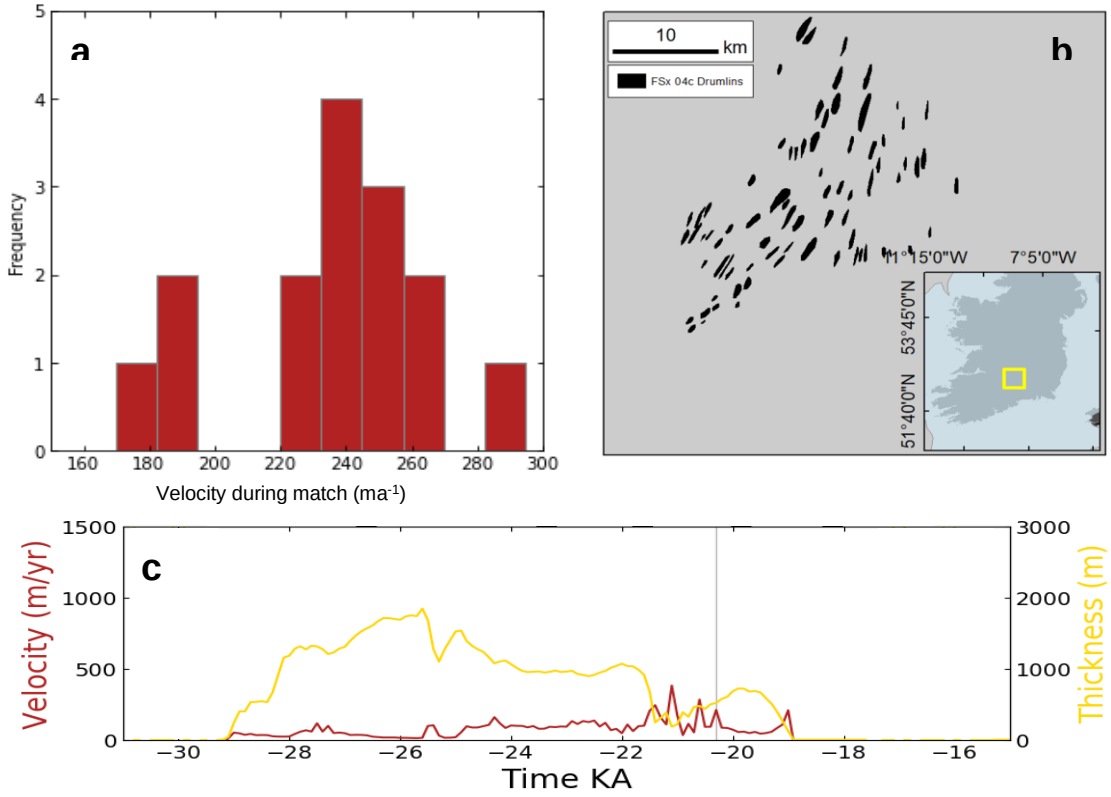

Figure 4.9: Short 100 year match of FSx 4c. 4.9a shows the frequency distribution of velocities of ice parallel drumlins with no background noise scaling. 4.9b slows location of drumlins in Southern Ireland, where ice is modelled to flow southwest. Figure 4.9c shows mean ice velocity and ice thickness of pixels within the flowset.

The second flowset I identified as having low timing uncertainty with a short model data match, was FS 35 (see Figure 4.10). FS35 is located south of the Moray Firth, and represents a rare example (for the BIIS) of onshore ice flow (see Figure 4.10b). Modelled velocity observations indicate that ice flow was faster than that of the natural ice sheet variation (anticipated coincidental signal) with modelled velocities ranging between 60 and 120 ma^{-1} with a mean velocity of 100 ma^{-1}. Neither of the short matches (FSx4c or FS 35) required filtering to remove 'background' signal and both flowsets matched velocities consistently above that of the 'background' ice which would be anticipated from a natural distribution in ice sheet velocities.

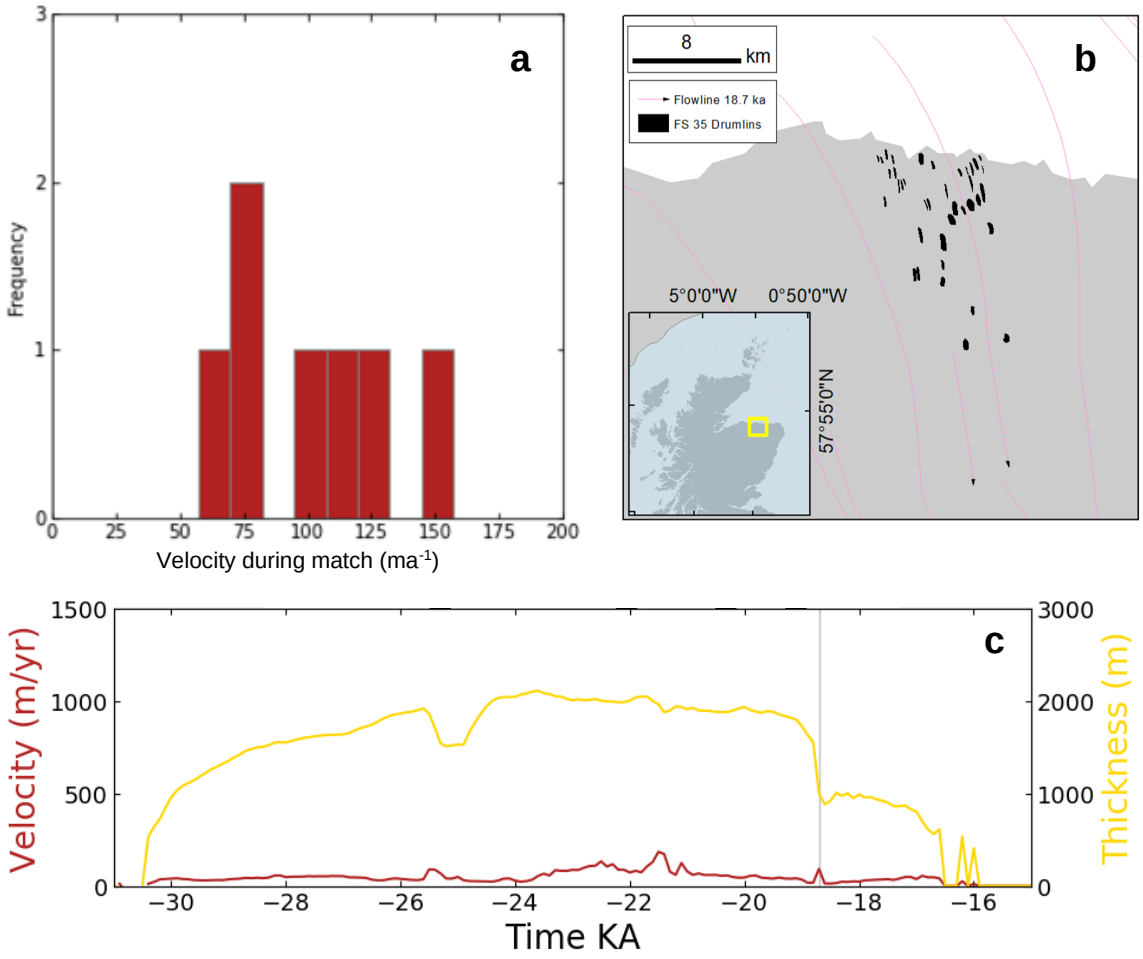

Figure 4.10: Short, 100-year, match of FS 35. 4.10a shows the frequency distribution of velocities of ice parallel drumlins with no background noise scaling. 4.10b slows location of drumlins in northern Scotland, with an onshore ice flow. Figure 4.10c shows mean ice velocity and ice thickness of pixels within the flowset.

An important consideration when selecting short matches was to validate the thickness estimates from the filtered matches of the full dataset. In Chapter 3 I conducted a second pass to assess model fidelity to ice thickness through a best estimate simulation nudged to fit the GIA signal (BC model; Clark et al., 2022). I identified a potential bias that means that ice thickness may be overestimated in this model simulation by 200 m. This overestimate would be most pronounced between 27 ka and 19 ka (see Figure 3.11/3.12). The majority of short to medium length matches occur outside this time window of highest misfit and sit within the range of the full filtered dataset (Figure 4.6).

FSx4c and FS35 were the only single, 100-year matches observed to occur on the ensemble run. I therefore gradually increased the match length to ascertain if these observations were consistent over longer matches. FSx18 is located in Ireland and

matched for 200 years during the deglaciation of the southern sector the BIIS (see Figure 4.11c). FSx18 showed a clear bimodal distribution, therefore I applied distribution filtering to isolate the second peak. The filtered data shows a clustering of velocity generally above 100 ma^{-1} with a modal velocity of 150 ma^{-1}. This aligns with observations of both the full dataset and unfiltered sites (see Figure 4.11a). Thickness observations also align with those of the full database with a modal thickness of 950 m (see Figure 4.11b). Unlike velocity observations which have a high variance, I predominantly present unfiltered thickness observations as neither a baseline or anomalous signal is obvious.

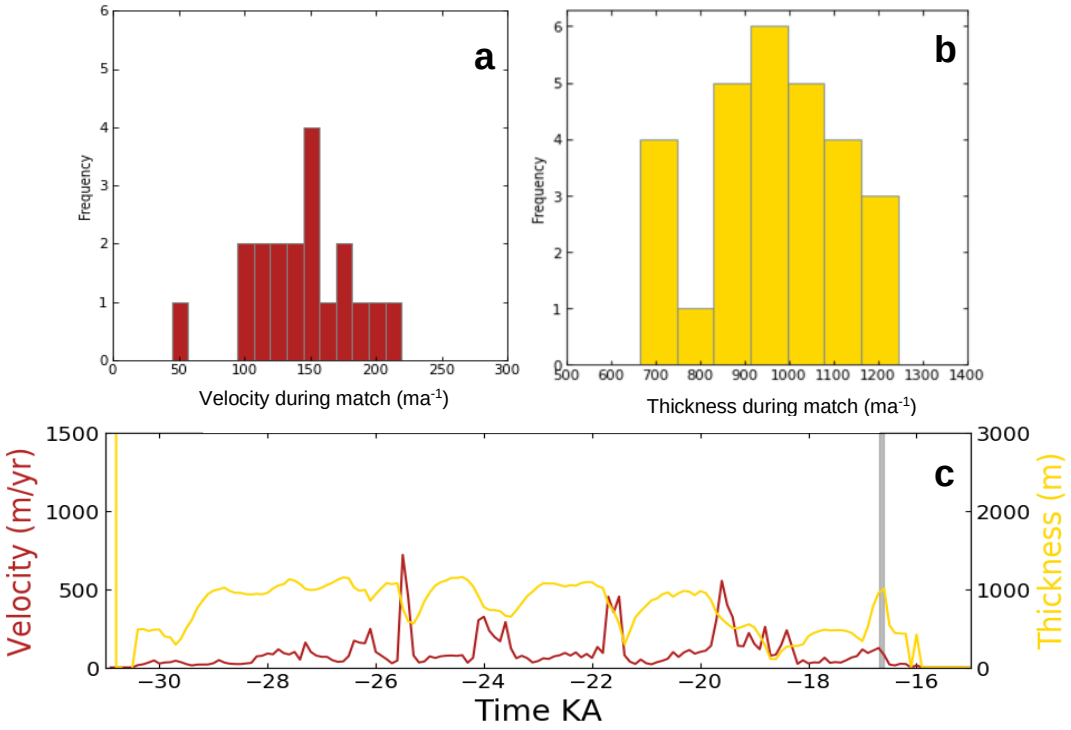

Figure 4.11: Velocity and thickness during match of FSx 18 in Ireland. 4.11a shows a cumulative frequency distribution of Fsx18 with a modal velocity of 150 ma^{-1}. Note a scaling factor of two is used on the background velocity signal. 4.11b shows ice thickness during match with a range and modal thickness similar to those of the full dataset. 4.11c shows the mean ice thickness and velocity over time and a grey band where model data match is met.

A clear bi-modal distribution can be observed in matches up to approximately 1000 years. FSx 32 matches for 900 years and shows a strong modal after distribution filtering. (see Figure 4.12). A pronounced mode in velocity can be observed at ~125 ma^{-1}, with no observations below 50 ma^{-1} (see Figure 4.12a). Bi-modal distribution are observed in longer matches. As the coincidental match component increases (i.e. with longer model data matches) it becomes harder to distinguish a pronounced modal

distribution after filtering single flowsets. Despite this, a pronounced mode can still be observed after filtering velocities of all matches combined (see Figure 4.6).

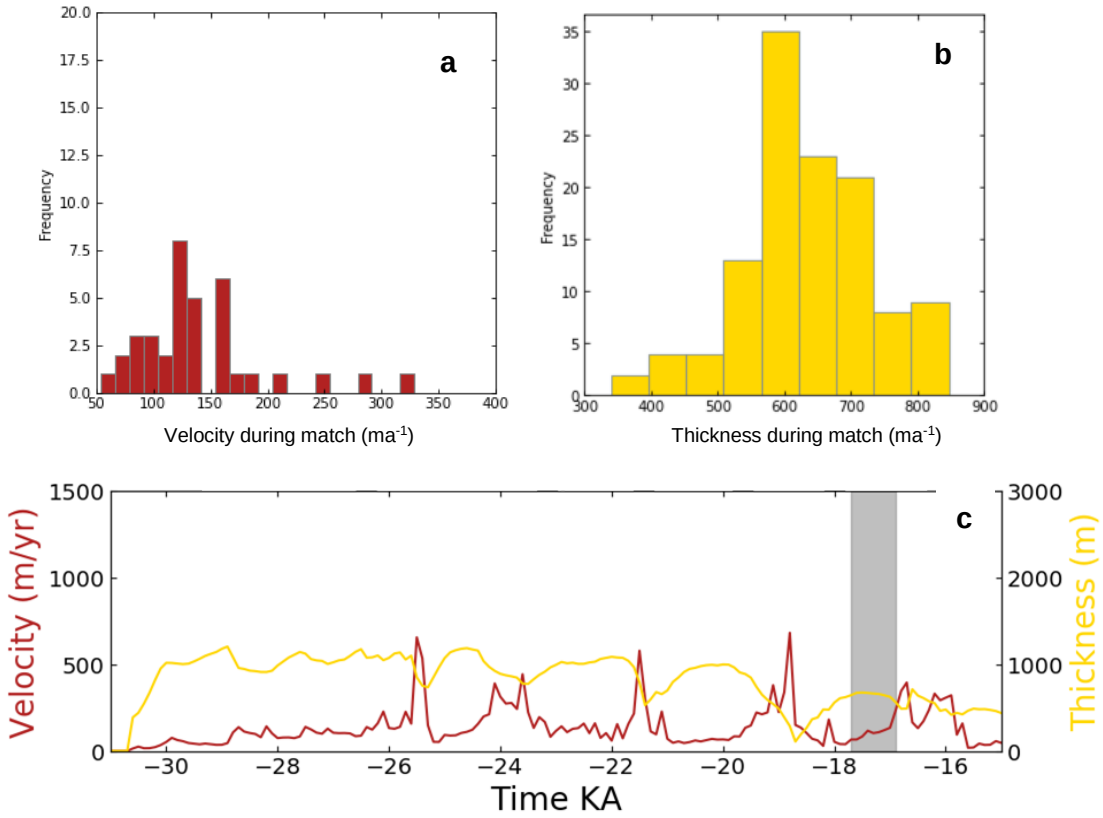

Figure 4.12: Velocity and thickness during match of FSx 32 in Ireland. 4.12a shows a cumulative frequency distribution of FSx32 with a modal velocity of 130 ma^{-1}. Note a scaling factor of three is used on the background velocity signal. 4.12b shows ice thickness during match with lower modal range and modal thickness than the full dataset. 4.12c shows the mean thickness of and velocity over time and a grey band where model data match is met. Note the match takes place during a period of moderate ice thinning.

4.4.2 - Does bedform length relate to ice flow conditions?

One of the key premises of the drumlin continuum hypothesis is that bedform length increases as a function of ice velocity (Clark, 1993;1997; Stokes and Clark 2002; Stokes et al., 2013). To assess this, I used a metric for glacial activity I call cumulative velocity (CV) (see section 4.3.3). This metric is in effect a measure of the number of metres of ice which travel over a point on the bed in the orientation of the bedform (e.g. Jamieson et al., 2016). The benefit of using CV for comparing against observations of the palaeo record is its ability to in effect control (normalise) for time when comparing two palaeo records against one another and the infer a measure of flow consistency.

FS 56 (near the Forth of Firth in Scotland) Shows a modal CV of 250 km, with a negatively skewed distribution (see Figure 4.13a). When we compare this to the spatial distribution of CV at a flowset scale a relationship generally exists between the highest CV and the longest bedforms (see Figure 4.13b). Notable outliers can be observed specifically with high CV and short bedforms.

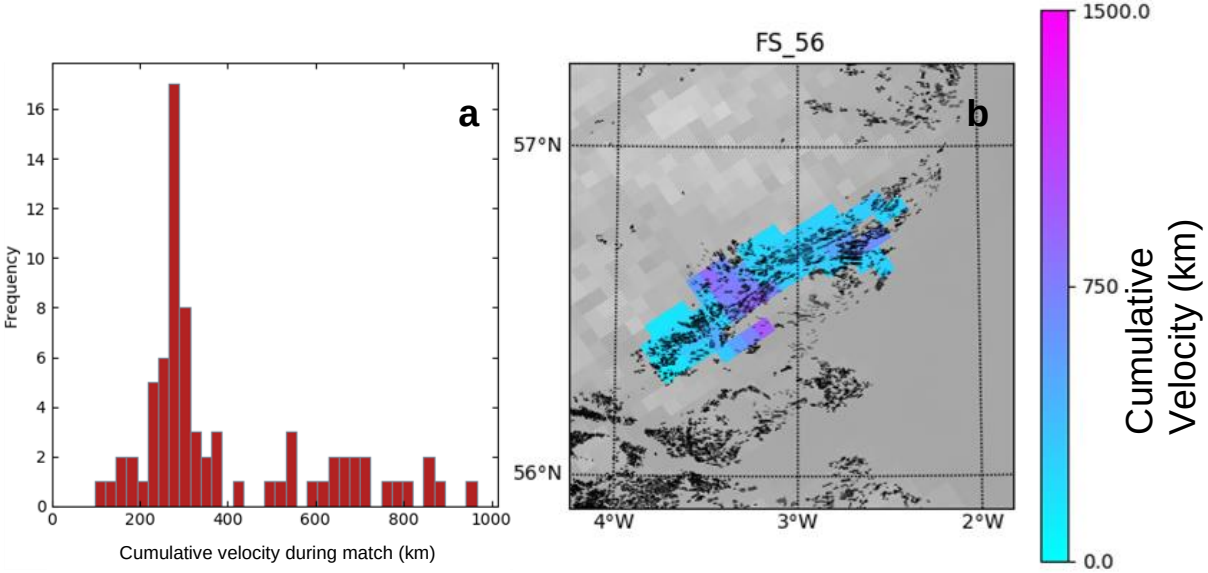

Figure 4.13: Cumulative velocity of FS 56. 4.13a shows frequency distribution of FS 56 showing a modal CV of 300 km. 4.13a shows the spatial distribution of CV with drumlins plotted on top. The longest drumlins generally relate to the areas of highest CV.

When we consider CV and drumlin length at a flowset scale the data show a stronger relationship. When we consider bedforms of drumlin lengths (e.g. >1000 m) (Ely et al., 2016) we note flowsets with higher CV have on average longer bedforms. This relationship becomes more pronounced when we only consider CV above the minimum threshold of 50 ma^{-1} to remove a degree of background from non-drumlin forming ice flow (see Figure 4.14).

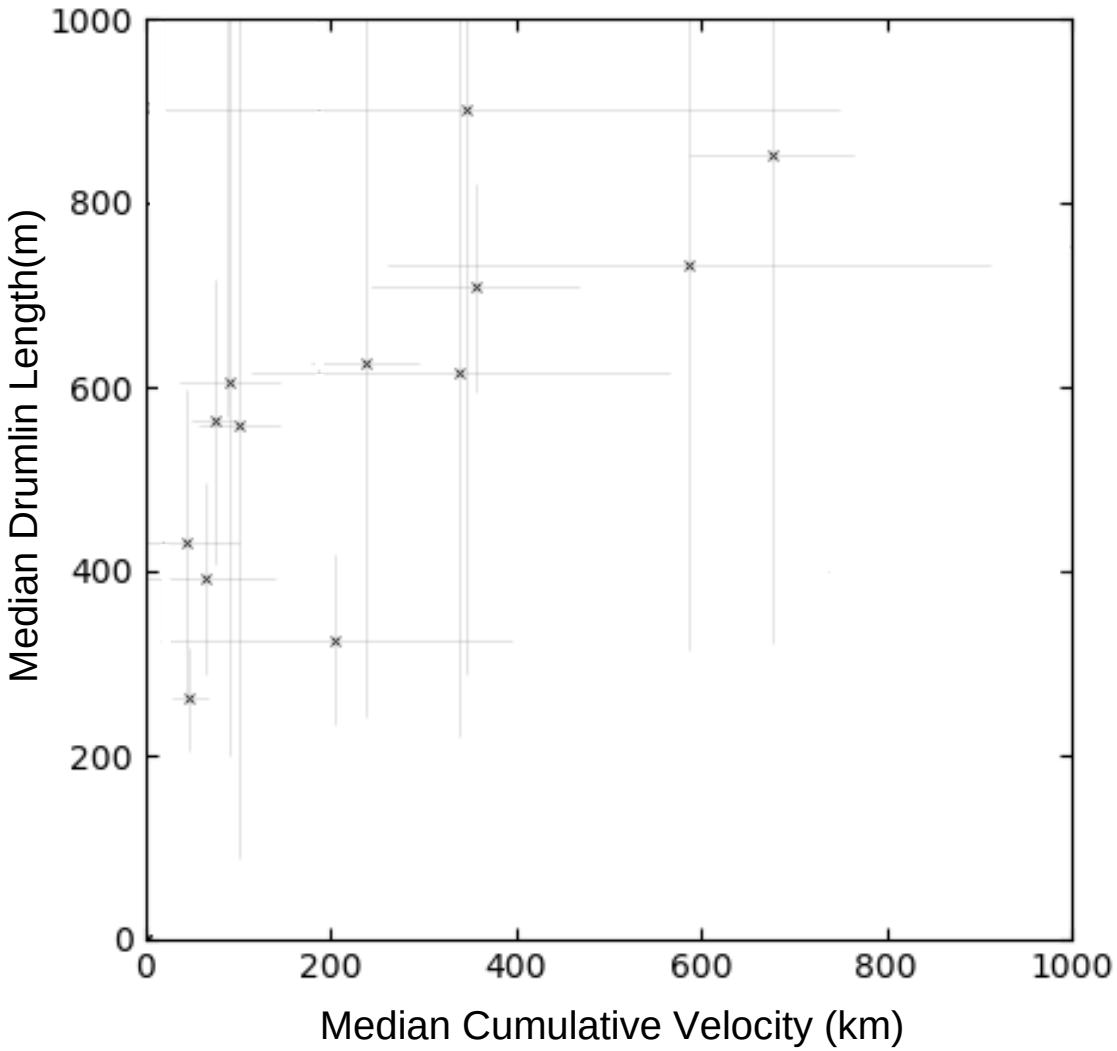

Figure 4.14: Bedform Length over cumulative velocity. Median drumlin length of British drumlins over cumulatively velocity showing drumlins are longer in regions of higher median sliding distance. Each point represents a single flowset. Median metrics are calculated from all pixels within the flowset (not each drumlin). Error bars represent the two standard deviations within the flowsets. Note flowsets with median lengths >1000 have not been included.

4.5 – Discussion

4.5.1 - Progress with the drumlin problem

Drumlin formation is a contentious issue, specifically with regards to how drumlins develop from an initially flat bed (see Section 4.2.4). In this thesis, I do not attempt substantial conjecture as to how drumlins form. However, I do propose a specific range of velocities and thicknesses under which drumlin formation (or reorientation) may occur. Both observations (i.e. specific velocity and thickness) and the broader conceptual observation of a distinct range of conditions under which formation occurs may prove important for testing existing drumlin formation hypotheses.

I interpret the observation of an upper and lower threshold of thickness and velocity to be indicative of the conditions under which drumlin form, which can be used to validate current and future drumlin formation hypotheses. This premise is consistent with the instability hypothesis as a mechanism for drumlin genesis, as Ely et al. (2023) note that bedform forming only occurred within a specific range of conditions relating to the effective pressure at the ice bed. In their physics-based model, too little pressure being transmitted into the sediment below (e.g. low effective pressure), led to decoupling of the ice-bed interface and a lack of bedform formation. Too much pressure at the ice-bed interface (high effective pressure) led to the bedforms being destroyed. Ely et al. (2023) highlight that this mechanism acts as a switch turning bedform formation on and off. The premise of a conceptual drumlin forming switch or upper and lower bounds of formation thresholds is potentially highly significant.

Data from the BIIS shows evidence of such a ‘switch’ and may quantify specific thresholds for this mechanism previously not specified in the instability model of Ely et al. (2023). This thesis finds evidence that drumlin formation in the BIIS likely does not occur below 50-100 ma^{-1} or above a 350-400 ma^{-1}, nor does it occur below ice thicknesses of 850 m or above ice thicknesses of 1200 m. It should be noted that although I find an association with specific velocity and thickness ranges it is possible that velocity or thickness do not directly drive drumlin formation, but in fact are markers of a more complex set of conditions which have combined to result in drumlin formation (perhaps balancing effective pressure at the base). The instability hypothesis model for example proposes that a range of dimensionless bed coupling parameters combined to create this zone between which drumlin formation can occur (Stokes et al., 2013; Ely et al., 2023). Multiple combinations of pore water pressure and overburdening pressure

can be combined to produce this range in the instability model, but significantly if this dimensionless value is too low or two high drumlin formation ceases.

I stress that the conditions I have identified may not be those that are initially required to perturb an initially flat bed into a regular field. I may in fact only have identified the glacial conditions required to reorientate and preserve a drumlin field. I have found no evidence to suggest a systematic set of conditions consistently occurring prior to the periods of ice flow associated with ice parallel bedforms,

As a final observation in support of a drumlin forming switch, I highlight the signal to noise ratio relative match length, and number of likely drumlin forming matches. When considering a single flowset, (and therefore possibly only a signal set of conditions required to form a field of drumlins), as match length increases the signal I interpret to be drumlin forming decreases. Despite this, when all flowsets are combined, the coincidental signal increases as does the modal peak I interpret as drumlin forming. I interpreted this to imply that when a single match is paired with a large coincidental signal, the drumlin forming signal is lost. In contrast when multiple drumlin forming events are combined the drumlin forming signal increases at a greater rate than the coincidental match giving a stronger signal to noise ratio. This is interpreted to suggest drumlins can exist under ice flowing parallel to their long axis without changes to their morphology occurring.

With regards to the initial perturbation required for drumlin formation through an instability mechanism (or other) the data from regional observations (e.g. Solway Firth) shows that drumlins form during periods of reconfiguration (i.e. non steady state). This reconfiguration is predominantly a period of net retreat (primarily retreat) with 52% of potential drumlin forming events occurring during periods of net retreat. This may either be due to preservation or be related to some form of preconditioning mechanism. These periods are likely to be prone to reconfiguration of the subglacial environment, perhaps with rapid changes in subglacial hydrology or rheology. These would likely promote the development of bed perturbations which are required to allow the initial instability to occur. These are largely speculative propositions, but may be of relevance to future works on the drumlin problem.

One method of finally resolving the drumlin conundrum, is to develop a model of drumlin formation which can explain the breadth of drumlin forms observed in the landscape using appropriate glacial conditions. As well as explaining the morphometry of drumlins, such a model must also be founded on observations of the environment drumlins are believed to form (e.g. velocity, thickness, effective pressure, shear stress). Although many would argue this has already been achieved, (e.g. Eyles, 2016;

Barchyn et al., 2016; Iverson et al., 2017; Ely et al., 2023), no single model combines real world velocities, with the ability to develop known patterns of bedforms from an initially flat bed. In this work I have observed what I propose are the thickness and velocity conditions. These observations should be used in future for further testing of all drumlin formation models.

4.5.2 - Implications for palaeo-ice sheet reconstructions

The finding of a narrow range of modelled velocities and thicknesses under which palaeo drumlins can persist represent a potentially powerful tool for forcing future palaeo-ice sheet reconstructions. Three key ice sheet scenarios arise from this work for application in future palaeo-ice sheet reconstructions: i) Magnitude of ice sheet velocities ii) timing of ice sheet velocities and iii) duration of flow conformity events.

The implication of point i) is that ice sheet velocity could be compared and nudged when aligning with drumlins fields to fit within the 100-350 ma^{-1} range. This nudging approach would work for well constrained events (i.e. where confident in the timing as a result of a short match). The implication of point ii) is that increased confidence in timing of velocity magnitude could be achieved based on the observation that preserved drumlin fields are a record of the net deglaciation signal. For example, if a flowset matches twice, once during the build up and once during retreat, the retreat signal could be used to constrain ice flow conditions. Under such a scenario it might be possible to force numerical modelled glacial retreat to specific geometries and velocities. Furthermore, the implication of point iii) is that if cumulative velocity does indeed result in elongation of bedforms this would provide a powerful tool for adjusting the retreat geometry, either by increasing ice velocity (within the observed range) or by prolonging the active duration of the deglaciating sector so as to align with the most elongate bedforms. I believe an important future test would be to compare observation of ice parallel drumlins with numerical modelling simulations of other ice sheets, such as the Laurentide or the Eurasian Ice Sheet.

To examine the implications of this chapter, that velocity acts like a ‘switch’ with specific windows of drumlin forming conditions, I used AFDA, in conjunctions proposed velocity window to independently refine the timing of a long drumlin-forming event (e.g. point ii, above). I then verified this against empirical observations. To conduct this test, I identified a flowset with uncertain AFDA timing (e.g. multiple long matches) in a regions with a good level of independent (empirical) chronological data to validate model-data interpretation. I selected FS 58 in the Solway Firth in Southern Scotland,

which matches three times for a total of 5 ka (see Figure 4.15). The Solway Firth region is well studied with several detailed local reconstructions based on erratics, sediment stratigraphy and decades of field observations (e.g. Trotter, 1929; Hollingworth, 1931; Livingstone et al., 2008; 2009;2012; Evans et al., 2009; Hughes et al., 2014; Ballantyne and Small 2018). Furthermore, FS 58 has a crosscutting relationship with FS 57, which is well constrained by empirical observations. The drumlins of FS 57 are cross cut by those belonging to FS 58 (Hughes et al., 2014). The drumlins of FS 57 are also capped by the Gillcambon Till, which pertains to the Scottish Readvance at 19.2-18.2 ka (Trotter, 1929; Hollingworth, 1931; Ballantyne and Small 2018 Chiverrell et al., 2018). Together, this has been interpreted to show that FS57 formed first, and was later overprinted by the drumlins of FS 58 (Livingstone et al., 2012; Livingstone et al., 2015).

FS 57 only matches once during the model simulation at 25.1 ka, consistent with empirical estimates of 23-29 ka (Livingstone et al., 2008). This provides an important reference point for independently validating the timing of FS 58 formation, which occurred afterwards given the cross-cutting relationship. Of the three model-data matches of FS 58, only two partly sit within the observed thickness velocity threshold (starting at 29.9 ka and 18 ka). The first model data match has comparatively high mean residual vector (18) and variance (0.09) only just within the thresholds of 20 and 0.1 respectively. In contrast the latter match has a very low mean residual vector and variance (8 and 0.007 respectively). Modelled ice velocities and ice thicknesses show two phases of ice flow during the 2000 year match following the Scottish readvance. A 1400 year ‘slow’ period characterised by a minor advance followed by an 800 year long ‘fast’ period of retreat. This initial slow period sits within the threshold of drumlin formation velocities. My interpretation, based on the threshold found for drumlin formation in section 4.4.1, and AFDA scores is that the drumlins formed during the initial slow period (18 ka year to 16.8 ka year, 50-350 ma^{-1}) (see Figure 4.15a,b), but were then preserved under the faster flowing ice that occurred later (16.8 year to 15.9 year, 500-800 ma^{-1}). The switch was on in the earlier flow but turned off in the later flow. This would imply the drumlins formed during the early phase of the Scottish Readvance which is consistent with empirical observations, and the deposition of till on the pre-existing drumlins. However, this hypothesised velocity mechanism remains to be tested against further data, and observations of drumlin formation beneath contemporary ice sheets. This example highlights a potentially important avenue for future works to explore in palaeo model-data comparison.

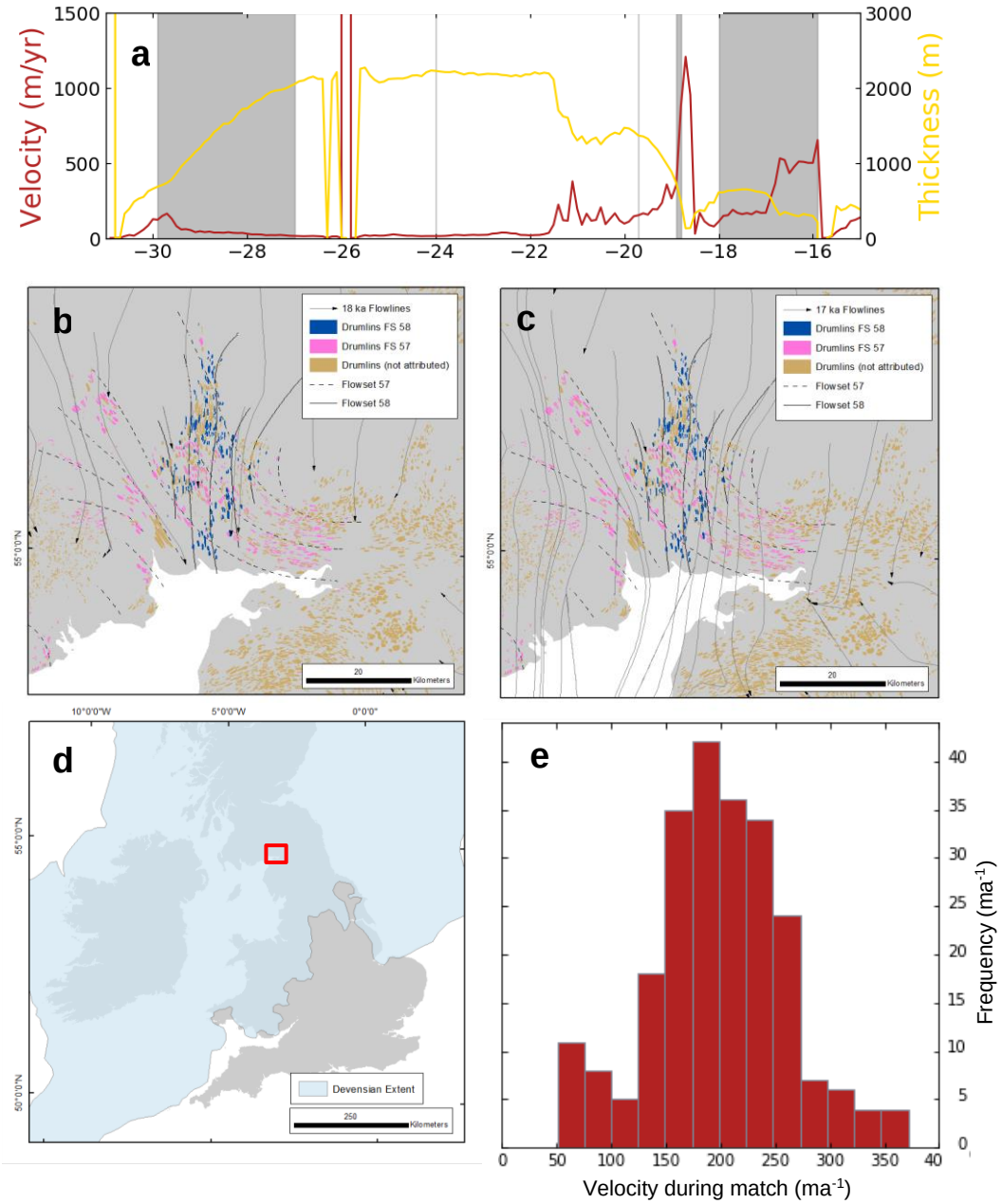

Figure 4.15: Proposed formation event of crosscutting drumlin field in the Solway Firth in southern Scotland. 14.9a Mean modelled ice thickness and velocity of FS 58 in the Soloway Firth. Grey bounding box used to delineate timing of match (e.g. vector score <20, variance grounded ice, velocity >10 ma^{-1}, thickness >10 m). 4.15b 18 ka flowlines interpreted to relate to ice flow at the beginning of the formation of the drumlins of FS 58 (blue), which crosscuts the drumlins of FS 57 (pink) which had previously formed. 4.15c 17 ka Flowlines, 200 years prior of proposed formation period of FS 58. 4.15d insert map showing approximate location of figures b/c). 4.15e frequency distribution of velocities from 'refined' match. Note no distribution filtering has been applied to this FS 58, we may therefore be observing some non-drumlin forming pixels resulting in the peak at 50 ma^{-1}.

4.5.3 - Implications for contemporary ice sheets.

The findings of this chapter are applicable to future glacial modelling, and historic and prospective observations of subglacial drumlins. Firstly, in the context of future work using numerical ice sheet models the presence of a drumlin forming switch may form the basis of an improved bed classification when assigning basal sediment models and regimes to ice sheet models. In a contemporary glacial setting, it may be possible to infer the presence of active drumlins (and in turn basal conditions) from specific thickness, and velocity observations. However, an important first step before inferring the presence of drumlins, would be to further test the association of thicknesses and velocities against the presence of drumlins beneath active ice. Short of proposing new radar investigations of regions where such bedforms would be anticipated I have combined the location of observations of subglacial lineations in Antarctica with velocity. To this end, I have identified regions of the Antarctic Ice Sheet where drumlin formation may be occurring based on surface velocities of grounded ice (see Figure 4.16).

The regions where I predict the presence of drumlins align well with locations in Antarctica where subglacial bedforms may have been identified (be these drumlins or MSGL). Significantly, all but two regions (out of twelve) sit either in a region predicted to be conducive to drumlinisation or in a transitional area proximal to predicted regions (See figure 4.17). For example, lineations observed by Schlegel et al. (2022) on the Rutford Ice Stream, overlap a region of predicted flow with the central of their study site having a mean velocity of 370 ma^{-1} (just above the 350 ma^{-1} threshold). This study site predominantly consists of MSGL, however published velocities for the region suggest the shortest bedforms (drumlins) sit under lower velocities closer to 200 ma^{-1}. It seems possible such a region highlights the transition from drumlins to MSGL as ice flow conditions exceed the approximate 350 ma^{-1} upper threshold.

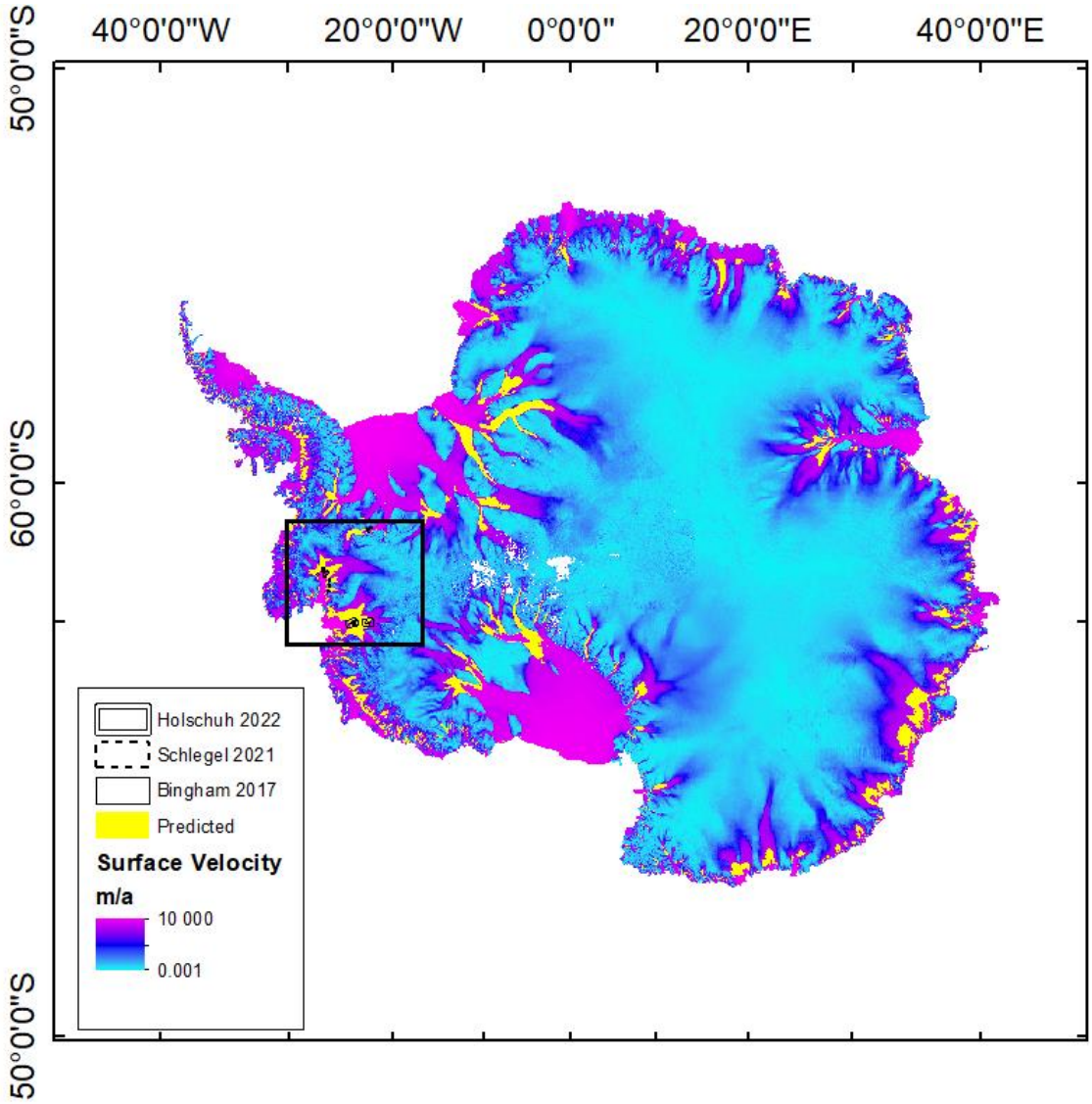

Figure 4.16: Velocities zones in Antarctica where drumlin formation may take place. A drumlin forming velocity threshold was set between 100 and 350 ma^{-1} using velocity data from Rignot et al. (2011) and grounding line data from Rignot et al. (2016). Regions where subglacial drumlins have been observed through GPR surveys of Schlegel et al. (2022), Holschuh et al., (2020), and Bingham et al. (2017).

Lineations of the Pine Island Ice Stream span a region of predicted drumlin formation and a region of fast flow considerably above that of proposed drumlin formation (Bingham et al., 2017). However, it seems likely that such bedforms could recently have been associated with slower flow proposed for drumlin formation and may therefore now represent relic bedforms. Or that as in the Rutford Ice Stream, the faster velocities relate to more elongate MSGL. The Pine Island Ice Stream has experienced almost 70 years of thinning and retreat and therefore aligns well with the observations of similar flow regimes in the BIIS associated with bedforming (Gillet-Chaulet et al., 2016).

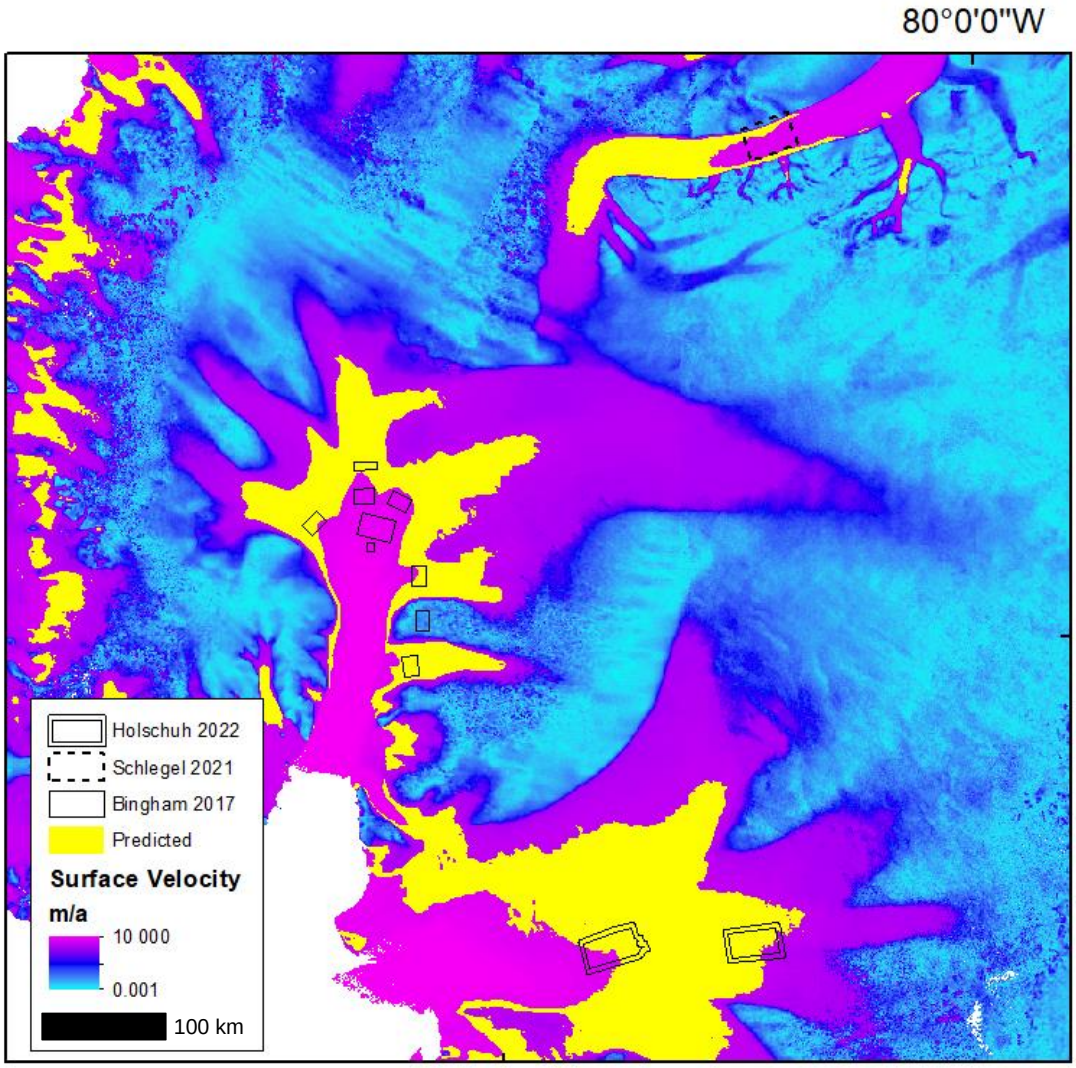

Figure 4.17: West Antarctica velocities zones where drumlin formation may take place. A drumlin forming velocity threshold was set between 100 and 350 ma^{-1} using velocity data from Rignot et al. (2011) and grounding line data from Rignot et al. (2016). Regions where subglacial drumlins have been observed through GPR surveys of Schlegel et al. (2022), Holschuh et al. (2020), and Bingham et al. (2017).

In addition to the good association with my predictions of velocity and observation of lineated bedforms in Antarctica I also find my velocity predictions sit within the range of those generally observed in the literature (see section 4.4). My data on the velocity of drumlin formation is consistent with 'best estimates' from inference of the palaeo glacial record (e.g. Stokes et al., 2013) and from those used in previous first principal numerical models (e.g. Eyles et al., 2016). Observations of lineated bedforms beneath Antarctica shows drumlins in the onset zone, with velocities between 72 and 200 ma^{-1}, and with MSGL in regions of 375 ma^{-1} (King et al., 2007; 2009; Smith et al., 2007; Stokes et al., 2015). This supports the observed velocities in this thesis of a

lower bound of drumlin formation velocity at 50-100 ma^{-1} and an upper bound of 350-400 m^{-1}. Here I predict notably lower velocities than observed in Jamieson et al. (2016), although the bedforms studied in that paper are MSGL, and often an order of magnitude longer than those presented in this thesis for the BIIS. This interpretation is consistent with the long-held association between MSGL and ice streams (Clark, 1993).

My observations from the BIIS, complement those of Pine Island, Thwaites and Marguerite Bay highlight the potential of velocity indeed being an important element to length in a landform continuum (e.g. Clark 1993; King et al., 2007; 2009; Smith et al., 2007; Stokes et al., 2015; Jamieson et al., 2016; Ely et al., 2016). Tentatively one could propose these to be snapshot observations of end members of an elongation spectrums in which bedforms transition from shorter to longer features. Perhaps Thwaites and Pine Island Ice streams are in fact examples of locations where this transition occurring? This transition, and the importance of velocity to bedform length is also illustrated in cumulative velocity over bedform length data presented in Section 4.4.2. This data shows more elongate bedforms are associated with more active beds (more cumulative metres of ice flow). Although in this thesis an association was only found in bedforms of <1 km, Jamieson and others found that cumulative velocity had a significant association with maximum lineation length (2016) for longer bedforms (MSGL). However, the size and scale of bedforms in the BIIS has meant limited examples of true MSGL exist. As such I have not been able to adequately test the relationship with CV over bedforms longer than 1km for the context of the BIIS. This is, however, an important area to expand upon in future work.

These data also show an upper and lower bound for ice thicknesses associated with bedforming with a range of 850 to 1200 m. These are similar to those from other model-data comparisons of lineated bedforms (e.g. Jamieson et al., 2016 for MSGL), but sit at the upper range of those proposed by Patterson and Hooke (1995) for drumlins, and below those observed on the Rutford Ice Stream (Schlegel et al., 2022 for MSGL). It seems prudent to caveat these findings for ice thickness, with the need for further investigation to test proposed ice sheet thicknesses. I found the ensemble to overestimate ice thickness from the GIA estimate by approximately 206 m (see Section 3.4.2). In light of the variation in observed ice thickness from the drumlin literature and the potential overestimation of ice thickness of the full dataset it seems well reasoned to caveat observations of thickness as the likely upper bound of drumlin forming thicknesses. An overestimate of approximately 200 m would put these observations more in line with those previously proposed for drumlins in the literature (e.g. Patterson and Hooke, 1995).

More broadly, it seems wise to compare these findings against other palaeo-ice sheets simulations and where possible empirical observations. This will ensure we can calibrate our understanding of drumlin forming processes against a variety of ice sheet styles and locations. When we consider broader drumlin observations (outside of the BIIS and Antarctica), some have most likely formed under much thinner ice than observed in this thesis. For example, those beneath contemporary Hofsjökull Ice Cap in Iceland relate to ice marginal geometries rather than the onset zone. These geometries are unlikely to have formed under the median range of thicknesses observed in this thesis. Although with generous interpretation the lower end of observed thickness in this thesis could be applied (e.g. >700 m and a potential thickness overestimate of 200 m see Section 3.4.2), existing formation hypothesis for the region refute the timing required for such thicknesses (e.g. Johnson et al., 2010; Benediktsson et al., 2016; Iverson et al 2017). As a result, if thickness is indeed a proposed metric which relates to bedforming, it is perhaps only one of a number of factors which combine to result in drumlin forming conditions and therefore requires further investigation to be clarified. The need for a number of factors to combine for drumlin formation seems probable, and is supported by the instability hypothesis of drumlin formation (e.g. Ely et al., 2023 see chapter 4). Therefore, although the data shows a combination of thicknesses and velocities to be associated with drumlin formation beneath the BIIS, these may in fact only be two dials of a more complex system.

4.6 - Conclusion

In this chapter I use numerical ice sheet simulations as an observational environment to explore the conditions of drumlin formation for the first time. Doing so has allowed me to produce the largest comparison dataset of 85,834 drumlins against ice flow conditions over 16 thousand years. This matching was performed using automated flow comparison tools which allowed for the scale of comparison to be dramatically expanded and compared to manual or visual comparison methods. This thesis has shown a distinct range of velocities between 100 and 350 m/a which are proposed to be those required for drumlin formation. The presence of a large coincidental match signal is interpreted as evidence to suggest that drumlins frequently exist in ice parallel conditions likely without suitable conditions for changes in morphometry. The presence of an upper and lower bound of drumlin forming velocities is interpreted to be part of a drumlin forming switch. Ice thickness is also proposed to contribute to this mechanism which controls drumlin formation. These observations may be the first to pin down two of the key concepts of drumlin formation when and

where they form as well as under what conditions. In the context of the BIIS, I observe model/data matches occurring at both the onset zones of the largest ice streams and the margins of smaller ice streams. In the context of Antarctic Ice Sheet regions of flow at these velocities are primarily found in the onset zone on large ice streams. The data shows drumlins to be associated with comparatively thick ice in the region of 700-1200 m thickness, however this is likely to represent the upper bounds of drumlin forming thicknesses with the threshold perhaps being 200 m thinner.

The drumlin problem is perhaps one of the longest and most substantial studied glacial discourses of the field. With these new observations of the parameters under which drumlins form we are perhaps the closest the academic field has ever been to resolving the drumlin conundrum. Numerical modellers will be able to use these observations to test their first principal models, and field glaciologists will be able to search for more subglacial bedforms. It seems possible that within a matter of years one of the largest intellectual debates of the field could come to closure.

Chapter 5. A shifting flowline approach for comparing simulated erratic dispersal to erratic distribution data.

5.1 - Introduction

No matter your understanding of geology, large erratic boulders without an obvious source or delivery mechanism are likely intriguing. Be this a Victorian traveller finding a granite boulder perched on a col, or a modern construction worker unearthing a 200-tonne boulder when digging the foundations of an apartment block. Humans want to know how these stones arrived in their current locations. This fascination with unusual rocks can be seen in the rock selection of Stonehenge, or early Stone Age axe makers; it's clear that humans have always appreciated unusual rocks (Knowles, 1903; Briggs 1988; Corradi et al. 2014; Pearson, 2016). Despite this, the written record of the delivery mechanism of these boulders in the British Isles does not start until the end of the enlightenment (in the late 18th century). The incomprehensible nature of these rocks is exemplified by Darwin recalling being told that 'the world would come to an end before anyone would be able to explain how this stone came where it now lay' (1887). Early scientists proposed a wide variety of hypotheses varying from the great flood (Greenough, 1819; Buckland, 1823) to the toys of great trolls to explain how they arrived in their current resting places. These intriguing boulders eventually became known as glacial erratics, and modern thought now attributes these rocks to past glacial activity. The term 'erratic' is commonly applied only to large boulders (>50 tonnes), which in early work added to the mystique of how they travelled so far from their geological source. In this thesis, the term 'erratic' is used more broadly to describe surface boulders, cobbles (lodged in till), and indicator grains (constituting till) which have been found outside of their geological source area. This work assumes erratics are glacially transported unless otherwise stated.

The popularity of studying erratic boulders has varied over time. The 19th century, it could be argued, marked one of the most popular periods in erratic boulder exploration, with the advent of the Boulder Committee (Buckland, 1823; Christison et al., 1871). Although experiencing a notable decrease in public interest in the 20th century, scientific interest in erratic boulders has continued into the 21st century (Clark et al., 2004b; Greenwood and Clark, 2009b; Jouvet et al., 2017, Carling et al., 2023).

With the increased interest in glacial reconstructions, both from numerical modelling and traditional mapping-based approaches, interest in the study of glacial erratics has grown in the last decade (Clark et al., 2004a; Clark et al., 2004b; Greenwood and Clark, 2009b; Jouvet et al., 2017). This interest is in part fed by the wealth of information glacial erratics can hold about past glacial conditions. Erratics intrinsically record information on the start and end of a glacial transport route. When this information is paired with a numerical ice sheet model (Jouvet et al., 2017) or other observations of flow direction (Sutherland 1984; Clark et al., 2004b; Greenwood, 2008), it can be used to recreate erratic transport pathway. Erratic transport pathways have mostly been ignored by numerical ice sheet modellers to date. This chapter looks to explore and develop the potential of using erratic transport pathways to decipher past glaciations and assess how well ice sheet simulations recreate the past.

5.2 - A history of erratic research in Britain and Ireland

Scholarly explanations for erratic boulders in Britain and Ireland began in the 18th century (Greenough, 1819, Buckland, 1823; Lyell, 1830; Rudwick, 2009). The first widespread explanation for glacial erratics that gained traction in Britain and Ireland was that of the diluvium, or a large alluvial flood referenced in the Bible as Noah's Flood. Early Diluvialists proposed erratic boulders to be the result of a catastrophic flood which deposited both till, and erratic boulders in a single event (Greenough, 1819; Buckland, 1823). Variations on this theory persisted for almost a century, as it fit well within the existing Western Christian model of the Earth. It became increasingly apparent, however, that the glacial deposits in Britain and Ireland were not the result of a single catastrophic event but were in fact the result of a gradual process.

By the 1830's the majority of geologists had moved away from the Diluvialism in favour of ice rafted debris (Boyland, 1998). These initial theories for ice rafting of erratics proposed that icebergs from higher northern latitude drifted over a submerged unglaciated Britain and Ireland, with boulders intermittently freezing onto the base (Darwin, 1848). Variations in the theory of iceberg rafting of debris remained popular for several decades. Attempts to move towards theories of widespread glaciation were widely disregarded in Britain and Ireland, with the Geological Society of London going so far as to censor publications supporting widespread glaciation (Darwin, 1848; Boylan, 1998). Despite limited evidence, by modern standards, for the required transcontinental ice rafting of erratics, substantial innovations were made on the scale of distances erratics had travelled (See Figure 5.1). A key reason for hesitation in

moving away from the ice rafting hypothesis was the influence of the church in British Geology and Oxbridge at the time, who are proposed to have censored early glacial observations out of publications (Boylan, 1998; Rudwick, 2009; Roberts, 2012). It was not until the 1840's when Agassiz visited the British Isles and proposed the notion of past glaciations that the possibility of glacial transport began to arise as an explanation for erratic boulders in Britain and Ireland. Over the two years following Agassiz's visits to Britain and Ireland in 1840, a large body of evidence was laid down for widespread glaciation, including 22 sites where erratic boulders were interpreted to have been glacially transported (Buckland, 1841; Lyell, 1841; Agassiz, 1841; Boylan, 1998). Despite this, it took many decades for glacial transport of erratics to gain traction over the iceberg transport hypothesis, with a hybrid model proposing mountain glaciation and iceberg transport over the lowlands (Darwin, 1848).

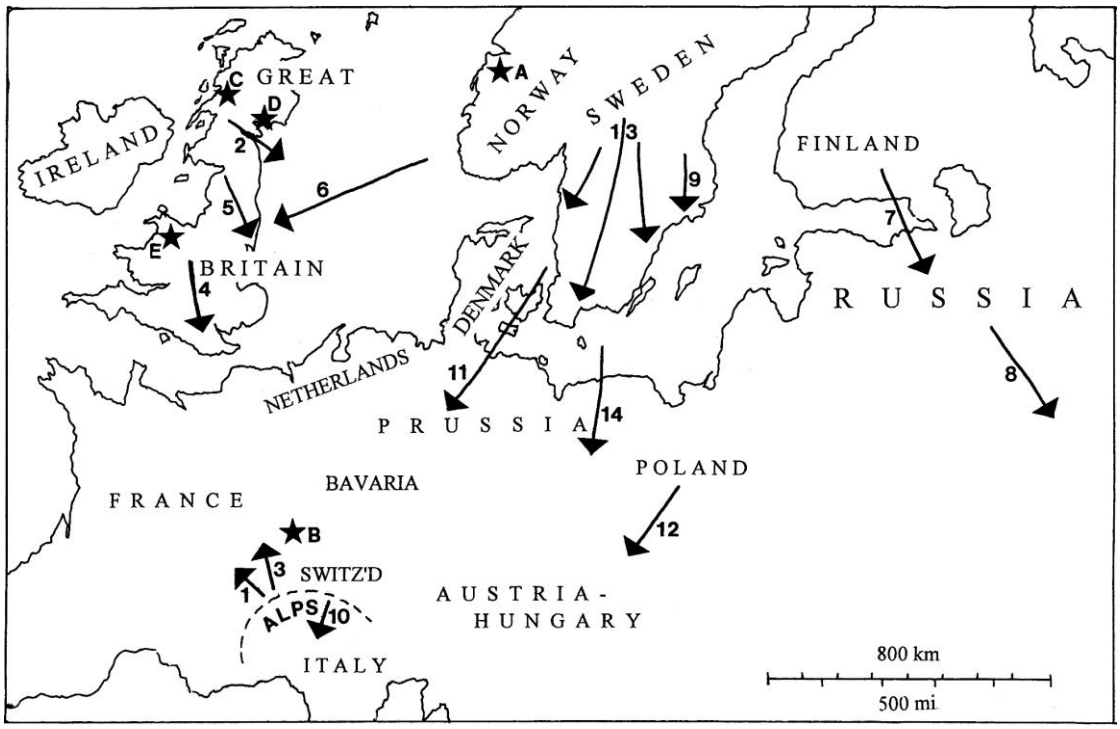

Figure 5.1: Map of proposed transport pathways by early Diluvialist. Diluvium transport pathways to current erratic locations, proposed by academics in the 1820s and 30s. Reproduced from Rudwick (2009).

Progressively, over the following 50 years, the regions in which glacial transport was deemed possible (rather than iceberg rafting) increased until widespread glaciation of the British Isles became accepted (Geikie, 1894). Undoubtedly, a major step forwards in deciphering the glacial origin of erratic boulders in Britain and Ireland was

the work of the Royal Society of Edinburgh's Boulder Committee. In 1871, the first call went out from the Boulder Committee of the Royal Society of Edinburgh to catalogue all erratic boulders of Scotland (Christison et al.,1871). This call mobilised academic geologists and reverends of each local parish to help resolve the issue of ice rafting of erratics or glacial transport. The early work of the Boulder Committee was supported (and part funded by) the clergy to add evidence to Diluvialism and in turn the Bible's great flood (Christison et al., 1871). Ten reports were issued between 1871 and 1884, with the consensus gradually shifting towards that of glacial transport (Christison et al., 1871 and 1884). By the late 19th century, the academic consensus was that erratic boulders across Britain and Ireland were glacially transported. However, there was still resistance to this hypothesis, specifically within the clergy.

Over the next century, research into erratics experienced sporadic popularity. Geikie (1894), who was a member of the Boulder Committee, used glacial erratics to produce his glacial reconstruction of the British and Irish Ice Sheet (BIIS). In the early 20th century, numerous studies used lodgement erratics as a central tool to understand the origins of till (Bremner, 1928, 1931, 1939; Jamieson 1906) and surface erratic boulders in Scotland (Makie, 1901; Raistrick, 1931; Cumming and Bate 1933; Charlesworth, 1953). Work by Makie (1901) stands out for its early use of a microscope to identify subtle differences in Highland granite erratics. In this work, Makie (1901) was able to identify variation in ice flow directions over time of up to 140 degrees in the Moray Firth basin. Charlesworth (1953) used erratic origins to delineate zones of convergence over Ireland, mapping the confluence of Scottish and Irish Ice (see Figure 5.2) and resulting ice flow. Similarly, Charlesworth (1953) used erratic dispersal of Galway Granite and numerous regions of striations to reconstruct the build-up of the Irish Ice Cap. The insight from erratic dispersal was used in Charlesworths' 1956 reconstruction of the BIIS.

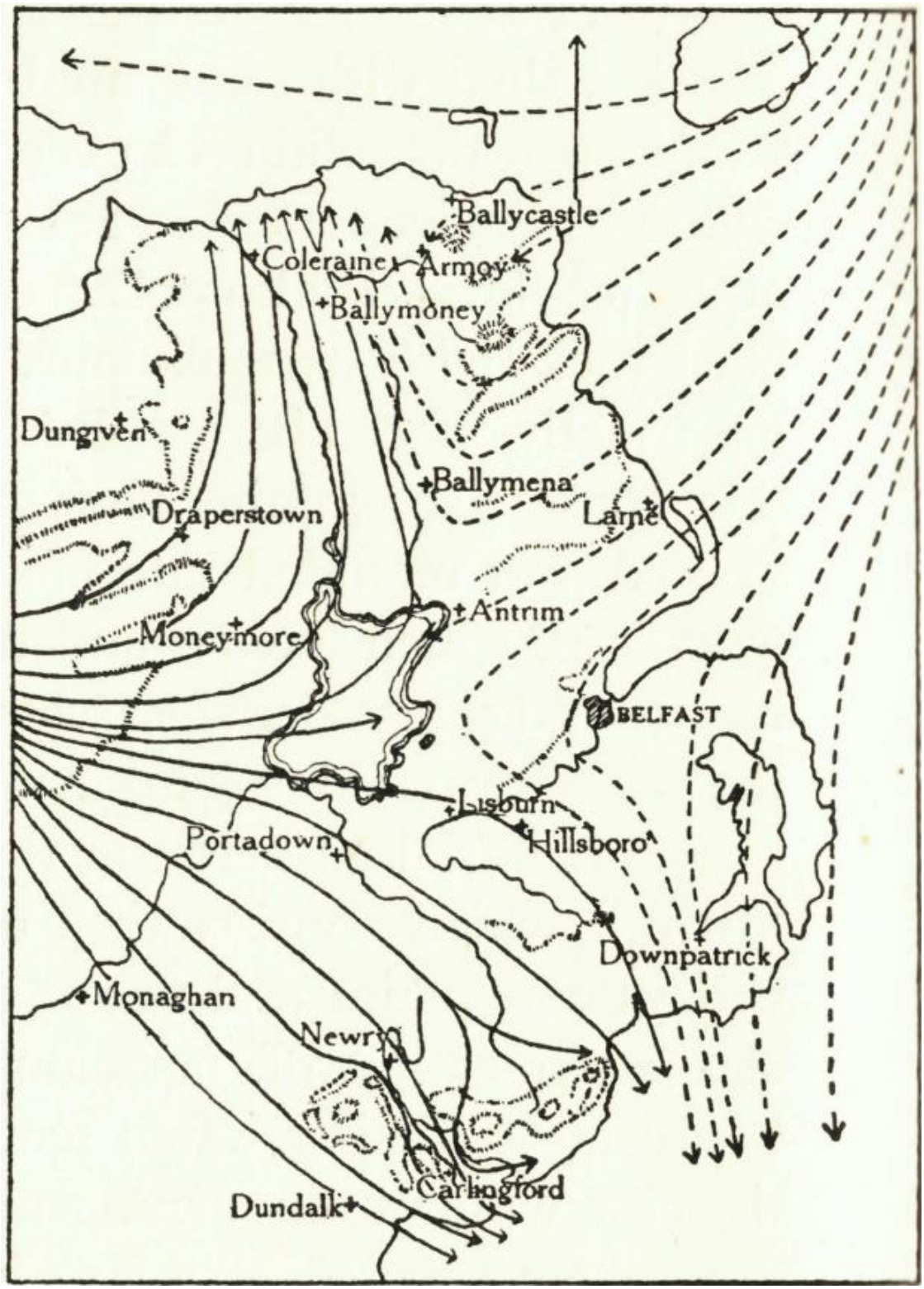

Figure 5.2: Convergence of the Irish and Scottish Devensian ice reproduced from Charlesworth (1953). Erratics from Scotland were used to infer locations of ice divides and resulting ice streams.

Erratics gradually drifted out of popular academic interest in Britain and Ireland throughout the mid-20th century and it wasn't until the 1980's that renewed interest

came in the form of larger scale glacial interpretations of erratics in the Scottish Highland, with the work of Sutherland (1984). Sutherland (1984) compiled 'all known' major erratics in Scotland at the time, with observations of flow direction and geological source areas, to create a map of erratic transport paths (see Figure 5.3). This work can, in many ways, be seen as the foundation of erratic flow path routing completed in this thesis and that of Clark et al. (2004) and Greenwood (2008).

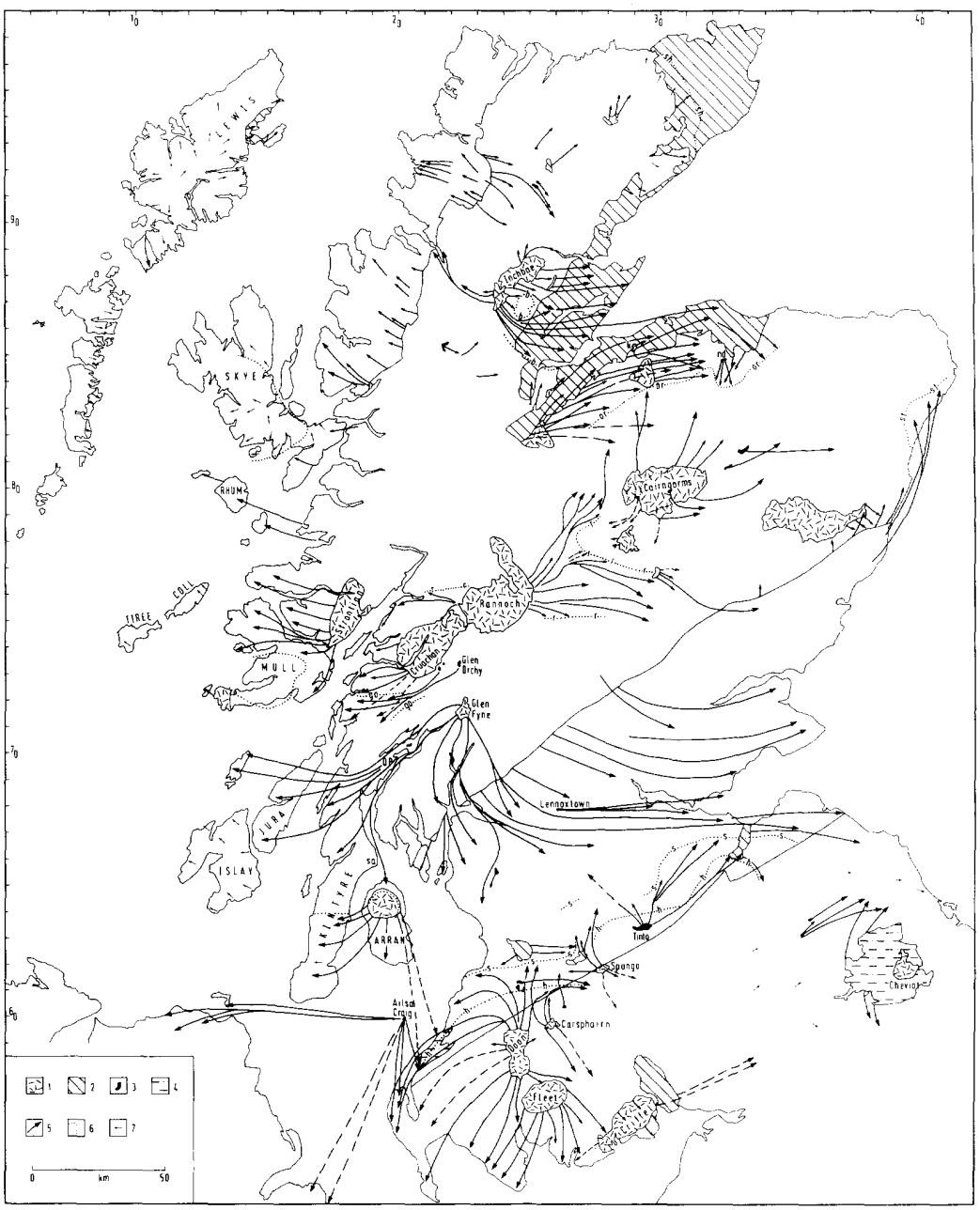

Figure 5.3: Erratic dispersal of the Late Devensian ice sheet from Sutherland (1984). Pathways are produced using observations of lineated landforms and dispersals of erratics. Legend item key: 1. Granite/foliated granite; 2 Particular sedimentary outcrops; 3 Minor igneous intrusions; 4 Large igneous bodies; 5 Erratic transport pathways; 6 margins of erratic distributions; 7 Direction of ice flow (striation/ ice moulding).

More recently, erratics have seen revived interest in Britain and Ireland. Clark et al. (2004) compiled evidence for major erratics for the BRITICE project. This work updated the work of Sutherland (1984) and similarly used lineated landforms to propose dispersal pathways. Clark et al. (2004) expanded the dataset to include more erratics including those in northern England. In Ireland, Greenwood (2008) compiled erratic dispersal from the literature. As with the work of Sutherland (1984), source and sinks were defined on an ice cap scale (e.g. Irish Ice Cap). Unlike previous work, Greenwood (2008) delineated regions of erratic dispersal, rather than paths specific erratics might have taken from source to sink.

In 2019, Les Knight approached the BRITICE-CHRONO project with a new dataset he had compiled. This dataset consisted of a digitization of over 23,053 erratic boulders across Britain including (but not limited to) their proposed geological province, size and notes about location. The database is founded on the early work on the Boulder Committee, from which the majority of the erratics were identified and resurveyed. The work has, however, been expanded upon dramatically with a resurveying of boulders, and the attribution of modern GPS coordinates. Similarly, clast lithology, size and other observations were recorded. The first work publishing with this dataset was by Carling et al. (2023), who used dispersal of Shap Granites to elucidate a Devensian glacial reconstruction of the ice divides over the northern Pennines. However, at the time of writing the full dataset is not published (see Figure 5.4).

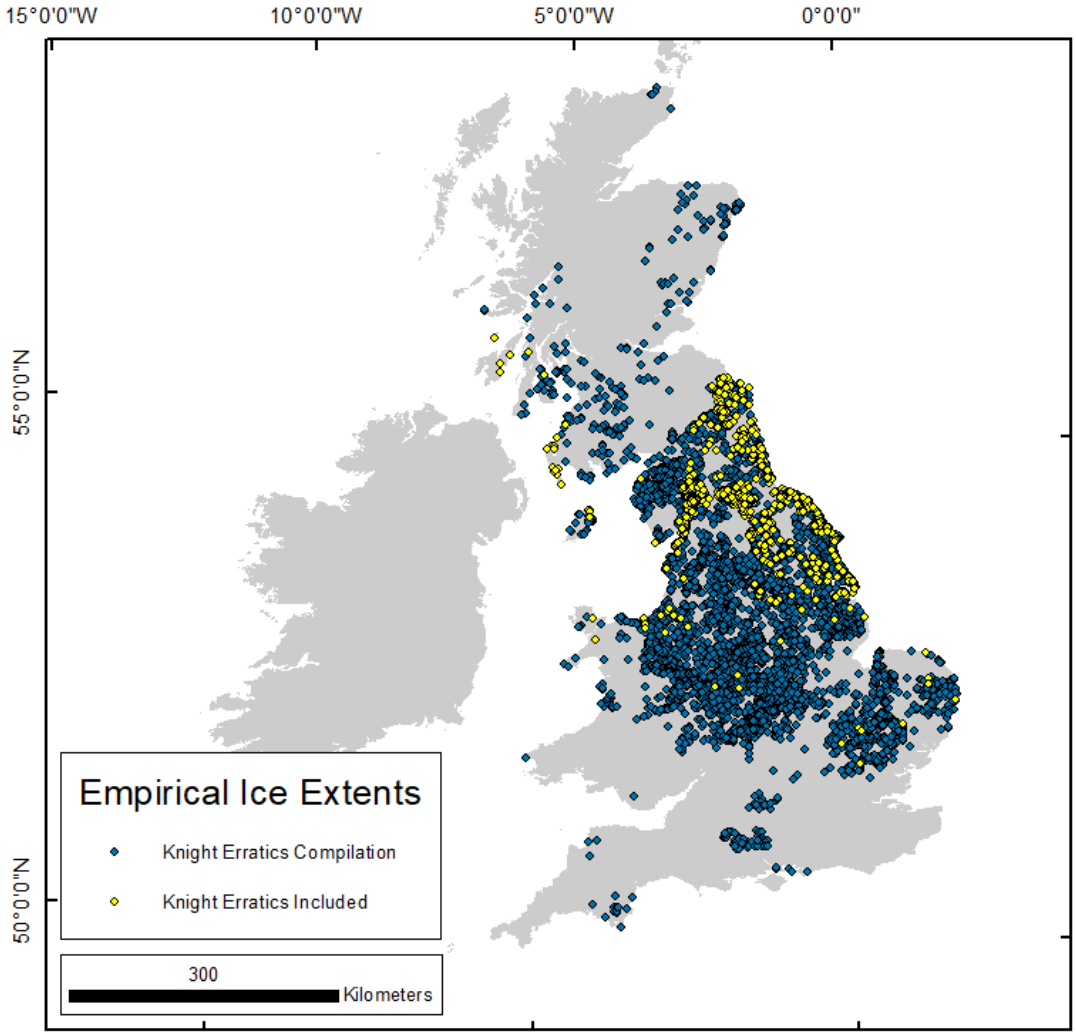

Figure 5.4: Glacial erratics database produced by Knight (pers. comm. 2021). Erratics from the database included in this thesis are highlighted in yellow. The full selection of erratics used in this work are included in Figures 5.7 & 5.20. Those from the database not included in this work are in blue. Note the Knight (pers. comm. 2021) erratic database does not cover Ireland and has a lower concentration of erratics in the Northern Highlands of Scotland than in England.

5.3 - Understanding the pathway taken by erratics

Reconstructing glacial transport of sediment is a complex issue. On first inspection, the problem of glacial transport of erratics is simple; ice flows from a known source rock to the location of deposition, taking the most direct route. However, once we begin to consider the complexities of the glacial conveyor belt, it becomes apparent that the issue is likely not so simple. Erratics may travel via several glacial pathways, be that supraglacial (Figure 5.5a), englacial, or subglacial (Figure 5.5b). Each pathway represents a different set of transport conditions and resulting transport trajectory (Figures 5.5e & 5.5f). Take for example a boulder falling onto the ice surface from a nunatak in the ablation area (see Figure 5.5a). This boulder will likely spend its entire

transport journey on the ice surface travelling at the speed of the ice surface. At the same time, material beneath the ice, from the same rock source as the nunatak, may release an identical boulder into the bed of the ice sheet through plucking (Figure 5.5b). This boulder may spend its entire transport trajectory at the ice sheet's bed, first being abraded, then being incorporated into a thick tractional till. Both boulders, entrained at the same horizontal location, but different vertical places within the ice sheet, will travel at different speeds. This difference in transport velocity is more significant than simply changing the distance both clasts move. Over the duration of transport journeys, the geometry of the ice sheet flow is changing. This changing geometry means the direction a clast will be transported varies over time. It is therefore possible that both boulders entrained at the same horizontal location at the same time may travel to different final locations.

Despite numerous past efforts to account for the distribution of glacial erratics, both in the BIIS and on other ice sheets, the issues of entrainment process uncertainty and transport velocities have thwarted previous attempts to effectively recreate and account for the glacial transport of erratics. In an attempt to overcome such issues, through modelling the transport pathway of erratics, this thesis looks to resolve only the maximum potential dispersal area of erratics. The fundamental assumption of this work is that, as a result of ice movement, an erratic will always be displaced in the direction of ice flow at between 0-100% of the velocity until it reaches the ice margin. The rationale for this assumption is that it allows all possible 2D (x/y) displacement scenarios to be accounted for, without the need to numerically constrain the complex systems which characterise erratic production, entertainment and transport (e.g. Hildes et al., 2004; Melanson et al., 2013; Ugelvig et al., 2016). We thus ask: given this source rock, which areas could this erratic end up in and where could it not?

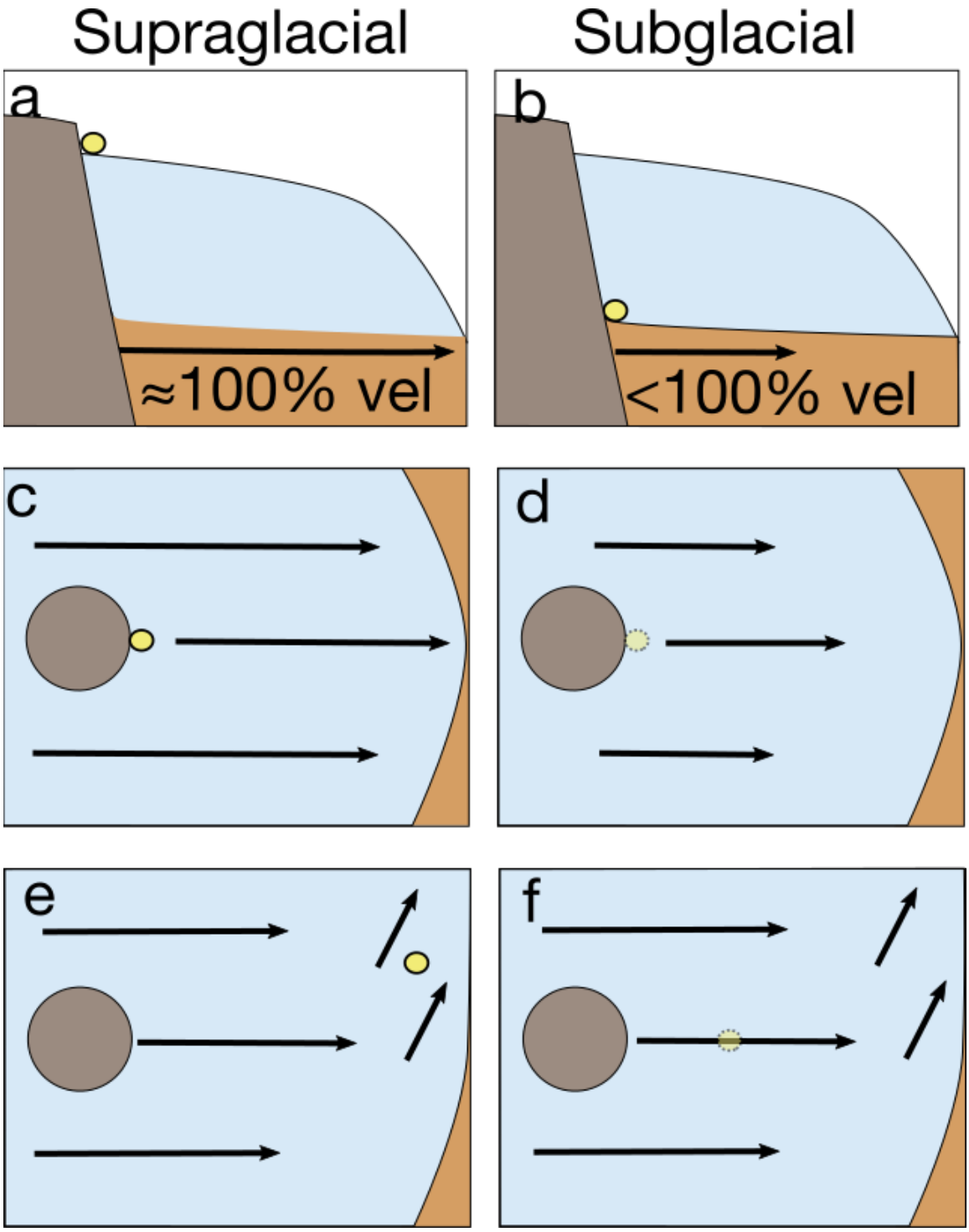

Figure 5.5: How erratic placement (yellow dot) influences transport velocity and direction. Panels a, c & e show transport of an erratic on the ice surface travelling at or near ice sheet surface velocity. In this supraglacial scenario the erratic travels far enough to enter a tangential flow field which diverts the original transport vector. Panels b, d & f show a subglacial transport pathway in which the erratic travels at less than the ice sheet velocity; this subglacial pathway is slower as the erratic spends a fraction of the transport time being slowed down (e.g. in lodgement in subglacial cavities for example). This subglacial pathway does not allow the erratic to enter the tangential flow field.

5.4 - Methods

To predict the likely footprint of erratic dispersal one could devise a scheme of seeding rocks into an ice sheet model simulation and then tracking and plotting their dispersal. Here I take a simpler approach and extract ice flowlines from a pre-existing ice sheet simulation selected in Chapter 3. I use these flowlines as part of an ArcGIS workflow to create a flow path along which erratics could move. This workflow produces possible flow paths an erratic could take, irrespective of the exact transport distances actually undertaken. It will always therefore represent an overprediction.

5.4.1 - Creating composite flow paths

The maximum potential erratic dispersal was derived using an ArcGIS workflow which combines flowlines to create a composite flow path for a specific geological source area. When conducted at coarse temporal resolutions (≈1000 year increments), it is feasible to conduct this work in ArcGIS rather than writing bespoke code. The workflow can be split into two main steps, S1 and S2 (see figure 5.6).

1. (S1) For time 1 (t1) modelled flowlines intersecting the erratic source are extracted (Figure 5.6a).
2. (S2) Extracted flowlines are truncated to remove all flowline upstream of the erratic source (see Figure 5.6b).
3. (S1) For the following time step (t2), all flowlines which intersect either the erratic source or the truncated flowlines generated in t1 are selected and extracted (see Figure 5.6c & f).
4. (S2) As in step 1 all flowlines which extend upstream of the source or the footprint delineated in t1 are removed (see Figure 5.6e & g).
5. Flowlines for t1 & t2 are merged to create a new grouping of flowlines which is used to repeat steps 3 and 4.

This work assumes maximum lateral dispersal of 1 model grid cell (5 km). Therefore, flowlines which are within 5 km of an existing flowline are included in the selection (e.g. within a 5 km buffer).

When working on coarse temporal resolutions (1000 years) on the BIIS, it is reasonable not to truncate the downflow line segments as these are likely to be shorter

than the maximum transport distance possible over the timescale. This is because assuming a mean ice velocity along a flowline of 200 ma^{-1}, erratics could be expected to travel 200 km during a 1000 year time period. Under such assumptions it is reasonable to assume an erratic travelling at the velocity of the ice could have reached the margin of the ice sheet. However, as either the temporal resolution of the ice sheet increases or the spatial extent of the ice sheet increases, the likelihood of flowlines being longer than the maximum transport distance at the ice sheet velocity increases. It is therefore preferable to truncate the downstream end of the flowline to limit the length of the flowline to that of maximum transport distance. Although such modifications are possible in a GIS, the process becomes unreasonable to complete by hand and the use of automation is required.

Three model simulations are used to generate maximum simulated dispersal areas. This work primarily uses the best ranking model selected in Chapter 3 - MR 441, as I identified it as the best candidate for capturing the flow geometry. I also examine a subset of erratics using MR 549, which represents the run with the lower 75th percentile score from model data comparison tests in chapter 3. In addition to the two simulations selected in this thesis, I used the best estimate BC model (Clark et al., 2022). The BC model run should represent the best match to ice margins, as it is 'nudged' to fit these (c.f. Clark et al., 2022). This gives me three models with different traits: MR 441 best matches flow direction; BC MR best matches margins; and 549 aligns poorly with flow direction and ice extent indicators.

I compare maximum simulated erratic dispersal area against a subsample of 2295 erratics composed from the literature (Lamplugh, 1903; Charlesworth, 1953; Sutherland,1984; Warren, 1991; Clark et al; 2004; Knight pers. comm., 2021), including 2295 erratic boulders, the majority of which are in Britain (see figure 5.7). Erratics are considered to be accounted for if they sit within 5 km (one model grid cell) of the maximum erratic dispersal area. Six geographically dispersed erratic sources spread across Scotland, England, and Ireland are examined. These were Shap, Glen Fyne, Galway Granites, Ailsa Craig, Cheviot Hills, and the Sperrin Mountains. The erratics used in this work were primarily sourced from the Les Knight database i.e. georeferenced Boulder Committee (Christison et al., 1971; 1884), with supplementary observations across Scotland being taken from Clark et al. (2004) and Sutherland (1984). I also supplemented the Ailsa Craig erratic records of erratics on the Isle of Man (Lamplugh, 1903; Moore, 1931) and the Pembrokeshire coast (Jehu, 1906). The erratic database compiled by Knight (pers. comm. 2021) did not cover Ireland. Erratics in Ireland were therefore taken from the work of Greenwood (2008), who compiled data from Charlesworth (1953) and Warren (1991).

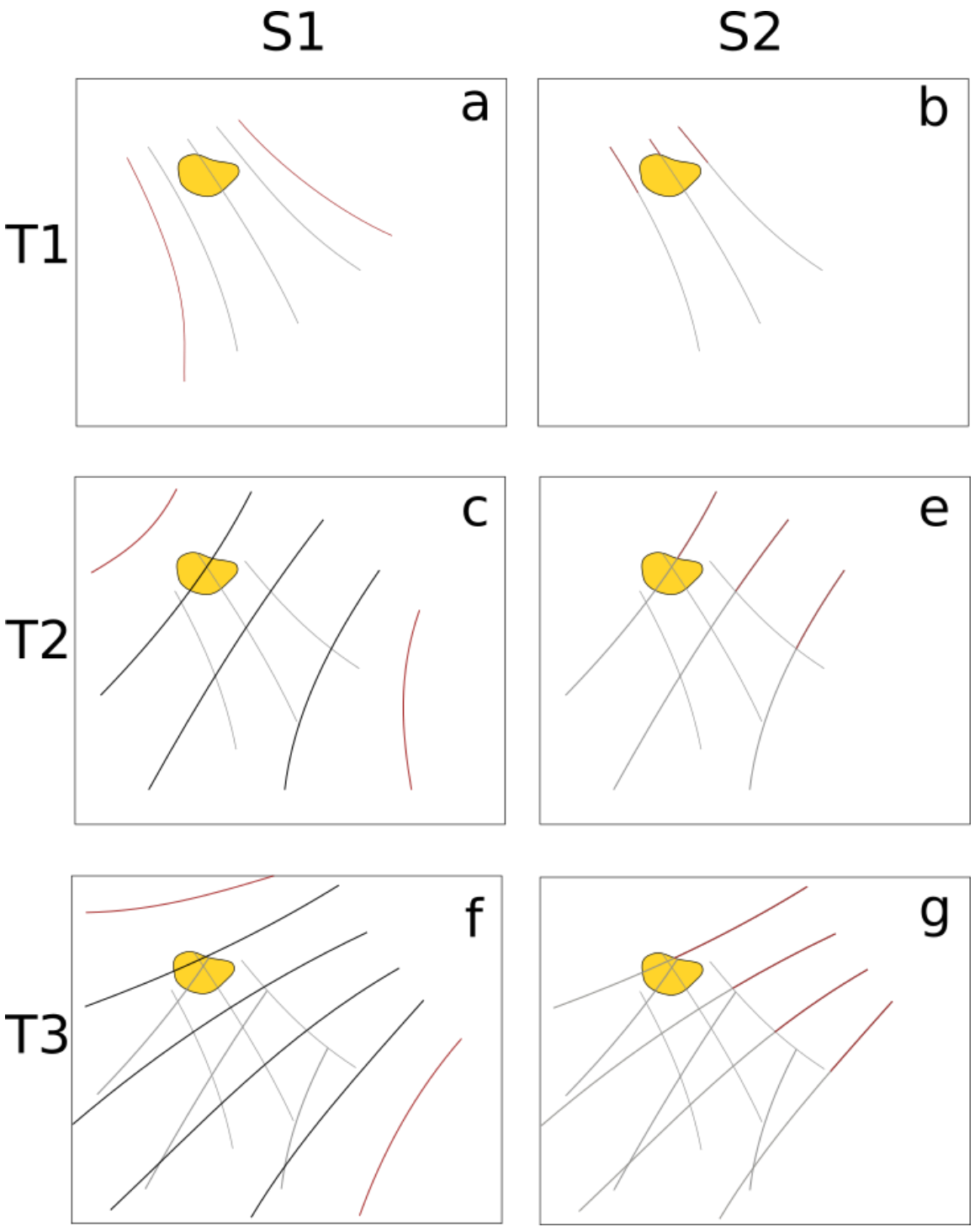

Figure 5.6: Simple sediment transport model used to predict the footprint of possible erratic deposition. An outcrop rock source (yellow) experienced ice flow towards the SE at T1 and SW (at T2), then finally experiencing a more westerly flow direction in T3. This results in a predicted footprint (Figure 5.6G). In step 1 (S1) flow lines are selected that either intercept the source, or a flowline from a previous step. In S2 flowlines are truncated to remove up flow line segments. Red line(s) are used to indicate areas which are removed due to being either too far from the source/transport path or up flow from the source.

5.4.2 - Choice of erratics to investigate.

Erratic source selection was primarily motivated by three characteristics: geographic distribution, data availability, and anticipated complexity of ice flow. I strived to select sites spread across the BIIS to identify geographic regions where simulations performed differently. A sufficiently large body of observed erratics was considered desirable so as to ensure a variety of flow routing scenarios could be tested. Finally, regions with wide variation of flow direction or historically popular due to known complexities in the flow geometry were preferred. These criteria were not strictly enforced, but were generally used to guide site selection.

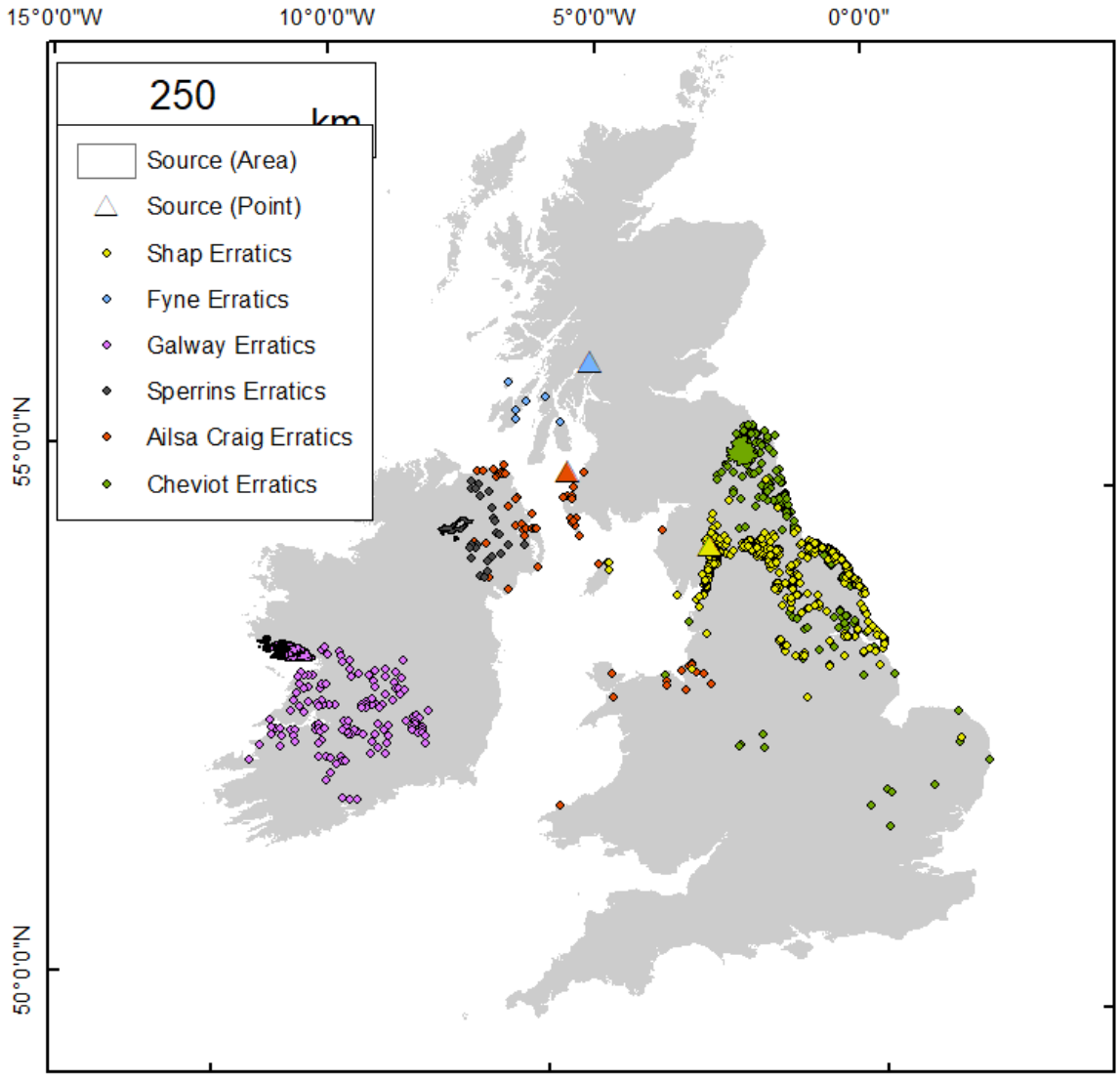

Figure 5.7: Erratic boulders and source areas compiled and used in this thesis. Where source areas are <5 km diameter they are simplified to a point (triangle for illustrative purposes). Otherwise published polygon extents are used from Clark et al. (2004).

Shap Granite is perhaps the most famous and popular glacial erratic of the early boulder collective and has long since drawn the intrigue of glaciologists and geologists (Dakyns, 1877; Raistrick, 1931; Johnson 1953; Clark, et al., 2004; Carling et al., 2023). Shap Granite originates from a small (<5 km) magmatic pluton in the east of Cumbria. It is readily distinguished from other granites by its large K-Feldspar mega crystals and is easily identifiable by its pink tint (Nicolson, 1868; Cox et al., 1996). In this work, Shap will be used to refer to this granitic source, rather than the nearby village from which the granite takes its name. Shap is located east of the mountains of the Lake District and west of the Pennines at the crest of the col between the Pennines and the Lake District. Shap is therefore likely to be influenced by both the Cumbrian and the Pennine Ice Caps, in addition to experiencing ice flowing down from Scotland. This critical location is key to glacial variation in transport direction and distance observed in Shap granite.

The Glen Fyne igneous complex is in a small (20 km^2) valley situated on the west coast of Scotland (Nockolds, 1940). The site is of particular interest to the dispersal of erratics as it is located in a region of fluctuating ice divides, and has a relatively large number of erratic boulders attributed to it. The majority of the erratics used for the Fyne valley (26) are discussed in Sutherland (1984), and further reproduced in Clark et al., (2004). Six erratics are also described in the Knight Database (Pers. Comm. 2021) which have been included in this thesis. In recent years, interest in Glen Fyne has increased with Scotgold Resources proposing the site may have geochemical potential for a commercial gold mine (Grampian Project- Scotgold resources, 2018).

The Galway granites have intrigued glaciologists for decades, with numerous attempts to explain their history and origin (Charlesworth, 1953; Warren, 1991). The Galway Hills are located on the west coast of Ireland. Erratics in this section are taken from the work of Greenwood 2008, which were in turn reproduced from Charlesworth, (1953) and Warren (1991). The Galway granites are found in a roughly south to east arc radiating up to 100 km away from the source. One hundred and twenty eight erratics of Galway Granite were included representing the most westerly and the most southern source region used in this thesis.

The Cheviot hills contain an igneous collection of outcrops In the Southern Uplands of Scotland. The geology is dominated by andesites and granites and formed as part of a period of volcanic activity in the early Devonian (Thirlwall, 1988). The

igneous rocks of the Cheviots have been observed as far south as Norfolk which made them a popular erratic of interest to the early pioneers of the Boulder Committee (Christison et al., 1871; 1884). Three-hundred and thirty-three of the erratics used in this work were identified to have originated from the Cheviot Hills.

Ailsa Craig is a small magmatic pluton (1.2 km in diameter) forming a granite island off the west coast of Scotland (Harrison et al., 1987). The micro granites of Ailsa Craig are widely recognisable due to their fine grain structure and blue tint. They are so distinctive that they are the only rock from which curling stones can be made for competitive curling (Leung and McDonald, 2022). The location and distinct geology have historically made Ailsa Craig a well-studied erratic, which has resulted in numerous reported finds (Charlesworth, 1953). For this thesis the small source area, distinctive geology and location near the Irish channel make it of significant interest when looking to constrain the transport of glacial erratics. Twenty-five Ailsa Craig erratics were identified in the work of Knight (pers. com. 2021), with an additional 26 compiled from the literature across Ireland by Greenwood (2008). Three additional sites were identified in the literature, in Pembrokeshire, the Isle of Man and the Isle of Tievebulliagh (Knowles 1903, Lamplugh, 1903; Jehu, 1906, Moore, 1931; Briggs, 1988). Reports in the literature Ailsa Craig boulders on Tievebulliagh in Northern Ireland with clasts of Ailsa Craig reported as far inland as Ballymena (Knowles 1903; Briggs 1988). Clasts on the Isle of Man were identified in coastal till sections (Lamplugh, 1903; Moore, 1931), whilst samples in Pembrokeshire have been identified in both till and beach deposits (Jehu, 1906).

The Sperrins Mountains of Northern Ireland are an igneous mountain range in the northern centre of the island. The geology consists mainly of metamorphic Greenschists (Alsop and Hutton, 1992) and glacial erratics have not received the historic attention of other glacial erratics and are therefore not as extensively documented as other geologies included in this thesis. The location of the Sperrins makes them a potentially useful study site for the confluence of the British and Irish Ice sheets as they sit close to the zone of confluence (Charlesworth, 1953; Greenwood, 2008). The Sperrins also offer a good example of mountain glacier build up as erratics radiate away from the mountain range to the east. Twenty-four erratics are used in this study for the Sperrin Mountains.

5.5 - Results

Using the maximum dispersal area method I was able to successfully recreate the transport pathways of 82% of all erratics in this study with a mean match of 75% using Ensemble Run 441 (see Table 5.1). The erratic transport model is therefore deemed successful in recreating the majority of transport paths for erratic source with the notable exception of Galway Granites, where the model is not successful with any of the three model runs.

5.5.1 - Shap

The flowline transport model for model ensemble 441 performs well at recreating erratic transport for Shap accounting for 84% of erratics. Shap has the largest number of erratic boulders of any of the sites included in this work and performs above average across all three ensemble simulations. Using model ensemble simulation 441, I am able to recreate the erratics of the Vale of York, and the Vale of Eden (see figure 5.8). The maximum extent of the model run aligned well with observations of erratics (despite exceeding the proposed Devensian limit from Clark et al., 2022).

A large number of Shap Granites are found along the Vale of Eden. The erratics of the Vale of Eden could be recreated by advance flow paths (blue lines fig 5.8), but are best accounted for by retreat flowlines (pink lines Figure 5.8). Simulation suggests the ice flowed south along the Lune Valley for <3000 years during the ice sheets retreat around 21 ka - 19 ka. During this period of retreat, marginal or subglacial deposition could account for all the erratics of the Vale of Eden. Although the ensemble is successful in accounting for the southern branch of the Vale of Eden, clasts distributed north from the source are not accounted for with simulation 441.

Four regions are noted for not being explained by the maximum simulated extent of erratic dispersal. These regions are: i) the East Coast of Yorkshire and Northumberland; ii) inland Northern Northumberland; iii) the Tweed Valley; and iv) the Isle of Man (see Figure 5.8). The main region of erratics not accounted for by the simulated erratic dispersal is the east coast deposits. These clasts are primarily in lodgement tills and beach deposits. Erratics of inland Northumberland which were not accounted for were primarily surface erratic boulders. The four erratic boulders north of Shap in the Tweed Valley were also not accounted for as were erratic boulders of the Isle of Man.

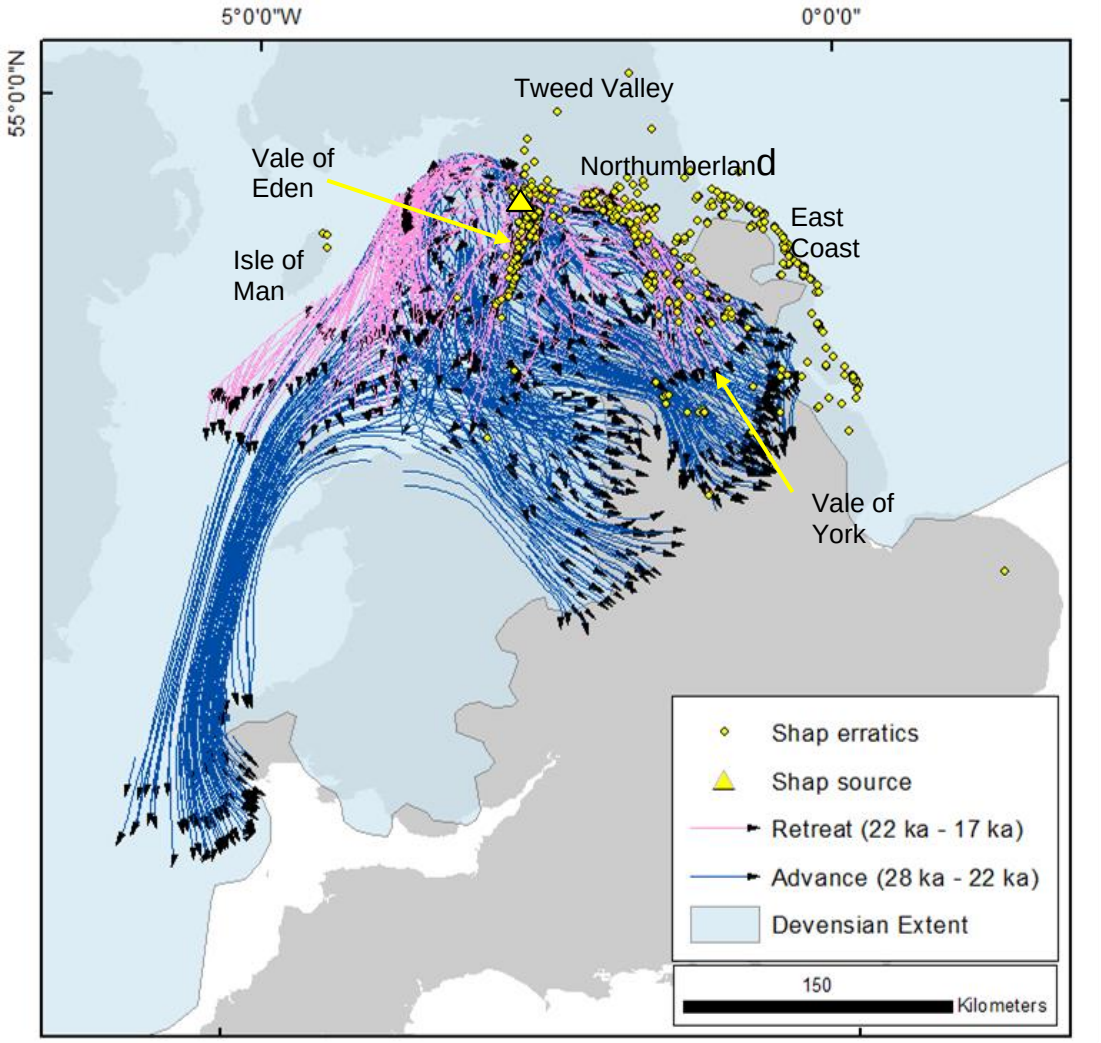

Figure 5.8: Shap transport pathways from ensemble run 441 from 28 ka to 17 ka depicted as coloured lines along which an erratic could have been deposited. Erratic boulders of Shap granite from Knight (pers. comm. 2021) are shown in yellow. Pathways are split into advance and retreat of the southern margin, with the retreat running from 21 ka to 17 ka and the advance from 28 ka – 22 ka. The simulated dispersal extends beyond the empirically reconstructed margin from Clark, et al.,2022 and accounts for a number of erratics beyond the supposed Devensian ice limit.

In addition to using MR 441, the BC simulation was also used to reconstruct the distribution of glacial erratics from Shap (see Figure 5.9). Unlike ensemble run 441, the BC model did not substantially exceed the empirically reconstructed glacial extent. As a result, erratic boulders exceeding the empirical Devensian limit were not accounted for in the Pennines. Unlike ensemble run 441, the BC model run produced a notable north flowing lobe during its retreat. Similarly to ensemble 441, erratics along the northeast coast are not recreated.

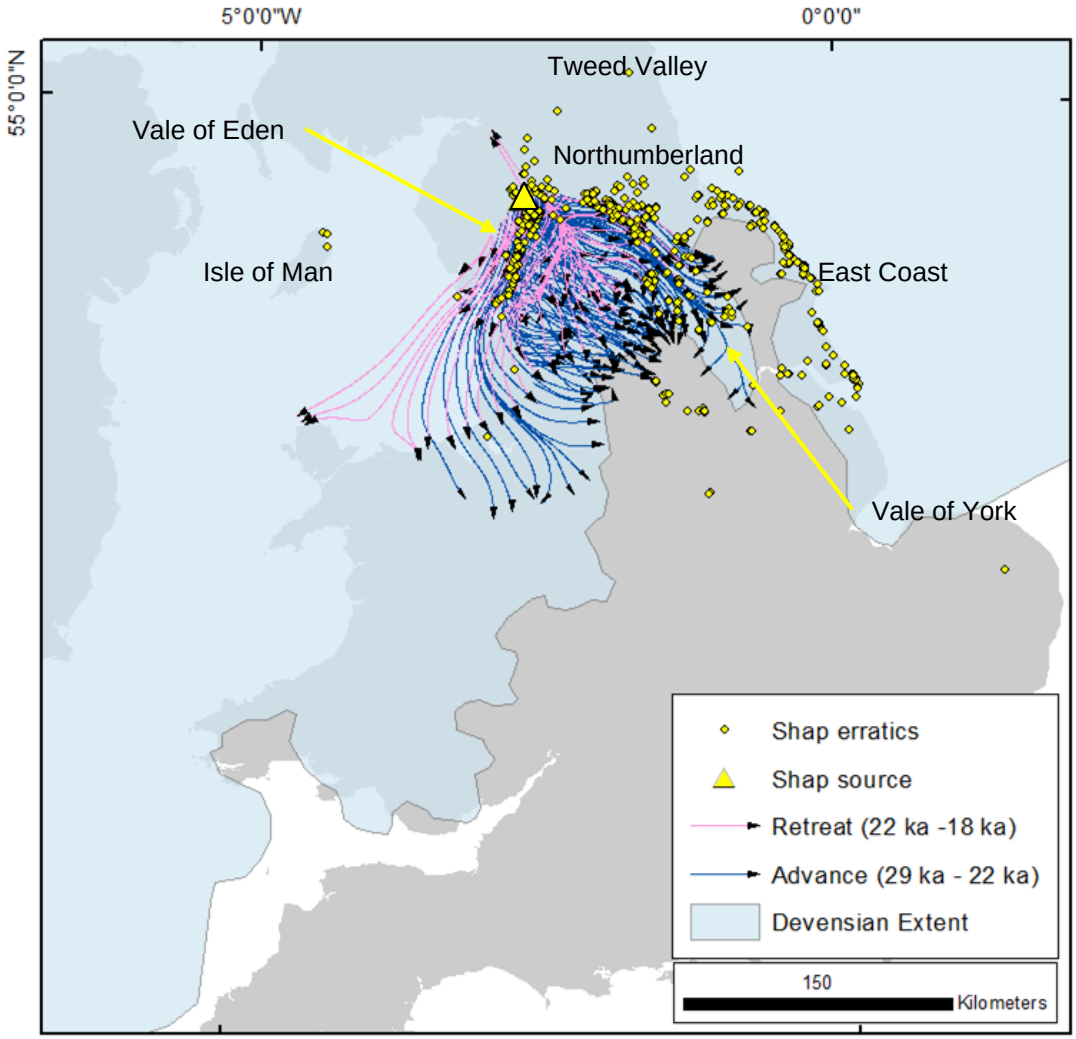

Figure 5.9: Shap transport pathways from the BC model run from 29 ka to 18 ka depicted as coloured lines along which an erratic could have been deposited. Erratic boulders of Shap granite from Knight (pers. comm. 2021) are shown in yellow. Pathways are split into advance and retreat of the southern margin of Shap with the retreat running from 22 ka to 17 ka and the advance from 28 ka - 22 ka. The model (and transport pathways) predominantly sit within the empirical margin from Clark et al. (2022) and therefore does not explain a number of erratics beyond the supposed Devensian ice limit.

The final simulation used to recreate the erratic dispersal of Shap Granites was ensemble run 529. This accounted for 99.7% of erratics with the best simulated reconstruction of Shap erratics included in this work. MR 529 rapidly grows a large Pennine Ice Cap which disperses North, before flowing into the Tweed Valley Ice Stream and south down the Northeast Coast (see Figure 5.10).

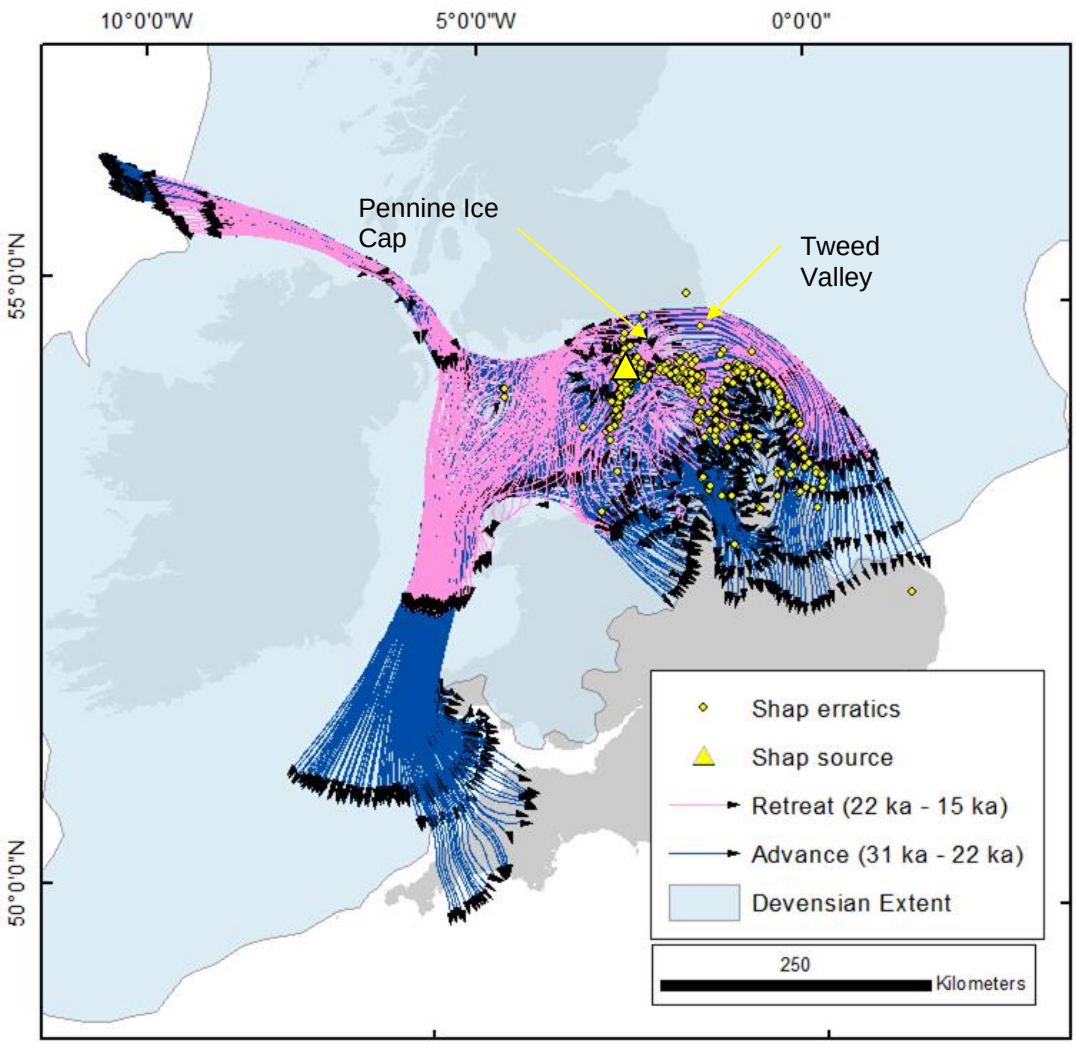

Figure 5.10: Shap transport pathways from ensemble run 529 of the BIIS from 31 ka to 15 ka and erratic boulders of Shap granite from Knight (pers. comm 2021.). Pathways are split into advance and retreat of the southern margin of the BIIS. A large Pennine ice cap is during the ice sheet build up which sends Ice North and subsequently into the tweed ice stream. The model (and transport pathways) predominantly extend beyond the empirically reconstructed margin from Clark et al. (2022) accounting for a number that explains a number of erratics beyond the proposed LGM extent.

5.5.2 - Glen Fyne

The maximum simulated erratic dispersal area of Glen Fyne using the preferred ensemble model run (441) was not successful in recreating the majority of the glacial erratics. Only 47% of erratics were simulated, these being situated on the West Coast of Scotland and the Hebrides (see figure 5.11). It is likely that a large number of erratics were deposited offshore in the Irish Sea given the marine dominated simulated transport pathway. Model run 441 did not recreate any eastern central belt erratics identified in the literature (Sutherland, 1984; Clark et al., 2004a). Of note, a number of the West Coast erratics are only recreated by a single time step in the model at 15 ka

just prior to deglaciation. The Highlands ice divide sat approximately 10-15 km east of Glen Fyne in this run. Despite not recreating the eastern erratics of Glen Fyne, the flow geometry is such that if the divide was offset 10 km west 100% of erratics would have been accounted for.

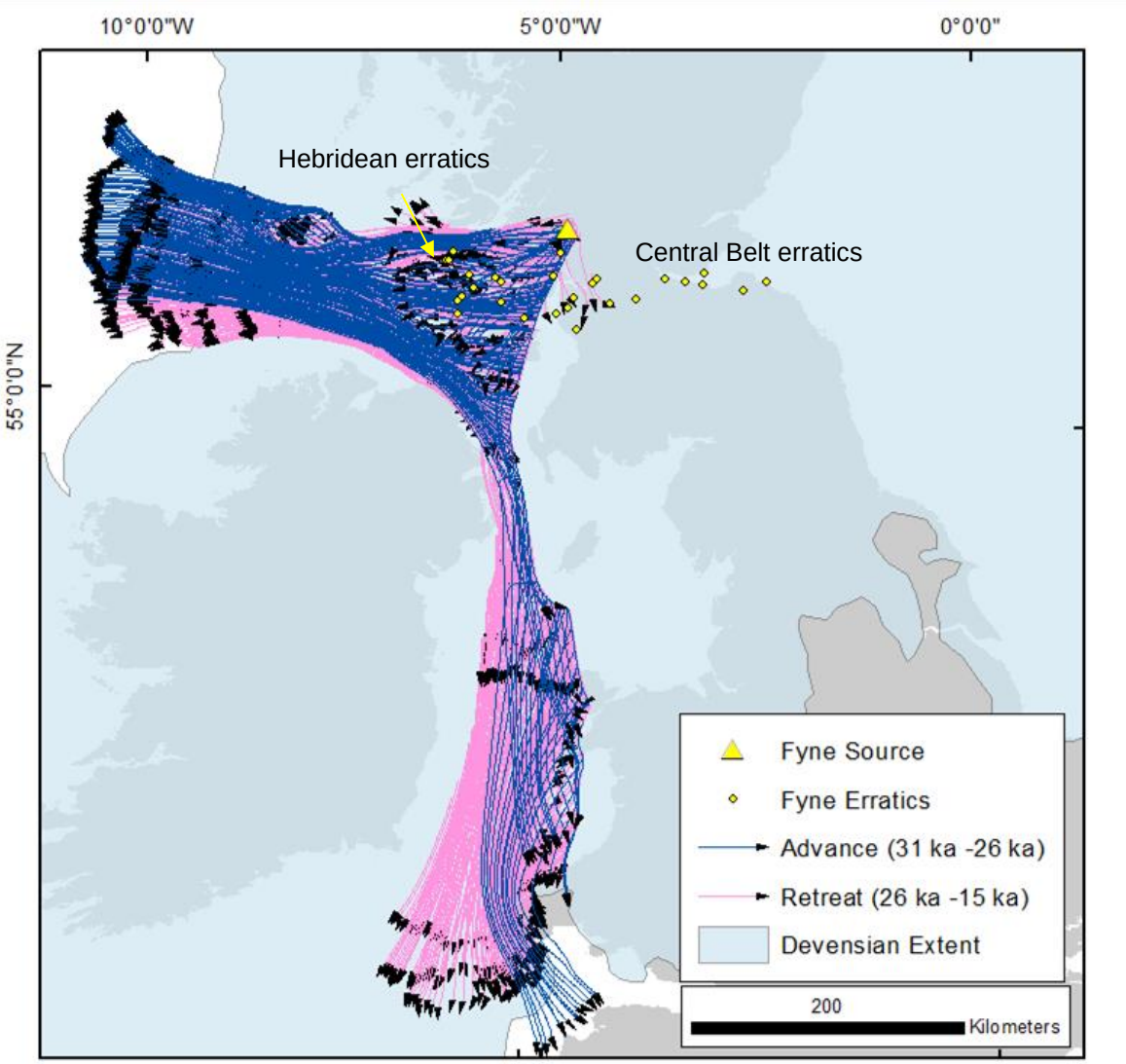

Figure 5.11: Glen Fyne erratic transport pathways from the ensemble model run 441 of the BIIS from 31ka to 15 ka and erratic boulders of Glen Fyne igneous complex from Knight (pers. comm. 2021) and of Sutherland, 1984/Clack et al., 2004. Pathways are split into advance and retreat based on the Irish Sea Ice Stream with the retreat running from 26 ka to 15 ka and the advance from 28 ka - 22 ka. The model (and transport pathways) exceed the empirical margin from Clark et al. 2022 in both outlets. The model run does not account for erratics around the Firth of Forth.

The BC model run of the Glen Fyne erratics showed the most significant difference between any two runs, accounting for 100% of erratics. This higher success

rate than ensemble 441 comes from the location of the West Highlands Ice Divide during the build-up of the Caledonian Ice Cap (see figure 5.12). The West Highlands Ice Divide in the BC run sits approximately 15 km west of that of ensemble 441, which allows erratics to be entrained into the Firth of Forth Ice Stream. Entrainment into this stream would also allow for significant distribution of erratic into the North Sea. Although evidence for this has not been recorded, searching for geochemical evidence for such dispersal poses an interesting avenue for future work.

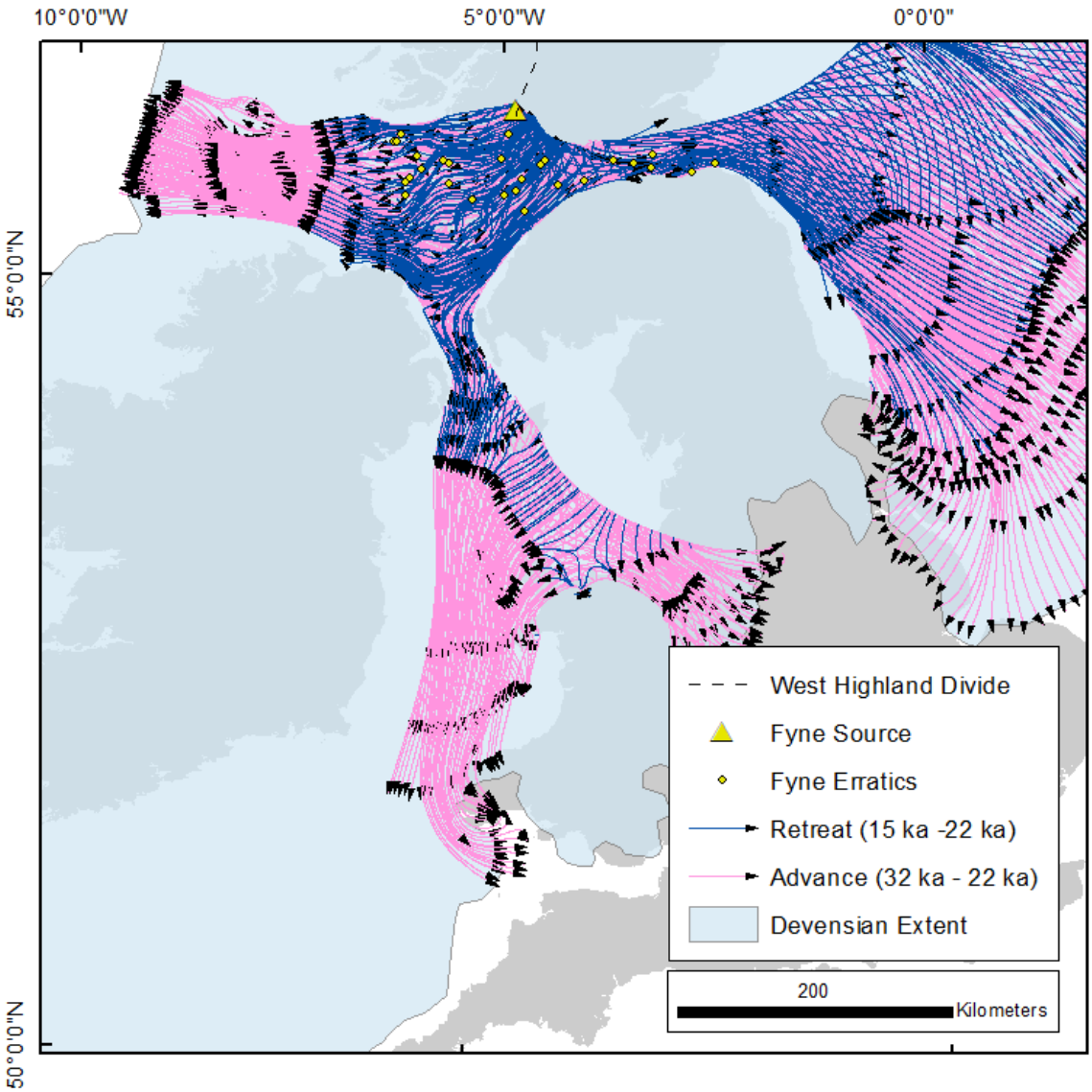

Figure 5.12: Glen Fyne erratic transport pathways from the BC model run of the BIIS from 32ka to 15 ka and erratic boulders of Glen Fyne igneous complex from Knight (pers. comm. 2021) and of Sutherland (1984) and Clark et al. (2004). Pathways are split into advance and retreat based on the North Sea Ice Extent with the retreat running from 26 ka to 15 ka and the advance from 28 ka - 22 ka. The model (and transport pathways) predominantly sit within empirical margin from Clark et al. (2022) on the southern and western extents. The BC model successfully accounts for erratics around the Firth of Forth.

The final simulation used to reconstruct the dispersal of erratics was MR 529 (see Figure 5.13). This simulation matched the least erratic of all three used in this study at 64%. As with MR 441, these were located along the western coast of the UK (primarily in the Hebrides). Similarly to MR 441, this relatively poor performance can be attributed to the location of the West Highlands Ice Divide.

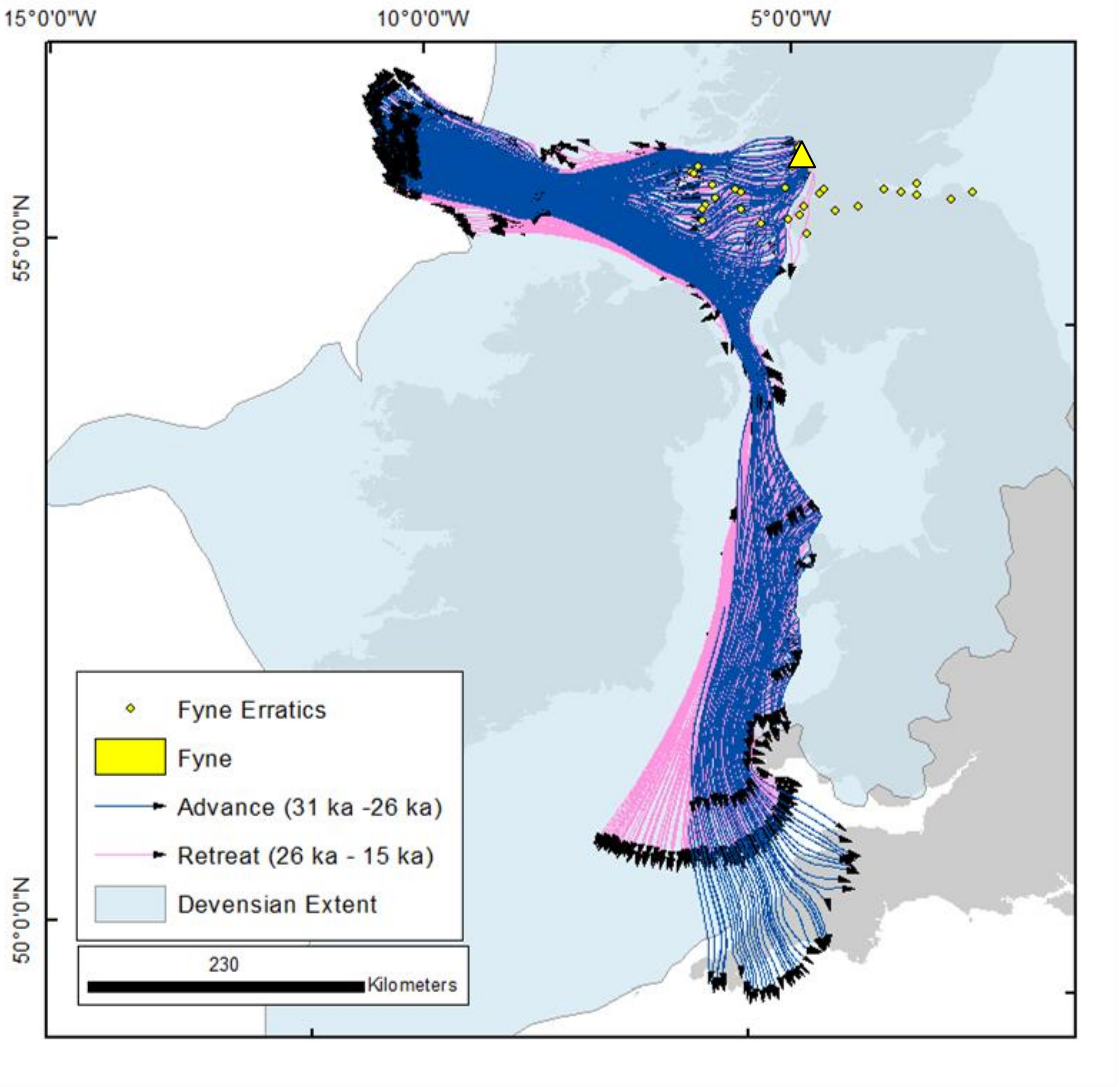

Figure 5.13: Glen Fyne erratic transport pathways from the MR 529 model run of the BIIS from 31ka to 15 ka and erratic boulders of Glen Fyne igneous complex from Knight (pers. comm. 2021) and of Sutherland)1984) and Clark et al. (2004). Pathways are split into advance and retreat based Irish Ice Stream with the retreat running from 26 ka to 15 ka and the advance from 28 ka - 22 ka. The model (and transport pathways) exceed the empirical Devensian margin from Clark et al. (2022). The simulation accounts for the erratics of the Inner Hebrides.

5.5.3 - Galway Granite

The erratic transport model in conjunction with model run 441 is unable to account for the majority of the glacial erratics of Galway Granite, barring a few located South of the main erratic source (See figure 5.14)

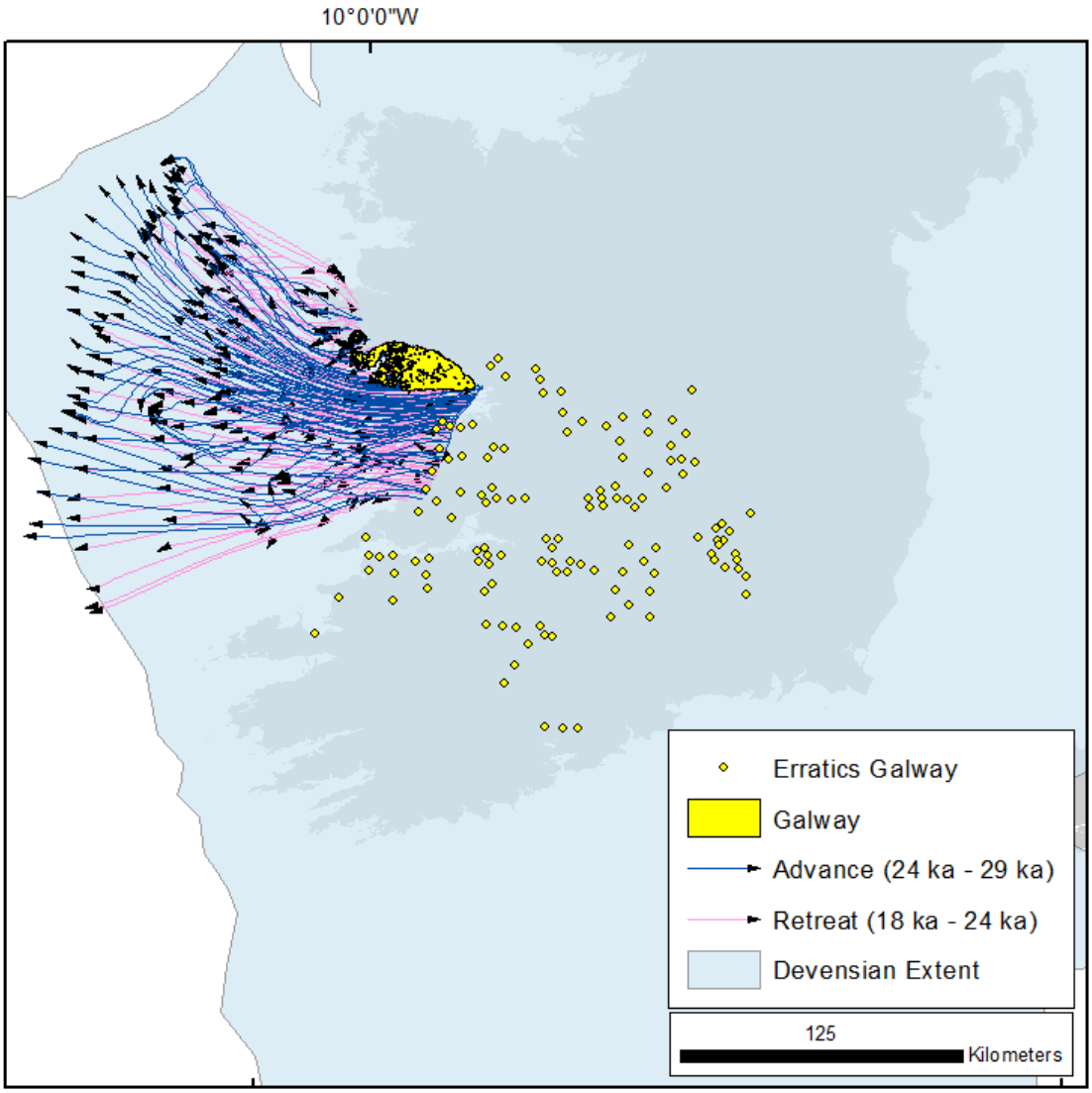

Figure 5.14: Galway erratic transport pathways from the ensemble model run 441 of the BIIS from 29ka to 18ka and erratic boulders of Galway granite from Greenwood (2008), which were in turn reproduced from Warren (1991). Pathways were split into advance and retreat based on the western margin of the Irish ice sheet with the retreat running from 24 ka to 18 ka and the advance from 29 ka - 24 ka. The model (and transport pathways) largely sit within the empirically reconstructed ice margin, and when exceeding the margin do so offshore.

The BC simulated dispersal extent stands out as the only instance where the BC model and the erratic transport model accounts for no glacial erratics (see figure 5.15). This is largely due to lack of sufficient southwards ice flow in the model.

Increased southwards flow is observed during the retreat, and it is conceivable this flow migration could have continued to arc around anti clockwise to account for some of the erratics of County Clare, Limerick and Kerry. However, arcing of flow over the erratics was not observed in any of the three model runs considered in this work.

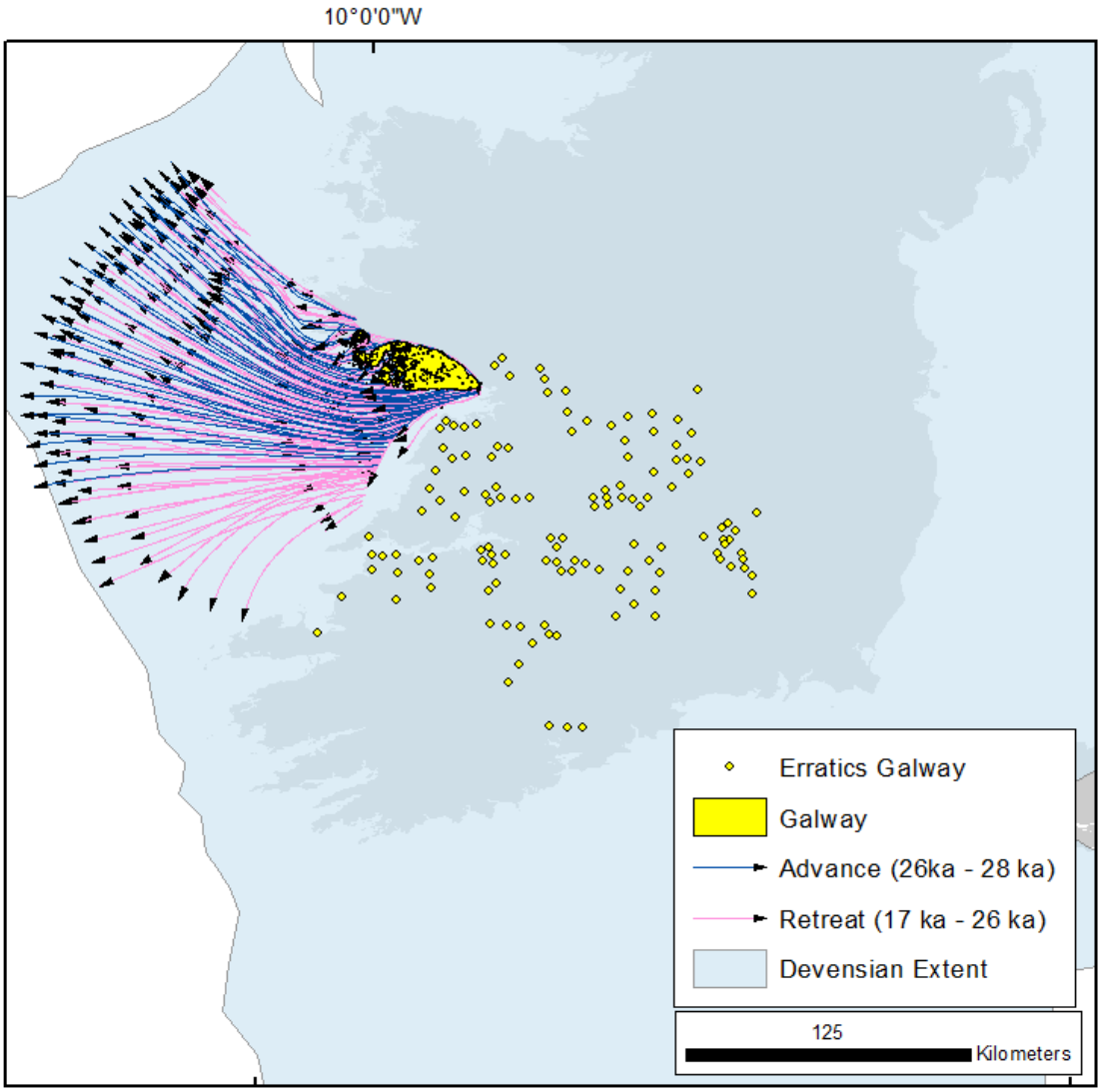

Figure 5.15: Galway erratic transport pathways from the BC model run of the BIIS from 28ka to 17ka and erratic boulders of Galway granite from Greenwood (2008) which were in turn reproduced from Warren (1991). Pathways are split into advance and retreat based on the western margin of the Irish ice sheet with the retreat running from 26 ka to 17 ka and the advance from 28 ka - 26 ka. The model (and transport pathways) sit within the empirically reconstructed ice margin.

5.5.4 - Cheviot Hills

The maximum simulated erratic dispersal area of the Cheviots using MR 441 performed above average accounting for 96% of the glacially transported erratics (see

Figure 5.16). The majority of these erratics are found on or near the east coast, with the model predicting the majority of advancing ice to transport clasts offshore. The majority 92% of Cheviot erratics are accounted for using glacial retreat flowpaths. The prediction of the erratic on the Fylde Coast in Lancashire stands out due to the narrow-modelled pathways which appear to recreate it perfectly. It is of note that ensemble run 441 reproduces flow along the Vale of York to recreate the erratics of North Yorkshire during its retreat. However empirical evidence suggests this region remained ice free during the LGM (c.f. Clark et al., 2022). Despite this, similar ice flow patterns could recreate the observed erratics without the need for ice to flow along the Vale of York.

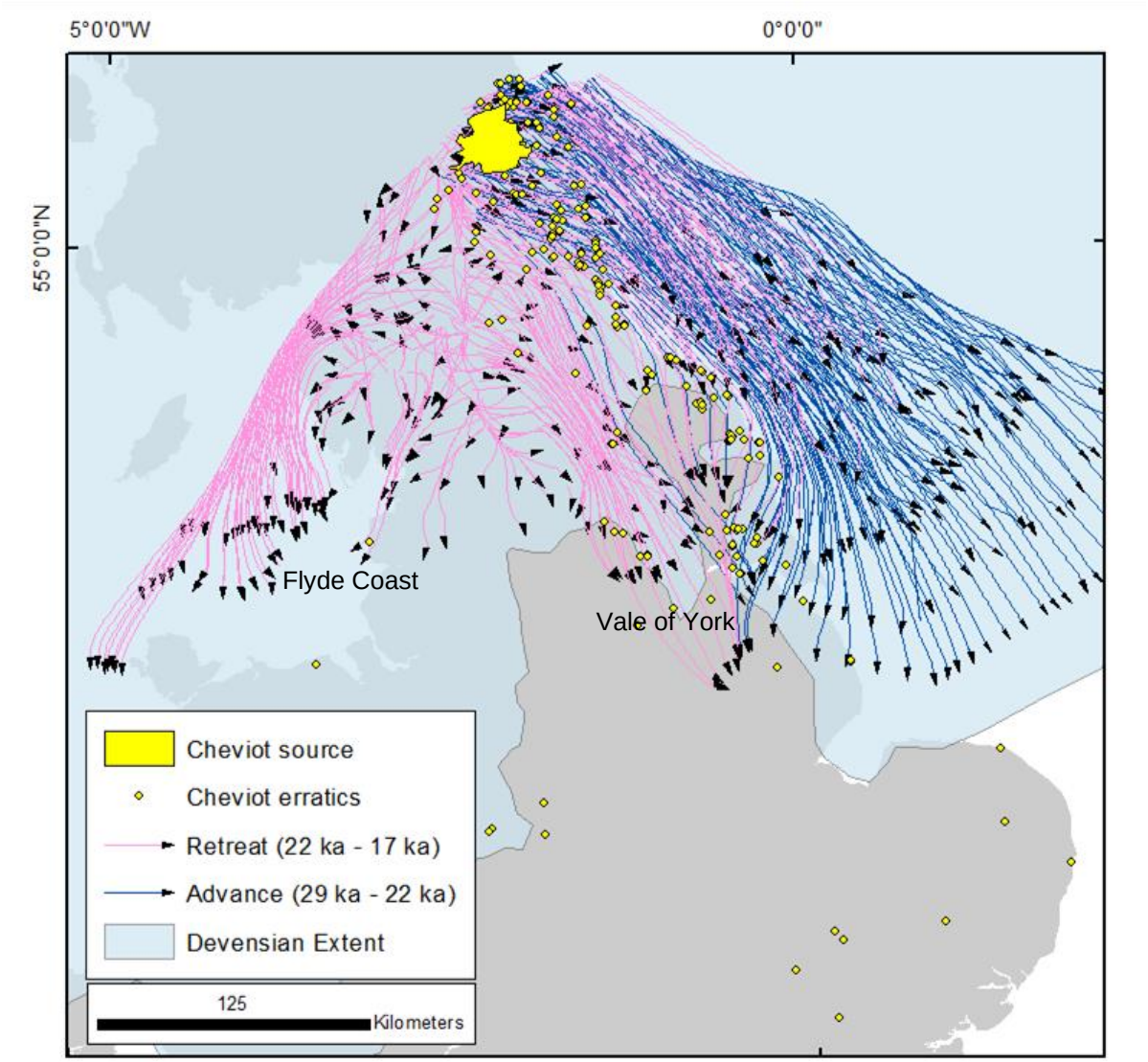

Figure 5.16: Glacial erratics transport pathways from the ensemble model run 441 of the BIIS of the Cheviot Hills igneous group and modelled advance and retreat deposit locations. All erratics are from the Knight pers. comm. database (2021). Pathways are split into advance and retreat based on the southern margin of the north sea with the retreat running from 22 ka to 17 ka and the advance from 29 ka - 22 ka. The model (and transport pathways) largely sit within the empirical reconstructed ice margin with the exception of the Vale of York.

Notable regions where the simulated deposit area failed to reproduce the depositions are those of Norfolk. The erratics of Norfolk were beyond the modelled extent and palaeo glacial evidence of the last glacial maximum. It is therefore most likely these are the result of previous glaciations (Clark and Gibbard, 2004; Gibbard and Clark, 2011).

If we assume the erratics of Shropshire are deposited during the Devensian, these can be accounted for by the maximum simulated deposit area if we allowed for a larger Cheviot ice cap during the build-up of the ice sheet. A larger Cheviot Ice Cap would send erratics 40 km northeast during the build-up the ice sheet which could then be transported to the margin in Shropshire.

5.5.5 - Ailsa Craig

Ailsa Craig erratics are well accounted for with the maximum simulated erratic dispersal of run 441. The simulation accounts for 91% of the erratics compiled in this work. Significantly the transport model predicts deposits on the Northwest Pembrokeshire coast, but not in the eastern section of Cardigan Bay, which aligns well with observations (see figure 5.17). Similarly, erratics are estimated to appear on Rathlin and Tievebulliagh in Northern Ireland, a region where glacial erratics had not been explicitly described in the geological literature. However, extensive archaeological literature commented on the use of Ailsa Craig in the use of Stone Age axes which were believed to have been made on the island (Knowles, 1903; Briggs, 1988).

The main notable erratics which are not accounted for by the simulated deposition area are the four erratics inland in Ireland which were compiled in the thesis of Greenwood (2008) (see Figure 5.17). These Ailsa Craig could be accounted for by increased westwards ice flow (of approximately 50 km) shifting the confluence zone as described in Charlesworth (1953). The converging flow regime of the upper Irish Sea Ice Stream would then sufficiency evacuate all clasts into the Irish Sea, explaining the lack of Ailsa Craig deposits further south in Ireland. This hypothesis would account for both the presence of the erratics outside the modelled deposition area, and the absence of erratics further south in Ireland. Erratic boulders in Northern Cumbria are not accounted for by the simulation but may be the result of iceberg rafting of clasts during the ice sheet retreat or of misinterpretation.

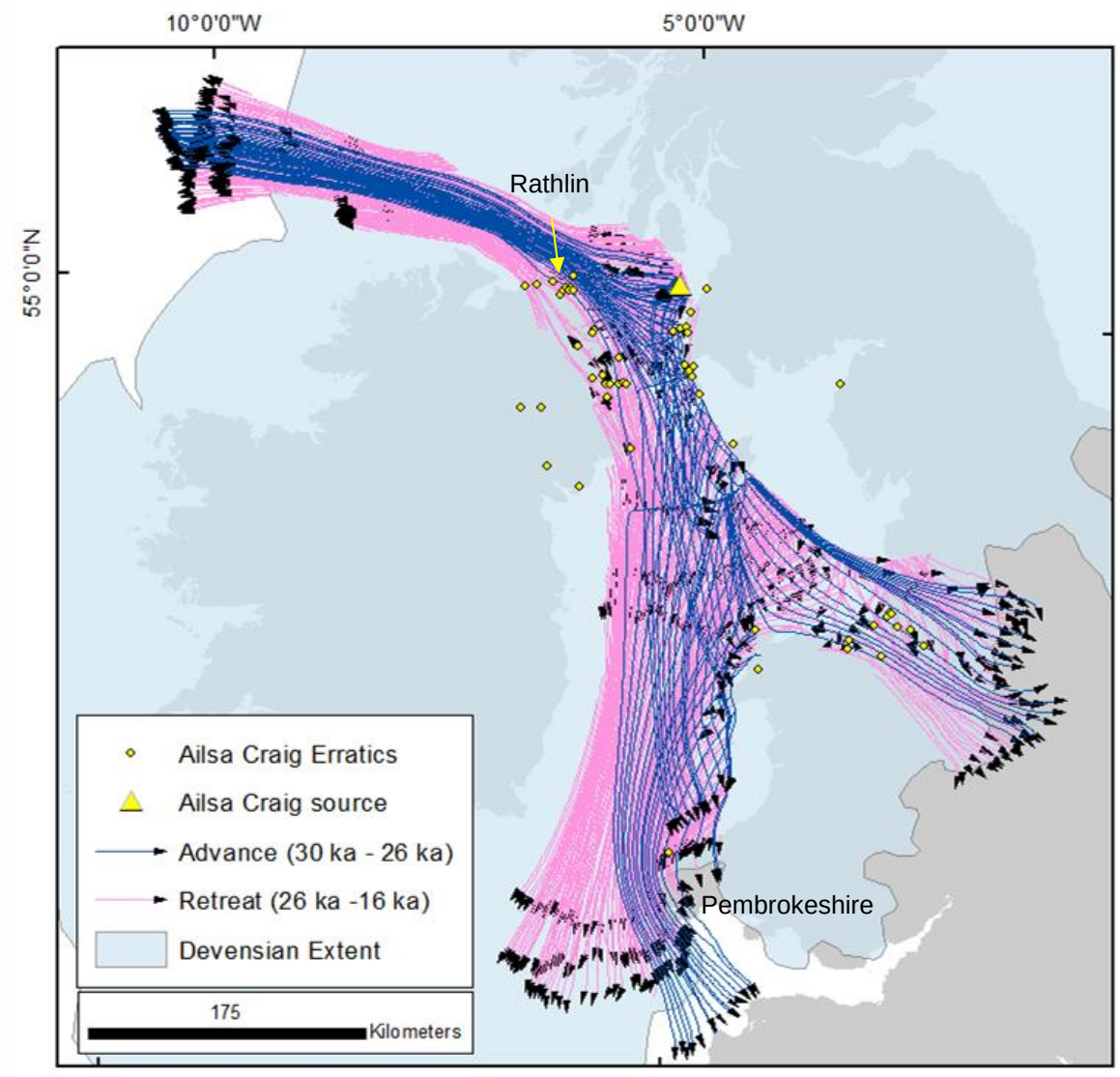

Figure 5.17: Glacial erratics transport pathways from the ensemble model run 441 of the BIIS of Ailsa Craig and modelled advance and retreat deposit locations. All erratics are from the Knight pers. comm. Database (2021) or the work of Greenwood (2008). Pathways are split into advance and retreat based on the Irish Channel Ice Stream a with the retreat running from 26ka to 16 ka and the advance from 30 ka - 26 ka. The model (and transport pathways) largely exceed the empirical reconstructed ice margin on outlets.

5.5.6 - Summary

Of all the erratics tested (2295), 1872 were recreated by model 441 yielding a success of 82%. However, this metric of total erratics recreated can be misleading due to the varying sample size of boulders attributed to each erratic source and the spatial distribution of erratic boulders. To account for the varying sample sizes I summarise the simulation by providing the mean match score, which is normalised by source region (Table 5.1). I opt to present the mean score of all reconstructed erratics rather than total percentage, as this provides a better spatial assessment of model performance. Furthermore each erratic source has a significant variation in the number of erratic boulders (discussed further in section 5.5.2) which would skew the scores to regions with more boulders.

Mean match scores show a spatial trend in matches with some areas of persistent mismatch (Galway) and others which have more nuanced differences (Table 5.1). Model run 441 (ensemble selected for ice flow geometry good) performed best overall, followed by BC (nudged to extent), followed by model 529.

Erratic source	*Total erratics*	*Model 441 Simulated best matched ice flow*		*BC model Simulation best matched extent*		*Model 529 75th percentile ice flow*	
		Erratics matched	*Percent matched*	*Erratics matched*	*Percent matched*	*Erratics matched*	*Percent matched*
Shap	1727	1451	*84%*	*1414*	*82%*	*1722*	*100% (99.7%)*
Fyne	28	21	*75%*	*28*	*100%*	*18*	*64%*
Galway	*128*	6	*5%*	*0*	*0%*	*0*	*0%*
Ailsa Craig	55	50	91%				
Cheviots	333	320	96%				
Sperrins	24	24	*100%*				
Total	2295	1872	*Mean match 75% Percentage 82%*	*1442 (of 1,883)*	*Mean match 61% Percentage 77%*	*1740 (of 1,883)*	*Mean match 55% Percentage 92%*

Table 5.1: Summary of erratic transport modelling. Quantification of success of the erratic transport model in explaining erratic dispersal. Using three model runs, the number and percentage of erratics matched is normalised by the number of erratic sources used.

5.5 - Discussion

This chapter demonstrated the feasibility of using simple transport rules and numerical ice sheet simulations to account for and predict the transport of glacial erratics. I find evidence that simulation erratic dispersal has the potential to be used as a test of model fidelity showing a hierarchy in percentage of erratics simulated. Of note, the simulation identified in Chapter 3 (441) which was the best performing with regards to flow direction, was able to match the highest weighted percentage of erratics (75%) as expected.

5.5.1 - What can be learnt from erratic records?

This work highlights the potential for understanding past ice sheet flow geometry through variation in simulated erratic dispersal relative to the erratic record. Several examples stand out where choosing different model simulations resulted in a 25% or more improvement in the simulated erratic dispersal (e.g. Glen Fyne). These variations could be the result of different model parameters (e.g. climate/ice parameters etc.). However, they could also be a result of better fit to ice margins and thus ice flow geometry. Although hypothetically one might assume the best match with lineations would also mean the best flow direction (e.g. ensemble 441), we do not have a uniform distribution of flowsets across the spatial or temporal ice sheet domain. This means some flow events are not captured or tested using solely lineations. This highlights an important potential future use for simulating erratic dispersal - which is to use erratic dispersal to score and choose between ensemble simulations. Erratics have the potential to shed light on events that lineations may not be able to account for. Unlike drumlins, which likely require warm based ice to form, erratics could be entrained without the need for specific basal conditions (e.g. transported supraglacially) (Stokes et al., 2015). As such, erratics could be used as evidence for km scale interpretation of ice divides. In this work, erratics have been shown to highlighted regions where simulations successfully (and unsuccessfully) recreate ice divides e.g. Glen Fyne with an accuracy of ≈ 10 km (see Figure 5.11, 5.12 & 5.13). Furthermore, I demonstrate how modelled erratic dispersals have the potential to delineate zones of confluence between two ice sheets e.g. Ailsa Craig over Ireland (see Figure 5.17). Although not addressed in detail in this work, it seems plausible that in future, numerical modellers could incorporate model assessment tools using erratics, much in the same way this work has used drumlins and moraines to test ice flow geometry (Ely et al., 2019a). These tools could test the zones of confluence and divergence in

numerical ice sheet models to within a matter of km (assuming we have observations or erratics in the right areas).

An interesting result of comparing model simulations to data on erratic dispersals, is that erratic deposition is predicted in locations where there are currently no observations of erratics. The results presented in this work can be seen as a foundation for expanding and testing the observational record. Specifically testing regions where we do not see observations of erratics, yet we consistently simulate dispersal. Several islands and regions stand out as being potential sinks for erratics, yet no observations of such deposits exist. For example: simulations suggest erratics from Glen Fyne should be found in Anglesey, along the North Welsh Coast and in Pembrokeshire (see figure 5.11). These regions have a low number of erratics recorded in the literature (see figure 5.4). This may in part be due to the long potential transport distances abrading boulders down to smaller more discrete sizes; or the difficulty in distinguishing small pieces of (Glen Fyne) igneous rocks from one another. This leaves an open question: Can erratics or indicator grains of Glen Fyne erratics be observed in these regions, as the simulation suggests? Similarly, despite its proximity, we do not simulate the deposition of Ailsa Craig erratics in the Forest of Galloway in southern Scotland – Is this indeed the case, and can indicator grains be identified in this region? Such investigations would be invaluable for furthering our understanding of how, when and why glaciers move sediment. For example, if we can delineate the boundary beyond which recognizable hand samples degrade into indicator grains along the simulated pathways we can answer questions such as: what rate of abrasion should we expect erratics to be exposed to during the Devensian? These are important questions for glaciology which would help improve existing and future modelling efforts.

5.5.2 - Unaccounted for erratics.

Despite the majority of erratics being reproduced by the simulated maximum dispersal, several erratic sources were not well accounted for. This offers an interesting opportunity to explore possible causes for these discrepancies. One of the benefits of using such broad and simple assumptions for a dispersal ‘model’ is that the reasons erratics may be unaccounted for lies in either the data, the simulation, or a combination of the two.

5.5.2.1 - Galway Granite

The most obvious simulation-data discrepancies occurred in the case of Galway granites (see Figures 5.14 & 5.15). The challenge of simulating these erratics arises from their odd location with respect to the coastline and interior of the ice sheet - the boulders must move eastward from Galway towards central Ireland.

No simulation in this study recreates a significant proportion of observed Galway Granite erratics in the interior (see Table 5.1). This suggest an event or process is missing from these simulations. One potential solution is the long-standing Connemara Mountain glaciation hypothesis (Hull, 1878; McCabe, 1984; Charlesworth, 1953; Warren, 1992). This proposes that glaciation in Ireland stemmed from the mountain regions (around the rim of Ireland) and expanded inwards, prior to substantial glacial interaction with the Scottish Mountain Ice Sheet (see Figure 5.18). This hypothesis seems plausible. However, it would require the Connemara ice caps to expand over 100 km eastwards before incoming ice from the west altered the ice flow direction. None of the model simulations used in this work support the Connemara Mountain glaciation hypothesis. However, this may be a limitation of the ability of the model to simulate ice cap build up, which is sensitive to climatic processes and simulation resolution targeting ice sheet scale processes and which failed to capture the inception and growth of mountain centred ice. One hypothetical method of achieving the Connemara Mountain glaciation would be to increase precipitation over the west coast of Ireland, so as to rapidly grow large ice caps which could expand east into the interior of Ireland (see Figure 5.18c). This initial distribution by the ice cap could then be reworked south during subsequent ice sheet glaciation.

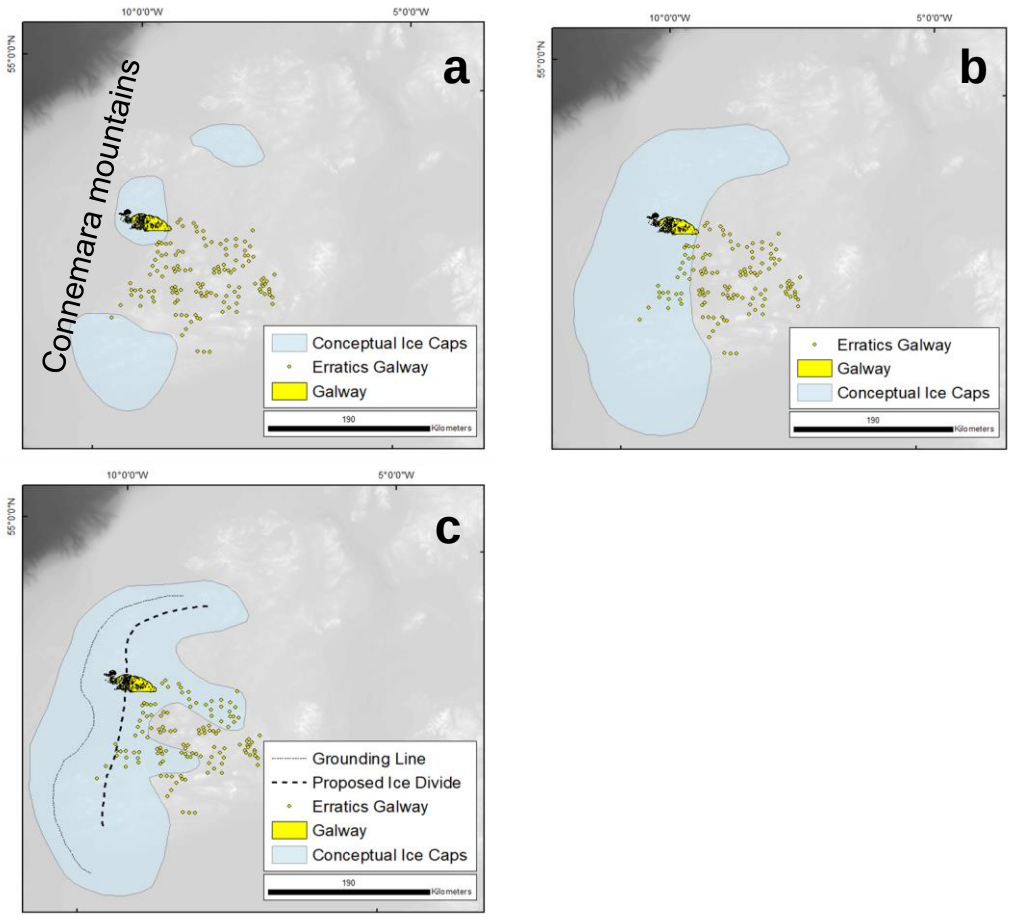

Figure 5.18: Conceptual reconstruction of the Connemara Mountain glaciation hypothesis to account for eastwards transport of glacial erratics. 5.18a shows initial build up of small mountain ice caps along the west coast, 5.18b: shows the marine termination ice cap which casts a rain shadow over the Irish interior reducing accumulation to the west. 5.19c shows the westward expansion of outlet glaciers encouraged by increased accumulation over Galway, and the buttressing of the marine terminating sector. Once the Caledonian Ice Cap crosses the Irish Sea and brings Scottish ice south, erratics transported west would be driven south into the observed distribution.

Another potential for producing the required eastwards flow of ice (and erratics) is for the ice divide of the Irish Ice dome to move further west. Such an ice sheet configuration might be achieved if the catchment size of the Irish Sea Ice Stream was larger than typically reconstructed (Chiverrell, et al., 2013). This would likely require an ice divide and considerable ice thickness on the continental shelf. Recent work has suggested the BIIS extended to cover Porcupine Bank to the west of Ireland (e.g. Peters et al., 2015; Callard et al., 2020; Ó Cofaigh, et al., 2021; Clark et al., 2022). This would increase the current margin some 80 km further west than simulated in model runs used in this thesis. If this were combined with a larger, more active Irish Ice Sea Stream, it is conceivable that the ice divide could be significantly further west than

currently observed in the simulations (see figure 5.19). Considerable geomorphic evidence has been found to suggest the Irish Sea Ice Stream was larger and more active than included in these simulations. However, it has not been possible to create a large stable Ice Stream in the Irish Sea using existing numerical modelling techniques. Such a flow geometry configuration would also be supported by observations of drumlin orientation (e.g. Charlesworth, 1953; Greenwood 2008; Greenwood and Clark 2009b). Increasing the catchment size of the Irish Ice Stream to such an extent is not unreasonable based on observations of current ice streams e.g. Evans Ice Steam in Antarctica which reaches back to within 100 km of the west Antarctic coast, yet feeds an ice stream which terminates 500 km North (Rignot et al., 2011).

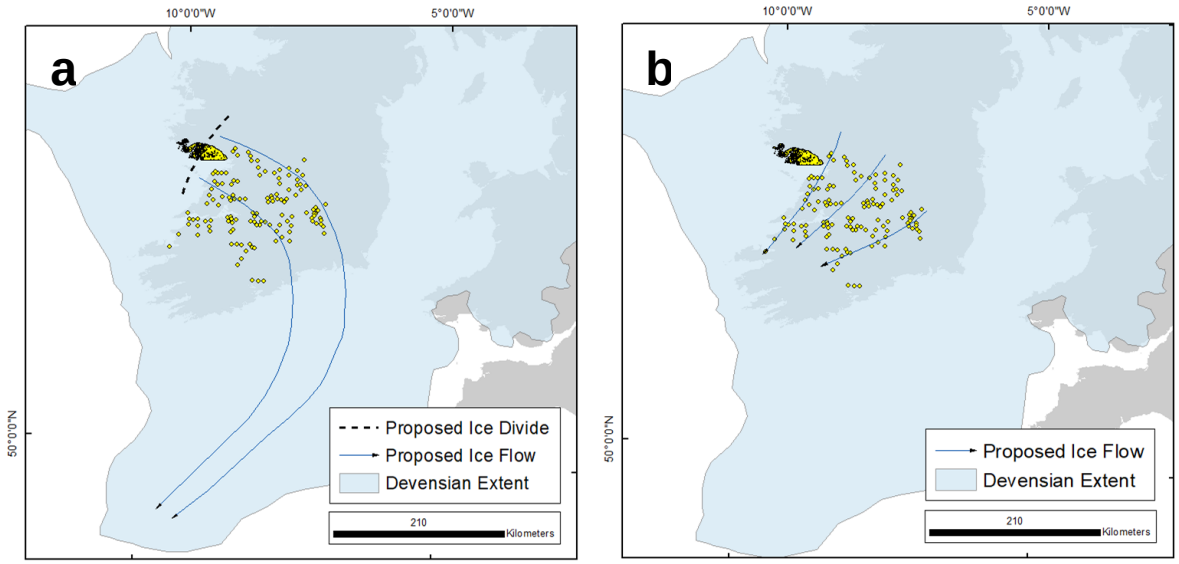

Figure 5.19: Irish sea ice stream scenario to explain Galway Granites. 5.19a larger more active Devensian Irish Ice Steam drawing ice in from the west (over Galway Granites). 5.19b remobilisation later in the Devensian moving erratics South to recreate the observed Galway erratics.

5.5.2.2 - Shap Granite

With regards to the number of erratics which different simulations recreated, Shap Granites stands out (Table 5.1). A large number of erratics were not matched by MR 441 and the BC model, which were anticipated to perform best. In contrast MR 529, which was anticipated to perform poorly being the 75th percentile in ranking in Chapter 3, matched almost all erratics. This highlights two significant factors about Shap: i) the large volume of erratics observed to originate from Shap; and ii) the complexity of the flow associated with the region (near the centre of the British Ice Sheet). Regarding point i), it must be pointed out that more Shap granite erratics have been included in this study than all other erratics combined. The quantity of erratics

included is likely due to a number of reasons including geological, cultural and glaciological. Shap granite is easily identified geologically. This makes Shap more likely to be randomly found, or to be noticed when not directly looking for erratics (or by amateur geologists). The relative hardness of the rock makes it less readily abraded during transport. This would mean it may remain intact in large samples after long transport distances (Boulton, 1978). Shap has also experienced prolonged periods of comparative literary vogue (e.g. during the time of the Boulder Committee). This led individuals to be more likely to return to areas where Shap has been found with a view of finding more erratics. It may also have been preferentially chosen long before the Boulder Committee due to its colour, weight and potential as a building material (Corradi et al., 2014). This may have meant boulders were dug out of lodgement, or moved by humans making them easier to find today. Finally, the glaciological conditions associated with Shap may provide an abnormally good source of glacial erratics both in terms of production and dispersal. In the following, I discuss some of these hypotheses in more detail.

Significant variation in ice flow directions is required around Shap to recreate observed erratic dispersal because it is observed in all compass quadrants around Shap. As a result, Shap provides a number of regions where the simulated erratic dispersal at 1 ka temporal resolution does not sufficiently account for observation of erratics. These can be split into four regions: i) Northern Northumbria; ii) the Northeast Coast of England; iii) Isle of Mann; and iv) the Tweed Valley (see Figure 5.8 & 5.9). In an effort to understand the reason erratics were not accounted, for I ran a second experimental transport set up at higher temporal resolution. This simulation used the same method described in Section 5.4 and Figure 5.6, but increased the temporal resolution from 1000 to 300 years. Using a higher temporal resolution, I was able to recreate erratics in the Tweed Valley and the Northeast Coast of England.

The experiment of increasing the temporal resolution highlights the significance of high spatial and temporal resolution during the ice cap build up stage. In the case of Shap and the Tweed Valley, erratics are transported north, then northeast during two phases of ice flow (e.g. 600 years). Significantly this allows sediment to enter the Tweed Ice Stream and for this to be rapidly transported eastwards into the observed locations. Unfortunately, the manual nature of my analysis prohibits examination of other erratic sources at this temporal scale. This is because increasing the temporal resolution of the simulated erratic dispersal without truncating the flowline length by velocity results in a higher probability of likely unrealistic flowline lengths and/or transport distances. For this experiment, each flowline could be manually checked to ensure the flowline length remained shorter than the maximum potential transport

distance. However, it is unfeasible to perform these checks at ‘large scale’ using manual methods. These higher resolution results are therefore not presented, or extended upon in this work but form an important discussion point on the significance of temporal resolution.

Experimenting with temporal resolution raises several important potential points about the use of erratic dispersal simulations. Firstly, ice sheet flow geometries can change in tens of years, with short term major reconfigurations possible in hundreds of years. Care needs to be taken when accounting for such short-term events, as small-, scale variations in geometry (e.g. of just 10 km in the case of Glen Fyne) can significantly alter where erratics can potentially be transported too. At this stage in the development of the method, balancing temporal resolution with projected scalability needs to be considered carefully. Secondly, ice cap build-up during inception can be seen in many cases as essential preconditioning of erratics for subsequent transport (e.g. Shap ice cap build up, Cheviot Hills ice cap build up). Ice sheet models generally run at several km spatial resolution. This is often insufficient for resolving small, 10’s of kms, ice caps. The issue is further exacerbated when we consider the geomorphic evidence generally used to select which is the best ensemble run relates to ice sheet scale geomorphology or at best ice cap retreat.

The Shap granite erratics of the Northeast coast of England may also offer an important and intriguing case study for preferential boulder deposition, emergence or observations (see figure 5.8). The majority of unexplained for boulders along the Northwest Coast are recorded as surface boulders, though lodgement placements are also observed. The following questions arise; Does the coastal nature of many of these boulders relate to their prevalence? Are the boulders preferentially eroded out of soft cliffs by coast processes? Could ice rafting (through ice bergs) have increased the concentration of Shap Granites along the coast? Or, could anthropogenic activity have resulted in redistribution of glacial erratics along the coast? One hypothesis for remobilization of erratics is by early Viking settlers. The majority clasts along the east coast are of the size reportedly favoured by Vikings as use for ballast rocks in their ships. Boulders were of a size that could be held with one in each hand and would be loaded into the bed of the Viking long boats. When mooring, the rocks would be removed from the boat so as to drag the ship on shore (Haynes et al., 2023). Under this hypothesis, the clasts would have likely been initially glacially transported to the River Humber which had a large Viking settlement. It is possible that at this point the boulders were loaded onto ships for travelling along the east coast before being unloaded. A similar explanation may account for the erratics found on the coasts of the Isle of Mann.

5.5.3 - The multiple glaciations problem

One trait of the erratics included in this work is the presumed largely Devensian nature of their proposed transport. Some erratics which sit within the Devensian limit (and have therefore been accounted for by the transport model) may have been the result of past glacial activity (Anglian or Wolstonian). However, the Devensian will have been important for defining their current position. Of the clasts included in this study all bar 32 of the erratics lie within either the empirically observed Devensian limit or are accounted for by model simulations of Devensian climate forcings (see figure 5.20). Of these approximately half can only be glacial accounted for through Anglian ice extent.

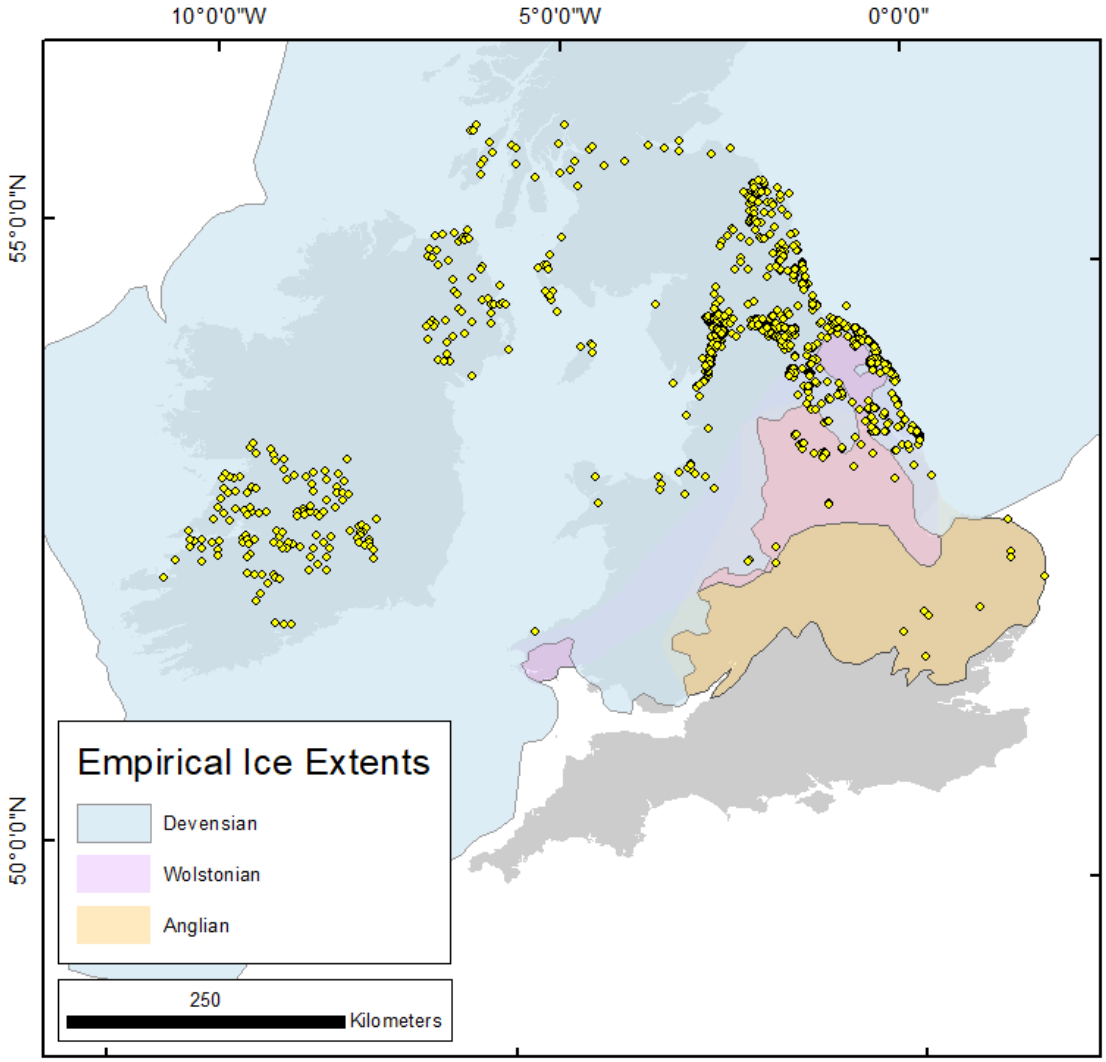

Figure 5.20: Location of Erratics in this study relative to past terrestrial glacial ice extents derived from empirical observations (Clark et al., 2022). The Devensian limit is derived from the BRITICE-CHRONO project and includes both on and offshore indicators of ice extent. The Wolstonian and Anglian limits only use terrestrial limits and therefore do not account for potential offshore erratic dispersal.

5.6 - Summary and conclusions

This chapter has presented a new dataset of glacial erratics across Britain and Ireland. These boulders were compared against the maximum simulated extent of erratic dispersal tracked within ice sheet model simulations and generated using a new workflow developed in this thesis. The simulated erratic dispersal extent presented here represents a first effort at using numerical ice sheet models to account for the distribution of records of glacially transported clasts. The tool benefits from using a simple set of assumptions as to how a clast may travel through a glacial system. It has been shown that in using these assumptions, 82% of erratics could be reproduced using the (preferred) PISM ensemble simulation (441). The novelty of this work stems from its acceptance that we cannot yet model erratics transport from first principles. Despite this, we can explain a large proportion of erratic boulder observations by using a simple set of transport and deposition rules which account for varying transport directions and distances.

In using this composite approach, I am able to account for all possible variations within the simulated ice flow without having to calculate one specific transport route. By using this composite flowline approach, a systematic comparison of all plausible transport pathways can be created without the need to parameterise unknown transport variables such as the physical processes of entrainment and deposition which in turn alter the average transport velocity. It is anticipated that this work could be used as a foundation for future testing of ice sheet simulations, identification of areas of undocumented erratics, and inform future empirical ice sheet reconstructions with regards to the location of ice divides and confluences.

This work also can be seen as proof of concept that using model data comparison to select ensemble runs for specific tasks (e.g. chapter 3) is a powerful approach. Specifically in this work we demonstrated the best performing model run with regards to reconstructing the transport of erratics was indeed MR 441 which matched on average 75% of erratics in comparison to 61% for the BC model and 55% for MR 529.

Chapter 6 - Discussion and Conclusions

6.1 - Summary

In recent years, numerical ice sheet modelling investigations have increased in number and popularity. Modellers have increasingly high confidence that model formulation appropriately captures the range of required processes and that models have finally, after many decades (Andrews, 1982), reached a point where they require confronting with observational data for testing. That models are now used for predictions of sea level rise for the benefit of society (Hock et al., 2019; Edwards et al., 2020; 2021), rather than just academic inquiry, also pushes a need for model testing and improvement. From the empirical side, there is also an increasing sophistication and confidence in that data sets are now routinely assembled, quality controlled and made available (e.g. Hughes, et al., 2016; Davies, et al., 2020; Clark et al., 2022; Leger et al., 2023) as open access, and which can then be compared to models. In response to these developments, an emerging field of model-data comparison is now underway (Tarasov and Peltier 2004; Tarasov et al., 2012; Jamieson et al., 2012; 2016; Lecavalier et al., 2014; Gregoire, et al., 2016; Ely et al., 2019a;2019b; Mas e Braga et al., 2021; Clark et al., 2022). However, glaciology has a long way to go to catch up with, for example, how climate scientists use models and data in combination (e.g. Compo et al., 2011; Jones et al., 2016).

The overall aim of the thesis was to add to the research base on model-data interoperability to reduce the disconnect between numerical ice sheet modelling and empirical observations. In this thesis, I used simulations of the British-Irish Ice Sheet (BIIS) and focussed on flow geometry, regarding it as a vital marker of the fidelity of a simulation. I have developed tools and explored both directions of model-data comparison, specifically: i) I used observations of former ice flow (drumlins) to compare, score or test a large number of ice sheet model simulations (objective 1); and ii) with model simulations that were judged good for capturing flow geometry, I explored the physical conditions under which drumlins might form (objective 2) and devised a new approach for modelling (objective 3) and exploring erratic transport. I then trialled using this transport model to assess the fidelity of PISM simulations (objective 4).

6.1.1 - Assessing model performance against ice flow geometry indicators

In Chapter 3 I identified criteria for a ‘good model simulation’ with a view of assessing the fidelity of a model ensemble which recreated the British and Irish Ice Sheet (BIIS). A core concept of this chapter is the notion that a perfect model simulation does not exist, as numerical models, and past climate proxies will never be perfect. Therefore, I scored 200 model simulations to identify which best represented the compromise on important metrics of ice sheet quality for processes related to ice flow geometry such as drumlins and erratic transport (Objective 1).

The importance of consciously choosing a testing protocol based on the desired model use is relevant. This is because with every layer of sieving, optimising for one aspect (e.g. ice extent vs. thickness vs. flow geometry) may inadvertently compromise another. This highlights the need for different model users to potentially use and combine different tests, protocols or weightings.

Using new tools and approaches for scoring model performance against data (as explained later), I sieved an ensemble of 200 simulations, sorting them from the most useful to least suitable in the context of capturing ice sheet flow geometry. Using this method, I curated a list of ten NROY simulations which ranked most highly. I then compared the ice volume and extent of the top three NROY’s with a simulation of a glacio-isostatic adjustment model that had been optimised to correctly approximate ice thickness and extent, judged against relative sea level records. This was to verify that my flow-geometry sieving had not inadvertently negatively affected unaccounted-for aspects such as a realistic ice thickness. In essence I combined the most important tests in parallel for the sieving, then ran through subsequent validation tests in series. Through this process, I was able to select a model simulation that best recreated ice flow geometry whilst not compromising on other potentially significant characteristics of the modelled ice sheet, such as ice extent.

Towards the overall aim of the thesis of improving interoperability between models and data, I also developed a number of tools, workflows and principles for model-data comparisons. These tools ranged across the full model data comparison workflow and included: a series of ArcMap Tools to re-grid observations into NetCDF’s, a series of python scripts to perform the model data comparisons (e.g. AFDA) and prepare large volumes of output data for interpretation. Automation across all sections of the workflow was required, due to the Big Data scale which is now possible in model-data comparison. For example, sieving was the culmination of 4,148,000 AFDA comparisons and 3,400,000 APCA comparisons. Furthermore, this work required

reformatting and aggregation of 85,834 landforms into 122 marine, onshore and offshore flowsets so as to convert them into an interoperable format. This represents an almost 20-fold increase in observations of flow direction (flowsets) than used in previous studies (e.g. Napieralski et al., 2007; Patton et al., 2016).

Finally, to combine these tools I implemented a novel method of combining model-data comparison tools into a single metric of simulation fidelity. This method produces a weighted suitability score encompassing flow geometry matching, which allows for simulations to be quantifiably distinguished from one another. The best performing simulation scored 18.5 on the weighted suitability score as a result of matching 110 flowsets and 55 margin positions.

Aside from the above methodological developments and outcomes, I also found evidence of the Mohr-Coulomb criterion paired with a prescribed till friction angle map to be the numerical scheme for prescribing basal conditions to consistently create higher ranking models. Of the top 10% of model simulations (ranked using the weighted suitability score), most (70%) used calculated yield stress using the prescribed till friction, whilst most (80%) of the lower 10% scoring simulations used prescribed yield stress to calculate sliding. This is perhaps a useful guide for future modelling endeavours, affirming the rather laborious task of compiling maps of bed geology and ascribing shear stress values to different substrates is indeed preferable.

6.1.2 - Under what physical conditions do drumlins form?

Despite concerted investigation for one and half centuries, drumlin formation is still highly contentious (e.g. Davis, 1884; Fairchild, 1929; Prest, 1969; Patterson and Hooke, 1995; Hart, 1999; Stokes et al., 2013; Eyles et al., 2016; Iverson et al., 2017; Ely et al., 2023). I propose that one of the key bottlenecks in resolving the problem of drumlin formation is the lack of contextualising observations on the physical conditions under which they form. In Chapter 4, I address this by using well-constrained numerical ice sheet simulations as an ‘observational’ environment in which to explore drumlin formation (objective 2) across the British Isles. A similar approach had been taken with regards to the formation of MSGL for a cross-shelf trough in Antarctica (Jamieson et al., 2016), but in this thesis the focus is on drumlins, and at a larger ice sheet scale. The premise is that when drumlins are found to match flow directions within the ice sheet model simulation, the physical conditions of ice velocity and thickness could be the conditions under which the drumlins were created. Using such an approach, I collate the largest database of drumlin ‘observations’ paired with glacial conditions,

which could provide a central piece of evidence for future drumlin formation models or hypothesis testing.

The main conclusion based on drumlins of the BIIS is that drumlins are likely associated with a specific range of velocities and thicknesses; velocities of between 100 and 350 ma^{-1}; and ice thicknesses of between 850 m and 1250 m. These results are consistent with the small number of observations of drumlins and MSGL imaged beneath the Antarctic Ice Sheet (King et al., 2007; 2009; Smith et al., 2007; Schlegel et al., 2022; Holschuh et al., 2020; Bingham et al., 2017) and from previous model-data comparison (Jamieson et al., 2016). Velocities align with the range previously observed for drumlins beneath Antarctica and proposed in the literature, yet sit below the velocities of observations from MSGL (King et al., 2007; 2009; Smith, 2007; Stokes et al., 2015; Jamieson et al., 2016). I directly compare the velocity change predicted from my observations of the BIIS against current velocities in Antarctica and regions where MSGL and drumlins have been observed subglacial using GPR (King et al., 2007; 2009; Smith et al., 2007; Rignot et al., 2011; 2016; Schlegel et al., 2022, Holschuh et al., 2020 and Bingham et al., 2017). In doing so I found predicted velocities from this study aligned with 50% of regions where lineated bedforms had been mapped beneath the Antarctic Ice Sheet. Only 16% sites (two) where lineated bedforms were identified beneath ice in Antarctica had velocities lower than those identified in this thesis. In contrast 34% were identified in regions of greater velocity. Thicknesses ‘observed’ in this thesis were greater than those generally suggested in the literature for drumlins, although they sit within the upper limit of palaeo estimates (Patterson and Hooke, 1995) and well below observed thicknesses in Antarctica (Schlegel et al., 2022). Ice thicknesses observed in this work spanned the same range as those identified by Jamieson et al., (2016).

A problem with all data on drumlin formation conditions (i.e. an upper and lower parameter bound) is the fact that some degree of drumlin-forming switch likely exists. They do not always and continuously develop, rather, conditions come and go and they intermittently grow and develop (see Chapter 4). This is important because an observation of a drumlin beneath present day ice does not mean it is actively forming under those conditions. This thesis also found further evidence to support the hypothesis that regions of cross-cutting drumlins are evidence of a potential drumlin-forming switch. I observed cross cutting drumlin fields and find they likely formed over hundreds of years through repeat periods of drumlin-forming conditions associated with pulses of partial advance and retreat.

Through the examination of thousands of model-data matches, and the resulting bedform morphometry it is apparent that bedforms are not simply the result of ice parallel flow, and that a mechanism is required to begin the formation process. I find flowsets which match for the longest time have a characteristic background signal, similar to non flowset match conditions which I propose is a superimposed 'coincidental match' (i.e. ice flow in the same direction without forming bedforms). Based on this signal, and observation of the length of velocity and thickness threshold observed in this thesis, I suggest that drumlin formation conditions tend to persist for between 10^2 and 10^3 years, which I suggest is likely indicative of the time needed for drumlin formation in the context of the BIIS. I also highlight that model data matches can persist for thousands of years before drumlin formation is believed to commence (as demonstrated by the large coincidental signal in observed velocities).

It has been a long-standing hypothesis that bedform length is associated with glacial conditions (Clark, 1993; 1998; Hart, 1999; Stokes and Clark, 2002; Stokes et al., 2013; Barchyn et al., 2016; Jamieson et al., 2016; Ely et al., 2023), notably longer bedforms equate with faster flow velocities. In this thesis, I found a relationship between bedform length and glacial conditions by investigating the effect of prolonged ice flow on bedform elongation. To achieve this, I used the cumulative velocity, a metric for normalising velocity by time, to allow for a comparison of drumlins at a flowset scale against velocity. Although not directly measuring basal sliding, this metric could be seen as a proxy for cumulative ice parallel basal sliding distance. Using cumulative velocity, I identified a relationship between drumlin length and cumulative velocity. In other words, I have found evidence to suggest bedform elongation is a function of velocity and time, i.e., more elongate drumlins arise from more metres of ice passing over them.

6.1.3 - Implementing erratic transport in ice sheet models

One of the first tools used for reconstructing palaeo-ice sheets was the transport of erratic boulders away from their source geology (Buckland, 1841; Lyell, 1841; Agassiz, 1841; Geikie, 1894; Charlesworth, 1953). However, in recent years their use has largely fallen out of favour. In Chapter 5, I demonstrated that erratic travel can be a powerful tool for helping to reconstruct palaeo-ice sheets and potentially test numerical models. I developed a simple, yet effective, flowline-based erratic transport model (objective 3). It is likely that one of the reasons past work has not widely used erratic transport within ice sheet models is due to the perceived complexity of the process of erratic entrainment and deposition mechanisms. The premise of this chapter

was to reconstruct the maximum possible dispersal distances from known erratic sources, ignoring the problems of how to formulate and parameterise entrainment and deposition factors. Instead, we focused on ice flow direction and its variation over time, and used the broadest possible assumptions of transport velocity. The great surprise is how little information is needed to successfully explain a large number (82%) of erratic transport observations. This demonstrates that only limited parameterisation is needed to estimate the maximum possible transport extent of glacial erratics, and that flow direction shifts, at least in this ice sheet, outweigh issues of sediment entrainment and deposition.

To build and test the erratic transport model I used 2295 erratics originating from six geologically distinct rock types (Shap, Ailsa Craig, The Sperrin Mountains, The Cheviot Hills, Glen Fyne and Galloway). I compared these against three model simulations of which two were from the ensemble and one from the nudged BC simulation.

Using this simple erratic transport model I have shown it is possible to identify kilometre-scale discrepancies between modelled ice sheet flow geometries and the empirical record from erratics (objective 4). For example in Chapter 5, the position of Ailsa Craig erratics in Northern Ireland record the confluence zone of the Irish and Scottish Ice Sheets, and suggest the modelled confluence zone was too far east. Similarly, variation in the dispersal of Glen Fyne erratics showed a 10 km shift in ice divide location altered the dispersal geometry from bifurcating (east-west) to single branched (eastwards). In doing so, a small change in dome geometry halved the approximate dispersal area. A surprise in this chapter was the significance of km-scale changes in dome geometry on the larger erratic dispersal record. Put differently, some erratic sources are highly sensitive markers of small changes in ice sheet geometry, especially near divides. Results from this study highlight the potential use of erratics as a test of ice sheet geometry as they are sensitive to small perturbations in ice divide location.

6.1.4 – Uncertainty of match timing

One of the challenges of this thesis has been to constrain the timing of drumlin forming events. In using a model data comparison approach, establishing this timing fundamentally relies on assumptions as to how drumlins relate to ice flow conditions. The core premise for identifying the timing of drumlin formation is that drumlins form in the direction of ice flow and so when they match with modelled flow direction they likely formed at one of these matches in time. I found evidence, which was interpreted to

suggest the timing of drumlin formation was the result of a combination of glacial conditions, rather than simply the imprint of the most recent ice flow. Significantly this means that to identify the timing of a drumlin forming event we may need to be confident in our modelled ice flow conditions.

Prior to making the observation that drumlin formation likely only occurs under a narrow range of glacial conditions (see section 4.5), I investigated the avenue of drumlin formation occurring during the most recent period of match (e.g. last 100, 300 or 500 year period). In these scenarios, the assumption is that although drumlins may have formed earlier, they were continually reshaped until the ice flow geometry no longer matched. Experiments, assuming the most recent ice parallel conditions relate to drumlin formation or reorientation were interpreted to be inconclusive as the glacial conditions during the last match were found to be inconsistent across different flowsets. This is interpreted to imply no consistent formation or reorientation mechanism across the most recent matches in time. These experiments are not presented in this thesis, because they were inconclusive.

When considering the dataset of ice parallel conditions (matching conditions) a distinct bimodal distribution could often be found. Subsequent investigation showed some flowsets which only matched once (e.g. single <500 year match). The rationale behind investigating flowsets which only matched once is that assuming both the model and data are correct there is no uncertainty in the timing of the formation event (and is discussed in more detail in section 4.3.4). Of these single matches only the short 100-300 year matches showed distinctive unimodal distribution in ice flow conditions (velocity) and these signals were interpreted to represent the conditions associated with formation.

With regards to the uncertainty of match timings it is of note that the matches used to sieve the model ensemble likely provide an overestimate (too wide) of possible ice flow conditions. However, addressing this overestimate risks introducing a circularity to the model-data comparison results and experiments. In an effort to avoid potential circularity in the results, rather than introducing bias by selecting matches based on ice flow conditions, I analysed the full match and filtered the results so as to remove what was interpreted to be a baseline signal on non-drumlin forming events. Using this filtering approach, results are found to be broadly consistent with previous hypotheses in the literature (e.g. Patterson and Hooke, 1995; Stokes et al 2017). It remains a problem though that selective filtering introduces a methodological bias towards observing drumlin formation under higher velocities ice flow. In other words, although the filtering appears necessary to develop observations of drumlin formation

and their timings, it may in turn eliminate important information though filtering (such as a lower velocity signal) which is in fact present in a drumlin forming event.

Adding to the challenges of constraining match timings, some flowsets may be incorrectly categorised as a single flowset (event in time) when in fact multiple drumlin forming events occurred. In such a scenario accurately estimating a single point in time for drumlin formation to have occurred would not be possible. This however highlights a benefit of distribution filtering in that, some of these errors (e.g. in coincidental matches or incorrect grouping of multiple flow events) will be averaged out proving a more representative sample of drumlins formation conditions. This stems from the aggregation of all pixel values from matching flowsets prior to filtered. This means that if a large flowset (where each pixel has a smaller contribution to the AFDA score) has a subset of pixels which are incorrectly grouped outlying values will be smoothed out.

It should be noted however that incorrect flowset grouping may still affect the sieving process, and in turn the NROY selection. As a result, some of these biases (incorrect timing of matches or grouping of flowsets) may still be affecting the resulting model output and drumlin forming conditions. Incorporating conditions required for drumlin formation into model-data comparison testing routines is therefore likely an important issue to be addressed to reduce timing uncertainty and is discussed in more detail in section 6.3.3.

In summary, there is perhaps still no perfect method of constraining the timing of model-data matches against drumlins. However in this thesis I have grappled with the challenges associated with using model-data comparison to understand how drumlins form, and understand ice sheet processes. In doing so I have helped reduce some of the uncertainty in the potential timing of some drumlin forming events but more work is needed to fully constrain the timing of model data matches.

6.1.5 - Synthesis of model data comparison results

In this thesis I have highlighted the importance of model-data comparison using a variety of tests against different types of data, namely ice extent and flow direction, for the purpose of sieving model ensembles to find the most realistic member. Specifically, I have highlighted how such a multi test approach can help reduce uncertainty with regards to issues of equifinality of the chosen simulated ice sheet. For example, a simulation might yield the correct ice volume judged against sea level records but have the wrong ice extent. To address this I used in-series tests, where key metrics (such as ice extent) are used in parallel for initial sieving, and metrics addressing equifinality (such as ice volume) are subsequently used to validate the

results of the sieving (see figure 6.1). The benefit of in parallel testing is that only the 'most important' metrics of ice the desired ice sheet are used for sieving. These can be combined using an explicitly defined weighting scheme, which makes the ensembles quality assessment priorities more transparent. This decreased the possibility of inadvertently sieving out models based on characteristics which are not a priority. Subsequent in series tests then help validate the initial sieving results. The ordering of these tests (which are performed in series vs in parallel) is specific to the model users desired traits required of the ice sheet simulation. By adopting a mixture of in-series and in-parallel testing, each layer of testing can be used to independently help support the rationale that the model is producing the correct answer through the correct process.

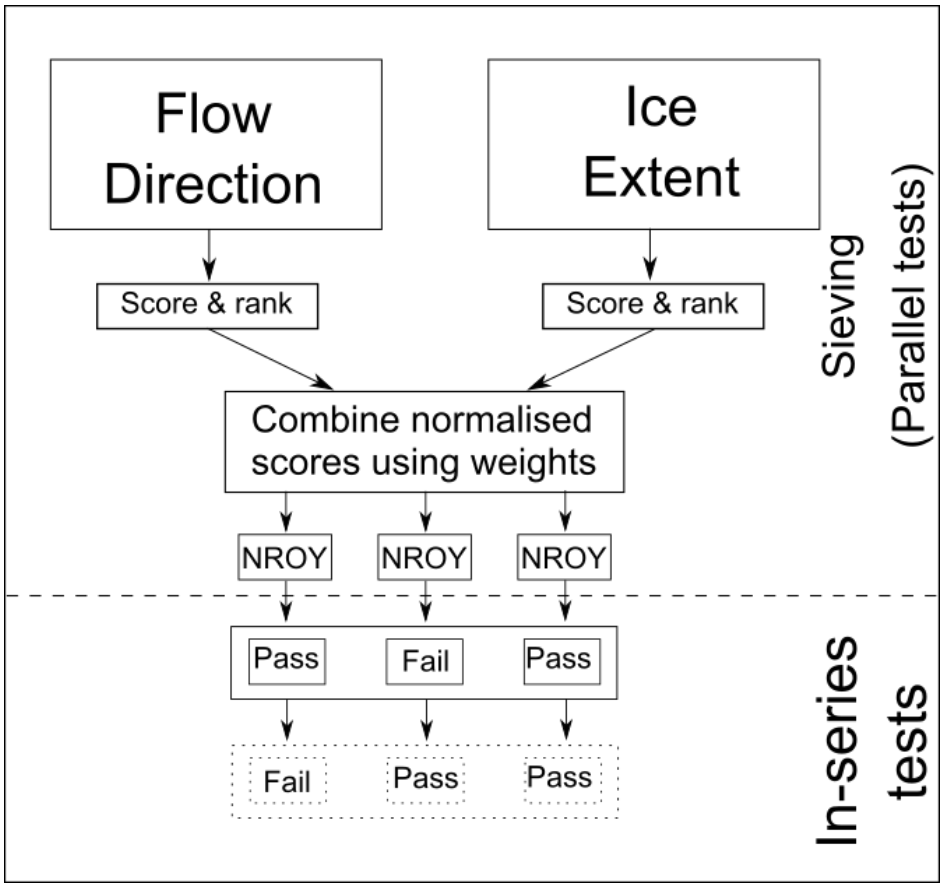

Figure 6.1: Combined parallel and in series tests of ice sheet model fidelity. Each test is conducted in isolation, before scores are normalised (in this thesis through ranking). Scores are then combined using user specific weights based on the modelling rationale and the perceived relative importance of each test. This produces an NROY list. Each NROY can then be evaluated using in series tests to ensure the right result has been achieved for the right reason. In this thesis I used ice sheet volume as an in series test and explored the use of erratics as such a test. Many tests can be run in series (idealised by the dashed boundary boxes). The test included both in series and in parallel and the weights used when combing them would be specific to the requirements of the model user.

Different tests may inherently have spatial discrepancies as a result of the availability of data (e.g. location of drumlins) or the glaciological processes implicit in the model data comparison tests (e.g. the need for warm based ice for drumlin formation). Using multiple tests can help address a breadth of scientific challenges in palaeo glaciology, such as the uneven spatial availability of observations, the varying precision of flow geometry tests and the tough requirement of creating a continuous reconstruction from a palimpsestic and patchy record. For example, not all tests address the same aspect or processes. Some flowsets of drumlins will have been judged to represent an isochronous imprint, and so a flow geometry at a point in time. Whereas other drumlins (in time-transgressive flowsets) likely represent a time span and gradient tracking flow during a timespan of deglaciation. This limits the number and location of such sites and the potential for use in model-data comparison tests. In contrast, the dispersal of erratics and of indicator grains can occur almost constantly, such that their final resting place is an integration of flow changes over wide timespans up to the entire duration of glaciation. So to correctly account for erratic dispersal requires better reconstruction of long term, large scale modelled ice flow geometry, but less precise regional flow geometries. This makes glacial transport of erratics a valuable tool to use in conjunction with other test such as drumlins. This can be exemplified in figure 6.2 where matching erratics and flowsets are combined on a single figure. In some regions model data mismatches are consistent e.g. Galway and the East coast/North Sea flowsets. These regions can more confidently be interpreted to suggest the simulated ice sheet does not recreate the ice sheet flow geometry. In contrast north Wales, North Yorkshire and the Tweed Valley show contradictory model data matches matching only erratics or flowsets. These regions offer useful examples for exploring the nuance of how numerical ice sheet models behave, and why they do or don't recreate the empirical record.

A key lesson in this thesis is the importance of considering the long term dispersal of erratics, and how these can be preconditioned by ice cap build up, and convergence between ice dome. Several sites stand out with regards to the importance of build-up geometries. Most notably, the north easterly dispersal of Shap Granite, both along the Tweed Valley Ice Stream, but also subsequently south, along the East Coast. I interpret the likely mechanism for this dispersal to have been a larger, more extensive Pennine Ice Cap during the initial build-up of the ice sheet, than is captured in the model. This interpretation is supported by the distribution of flowset matches confirming modelled ice flowing west along the Tweed overlain by erratics which were not reconstructed (see figure 6.2). This suggests the easterly flow mechanism was

simulated, but not the not the required northerly flow mechanism. However this ice cap driven mechanism was observed in higher temporal resolution erratic dispersal models (see section 5.5.2.2) suggesting short term flow events to be central to preconditioning the erratic distribution for subsequent ice sheet scale glaciation. Similarly, the most extensive south westerly dispersal of Cheviot erratics is best achieved by a more extensive ice cap, building up over the Cheviot Hills than exists in the model and pushing erratics further north-west prior to subsequent south-easterly ice flow. A tentative conclusion therefore from these sites suggests that the British and Irish Ice Sheet likely grew more rapidly in the southern sector (Pennines, Cheviots) than reconstructed by ensembles in this thesis.

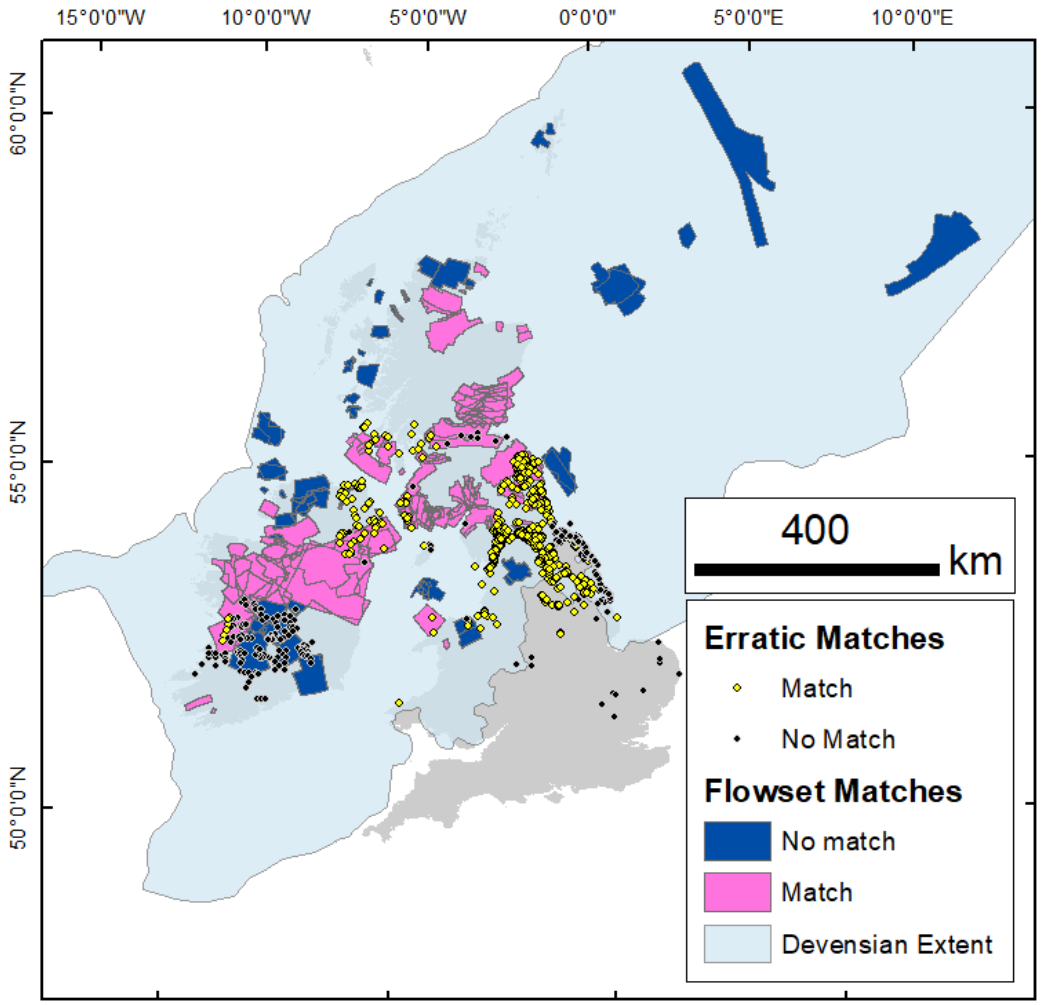

Figure 6.2 Flowset and erratic matches with modelled ice flow for MR 441. Flowsets which match with modelled flow at least once with a theshold of <20 degrees are shown in pink and erratics which can be explained (within 5 km) by modelled dispersal pathways in yellow.

In the south of Ireland the lack of matches of MR 441 with both flowsets and erratic's highlights the models poor performance in this region (see figure 6.2). It should be noted that no moraines were used in this region in the initial sieving (see figure

3.16). I discuss a number of mechanisms which could help explain the simulated ice sheet geometries which may be required to explain the dispersal of Galway Granites in section 5.5.2.1. However it also seems prudent to propose that Southern Ireland may also perform poorly due to the lack of ice marginal landforms (moraines) used in the initial sieving. Lacking these landforms in the parallel sieving stage would allow simulations which did not perform well in this region to pass through the NROY selection. This highlights the importance of using a breadth of tests in model data comparison as short comings in one single test in a region may not be sufficient to identify the source of simulation discrepancies.

The breadth of tests used to evaluate MR 441 in this thesis highlight a number of consistent model data mismatches, most notably peripheral flowsets and erratics. A central core of flowsets can be observed where the simulation also successfully recreates the majority of erratics (see figure 6.2). In contrast, with the exception of the west coast or Ireland, all peripheral sectors of the MR 441 simulation of the ice sheet perform poorly with regards to both flowsets matches and erratics matches. Several mechanisms may be at play in these patterns of model data misfit. The first may be a with regards to the statistical probability of recreating a palaeo record increasing with prolonged occupation (e.g. higher likelihood of coincidental matches). Although this may to some extend be true for flowsets, the complex time transgressive nature of many erratic dispersal pathways is interpreted to be less readily recreated by a coincidental combinations of flow directions. I therefore propose the spatial distribution of matches may be more directly a result of the nature of the maximum ice extent. By performing an in-parallel test of ice volume (see section 3.4.2), it can be inferred that the simulated ice sheet (or MR 441) likely exceed the true ice sheet thickness inferred from the GIA/RSL signal. This misfit in ice thickness is most pronounced during the maximum extent of the ice sheet. Under such a scenario it thicker ice at the ice sheet periphery could have been unhindered by local topography and therefore altered the ice flow direction or MR 441. Excess ice thickness could help explain several peripheral regions of persistent model data mismatch. One region which stands out where excess ice thickness could help explain model data mismatch is the Outer Hebrides where topographic relief from inter island troughs could have played an important role in driving ice flow direction of a thin ice sheet. Thicker peripheral ice could have flowed unimpeded over these regions. A similar explanation could explain the deep troughs of the Skagerrak, the Norwegian Channel and the North Sea. The thick ice exceeding topographic confinement could also in places explain the southern uplands of Ireland, however very thin ice would be needed to be affected by topography and I infer other mechanisms discussed in detail in section 5.5.2.1 likely play a larger factor.

6.2 - Current status of model data comparison of palaeo-ice sheets

The premise of comparing ice sheet simulations to data is not new, having been highlighted in Andrews seminal paper in 1982. In this work, Andrews (1982) highlights the need to reconcile the contradictory single dome ice sheets (produced by numerical models of the time) with the multi dome ice sheets of empirical reconstruction. In essence highlighting the importance of empirical observations in assessing model fidelity to flow geometry. However, in practice, implementation of such comparisons has been comparatively slow to gain traction.

An important example of model data comparison was that of Tarasov and Peltier (2004) where they used relative sea level (RSL) to assess model fidelity to the observational record. This work has both directly and indirectly prompted a continuous series of developments in comparison to RSL and in turn ice equivalent sea level contributions (e.g. Tarasov et al., 2012; Lecavalier et al., 2014; Gregoire et al., 2016). Some degree of RSL or GIA assessment is becoming increasingly popular as a tool for assessing model fidelity, likely because of the increased demand for models to answer questions of future sea level contributions (Clark et al., 2022). But also due to an early and proactive approach to increase communication between those creating empirical observations of RSL and numerical modellers (Stokes et al. 2015; Dalton et al., 2020).

However, a growing body of work (e.g. Ely et al., 2021; Gandy et al., 2021), including this thesis, demonstrates that RSL is not the only line of evidence that can be used to answer questions of model fidelity. Furthermore, there are many ice sheet configurations that can lead to the same answer, with RSL (Bradley et al., 2023) - this is the issue of equifinality. Therefore, in an effort to mitigate against equifinality it is important to also consider other metrics for assessing model fidelity. In essence these help us know we are getting to the right answer via the right ice sheet.

Methods of assessing ice sheet fidelity with geomorphology were pioneered by the work of Napieralski and Li through a series of papers, which they led through 2006 and 2007 (Napieralski et al., 2006; 2007; Li et al., 2007). In these works, they developed AFDA and APCA, the two tools used for testing fidelity of ice flow geometry in this thesis. These tools initiated the integration of GIS based observations into model-data comparison. Unfortunately, uptake of these tools has been comparatively slow outside of the context of the BIIS. A steady series of papers have integrated AFDA into their sieving workflow (Hubbard et al., 2009, Patton et al., 2016 a, b; Gandy

et al.,2021; Ely et al., 2019a; 2021). Other works have looked to develop new Bayesian methods of assessing ice sheet fidelity to flow direction for use in ice sheet emulators (Archer et al., 2023). Currently, similar model-data comparison studies have mainly focussed on the component ice sheets of the Eurasian Ice Sheet (EIS) complex (BIIS, EIS, Welsh Ice cap) and have yet to be implemented on the Laurentide Ice Sheet. Despite the breadth of observational data on ice flow direction (across the BIIS and EIS), the number of flowsets used in previous works has generally numbered less than ten.

Ice sheet extent is also experiencing increased incorporation into sieving routines. This has been both through the use of APCA (Ely et al., 2021) directly comparing against specific moraines, but also through the use of grounding line wedges to assess grounded ice extent for marine terminating outlets (e.g. Jamieson et al., 2012). Other methods have also been implemented for comparing ice sheet extent at a marginal feature scale, including using a flowline-based margin assessment against moraines in a topographical confined setting (Jouvet et al., 2017). At the other end of the spectrum of spatial extent, the Automated Timing Accordance Tool (ATAT) in essence tests for the timing of occupation of glaciated zones (Ely et al., 2019b). Unlike previous other methods of assessing extent at a feature scale which use a single margin (e.g. a moraine), ATAT uses a series of time transgressive occupation of regions (most frequently from isochrons which may incorporate many moraines and dates), to test the total occupation area and timing.

In summary, a plethora of methods already exist for assessing ice sheet geometry through sieving, but these still have not seen wide scale uptake across the field (other than perhaps RSL). I propose this disconnect may in part stem from systematic differences in methods used by modellers and those producing the empirical observations. Through improving automation of some of the tasks associated with preparing empirical observations I hope to have contributed to decreasing this disconnect. I also discuss a number of issues I propose still need to be addressed in the context of future work in the following section (Section 6.3).

6.3 - Future prospects for model data comparison

6.3.1 - Improving model-data interoperability

A core issue with integrating empirical observations into model simulations is the decentralised, inconsistent nature of much of the data. Systematic model data comparison relies on automation so as to efficiently assess large ensembles (Ely et al.,

2019a). If sufficient effort is not made to standardise the format in which observations are recorded and published, considerable if not insurmountable challenges are added to integrating observations into models.

One area where progress is being made in improving model data interoperability is numerical dating of ice margins. A good example of increasing interoperability of data sources is the DATED-1 Project (Hughes et al., 2016). The DATED-1 project compiled recorded dates of ice sheet extent and timing. The database calibrates all dates using a consistent routine and incorporates them into a series of ice margins. A key feature of this data product is the 'simple' quality assessment of all dates which constrain ice extent (with a traffic light system for data quality). This transparency in the data allows for the product to be more readily understood by the non-expert in the field making the data more accessible. In the DATED-1 project, dates are paired with an open access margin dataset which aligns with these dates. Crucially, the fact that both the age-based margins and the dates used for such margins are freely available, and in widely used file formats, means that the products can be readily incorporated into model data comparison testing in future works. Crucially, this data could either be incorporated as a margin (e.g. for use in APCA), or using the chronology data points (for use in ATAT). The DATED-1 project is not alone on this front and works such as PATICE (Davies, et al., 2020), BRITICE-CHRONO (Clark et al., 2022), PalaeoGriS (Leger et al., 2023) are also making considerable improvements on this front.

In contrast, perhaps one of the largest data sources left still untapped are the extensive records of till sections and boreholes (Elyes and McCabe 1989; Evans et al., 2006). Such data is spatially extensive across Europe and North America yet highly challenging to incorporate into model data comparison routines at a large scale. I believe this is in part due to the unstandardised method in which much of this data is recorded. Till stratigraphy is often included in empirical reconstructions which means at times it can be incorporated into model data comparisons (e.g. Evans et al., 2010; Livingstone et al., 2012; Davies et al., 2012). However, the route for such information into ice sheet simulations is usually only through an empirical reconstruction. Such methods of data incorporation are challenging as they limit the potential for future methodological improvements. For example, without the thickness of till sections they cannot be used to validate sediment flux. Similarly, as empirical reconstructions used for model data comparison predominantly use dated advances, the relative ages of advances and retreats stored in these sites is rarely released in such a way as to promote incorporation into numerical ice sheet models. Numerical ice sheet simulations could be a powerful tool in constraining advance and retreat records observed in till

sections, however this information is as of yet, not published in a format that is readily interoperable with ice sheet models.

The issue of interoperability is most evident from the numerical model users perspective. However it also applies to glaciologists looking to use model outputs to learn about glacial processes. In other words, the modeller may not be the only person who wishes to use the model simulation. As with empirical observations often not being published in such a way as to readily be incorporated, numerical modelling results are often challenging for third parties to re-evaluate. This in part stems from the methodological disconnect between empiricists and modellers which at times results in data formats which are not implicitly interoperable between both parties. To push the current boundaries of model data comparison, it is important that modellers strive to produce accessible datasets. These datasets should be accessible in terms of documentation, data formats, and where appropriate also through data products (e.g. margins, flowlines and velocity maps). An example of the style of data products which would be relevant for empiricists to test hypotheses can be found in the work of Patton et al. (2016), where they conduct a comparison of modelled retreat rates with observed moraine extents (see figure 6.3). Although the data were ultimately not published in reproducible format, the inclusion of intermediate data products represents a good example of how model outputs could be processed in such a way as to prompt further empirical observations. In this thesis I have attempted to bridge the gap from both the empirical and modelling perspectives.

Another example of a model product which could be more broadly accessible to other users is glacial flowlines. Producing these can make model output more intrinsically accessible to a range of users. For example, in this work I used flowlines as a tool for reconstructing glacial transport. Unlike more traditional flow routing algorithms which use the raw x/y displacement outputs of a model, the novelty of flowline routing is that they can be used to reconstruct transport in post processing (e.g. Chapter 5), without the need for the entire numerical ice sheet simulation to be published or accessed. In other words, a simple flowline data product can be published for a model and subsequently used in future work by users without the technical skill required to extract parameters from ice sheet model simulations. Given the demonstrated value of flowlines as a data product, I hope to encourage future modelling endeavours to readily publish their model outputs with flowlines and ice margins as open access shapefiles.

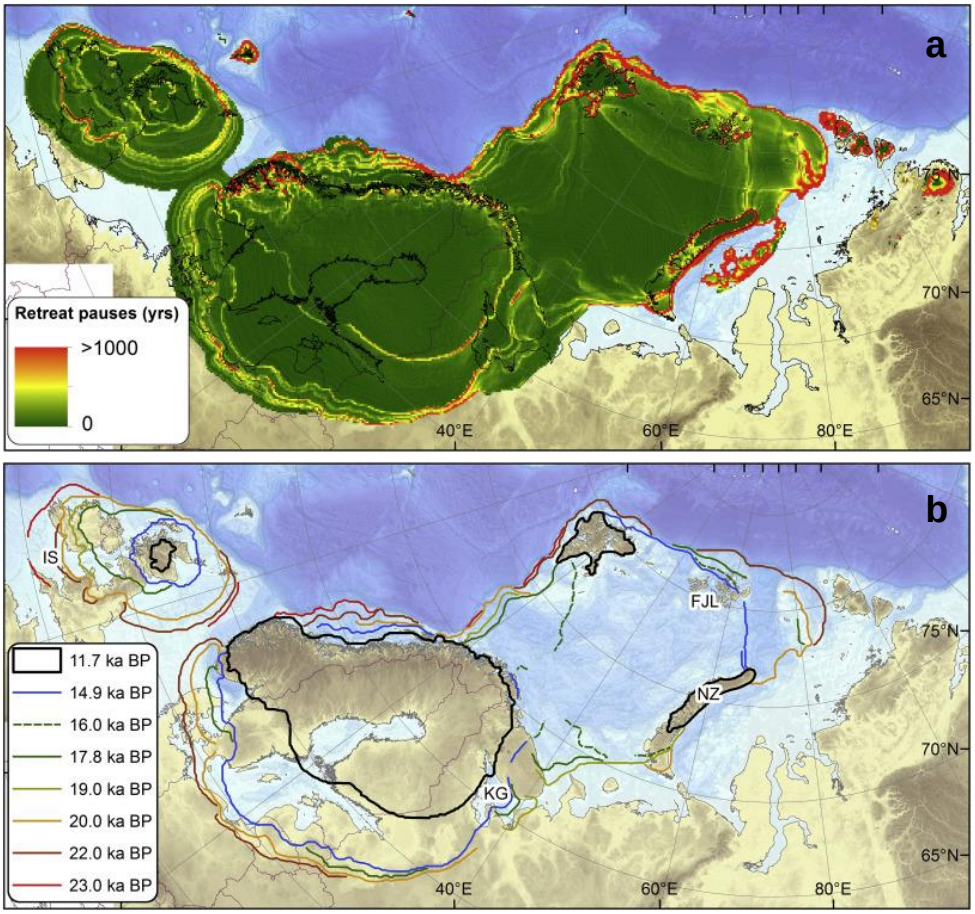

Figure 6.3: Using numerical ice sheet models to infer moraine formation. a) Pauses in glacial retreat of the EIS and b) mapped margins of the EIS. Both figures are modified from Patton et al., 2016

Overall, there are a large number of reasons why such data products (e.g. a till stratigraphy database, moraine/margin outputs, or modelled flow line) do not exist, the most obvious being the enormous effort such works can entail. However, more cynically, there has perhaps historically been a disinterest in making data interoperable as it opens the product up for others to criticise. It also makes it easier for others impinge in your area of expertise and possible future publications. Regardless of the reason, the long-term value of such data products is substantial and should be considered in future works.

6.3.2 - Future potential tools for model-data comparison using sediment dispersal

The observation that erratic transport may in fact be a comparatively simple process to derive from a model simulation was perhaps unexpected, but is certainly not

without value. For this reason, I believe using erratics as a proxy for glacial flow conditions may be useful to future modelling works. The use of erratics for glacial reconstruction is by no means a new concept, being extensively used by Geikie (1894) and Charlesworth (1953) for example. However, in this thesis, I have attempted to reinvigorate the use of such observations for approximating flow conditions in model simulation context. The benefit of such a system for numerical modellers is the potential to explore ice flow directions without the need for determining the conditions necessary to promote deformation of sediment (e.g. cold based ice conditions could still lead to erratic surface transport, but inhibit subglacial transport). Using erratics may also prove to be useful for testing zones of confluence or ice divides which are otherwise complex to reconstruct empirically (e.g. Dulfer et al., 2023). Further work would be beneficial to fully automate the process of generating erratic dispersal trails, and for assessing the degree of model-data fit. However, in this thesis I have demonstrated the effectiveness of the principal and the ability to distinguish between ensemble members.

Short of fully automating an erratic transport routine for sieving, in its current form, a simple erratic transport modelling ‘exercise’ could be replicated using the same manual method of this thesis. This could be used as ‘final check’ of ice flow direction before using the simulation for another use. This test could occur in much the same way as this thesis used a two-phase model data comparison process with initial quantitative sieving, paired with manual checks of the top three ranking NROY against ice volume and extent from nudged simulation.

Several works have looked to recreate the dispersal of fine sediment (Bougamont and Tulaczyk, 2003; Melanson et al., 2017; Hooke et al., 2013). A challenge with all of these models has been attempting to recreate entrainment before addressing transport geometry. There is considerable industrial interest in the implementation of a fine grain dispersal model for recreating the dispersal of rare earth elements. An important lesson with regards to sediment transport more broadly is that the maximum dispersal is comparatively simple to estimate, the issue may therefore not be in entrainment, but in dilution. Given this observation, development of models to recreate the maximum dispersal of finer grained sediments which could be entrained in till, taking a geometry first approach may be valuable until complex issues of entrainment, deposition and dilution can be thoroughly addressed. Thus, the potential exists for combining such models with the testing of till composition to provide a time transgressive test of flow geometry.

If models of fine grain sediment dispersal could be improved, these could allow for a powerful future avenue for model data comparison when used in conjunction with

till sections. A fine-grained sediment dispersal model could be used to recreated sequential dispersal plume events using point based sediment logs, as time transgressive model data comparison reference points.

Although this in this thesis I have focussed on the use of erratics to decipher palaeo glacial transport, the premise would be equally applicable to contemporary ice sheets. Specifically terrestrial terminating ice margins such those found around the GrIS. Extensive erratic boulders can be observed in the proglacial regions of the GrIS which likely hold information of the long-term stability of the catchment ice flow geometry. Exploring modelled dispersal of such erratic's could provide and powerful testing ground for questions of catchment migration over time.

6.3.3 - Future potential tools for model data using drumlins

Observations of ice flow direction (drumlins) are yet to be widely incorporated into sieving protocols for model data comparison (Stokes et al., 2015; Ely et al., 2019a). Therefore, proposing new methods of using drumlins in model data comparison may seem pre-emptive. However, their lack of inclusion could stem from both the lack of consensus on their formation conditions and the perceived lack of value in 'only indicating ice flow direction'. In this thesis, I have demonstrated that reconstructing ice flow geometry results also equates to replicating other popular measures of ice sheet fidelity (e.g. water equivalence/volume see Chapter 3.4.2) and therefore is of greater relevance than others have perhaps accredited it. However, in future model-data comparison works I propose improved understanding of drumlin formation can be leveraged for more advanced sieving tests. For example, the finding in this thesis that drumlins and their morphometry likely relate to specific glacial conditions (velocity and thickness) could have important implications for future ice sheet modelling works. For example, implementing the finding that drumlins relate to the 50-350 m a-1 velocity range. This could either be used to further reduce match quality uncertainty as section 4.5.2 (e.g. not consider coincidental matches), or in the extreme nudging velocities to remain within these conditions. Similarly, the association of bedform morphometry to flow conditions could also be used as a model-data comparison tool, to test CV or flow consistency. Finally this work omits to systematically use the chronological data stored in crosscutting flowsets to better constrain match timing but as demonstrated in section 4.5.2, this has the potential to help constrain the timing of glacial events and is still underutilised.

Hypothetically and optimistically looking forwards, with better understanding of the specific bed conditions of drumlin formation we could for example, improved bed

classification for future modelling work using a prescribed till friction map (e.g. the method used in this thesis which performed most favourably in ensemble ranking). In a forecasting context (e.g. where we can't access the bed) this understanding could be used to better define bed conditions from observations, or make inferences based on understanding of the surface characteristics of the ice above drumlin fields (e.g. as in Bowling et al., 2019 with subglacial lakes).

In essence, the more specifically we understand the conditions associated with drumlin formation, the more complete our empirical inversion models can become and better we can inform the model of the inferred glacial conditions (Kleman and Borgström, 1996).

6.3.4 - Recommendations for modellers and data scientists

To summarise this chapter and the broader findings of this thesis I here collate a short summary of recommendations for modellers. These focus on: output data; model set up; and model processes.

Firstly I highlight how it would be useful for the field, across both sides of 'data-modelling divide' if publications included a wide range of data products (e.g. flowlines & and margin maps) and format types (e.g. NetCDF's, geotiffs or shapefiles) see section 6.3.2 and 6.3.3. Where possible these should include many of the usable data outputs (e.g. by including parameters such a basal water pressure where calculated and not just ice velocity) or from a data collection side by including numerous metrics about the observations (e.g. drumlin length and elongation) where collected.

Investigating model data comparison results has demonstrated the importance of ice cap scale processes in preconditioning the transport of erratics. To account for this, modellers should use high temporal and spatial resolution or nested grids to improve performance in key areas (e.g. ice cap seed points). In this work, numerical modelling was performed at high temporal resolution with outputs saved every 100 years. However, a higher spatial resolution was likely needed for ice cap scale processes rather than the 5 km used in this thesis. Such high resolution may only be required for ice cap spin up.

Finally, several processes would be of wider benefit for future model data comparisons. Firstly, the importance of reconstructing and modelling the production of subglacial till. Two aspects would stand out from this work which were not available. Firstly the thickness of till at a pixel scale. Secondly a more robust calculation of shear stress. These would be useful for testing drumlin formation hypotheses as a function of till availability (e.g. Barchyn et al., 2016) or shear stress (e.g. Stokes et al., 2013).

In summary, although some new products are required, a key bottleneck in model-data comparison is that data products are often not made fully available in an accessible formats on both sides of the model-data divide.

6.4 - Closing remarks

The palaeo glacial record is rich and diverse, containing a breadth of information about how ice sheets have and likely will behave. Much of this information is either not yet fully understood, or adequately conveyed to numerical models. In this thesis, I have made progress to help close the disconnect between empirical observations and numerical ice sheet simulations within the context of ice flow geometry. I have done this through methodological improvements to how numerical ice sheet simulations can be combined with observational data. In doing so, I improve understanding of the conditions of drumlin formation and provide explanations of the varied pathways that erratic transport can take. I suggest that over the coming decades, data-modelling comparisons will further improve with new methods, applications, and sources of data enhancing the robustness of modelling approaches and our knowledge of ice sheets.

References

Agassiz, L., (1842) On glaciers, and the evidence of their having once existed in Scotland, Ireland, and England. *Proceedings of the Geological Society iii*, pp.327–332

Albrecht, T., Winkelmann, R. and Levermann, A. (2020) 'Glacial-cycle simulations of the Antarctic Ice Sheet with the Parallel Ice Sheet Model (PISM) – Part 2: Parameter ensemble analysis', *The cryosphere*, 14(2), pp. 633–656.

Alsop, G.I. and Hutton, D.H.W. (1993) 'Major southeast-directed Caledonian thrusting and folding in the Dalradian rocks of mid-Ulster: implications for Caledonian tectonics and mid-crustal shear zones', *Geological Magazine,* 130(2), pp.233-244.

Andrews, J. T. (1982). On the reconstruction of Pleistocene ice sheets: A review. *Quaternary Science Reviews*, *1*(1), 1-30.

Archer, R.E., Ely, J.C., Heaton, T.J., Butcher, F.E., Hughes, A.L. and Clark, C.D., 2023. Assessing ice sheet models against the landform record: The Likelihood of Accordant Lineations Analysis (LALA) tool. *Earth Surface Processes and Landforms*.

Aschwanden, A., Aðalgeirsdóttir, G. and Khroulev, C. (2013) 'Hindcasting to measure ice sheet model sensitivity to initial states', *The cryosphere*, 7(4), pp. 1083–1093.

Ballantyne, C.K. and Ó Cofaigh, C. (2017) 'The Last Irish Ice Sheet: Extent and Chronology', in P. Coxon, S. McCarron, and F. Mitchell (eds) *Advances in Irish Quaternary Studies*. Paris: Atlantis Press, pp.101–149.

Ballantyne, C.K. and Small, D. (2019) 'The Last Scottish Ice Sheet', *Earth and environmental science transactions of the Royal Society of Edinburgh*, 110(1-2), pp. 93–131.

Barr, I.D. and Lovell, H. (2014) 'A review of topographic controls on moraine distribution', *Geomorphology* , 226, pp. 44–64.

Bartholomew, I., Nienow, P., Mair, D., Hubbard, A., King, M.A. and Sole, A., (2010). Seasonal evolution of subglacial drainage and acceleration in a Greenland outlet glacier. *Nature Geoscience*, 3(6), pp.408-411.

Batchelor, C.L., Margold, M., Krapp, M., Murton, D.K., Dalton, A.S., Gibbard, P.L., Stokes, C.R., Murton, J.B. and Manica, A., (2019). The configuration of Northern Hemisphere ice sheets through the Quaternary. *Nature communications*, 10(3713), pp.1-10

Batchelor, C.L., Christie, F.D., Ottesen, D., Montelli, A., Evans, J., Dowdeswell, E.K., Bjarnadóttir, L.R. and Dowdeswell, J.A., (2023). Rapid, buoyancy-driven ice-sheet retreat of hundreds of metres per day. *Nature*, 617(7959), pp.105-110.

Bauer, E. and Ganopolski, A. (2017) 'Comparison of surface mass balance of ice sheets simulated by positive-degree-day method and energy balance approach', *Climate of the Past*, 13(7), pp. 819–832.

Benedict, J.B. (1967) 'Recent Glacial History of an Alpine Area in the Colorado Front Range, U.S.A.: I. Establishing a Lichen-Growth Curve', *Journal of Glaciology*, 6(48), pp. 817–832.

Benediktsson, Í.Ö., Jónsson, S.A., Schomacker, A., Johnson, M.D., Ingólfsson, Ó., Zoet, L., Iverson, N.R. and Stötter, J., (2016). Progressive formation of modern drumlins at Múlajökull, Iceland: stratigraphical and morphological evidence. *Boreas*, 45(4), pp.567-583.

Benetti, S., Chiverrell, R.C., Cofaigh, C.Ó., Burke, M., Medialdea, A., Small, D., Ballantyne, C., Bateman, M.D., Callard, S.L., Wilson, P. and Fabel, D., (2021). Exploring controls of the early and stepped deglaciation on the western margin of the British Irish Ice Sheet. *Journal of Quaternary Science*, 36(5), pp.833-870.

Benetti, S., Dunlop, P. and Cofaigh, C.Ó. (2010) 'Glacial and glacially-related features on the continental margin of northwest Ireland mapped from marine geophysical data', *Journal of maps*, 6(1), pp.14–29.

Bingham, R.G., Vaughan, D.G., King, E.C., Davies, D., Cornford, S.L., Smith, A.M., Arthern, R.J., Brisbourne, A.M., De Rydt, J., Graham, A.G. and Spagnolo, M., (2017). Diverse landscapes beneath Pine Island Glacier influence ice flow. *Nature Communications*, 8(1618), pp.1-9.

Boston, C.M., Evans, D.J.A. and Cofaigh, C.Ó. (2010) 'Styles of till deposition at the margin of the Last Glacial Maximum North Sea lobe of the British–Irish Ice Sheet: an assessment based on geochemical properties of glacigenic deposits in eastern England', *Quaternary science reviews*, 29(23-24), pp. 3184–3211.

Bougamont, M. and Tulaczyk, S. (2003) 'Glacial erosion beneath ice streams and ice-stream tributaries: constraints on temporal and spatial distribution of erosion from numerical simulations of a West Antarctic ice stream', *Boreas*, 32(1), pp. 178–190.

Boulton, G.S. and Clark, C.D., (1990). A highly mobile Laurentide ice sheet revealed by satellite images of glacial lineations. *Nature*, 346(6287), pp.813-817.

Boulton, G. and Hagdorn, M. (2006) 'Glaciology of the British Isles Ice Sheet during the last glacial cycle: form, flow, streams and lobes', *Quaternary science reviews*, 25(23), pp. 3359–3390.

Boulton, G.S. *et al.* (1977) ‘A British ice-sheet model and patterns of glacial erosion and deposition in Britain’. *British Quaternary Studies: Recent Advances*, pp. 231-246

Boulton, G.S. (1978) ‘Boulder shapes and grain-size distributions of debris as indicators of transport paths through a glacier and till genesis’, *Sedimentology*, 25(6), pp. 773–799.

Boulton, G.S. (1979) ‘Processes of Glacier Erosion on Different Substrata’, *Journal of Glaciology*, 23(89), pp. 15–38.

Boulton, G.S. and Hindmarsh, R.C.A. (1987) ‘Sediment deformation beneath glaciers: Rheology and geological consequences’, *Journal of geophysical research*, 92(B9), p. 9059.

Boulton, G.S. and Jones, A.S. (1979) ‘Stability of Temperate Ice Caps and Ice Sheets Resting on Beds of Deformable Sediment’, *Journal of Glaciology*, 24(90), pp. 29–43.

Boulton, G.S., Peacock, J.D. and Sutherland, D.G. (1991) ‘Quaternary’. G.Y. Craig (Ed.), Geology of Scotland (third ed.), The Geological Society, London (1991), pp. 503-543

Boyes, B.M., Linch, L.D., Pearce, D.M. and Nash, D.J., (2023). The last Fennoscandian Ice Sheet glaciation on the Kola Peninsula and Russian Lapland (Part 1): Ice flow configuration. *Quaternary Science Reviews*, 300, p.107871.

Boygle, J. (1993) ‘The Swedish varve chronology - a review’, *Progress in Physical Geography: Earth and Environment*, 17(1), pp. 1–19.

Boylan, P.J., (1998). Lyell and the dilemma of Quaternary glaciation. *Geological Society, London, Special Publications*, 143(1), pp.145-159.

Buckland, W., (1823). Reliquiae Diluvianae. John Murray, London.

Bradley, S.L., Ely, J.C., Clark, C.D., Edwards, R.J. and Shennan, I., (2023). Reconstruction of the palaeo-sea level of Britain and Ireland arising from empirical constraints of ice extent: implications for regional sea level forecasts and North American ice sheet volume. J*ournal of Quaternary Science*, 38(60), pp.791-805

Bradwell, T., Fabel, D., Clark, C.D., Chiverrell, R.C., Small, D., Smedley, R.K., Saher, M.H., Moreton, S.G., Dove, D., Callard, S.L. and Duller, G.A., (2021). Pattern, style and timing of British–Irish Ice Sheet advance and retreat over the last 45 000 years: evidence from NW Scotland and the adjacent continental shelf. *Journal of Quaternary Science*, 36(5), pp.871-933.

Bradwell, T., Small, D., Fabel, D., Clark, C.D., Chiverrell, R.C., Saher, M.H., Dove, D., Callard, S.L., Burke, M.J., Moreton, S.G. and Medialdea, A., 2021. Pattern, style and timing of British–Irish Ice Sheet retreat: Shetland and northern North Sea sector. *Journal of Quaternary Science*, 36(5), pp.681-722.

Bradwell, T., Stoker, M. and Krabbendam, M. (2008) 'Megagrooves and streamlined bedrock in NW Scotland: The role of ice streams in landscape evolution', *Geomorphology* , 97(1), pp. 135–156.

Bradwell, T., Stoker, M. and Larter, R. (2007) 'Geomorphological signature and flow dynamics of The Minch palaeo-ice stream, northwest Scotland', *Journal of Quaternary Science*, 22(6), pp. 609–617.

Bradwell, T. and Stoker, M.S. (2015) 'Submarine sediment and landform record of a palaeo-ice stream within the British−Irish Ice Sheet', *Boreas*, 44(2), pp. 255–276.

Bremner, A., (1928). Further problems in the glacial geology of north-eastern Scotland. *Transactions of the Edinburgh Geological Society*, 12(1), pp.147-164.

Bremner, A., (1934). The glaciation of Moray and ice movements in the north of Scotland. *Transactions of the Edinburgh Geological Society*, 13(1), pp.17-56.

Bremner, A. (1939) 'Notes on the glacial geology of east Aberdeenshire', *Transactions of the Edinburgh Geological Society*, 13(4), pp. 474–475.

Briggs, C.S. (1988) 'Stone Resources and Implements in Prehistoric Ireland: A Review', *Ulster Journal of Archaeology*, 51, pp. 5–20.

Buckland, W., 1823. "*Reliquiae Diluvianae*," p. 249; map pl. 27.

Buckland 1842. On diluvio-glacial phamomena in Snowdonia and adjacent parts of North Wales. Proceedings of the Geological Socieo" of London, 3. 579-584.

Bueler, E. and Brown, J., (2009). Shallow shelf approximation as a "sliding law" in a thermomechanically coupled ice sheet model. *Journal of Geophysical Research: Earth Surface*, 114(F3).

Bueler, E. and van Pelt, W. (2015) 'Mass-conserving subglacial hydrology in the Parallel Ice Sheet Model version 0.6', *Geoscientific model development*, 8(6), pp. 1613–1635.

Bulthuis, K., Arnst, M., Sun, S. and Pattyn, F., (2019). Uncertainty quantification of the multi-centennial response of the Antarctic ice sheet to climate change. *The Cryosphere*, 13(4), pp.1349-1380.

Callard, S.L., Cofaigh, C.Ó., Benetti, S., Chiverrell, R.C., Van Landeghem, K.J., Saher, M.H., Gales, J.A., Small, D., Clark, C.D., Stephen, J.L. and Fabel, D., (2018).

Extent and retreat history of the Barra Fan Ice Stream offshore western Scotland and northern Ireland during the last glaciation. *Quaternary Science Reviews*, 201, pp.280-302.

Callard, S.L., Cofaigh, C.Ó., Benetti, S., Chiverrell, R.C., Van Landeghem, K.J., Saher, M.H., Livingstone, S.J., Clark, C.D., Small, D., Fabel, D. and Moreton, S.G., (2020). Oscillating retreat of the last British-Irish Ice Sheet on the continental shelf offshore Galway Bay, western Ireland. *Marine Geology*, 420, p.106087.

Carling, P.A., Su, T. and Meshkova, L., (2023). Distribution of Devensian glacial erratics and related evidence elucidate complex ice flow changes across a former ice divide: Northern England. *Proceedings of the Geologists' Association*, 134(2), pp.139-165.

Carr, S.J. (2004) 'The North Sea basin', in J. Ehlers and P.L. Gibbard (eds) *Developments in Quaternary Sciences*. Elsevier, pp. 261–270.

Carr, S.J., Holmes, R.V.D., Van der Meer, J.J.M. and Rose, J., (2006). The Last Glacial Maximum in the North Sea Basin: micromorphological evidence of extensive glaciation. *Journal of Quaternary Science*, 21(2), pp.131-153.

Chapwanya, M., Clark, C.D. and Fowler, A.C. (2011) 'Numerical computations of a theoretical model of ribbed moraine formation', *Earth Surface Processes and Landforms*, 36(8), pp. 1105–1112.

Charlesworth, J.K. (1953) *The geology of Ireland: an introduction*. Oliver and Boyd.

Chiverrell, R.C., Thrasher, I.M., Thomas, G.S., Lang, A., Scourse, J.D., van Landeghem, K.J., Mccarroll, D., Clark, C.D., Cofaigh, C.Ó., Evans, D.J. and Ballantyne, C.K., (2013). Bayesian modelling the retreat of the Irish Sea Ice Stream. *Journal of Quaternary Science*, 28(2), pp.200-209.

Church, J.A. *et al.* (2001) 'Changes in Sea Level', in: J.T Houghton, Y. Ding, D.J. Griggs, M. Noguer, P.J. Van der Linden, X. Dai, K. Maskell, and C.A. Johnson (eds.): *Climate Change 2001: The Scientific Basis: Contribution of Working Group I to the Third Assessment Report of the Intergovernmental Panel*, pp. 639–694.

Christison, R., Brown, T., Geikie, G.A., Mitchell, A., Nicol, Stevenson, T., Thompson, W., White, T. P., Young, Home, D. H. (1871) 'First Report', Reports of the Boulder Committee of the Royal Society of Edinburgh. [Online]

Christison, R., Brown, T., Geikie, G.A., Mitchell, A., Nicol, Stevenson, T., Thompson, W., White, T. P., Young, Home, D. H. (1884) 'Tenth Report', Reports of the Boulder Committee of the Royal Society of Edinburgh. [Online]

Clark, C.D. (1993) 'Mega-scale glacial lineations and cross-cutting ice-flow landforms', *Earth Surface Processes and Landforms*, 18(1), pp. 1–29.

Clark, C.D. (1997) ‘Reconstructing the evolutionary dynamics of former ice sheets using multi-temporal evidence, remote sensing and GIS’, *Quaternary science reviews*, 16(9), pp. 1067–1092.

Clark, C.D., Evans, D.J., Khatwa, A., Bradwell, T., Jordan, C.J., Marsh, S.H., Mitchell, W.A. and Bateman, M.D., (2004a). Map and GIS database of glacial landforms and features related to the last British Ice Sheet. *Boreas*, 33(4), pp.359-375.

Clark, C.D., Hughes, A.L., Greenwood, S.L., Spagnolo, M. and Ng, F.S., (2009). Size and shape characteristics of drumlins, derived from a large sample, and associated scaling laws. *Quaternary Science Reviews*, 28(7-8), pp.677-692.

Clark, C.D. (2010) ‘Emergent drumlins and their clones: from till dilatancy to flow instabilities’, *Journal of Glaciology*, 56(200), pp. 1011–1025.

Clark, C.D., Hughes, A.L., Greenwood, S.L., Jordan, C. and Sejrup, H.P., (2012). Pattern and timing of retreat of the last British-Irish Ice Sheet. *Quaternary Science Reviews*, 44, pp.112-146.

Clark, C.D., Ely, J.C., Greenwood, S.L., Hughes, A.L., Meehan, R., Barr, I.D., Bateman, M.D., Bradwell, T., Doole, J., Evans, D.J. and Jordan, C.J., (2018). BRITICE Glacial Map, version 2: a map and GIS database of glacial landforms of the last British–Irish Ice Sheet. *Boreas*, 47(1), pp.11-35.

Clark, C.D., Ely, J.C., Hindmarsh, R.C., Bradley, S., Ignéczi, A., Fabel, D., Ó Cofaigh, C., Chiverrell, R.C., Scourse, J., Benetti, S. and Bradwell, T., (2022). Growth and retreat of the last British–Irish Ice Sheet, 31 000 to 15 000 years ago: the BRITICE-CHRONO reconstruction. *Boreas*, 51(4), pp.699-758.

Clark, C.D., Gibbard, P.L. and Rose, J., (2004b). Pleistocene glacial limits in England, Scotland and Wales. In: Developments in Quaternary Sciences (Vol. 2, pp. 47-82). Elsevier.

Clason, C.C., Greenwood, S.L., Selmes, N., Lea, J.M., Jamieson, S.S., Nick, F.M. and Holmlund, P., (2016). Controls on the early Holocene collapse of the Bothnian Sea Ice Stream. *Journal of Geophysical Research: Earth Surface*, 121(12), pp.2494-2513.

Compo, G.P., Whitaker, J.S., Sardeshmukh, P.D., Matsui, N., Allan, R.J., Yin, X., Gleason, B.E., Vose, R.S., Rutledge, G., Bessemoulin, P. and Brönnimann, S., (2011). The twentieth century reanalysis project. *Quarterly Journal of the Royal Meteorological Society*, 137(654), pp.1-28.

Corradi, M., Osofero, A.I., Coventry, K., Richardson, A.E., Udeaja, C. and Vo, T., (2014), July. Analysis and classification of historic construction within the north-east of England. *In Proceedings of the 16th International Conference Structural Faults & Repair-2014* (pp. 8-10).

Cox, R.A., Dempster, T.J., Bell, B.R. and Rogers, G., (1996). Crystallization of the Shap Granite: evidence from zoned K-feldspar megacrysts. *Journal of the Geological Society*, 153(4), pp.625-635.

Cumming, G.A. and Bate, P.A. (1933) 'The Lower Cretaceous Erratics of the Fraserburgh District, Aberdeenshire', *Geological magazine*, 70(9), pp. 397–413.

Dakyns, J.R., (1878). On the Southward Flow of Shap Granite Boulders. *Proceedings of the Yorkshire Geological Society*, 7(1), pp.60-65.

Dalton, A.S., Margold, M., Stokes, C.R., Tarasov, L., Dyke, A.S., Adams, R.S., Allard, S., Arends, H.E., Atkinson, N., Attig, J.W. and Barnett, P.J., (2020). An updated radiocarbon-based ice margin chronology for the last deglaciation of the North American Ice Sheet Complex. *Quaternary Science Reviews*, 234, p.106223.

Dardis, G.F. and McCabe, A.M. (1983). Facies of subglacial channel sedimentation in late-Pleistocene drumlins, Northern Ireland. *Boreas*, 12, pp. 263-278

Darwin, C. (1887) *The Life and Letters of Charles Darwin*. [Online] Available at: http://darwin-online.org.uk/content/frameset?viewtype=text&itemID=F1452.1&pageseq=1 (Accessed: 31 March 2023).

Davies, B.J., Darvill, C.M., Lovell, H., Bendle, J.M., Dowdeswell, J.A., Fabel, D., García, J.L., Geiger, A., Glasser, N.F., Gheorghiu, D.M. and Harrison, S., (2020). The evolution of the Patagonian Ice Sheet from 35 ka to the present day (PATICE). *Earth-Science Reviews*, 204, p.103152.

Davis, W.M. (1884) 'The distribution and origin of drumlins', *American journal of science*, s3-28(168), pp. 407–416.

DeConto, R. M., & Pollard, D. (2016). Contribution of Antarctica to past and future sea-level rise. *Nature*, *531*(7596), 591-597.

Doornkamp, J.C. and King, C.A.M. (1971) '*Numerical analysis in geomorphology: an introduction*', Hodder & Stoughton Educational

Dove, D., Arosio, R., Finlayson, A., Bradwell, T. and Howe, J.A., (2015). Submarine glacial landforms record Late Pleistocene ice-sheet dynamics, Inner Hebrides, Scotland. *Quaternary Science Reviews*, 123, pp.76-90.

Dowling, T. (2016) *The drumlin problem Streamlined subglacial bedforms in southern Sweden*. PhD. Lund University.

Dulfer, H.E., Margold, M., Darvill, C.M. and Stroeven, A.P., (2022). Reconstructing the advance and retreat dynamics of the central sector of the last Cordilleran Ice Sheet. *Quaternary Science Reviews*, 284, p.107465.

Dunlop, P., Shannon, R., McCabe, M., Quinn, R. and Doyle, E., (2010). Marine geophysical evidence for ice sheet extension and recession on the Malin Shelf: New evidence for the western limits of the British Irish Ice Sheet. *Marine Geology*, 276(1-4), pp.86-99.

Dunlop, P. and Clark, C.D. (2006) 'The morphological characteristics of ribbed moraine', *Quaternary science reviews*, 25(13), pp. 1668–1691.

Dyke, A.S., Andrews, J.T., Clark, P.U., England, J.H., Miller, G.H., Shaw, J. and Veillette, J.J., (2002). The Laurentide and Innuitian ice sheets during the last glacial maximum. *Quaternary Science Reviews*, 21(1-3), pp.9-31.

Ely, J.C., Clark, C.D., Spagnolo, M., Stokes, C.R., Greenwood, S.L., Hughes, A.L., Dunlop, P. and Hess, D., (2016). Do subglacial bedforms comprise a size and shape continuum?. *Geomorphology*, 257, pp.108-119.

Ely, J.C., Clark, C.D., Spagnolo, M., Hughes, A.L. and Stokes, C.R., (2018). Using the size and position of drumlins to understand how they grow, interact and evolve. *Earth Surface Processes and Landforms*, 43(5), pp.1073-1087.

Ely, J.C., Clark, C.D., Small, D. and Hindmarsh, R.C., (2019b). ATAT 1.1, the Automated Timing Accordance Tool for comparing ice-sheet model output with geochronological data. *Geoscientific Model Development*, 12(3), pp.933-953.

Ely, J. C., Clark, C. D., Bradley, S. L., Veness, R., Archer, R., Gasson, E., Gandy, N., Gregoire L., (in Prep.) The range of behavioural dynamics of the last British-Irish Ice Sheet from data calibrated numerical models.

Ely, J.C., Clark, C.D., Hindmarsh, R.C., Hughes, A.L., Greenwood, S.L., Bradley, S.L., Gasson, E., Gregoire, L., Gandy, N., Stokes, C.R. and Small, D., (2019a). Recent progress on combining geomorphological and geochronological data with ice sheet modelling, demonstrated using the last British–Irish Ice Sheet. *Journal of Quaternary Science*, 36(5), pp.946-960.

Ely, J.C., Stevens, D., Clark, C.D. and Butcher, F.E., (2023). Numerical modelling of subglacial ribs, drumlins, herringbones, and mega-scale glacial lineations reveals their developmental trajectories and transitions. *Earth Surface Processes and Landforms*. 48(5), pp.956-978

Ely, J.C., Clark, C.D., Hindmarsh, R.C., Hughes, A.L., Greenwood, S.L., Bradley, S.L., Gasson, E., Gregoire, L., Gandy, N., Stokes, C.R. and Small, D., (2021). Recent progress on combining geomorphological and geochronological data with ice sheet modelling, demonstrated using the last British–Irish Ice Sheet. *Journal of Quaternary Science*, 36(5), pp.946-960.

Evans, D.J., Livingstone, S.J., Vieli, A. and Cofaigh, C.Ó., (2009). The palaeoglaciology of the central sector of the British and Irish Ice Sheet:

reconciling glacial geomorphology and preliminary ice sheet modelling. *Quaternary Science Reviews*, 28(7-8), pp.739-757.

Evans, D.J., Roberts, D.H., Bateman, M.D., Clark, C.D., Medialdea, A., Callard, L., Grimoldi, E., Chiverrell, R.C., Ely, J., Dove, D. and Ó Cofaigh, C., (2021). Retreat dynamics of the eastern sector of the British–Irish Ice Sheet during the last glaciation. *Journal of Quaternary Science*, 36(5), pp.723-751.

Eyles, N., Putkinen, N., Sookhan, S. and Arbelaez-Moreno, L., (2016). Erosional origin of drumlins and megaridges. *Sedimentary Geology*, 338, pp.2-23.

Fairchild, H.L. (1929) 'New York drumlins', *Rochester Academy of Science.*

Fannon, J.S., Fowler, A.C. and Moyles, I.R. (2017) 'Numerical simulations of drumlin formation', *Proceedings. Mathematical, physical, and engineering sciences / the Royal Society*, 473(2204), p. 20170220.

Fowler, A.C., (2000) An instability mechanism for drumlin formation. *Geological Society, London, Special Publications*, 176(1), pp.307-319.

Fowler, A.C. (2010) 'The instability theory of drumlin formation applied to Newtonian viscous ice of finite depth', *Proceedings of the Royal Society A: Mathematical, Physical and Engineering Sciences*, 466(2121), pp. 2673–2694.

Fowler, A.C. (2018) 'The philosopher in the kitchen: the role of mathematical modelling in explaining drumlin formation', *GFF*, 140(2), pp. 93–105.

Fuchs, M. and Owen, L.A. (2008) 'Luminescence dating of glacial and associated sediments: review, recommendations and future directions', *Boreas*, 37(4), pp. 636–659.

Gandy, N., Gregoire, L.J., Ely, J.C., Clark, C.D., Hodgson, D.M., Lee, V., Bradwell, T. and Ivanovic, R.F., (2018). Marine ice sheet instability and ice shelf buttressing of the Minch Ice Stream, northwest Scotland. *The Cryosphere*, 12(11), pp.3635-3651.

Gandy, N., Gregoire, L.J., Ely, J.C., Cornford, S.L., Clark, C.D. and Hodgson, D.M., (2019) Exploring the ingredients required to successfully model the placement, generation, and evolution of ice streams in the British-Irish Ice Sheet. *Quaternary Science Reviews*, 223, p.105915.

Gandy, N., Gregoire, L.J., Ely, J.C., Cornford, S.L., Clark, C.D. and Hodgson, D.M., (2021). Collapse of the last Eurasian Ice Sheet in the North Sea modulated by combined processes of ice flow, surface melt, and marine ice sheet instabilities. *Journal of Geophysical Research: Earth Surface*, 126(4), pp.1-18

Geikie, James. *The Great Ice Age and its relation to the antiquity of man*. E. Stanford, 1894.

Gibbard, P.L. and Clark, C.D. (2011) ‘Chapter 7 - Pleistocene Glaciation Limits in Great Britain’, in: J. Ehlers, P.L. Gibbard, and P.D. Hughes (eds) *Developments in Quaternary Sciences*. Elsevier, pp. 75–93.

Michael Gibbons (2015). Drumlins from the air. Photo available online at: http://walkingireland.com/wp-content/uploads/2013/06/ Drumlins-from-the-air.jpg

Gillet-Chaulet, F., Durand, G., Gagliardini, O., Mosbeux, C., Mouginot, J., Rémy, F. and Ritz, C., (2016). Assimilation of surface velocities acquired between 1996 and 2010 to constrain the form of the basal friction law under Pine Island Glacier. *Geophysical Research Letters*, 43(19), pp.10-311.

Gowan, E.J., Tregoning, P., Purcell, A., Lea, J., Fransner, O.J., Noormets, R. and Dowdeswell, J.A., (2016). ICESHEET 1.0: a program to produce paleo-ice sheet reconstructions with minimal assumptions. *Geoscientific Model Development*, 9(5), pp.1673-1682.

Gowan, E.J., Hinck, S., Niu, L., Clason, C. and Lohmann, G., (2023). The impact of spatially varying ice sheet basal conditions on sliding at glacial time scales. *Journal of Glaciology,* 62(276), pp.1-15.

Graham, A.G.C., Lonergan, L. and Stoker, M.S. (2007) ‘Evidence for Late Pleistocene ice stream activity in the Witch Ground Basin, central North Sea, from 3D seismic reflection data’, *Quaternary science reviews*, 26(5), pp. 627–643.

Scotgold Resources (2018) *Grampian Project*. [Online]. Available at: https://www.scotgoldresources.com/projects/grampian-project/ (Accessed: 2 March 2023).

Greenough, G.B. (1819) ‘A Critical Examination of the First Principles of Geology’.

Greenwood, S.L., (2008). A palaeo-glaciological reconstruction of the last Irish Ice Sheet (Doctoral dissertation, University of Sheffield).

Greenwood, S.L. and Clark, C.D. (2009a) ‘Reconstructing the last Irish Ice Sheet 1: changing flow geometries and ice flow dynamics deciphered from the glacial landform record’, *Quaternary science reviews*, 28(27-28), pp. 3085–3100.

Greenwood, S.L. and Clark, C.D. (2009b) ‘Reconstructing the last Irish Ice Sheet 2: a geomorphologically-driven model of ice sheet growth, retreat and dynamics’, *Quaternary science reviews*, 28(27), pp. 3101–3123.

Gregoire, L.J., Otto-Bliesner, B., Valdes, P.J. and Ivanovic, R., (2016). Abrupt Bølling warming and ice saddle collapse contributions to the Meltwater Pulse 1a rapid sea level rise. *Geophysical research letters*, 43(17), pp.9130-9137.

Hart, J.K. (1997) ‘The relationship between drumlins and other forms of subglacial glaciotectonic deformation’, *Quaternary science reviews*, 16(1), pp. 93–107.

Hart, J.K. (1999) ‘Identifying fast ice flow from landform assemblages in the geological record: a discussion’, *Annals of Glaciology*, 28, pp. 59–66.

Haynes, R., Franklin, M., Goosney, J. and Goosney, D., (2023). Re-Visiting Viking Vinland: II.'Virtual Excavation' of 'Keelness', a Viking Shipwreck Site in North America.

Heidenreich, C. (1964) ‘Some observations on the shape of drumlins’, *The Canadian geographer. Geographe canadien*, 8(2), pp. 101–107.

Hildes, D.H., Clarke, G.K., Flowers, G.E. and Marshall, S.J., (2004). Subglacial erosion and englacial sediment transport modelled for North American ice sheets. *Quaternary Science Reviews*, 23(3-4), pp.409-430.

Hindmarsh, R.C.A. (1998a) ‘Drumlinization and drumlin-forming instabilities: viscous till mechanisms’, *Journal of Glaciology*, 44(147), pp. 293–314.

Hindmarsh, R.C.A. (1998b) ‘The stability of a viscous till sheet coupled with ice flow, considered at wavelengths less than the ice thickness’, *Journal of Glaciology*, 44(147), pp. 285–292.

Hindmarsh, R.C.A. (1999) ‘Coupled ice–till dynamics and the seeding of drumlins and bedrock forms’, *Annals of Glaciology*, 28, pp. 221–230.

Hollingworth, S.E., (1931). The glaciation of western Edenside and adjoining areas and the drumlins of Edenside and the Solway basin. *Quarterly Journal of the Geological Society*, 87(1-4), pp.281-359.

Holschuh, N., Christianson, K., Paden, J., Alley, R.B. and Anandakrishnan, S., (2020). Linking postglacial landscapes to glacier dynamics using swath radar at Thwaites Glacier, Antarctica. *Geology*, 48(3), pp.268-272.

Hooke, R.L., Cummings, D.I., Lesemann, J.E. and Sharpe, D.R., (2013). Genesis of dispersal plumes in till. *Canadian Journal of Earth Sciences*, 50(8), pp.847-855.

Howe, J.A., Dove, D., Bradwell, T. and Gafeira, J., (2012). Submarine geomorphology and glacial history of the Sea of the Hebrides, UK. *Marine Geology*, 315, pp.64-76.

Hubbard, A., Bradwell, T., Golledge, N., Hall, A., Patton, H., Sugden, D., Cooper, R. and Stoker, M., (2009). Dynamic cycles, ice streams and their impact on the extent, chronology and deglaciation of the British–Irish ice sheet. *Quaternary Science Reviews*, 28(7-8), pp.758-776.

Hughes, A.L., Gyllencreutz, R., Lohne, Ø.S., Mangerud, J. and Svendsen, J.I., (2016). The last Eurasian ice sheets–a chronological database and time-slice reconstruction, DATED-1. *Boreas*, 45(1), pp.1-45.

Hughes, A.L.C., Clark, C.D. and Jordan, C.J. (2010) 'Subglacial bedforms of the last British Ice Sheet', *Journal of maps*, 6(1), pp. 543–563.

Hughes, A.L.C., Clark, C.D. and Jordan, C.J. (2014) 'Flow-pattern evolution of the last British Ice Sheet', *Quaternary science reviews*, 89, pp. 148–168.

Hull, E. (1878) *The Physical Geology and Geography of Ireland*. E. Stanford.

Igneczi, A (2019) Streamline Script for Matlab. Pers. Comm.

IPCC, 2023: Climate Change 2023: Synthesis Report. Contribution of Working Groups I, II and III to the Sixth Assessment Report of the Intergovernmental Panel on Climate Change [Core Writing Team, H. Lee and J. Romero (eds.)]. IPCC, Geneva, Switzerland, pp. 35-115, doi: 10.59327/IPCC/AR6-9789291691647

Iverson, N.R., McCracken, R.G., Zoet, L.K., Benediktsson, Í.Ö., Schomacker, A., Johnson, M.D. and Woodard, J., (2017). A theoretical model of drumlin formation based on observations at Múlajökull, Iceland. *Journal of Geophysical Research: Earth Surface*, 122(12), pp.2302-2323.

Jamieson, S.S., Vieli, A., Livingstone, S.J., Cofaigh, C.Ó., Stokes, C., Hillenbrand, C.D. and Dowdeswell, J.A., (2012). Ice-stream stability on a reverse bed slope. *Nature Geoscience*, 5(11), pp.799-802.

Jamieson, S.S., Vieli, A., Cofaigh, C.Ó., Stokes, C.R., Livingstone, S.J. and Hillenbrand, C.D., (2014). Understanding controls on rapid ice-stream retreat during the last deglaciation of Marguerite Bay, Antarctica, using a numerical model. J*ournal of Geophysical Research: Earth Surface*, 119(2), pp.247-263.

Jamieson, S.S., Stokes, C.R., Livingstone, S.J., Vieli, A., Cofaigh, C.Ó., Hillenbrand, C.D. and Spagnolo, M., (2016). Subglacial processes on an Antarctic ice stream bed. 2: Can modelled ice dynamics explain the morphology of mega-scale glacial lineations?. *Journal of Glaciology*, 62(232), pp.285-298.

Jamieson, T.F., (1906). The glacial period in Aberdeenshire and the southern border of the Moray Firth. *Quarterly Journal of the Geological Society*, 62(1-4), pp.13-39.

Jauhiainen, F. (2008) 'Morphometric analysis of drumlin fields in northern Central Europe', *Boreas*, 4(4), pp. 219–230.

Jehu, T.J. (1906) 'IV.—The Glacial Deposits of Northern Pembrokeshire', *Earth and environmental science transactions of the Royal Society of Edinburgh*, 41(1), pp. 53–87.

Johnson, M.D., Schomacker, A., Benediktsson, Í.Ö., Geiger, A.J., Ferguson, A. and Ingólfsson, Ó., (2010). Active drumlin field revealed at the margin of Múlajökull, Iceland: a surge-type glacier. *Geology*, 38(10), pp.943-946.

Jones, J.M., Gille, S.T., Goosse, H., Abram, N.J., Canziani, P.O., Charman, D.J., Clem, K.R., Crosta, X., De Lavergne, C., Eisenman, I. and England, M.H., (2016). Assessing recent trends in high-latitude Southern Hemisphere surface climate. *Nature Climate Change*, 6(10), pp.917-926.

Jouvet, G., Seguinot, J., Ivy-Ochs, S. and Funk, M., (2017). Modelling the diversion of erratic boulders by the Valais Glacier during the last glacial maximum. *Journal of Glaciology*, 63(239), pp.487-498.

Jouvet, G., Cordonnier, G., Kim, B., Lüthi, M., Vieli, A. and Aschwanden, A., (2022). Deep learning speeds up ice flow modelling by several orders of magnitude. *Journal of Glaciology*, 68(270), pp.651-664.

Kageyama, M., Merkel, U., Otto-Bliesner, B., Prange, M., Abe-Ouchi, A., Lohmann, G., Ohgaito, R., Roche, D.M., Singarayer, J., Swingedouw, D. and Zhang, X., (2013). Climatic impacts of fresh water hosing under Last Glacial Maximum conditions: a multi-model study. *Climate of the Past*, 9(2), pp.935-953.

King, E.C., Hindmarsh, R.C.A. and Stokes, C.R. (2009) 'Formation of mega-scale glacial lineations observed beneath a West Antarctic ice stream', *Nature geoscience*, 2(8), pp. 585–588.

King, E.C., Woodward, J. and Smith, A.M. (2007) 'Seismic and radar observations of subglacial bed forms beneath the onset zone of Rutford Ice Stream, Antarctica', *Journal of Glaciology*, 53(183), pp. 665–672.

Kirchner, N., Hutter, K., Jakobsson, M. and Gyllencreutz, R., (2011). Capabilities and limitations of numerical ice sheet models: a discussion for Earth-scientists and modelers. *Quaternary Science Reviews*, 30(25-26), pp.3691-3704.

Klassen, R.A. (1994) 'A preliminary interpretation of glacial history derived from glacial striations, central Newfoundland', *Current Research, Part D. Geological Survey of Canada, Paper*, pp. 117–143.

Kleman, J. (1994) 'Preservation of landforms under ice sheets and ice caps', *Geomorphology*, 9(1), pp. 19–32.

Kleman, J. and Borgström, I. (1996) 'Reconstruction of palaeo-ice sheets: The use of geomorphological data', *Earth Surface Processes and Landforms*, 21(10), pp. 893–909.

Knight, L. (2021) Database of British Pleistocene Erratics and Glacial Striae-Version v2021-02-01 (Pers. Comm.)

Knowles, W.J. (1903) ‘Stone Axe Factories Near Cushendall, County Antrim’, *The Journal of the Anthropological Institute of Great Britain and Ireland*, 33, pp. 360–366.

Lambeck, K. and Chappell, J. (2001) ‘Sea level change through the last glacial cycle’, *Science*, 292(5517), pp. 679–686.

Lamplugh, G.W. (1903) *The geology of the Isle of Man*. HM Stationery Office.

Lecavalier, B.S., Milne, G.A., Simpson, M.J., Wake, L., Huybrechts, P., Tarasov, L., Kjeldsen, K.K., Funder, S., Long, A.J., Woodroffe, S. and Dyke, A.S., (2014). A model of Greenland ice sheet deglaciation constrained by observations of relative sea level and ice extent. *Quaternary Science Reviews*, 102, pp.54-84.

Leger, T.P.M.*, Clark, C. D; Huynh, C.; Jones, S.; Ely, J. C; Bradley, S. L; Diemont, C.; Hughes, A. L. C.* (2023) ‘A Greenland-wide empirical reconstruction of paleo ice-sheet retreat informed by ice extent markers: PaleoGrIS version 1.0’, *Climate of the Past Discussions*.

Leung, D.D.V. and McDonald, A.M. (2022) ‘Taking Rocks for Granite: An Integrated Geological, Mineralogical, and Textural Study of Curling Stones Used in International Competition’, *Canadian mineralogist*, 60(1), pp. 171–199.

Li, Y., Napieralski, J., Harbor, J. and Hubbard, A., (2007). Identifying patterns of correspondence between modeled flow directions and field evidence: an automated flow direction analysis. *Computers & geosciences*, 33(2), pp.141-150.

Libby, W.F. (1961) ‘Radiocarbon dating’, *Science*, 133(3453), pp. 621–629.

Livingstone, S.J., Evans, D.J., Cofaigh, C.Ó., Davies, B.J., Merritt, J.W., Huddart, D., Mitchell, W.A., Roberts, D.H. and Yorke, L., (2012). Glaciodynamics of the central sector of the last British–Irish Ice Sheet in Northern England. *Earth-Science Reviews*, 111(1-2), pp.25-55.

Livingstone, S.J., Evans, D.J., Cofaigh, C.Ó., Davies, B.J., Merritt, J.W., Huddart, D., Mitchell, W.A., Roberts, D.H. and Yorke, L., (2012). Glaciodynamics of the central sector of the last British–Irish Ice Sheet in Northern England. *Earth-Science Reviews*, 111(1-2), pp.25-55.

Livingstone, S.J., Cofaigh, C.Ó. and Evans, D.J., (2008). Glacial geomorphology of the central sector of the last British-Irish Ice Sheet. *Journal of Maps*, 4(1), pp.358-377.

Livingstone, S.J., Cofaigh, C.Ó., Stokes, C.R., Hillenbrand, C.D., Vieli, A. and Jamieson, S.S., (2012). Antarctic palaeo-ice streams. *Earth-Science Reviews,* 111(1-2), pp.90-128.

Livingstone, S.J. *et al.* (2015) 'Late Devensian deglaciation of the Tyne gap palaeo-ice stream, northern England', *Journal of Quaternary Science*, 30(8), pp. 790–804.

Livingstone, S.J., Stokes, C.R., Cofaigh, C.Ó., Hillenbrand, C.D., Vieli, A., Jamieson, S.S., Spagnolo, M. and Dowdeswell, J.A., (2016). Subglacial processes on an Antarctic ice stream bed. 1: Sediment transport and bedform genesis inferred from marine geophysical data. *Journal of Glaciology*, 62(232), pp.270-284.

Lockhart, E.A., Scourse, J.D., Praeg, D., Van Landeghem, K.J., Mellett, C., Saher, M., Callard, L., Chiverrell, R.C., Benetti, S., Cofaigh, C.Ó. and Clark, C.D., (2018). A stratigraphic investigation of the Celtic Sea megaridges based on seismic and core data from the Irish-UK sectors. *Quaternary Science Reviews*, 198, pp.156-170.

Lyell, C. 1841. On the geological evidences of the former existence of glaciers in Forfarshire. Proceedings of the Geological Societv of London, 3(72), 337-345

Mackie, W., (1901). Some notes on the distribution of erratics over eastern Moray. *Transactions of the Edinburgh Geological Society*, 8(1), pp.91-97.

Margold, M., Jansson, K.N., Kleman, J., Stroeven, A.P. and Clague, J.J., (2013). Retreat pattern of the C ordilleran I ce S heet in central B ritish C olumbia at the end of the last glaciation reconstructed from glacial meltwater landforms. *Boreas*, 42(4), pp.830-847.

Margold, M., Stokes, C.R., Clark, C.D. and Kleman, J., (2015). Ice streams in the Laurentide Ice Sheet: a new mapping inventory. *Journal of Maps*, 11(3), pp.380-395.

Mark, D.M. (1974) 'On the Interpretation of Till Fabrics', *Geology*, 2(2), pp. 101–104.

Mas e Braga, M., Selwyn Jones, R., Newall, J.C., Rogozhina, I., Andersen, J.L., Lifton, N.A. and Stroeven, A.P., (2021). Nunataks as barriers to ice flow: implications for palaeo ice sheet reconstructions. *The Cryosphere*, 15(10), pp.4929-4947.

McCabe, A.M., Clark, P.U., Clark, J. and Dunlop, P., (2007). Radiocarbon constraints on readvances of the British–Irish Ice Sheet in the northern Irish Sea Basin during the last deglaciation. *Quaternary Science Reviews*, 26(9-10), pp.1204-1211.

Melanson, A., Bell, T. and Tarasov, L. (2013) 'Numerical modelling of subglacial erosion and sediment transport and its application to the North American ice sheets over the Last Glacial cycle', *Quaternary science reviews*, 68, pp. 154–174.

Menzies (1979) 'A review of the literature on the formation and location of drumlins', *Earth-Science Reviews*, 14(4), pp. 315–359.

Milanković, M. (1920) *Théorie mathématique des phénomènes thermiques produits par la radiation solaire*. Gauthier-Villars et Cie.

Mills, H.H. (1987) 'Morphometry of drumlins in the northeastern and north-central USA', in *Drumlin symposium*, pp. 131–147.

Mitchell, W.A. (1994) 'Drumlins in ice sheet reconstructions, with reference to the western Pennines, northern England', *Sedimentary geology*, 91(1), pp. 313–331.

Moore, E.J. (1931) 'The Ecology of the Ayreland of Bride, Isle of Man', *The Journal of ecology*, 19(1), pp. 115–136.

Napieralski, J., Hubbard, A., Li, Y., Harbor, J., Stroeven, A.P., Kleman, J., Alm, G. and Jansson, K.N., (2007). Towards a GIS assessment of numerical ice-sheet model performance using geomorphological data. *Journal of Glaciology*, 53(180), pp.71-83.

Napieralski, J., Li, Y. and Harbor, J. (2006) 'Comparing predicted and observed spatial boundaries of geologic phenomena: Automated Proximity and Conformity Analysis applied to ice sheet reconstructions', *Computers & geosciences*, 32(1), pp. 124–134.

Nicholls, R.J. and Cazenave, A. (2010) 'Sea-level rise and its impact on coastal zones', *Science*, 328(5985), pp. 1517–1520.

Nicolson, H.A. (1868) 'On the granite of shap, in Westmoreland', *Transactions of the Edinburgh Geological Society*, 1(2), pp. 133–137.

Nockolds, S.R. (1940) *The Garabal Hill-Glen Fyne Igneous Complex*, *Quarterly Journal of the Geological Society of London*.

Ó Cofaigh, C., Callard, S.L., Roberts, D.H., Chiverrell, R.C., Ballantyne, C.K., Evans, D.J., Saher, M., Van Landeghem, K.J., Smedley, R., Benetti, S. and Burke, M., (2021). Timing and pace of ice-sheet withdrawal across the marine–terrestrial transition west of Ireland during the last glaciation. *Journal of Quaternary Science*, 36(5), pp.805-832.

Osman, M.B., Tierney, J.E., Zhu, J., Tardif, R., Hakim, G.J., King, J. and Poulsen, C.J., (2021). Globally resolved surface temperatures since the Last Glacial Maximum. *Nature*, 599(7884), pp.239-244.

Ottesen, D., Stokes, C.R., Bøe, R., Rise, L., Longva, O., Thorsnes, T., Olesen, O., Bugge, T., Lepland, A. and Hestvik, O.B., (2016). Landform assemblages and sedimentary processes along the Norwegian Channel Ice Stream. *Sedimentary Geology*, 338, pp.115-137.

Parker Pearson, M. (2016) ‘The sarsen stones of Stonehenge’, *Proceedings of the Geologists’ Association. Geologists' Association*, 127(3), pp. 363–369.

Patterson, C.J. and Hooke, R.L. (1995) ‘Physical environment of drumlin formation’, *Journal of Glaciology*, 41(137), pp. 30–38.

Patton, H., Hubbard, A., Andreassen, K., Winsborrow, M. and Stroeven, A.P., (2016). The build-up, configuration, and dynamical sensitivity of the Eurasian ice-sheet complex to Late Weichselian climatic and oceanic forcing. *Quaternary Science Reviews*, 153, pp.97-121.

Patton, H., Hubbard, A., Andreassen, K., Auriac, A., Whitehouse, P.L., Stroeven, A.P., Shackleton, C., Winsborrow, M., Heyman, J. and Hall, A.M., (2017). Deglaciation of the Eurasian ice sheet complex. *Quaternary Science Reviews*, 169, pp.148-172.

Pearce D.M., Ely, J. C., Barr, I.D. Boston, C.M. (2017) ‘Glacier Reconstruction’, in *Geomorphological Techniques*. *British Society for Geomorphology*, pp. 190–207.

Peters, J.L., Benetti, S., Dunlop, P. and Cofaigh, C.Ó., (2015). Maximum extent and dynamic behaviour of the last British–Irish Ice Sheet west of Ireland. *Quaternary Science Reviews*, 128, pp.48-68.

Pollard, D., DeConto, R.M. and Alley, R.B. (2015) ‘Potential Antarctic Ice Sheet retreat driven by hydrofracturing and ice cliff failure’, *Earth and planetary science letters*, 412, pp. 112–121.

Pollard, O.G., Barlow, N.L., Gregoire, L., Gomez, N., Cartelle, V., Ely, J.C. and Astfalck, L.C., 2023. Quantifying the Uncertainty in the Eurasian Ice-Sheet Geometry at the Penultimate Glacial Maximum (Marine Isotope Stage 6). *The Cryosphere Discussions*, pp.1-31.

Prest, V.K. (1969) ‘Retreat of Wisconsin and Recent ice in North America: speculative ice-marginal positions during recession of last ice-sheet complex’, Geological Survey of Canada.

Raistrick, A. (1931) ‘XI. GLACIATION’, Contribution to the Geology of Northumberland and Durham. *Proceedings of the Geological Association*, XLII, Part 3

Rignot, E., Mouginot, J. and Scheuchl, B. (2011) ‘Ice flow of the Antarctic ice sheet’, *Science*, 333(6048), pp. 1427–1430.

Roberts, D.H., Grimoldi, E., Callard, L., Evans, D.J., Clark, C.D., Stewart, H.A., Dove, D., Saher, M., Ó Cofaigh, C., Chiverrell, R.C. and Bateman, M.D., (2019). The mixed-bed glacial landform imprint of the North Sea Lobe in the western North Sea. *Earth Surface Processes and Landforms,* 44(6), pp.1233-1258.

Rose, J. and Letzer, J. M. (1977) Superimposed drumlins. *Journal of Glaciology* 18, 471-480.

Rudwick, M.J., (2009). Biblical Flood and geological deluge: the amicable dissociation of geology and Genesis. *Geological Society, London, Special Publications*, 310(1), pp.103-110.

Rutt, I.C., Hagdorn, M., Hulton, N.R.J. and Payne, A.J., (2009). The Glimmer community ice sheet model. *Journal of Geophysical Research: Earth Surface*, 114(F2).

Schlegel, R., Murray, T., Smith, A.M., Brisbourne, A.M., Booth, A.D., King, E.C. and Clark, R.A., (2022). Radar derived subglacial properties and landforms beneath Rutford Ice Stream, West Antarctica. J*ournal of Geophysical Research: Earth Surface*, 127(1), pp.1-18

Schoof, C. (2007) 'Pressure-dependent viscosity and interfacial instability in coupled ice–sediment flow', *Journal of fluid mechanics*, 570, pp. 227–252.

Scourse, J., Saher, M., Van Landeghem, K.J., Lockhart, E., Purcell, C., Callard, L., Roseby, Z., Allinson, B., Pieńkowski, A.J., O'Cofaigh, C. and Praeg, D., (2019). Advance and retreat of the marine-terminating Irish Sea Ice Stream into the Celtic Sea during the Last Glacial: Timing and maximum extent. *Marine Geology*, 412, pp.53-68.

Scourse, J.D. (1991) 'Late Pleistocene stratigraphy and palaeobotany of the Isles of Scilly', *Philosophical transactions of the Royal Society of London. Series B, Biological sciences*, 334(1271), pp. 405–448.

Scourse, J.D., Chiverrell, R.C., Smedley, R.K., Small, D., Burke, M.J., Saher, M., Van Landeghem, K.J., Duller, G.A., Cofaigh, C.Ó., Bateman, M.D. and Benetti, S., (2021). Maximum extent and readvance dynamics of the Irish sea ice stream and Irish Sea Glacier since the last glacial maximum. *Journal of Quaternary Science*, 36(5), pp.780-804.

Scourse, J.D. and Furze, M.F.A. (2001) 'A critical review of the glaciomarine model for Irish sea deglaciation: evidence from southern Britain, the Celtic shelf and adjacent continental slope', *Journal of Quaternary Science*, 16(5), pp. 419–434.

Sejrup, H.P., Clark, C.D. and Hjelstuen, B.O. (2016) 'Rapid ice sheet retreat triggered by ice stream debuttressing: Evidence from the North Sea', *Geology*, 44(5), pp. 355–358.

Shaw, J. (1983) 'Drumlin Formation Related to Inverted Melt-Water Erosional Marks', *Journal of Glaciology*, 29(103), pp. 461–479.

Shaw, J. (1989) 'Drumlins, subglacial meltwater floods, and ocean responses', *Geology*, 17(9), pp. 853–856.

Shennan, I., Bradley, S., Milne, G., Brooks, A., Bassett, S. and Hamilton, S., 2006. Relative sea-level changes, glacial isostatic modelling and ice-sheet reconstructions from the British Isles since the Last Glacial Maximum. *Journal of Quaternary Science*: Published for the Quaternary Research Association, 21(6), pp.585-599.

Siegert, M.J., Dowdeswell, J.A., Hald, M. and Svendsen, J.I., 2001. Modelling the Eurasian Ice Sheet through a full (Weichselian) glacial cycle. Global and Planetary Change, 31(1-4), pp.367-385.

Sigman, D.M. and Boyle, E.A. (2000) 'Glacial/interglacial variations in atmospheric carbon dioxide', *Nature*, 407(6806), pp. 859–869.

Smalley, I.J. and Unwin, D.J. (1968) 'The Formation and Shape of Drumlins and their Distribution and Orientation in Drumlin Fields', *Journal of Glaciology*, 7(51), pp. 377–390.

Smith, A.M., Murray, T., Nicholls, K.W., Makinson, K., Aðalgeirsdóttir, G., Behar, A.E. and Vaughan, D.G., (2007). Rapid erosion, drumlin formation, and changing hydrology beneath an Antarctic ice stream. *Geology*, 35(2), pp.127-130.

Smith, M.J., Rose, J. and Booth, S. (2006) 'Geomorphological mapping of glacial landforms from remotely sensed data: An evaluation of the principal data sources and an assessment of their quality', *Geomorphology* , 76(1), pp. 148–165.

Spagnolo, M., Clark, C.D., Hughes, A.L., Dunlop, P. and Stokes, C.R., (2010). The planar shape of drumlins. *Sedimentary Geology*, 232(3-4), pp.119-129.

Spagnolo, M., King, E.C., Ashmore, D.W., Rea, B.R., Ely, J.C. and Clark, C.D., (2014). Looking through drumlins: testing the application of ground-penetrating rada. *Journal of Glaciology*, 60(224), pp.1126-1134.

Stoker, M. and Bradwell, T. (2005) 'The Minch palaeo-ice stream, NW sector of the British–Irish Ice Sheet', *Journal of the Geological Society*, 162(3), pp. 425–428.

Stokes, C.R., Fowler, A.C., Clark, C.D., Hindmarsh, R.C. and Spagnolo, M., (2013). The instability theory of drumlin formation and its explanation of their varied composition and internal structure. *Quaternary Science Reviews*, 62, pp.77-96.

Stokes, C.R., Spagnolo, M. and Clark, C.D., 2011. The composition and internal structure of drumlins: complexity, commonality, and implications for a unifying theory of their formation. *Earth-Science Reviews*, *107*(3-4), pp.398-422.

Stokes, C.R., Tarasov, L., Blomdin, R., Cronin, T.M., Fisher, T.G., Gyllencreutz, R., Hättestrand, C., Heyman, J., Hindmarsh, R.C., Hughes, A.L. and Jakobsson,

M., (2015). On the reconstruction of palaeo-ice sheets: recent advances and future challenges. *Quaternary Science Reviews*, 125, pp.15-49.

Stokes, C.R., Tarasov, L., Blomdin, R., Cronin, T.M., Fisher, T.G., Gyllencreutz, R., Hättestrand, C., Heyman, J., Hindmarsh, R.C., Hughes, A.L. and Jakobsson, M., (2015). On the reconstruction of palaeo-ice sheets: recent advances and future challenges. *Quaternary Science Reviews*, 125, pp.15-49.

Stokes, C.R. and Clark, C.D. (2001) 'Palaeo-ice streams', *Quaternary science reviews*, 20(13), pp. 1437–1457.

Sugden, D.E. (1977) 'Reconstruction of the Morphology, Dynamics, and Thermal Characteristics of the Laurentide Ice Sheet at its Maximum', *Arctic and Alpine Research*, 9(1), pp. 21–47.

Sugden, D.E., Hulton, N.R.J. and Purves, R.S. (2002) 'Modelling the inception of the Patagonian icesheet', *Quaternary international: the journal of the International Union for Quaternary Research*, 95-96, pp. 55–64.

Sutherland, D.G. (1984) 'The Quaternary deposits and landforms of Scotland and the neighbouring shelves: A review', *Quaternary science reviews*, 3(2), pp. 157–254.

Tarasov, L., Dyke, A.S., Neal, R.M. and Peltier, W.R., (2012). A data-calibrated distribution of deglacial chronologies for the North American ice complex from glaciological modeling. *Earth and Planetary Science Letters*, 315, pp.30-40.

Tarasov, L. and Peltier, W.R. (2004) 'A geophysically constrained large ensemble analysis of the deglacial history of the North American ice-sheet complex', *Quaternary science reviews*, 23(3), pp. 359–388.

Teng, J., Potter, N.J., Chiew, F.H.S., Zhang, L., Wang, B., Vaze, J. and Evans, J.P., (2015). How does bias correction of regional climate model precipitation affect modelled runoff?. *Hydrology and Earth System Sciences*, 19(2), pp.711-728.

Thirlwall, M.F., (1988). Geochronology of Late Caledonian magmatism in northern Britain. *Journal of the Geological Society*, 145(6), pp.951-967.

Thomas, R.H. (1979) 'The Dynamics of Marine Ice Sheets', *Journal of Glaciology*, 24(90), pp. 167–177.

Trotter, F.M., (1929). The glaciation of eastern Edenside, the Alston block, and the Carlisle plain*. Quarterly Journal of the Geological Society*, 85(1-4), pp.549-612.

Tuckett, P.A., Ely, J.C., Sole, A.J., Livingstone, S.J., Davison, B.J., Melchior van Wessem, J. and Howard, J., (2019). Rapid accelerations of Antarctic Peninsula outlet glaciers driven by surface melt. *Nature Communications*, 10(1), p.4311.

Ugelvig, S.V., Egholm, D.L. and Iverson, N.R. (2016) 'Glacial landscape evolution by subglacial quarrying: A multiscale computational approach', *Journal of Geophysical Research: Earth Surface*, 121(11), pp. 2042–2068.

Van Landeghem, K.J.J. and Chiverrell, R.C. (2020) 'Bed erosion during fast ice streaming regulated the retreat dynamics of the Irish Sea Ice Stream', *Quaternary science reviews*, 245, p. 106526.

Warren WP. (1992). Drumlin orientation and the pattern of glaciation in Ireland. *Sveriges Geologiska Undersökning* 81, pp. 359-366.

Weertman, J. (1976) 'Milankovitch solar radiation variations and ice age ice sheet sizes', *Nature*, 261(5555), pp. 17–20.

Winkelmann, R., Martin, M.A., Haseloff, M., Albrecht, T., Bueler, E., Khroulev, C. and Levermann, A., (2011). The Potsdam parallel ice sheet model (PISM-PIK)–Part 1: Model description. *The Cryosphere*, 5(3), pp.715-726.

Winsborrow, M.C.M., Clark, C.D. and Stokes, C.R. (2010) 'What controls the location of ice streams?', *Earth-Science Reviews*, 103(1), pp. 45–59.

Woodard, J.B., Zoet, L.K., Benediktsson, Í.Ö., Iverson, N.R. and Finlayson, A., (2020). Insights into drumlin development from ground-penetrating radar at Múlajökull, Iceland, a surge-type glacier. *Journal of Glaciology*, 66(259), pp.822-830.

Wright, W.B. (1912) 'III.—The Drumlin Topography of South Donegal', *Geological magazine*, 9(4), pp. 153–159.

Zeitz, M., Reese, R., Beckmann, J., Krebs-Kanzow, U. and Winkelmann, R., (2021). Impact of the melt–albedo feedback on the future evolution of the Greenland Ice Sheet with PISM-dEBM-simple. *The Cryosphere*, 15(12), pp.5739-5764.

Zoet, L.K., Rawling III, J.E., Woodard, J.B., Barrette, N. and Mickelson, D.M., (2021). Factors that contribute to the elongation of drumlins beneath the Green Bay Lobe, Laurentide Ice Sheet. *Earth Surface Processes and Landforms*, 46(13), pp.2540-2550.